REPORT NO.
UCB/EERC-90/14
OCTOBER 1990

EARTHQUAKE ENGINEERING RESEARCH CENTER

INELASTIC SEISMIC RESPONSE OF ONE-STORY, ASYMMETRIC-PLAN SYSTEMS

by

RAKESH K. GOEL

ANIL K. CHOPRA

A Report on Research conducted under
Grant No. BCS-8921932 from the
National Science Foundation

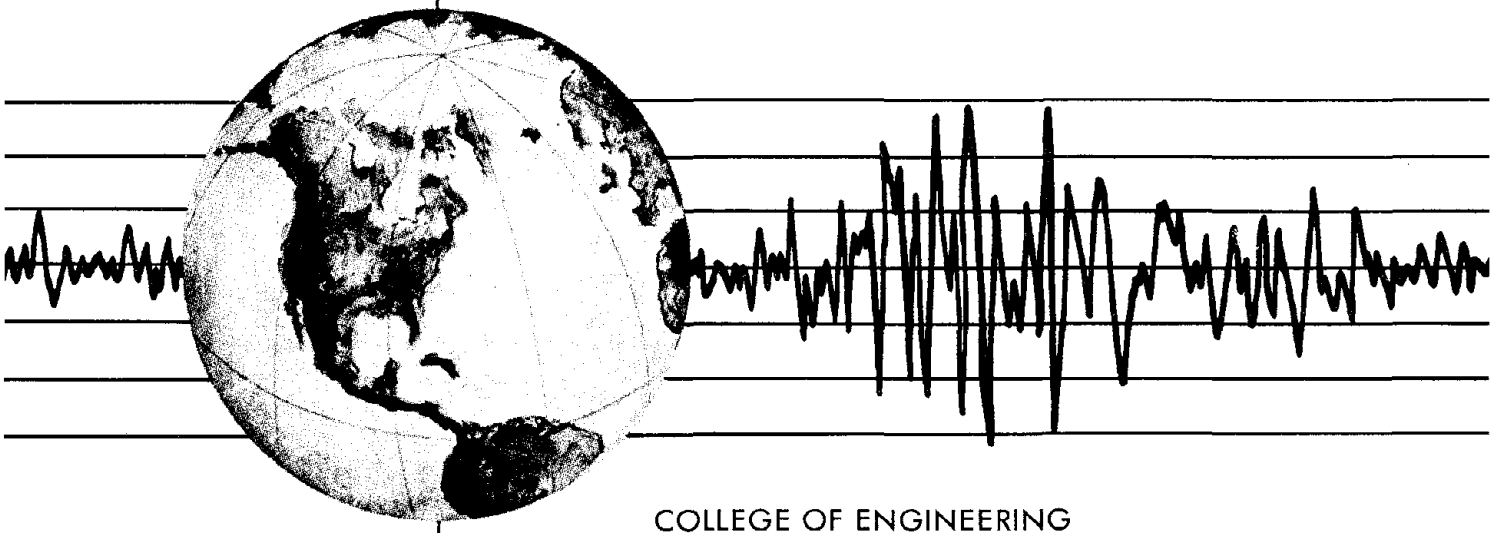

COLLEGE OF ENGINEERING

UNIVERSITY OF CALIFORNIA AT BERKELEY

For sale by the National Technical Information Service, U.S. Department of Commerce, Springfield, Virginia 22161

See back of report for up to date listing of EERC reports.

DISCLAIMER

Any opinions, findings, and conclusions or recommendations expressed in this publication are those of the authors and do not necessarily reflect the views of the National Science Foundation or the Earthquake Engineering Research Center, University of California at Berkeley.

REPORT DOCUMENTATION PAGE	1. REPORT NO. NSF/ENG-90008	2.	3 PB93-114767

4. Title and Subtitle
Inelastic Seismic Response of One-Story, Asymmetric-Plan Systems

5. Report Date
October 1990

6.

7. Author(s)
Rakesh K. Goel and Anil K. Chopra

8. Performing Organization Rept. No.
UCB/EERC-90/14

9. Performing Organization Name and Address
Earthquake Engineering Research Center
University of California, Berkeley
1301 So. 46th Street
Richmond, Calif. 94804

10. Project/Task/Work Unit No.

11. Contract(C) or Grant(G) No.
(C)
(G) BCS-8921932

12. Sponsoring Organization Name and Address
National Science Foundation
1800 G Street, N.W.
Washington, D.C. 20550

13. Type of Report & Period Covered

14.

15. Supplementary Notes

16. Abstract (Limit: 200 words)

The response was studied for a wide range of system parameters with the objective of: (1) evaluating the effects of plan-wise distribution of stiffness and strength on the response; (2) investigating how the response is influenced by the system parameters; (3) identifying how structural response is affected by plan-asymmetry and how these effects differ between elastic and inelastic systems; and (4) investigating how well the effects of plan-asymmetry on structural response are represented by torsional provisions in building codes. The inelastic responses are presented of several asymmetric-plan systems: with and without resisting elements along the direction perpendicular to the ground motion, with varying number of resisting elements along the direction of ground motion, with varying levels of overstrength and relative values of strength and stiffness eccentricities, and with eccentricity due to uneven distribution of stiffness and of mass. Plan-wise distribution of stiffness and strength is shown to significantly affect the inelastic response of asymmetric-plan systems. Based on these results, a simple system with two resisting elements along each of the two principal directions -- a system that encompasses all the important characteristics of many actual asymmetric-plan systems -- is selected for further study. Its inelastic responses to two excitations -- a simple input and an actual earthquake ground motion -- are presented for a wide range of system parameters: uncoupled lateral vibration period, uncoupled torsional-to-lateral frequency ratio, stiffness eccentricity, relative values of strength and stiffness eccentricities, and yield factor.

17. Document Analysis a. Descriptors

b. Identifiers/Open-Ended Terms

c. COSATI Field/Group

18. Availability Statement:	19. Security Class (This Report)	21. No. of Pages
Release Unlimited	unclassified	254
	20. Security Class (This Page) unclassified	22. Price

INELASTIC SEISMIC RESPONSE OF ONE-STORY, ASYMMETRIC-PLAN SYSTEMS

by

Rakesh K. Goel

Anil K. Chopra

A Report on Reseach Conducted Under
Grant No. BCS-8921932 from the
National Science Foundation

Report No. UCB/EERC-90/14
Earthquake Engineering Research Center
University of California
Berkeley, California

October 1990

ABSTRACT

The inelastic responses of one-story, asymmetric-plan systems to earthquake ground motions are presented for a wide range of system parameters and analyzed in this investigation with the objective of: (1) evaluating the effects of plan-wise distribution of stiffness and strength on the response; (2) investigating how the response is influenced by the system parameters; (3) identifying how structural response is affected by plan-asymmetry and how these effects differ between elastic and inelastic systems; and (4) investigating how well the effects of plan-asymmetry on structural response are represented by torsional provisions in building codes.

Presented first for a wide range of system parameters are the inelastic responses of several asymmetric-plan systems: with and without resisting elements along the direction perpendicular to the ground motion, with varying number of resisting elements along the direction of ground motion, with varying levels of overstrength and relative values of strength and stiffness eccentricities, and with eccentricity due to uneven distribution of stiffness and of mass. Plan-wise distribution of stiffness and strength is shown to significantly affect the inelastic response of asymmetric-plan systems. Based on these results, a simple system with two resisting elements along each of the two principal directions -- a system that encompasses all the important characteristics of many actual asymmetric-plan systems -- is selected for further research investigation.

The inelastic responses of this asymmetric-plan system to two excitations -- a simple input and an actual earthquake ground motion -- are presented for a wide range of system parameters: uncoupled lateral vibration period, uncoupled torsional-to-lateral frequency ratio, stiffness eccentricity, relative values of strength and stiffness eccentricities, and yield factor. Based on these response results, we identify how various system parameters and yielding of the system influence the response of asymmetric-plan systems in various spectral regions of the excitation. In particular, the lateral deformation decreases and the torsional deformation increases as the system becomes increasingly asymmetric in plan and

increasingly flexible in torsion. Inelastic behavior influences the lateral deformation of asymmetric-plan systems in a manner similar to symmetric-plan systems. The torsional deformations are shown to generally decrease with yielding; however they may increase for systems with large stiffness eccentricity, small yield strength, and equal values of stiffness and strength eccentricities.

Subsequently, the dynamic responses of asymmetric-plan and symmetric-plan systems are compared for a wide range of system parameters. Based on these response results, we identify how the structural response is affected by plan-asymmetry, how these effects depend on the system parameters and how these effects differ between elastic and inelastic systems. The response of inelastic systems is affected less by plan-asymmetry compared to elastic systems. Between the two types of inelastic systems considered, the response of strength-symmetric systems is affected by plan-asymmetry generally to a smaller degree compared to systems with equal strength and stiffness eccentricities. In particular, the dynamic amplification of torsional deformation is smaller, and the increase in element deformation due to plan-asymmetry is less in strength-symmetric systems.

Finally, the responses of asymmetric-plan systems designed by various building codes are presented and analyzed to determine how well the effects of plan-asymmetry are represented by the torsional provisions in building codes. Building code provisions do not ensure that the deformation and ductility demands on an asymmetric-plan system are similar to those on a similarly-designed symmetric-plan system. This goal can usually be achieved for stiff-side elements by precluding any reduction in their design forces below their symmetric-plan value; $\delta=0$ in the design eccentricity, e_d, is equivalent to this requirement. Similarly, the ductility demand on the flexible-side element can be kept below and close to its symmetric-plan value by modifying the coefficient α in the design eccentricity, e_d. The optimal value of α depends on the design value of the reduction factor R and may differ with the ground motion. However, it does not appear possible to reduce the additional element deformations due to plan-asymmetry by modifying the design eccentricity; these larger

deformations should be provided for in building design. Furthermore, the design eccentricity should be defined differently for elastic and inelastic systems; in the latter case, it should vary with the design force level and anticipated degree of inelastic action.

ACKNOWLEDGEMENTS

This research investigation was supported by the National Science Foundation under Grant No. BCS-8921932. The authors are grateful for this support.

This report is the same, except for some editorial changes, as Rakesh K. Goel's doctoral dissertation submitted to the University of California at Berkeley. The dissertation committee consisted of Professors Anil K. Chopra (Chairman), Stephen A. Mahin and Bruce A. Bolt. The authors are thankful to Professors Mahin and Bolt for reviewing the dissertation manuscript.

Table of Contents

1. INTRODUCTION

Buildings subjected to lateral ground motion simultaneously undergo lateral as well as torsional motions if their structural plans do not have two axes of mass and stiffness symmetry. As a result of coupled lateral-torsional motions, the lateral forces and deformations experienced by various resisting elements (frames, shear walls, etc.) in such buildings would differ from those experienced by the same elements if the building had symmetric plan and hence responded only in planar vibration.

The effects of coupling between lateral and torsional motions on the earthquake response of asymmetric-plan buildings has been a subject of numerous studies. Initially, most studies were concerned with the elastic response of buildings, and the effects of lateral-torsional coupling for such systems are now well established [2,7,11,12,18,29]. Based on the elastic response results, the torsional provisions in seismic codes have been evaluated [2-4,6,13,14,25,26,29,33,34]. Several of these investigations have suggested a larger eccentricity, compared to current codes, in order to reflect the dynamic amplification of the torsional response arising from plan-asymmetry. However, the results of these studies may not be directly applicable to the calculation of earthquake design forces for buildings because they are usually designed to deform significantly beyond the yield limit during intense ground motions.

In recent years, the research focus has shifted to the inelastic response of asymmetric-plan systems in order to obtain results applicable to design of buildings [1,7,8,17,19,20,24,30,31,35,36]. One of the difficulties in investigating the coupled lateral-torsional response of asymmetric-plan systems in the inelastic range of behavior is that many more parameters are required to characterize such systems compared to their elastic counterparts. In particular, the linear elastic response of a one-story, asymmetric-plan (or torsionally-coupled) system depends on the lateral and torsional vibration frequencies of the corresponding symmetric-plan (or torsionally-uncoupled) system, the eccentricity between the center of stiffness and center of mass, and the damping ratio, but not independently on

the number, location, or stiffness of the individual resisting elements, nor on the plan geometry. In contrast, the distribution of stiffness and strength in plan influences the response of the system in the inelastic range. Thus the results and conclusions of each of the earlier research investigations may be restricted to the particular system analyzed and not valid in general. This becomes apparent from the following review of previous work on inelastic response of asymmetric-plan systems.

In one of the earlier investigations [19], using a single element model (Figure 1.1a), the effects of torsional coupling on the earthquake response of a one-story structure in the inelastic range of behavior were investigated for a range of system parameters. It was shown that the inelastic response is affected by torsional coupling to generally a lesser degree than elastic response. In particular, the torsionally coupled system, after initial yielding, has a tendency to yield further primarily in translation and behave more like an inelastic single-degree-of-freedom (SDF) system, responding primarily in translation.

In another study [17], using a two-element mass-eccentric model (Figure 1.1b), it was shown that ductility demands in the resisting elements are insensitive to the normalized eccentricity and the uncoupled torsional-to-lateral frequency ratio; in contrast, both of these parameters are known to be important in elastic response. Furthermore, the ductility demand on the worst loaded frame was shown to be rarely more than thirty percent greater than the ductility demand in a similar symmetric-plan structure.

The validity of the findings in both of the above-mentioned studies were re-examined using a three-element model (Figure 1.1c) in Reference [35] which demonstrated that, in contrast to earlier work [19], torsionally-coupled systems did not respond primarily in translation when they were excited well into the inelastic range. On the contrary, significant rotational motion was shown to exist at the instant where peak ductility demand is reached. It was also shown that an increase by a factor of two in ductility demand is not uncommon for systems with large eccentricity as compared to a symmetric-plan system, which is much larger than the increase reported in Reference [17]; however, the ductility demand was not

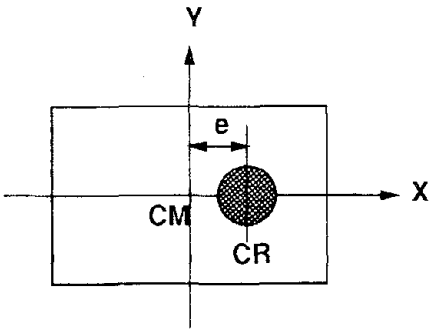

(a) One-Element System [19]

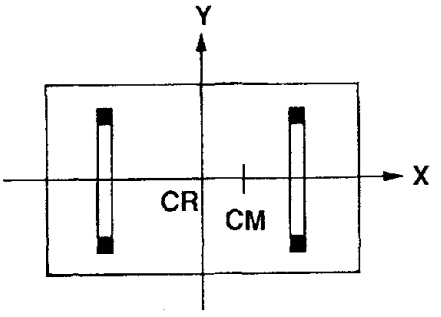

(b) Two-Element System [17]

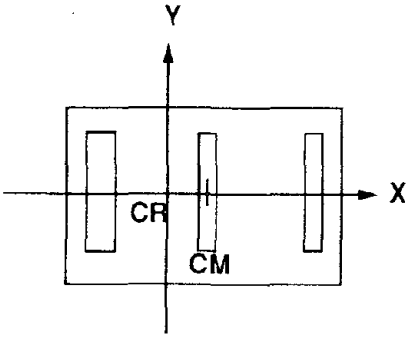

(c) Three-Element Stiffness-Eccentric System [1,35]

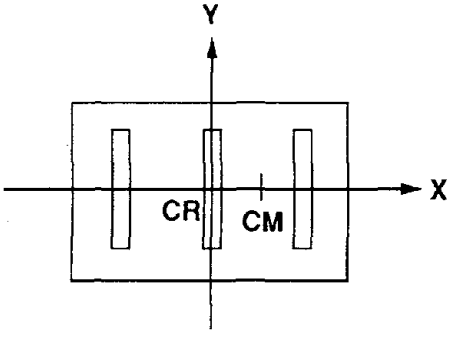

(f) Three-Element Mass-Eccentric System [8]

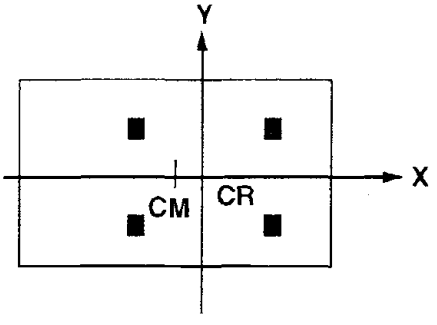

(d) Four-Element System [7]

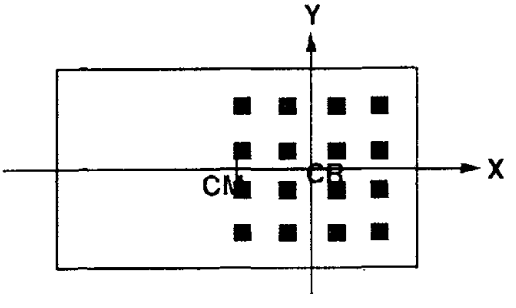

(e) Sixteen-Element System [7]

Figure 1.1 Systems Considered in Previous Investigations

sensitive to the ratio of uncoupled torsional and lateral frequencies. Using the same structural model, another study [1] confirmed these observations and concluded that the edge displacement, which is affected more by plan-asymmetry than the ductility demand, can be more sensitive to the uncoupled torsional-to-lateral frequency ratio, and that the lateral displacement at the center of mass is not sensitive to the normalized eccentricity.

The response of four- and sixteen-element mass-eccentric models (Figures 1.1d and 1.1e) demonstrated that for small eccentricities the torsionally-coupled system behaves more and more like an inelastic SDF system responding in translation after initial yielding [7]. Obviously, this investigation supports the conclusion of Reference [19] but contradicts the results of References [1,35]. Using a four-element model similar to the one shown in Figure 1.1d, a recent study [24] concluded that a marked amplification of ductility demand occurs when the uncoupled torsional and lateral frequencies are coincident. Obviously, this investigation contradicts the results of Reference [17].

Most building codes require that the lateral earthquake force at each floor level of an asymmetric-plan building be applied eccentrically relative to the center of stiffness. Some codes specify two formulas for the design eccentricity, e_d. The design force for a resisting element is computed as the larger of the two force values corresponding to the values of e_d. The resulting element design forces, when compared to their values in the corresponding symmetric-plan system, are always larger for resisting elements on the flexible side of the building but may be smaller for elements on the stiff side of buildings with large stiffness eccentricity. Such a reduction of the design forces is not permitted by several building codes. Because of this restriction, and because for each element the more unfavorable of two values of e_d is used to compute the element design forces, these as well as the total design force for an asymmetric-plan building are larger than for the corresponding symmetric-plan building. The resulting overstrength of the building has not been recognized in most earlier studies of inelastic response of asymmetric-plan systems, where the element yield forces have been assumed to be the same as in the symmetric-plan system [1,7,17,19,20,24,35]. Thus the

results of these studies may not be directly applicable to code-designed buildings.

The inelastic response of systems with plan-wise strength distribution representative of code-designed buildings was a subject of two recent investigations which reached different conclusions [30,36]. In one of these investigations [36], the strength eccentricity of code-designed systems was determined to be approximately zero even if their stiffness eccentricity is large, and the ductility demand on the resisting elements of asymmetric-plan systems was shown to be about the same as if the plan were symmetric. Another study [30] demonstrated that the largest ductility demand among all the resisting elements may not occur in flexible-side elements, although they experience the largest deformation, but in stiff-side elements; moreover, it was shown, in contrast to Reference [36], that the peak ductility demand in asymmetric-plan systems may significantly exceed that in symmetric-plan systems.

Two investigations were concerned with three-element systems with strength eccentricity much smaller than the stiffness eccentricity, a situation typical of code-designed buildings. Using stiffness-eccentric systems (Figure 1.1c), it was concluded that torsional coupling due to plan-asymmetry leads to little additional ductility demand [36], but mass-eccentric systems (Figure 1.1f) were shown to experience unusually high ductility demand [8]. In order to reduce the ductility demand, the Mexico Federal District Code was modified to impose a minimum value on the strength eccentricity [8].

It is apparent from this brief review of earlier work that different studies of the inelastic response of buildings with asymmetric plan have not always arrived at consistent conclusions applicable to code-designed buildings. The differences in the various results indicate that the conclusions of each of these investigations are not valid in general, but are restricted to the particular system and underlying modeling assumptions. Obviously there is a need for a more comprehensive investigation of the inelastic response of asymmetric-plan systems in order to arrive at consistent, generally applicable conclusions which can provide the basis for improving torsional provisions in building codes.

Aimed towards this long-term goal, the objectives of this investigation are: (a) to evaluate the effects of plan-wise distribution of stiffness and of strength on the inelastic response of systems; (b) to investigate how the response of yielding, asymmetric-plan systems is influenced by the system parameters; (c) to identify how structural response is affected by plan-asymmetry and how these effects differ between elastic and inelastic systems; and (d) to investigate how well the effects of plan-asymmetry on structural response are represented by torsional provisions in building codes.

A general procedure for the earthquake response analysis of one-story, asymmetric-plan system is presented in Chapter 3. The parameters that control the elastic response of such systems are identified. Subsequently, a limited number of additional parameters that are believed to be the most important in characterizing the inelastic response of asymmetric-plan systems are introduced.

The objective of Chapter 4 is to investigate how the inelastic response of asymmetric-plan systems is affected by the plan-wise distribution of stiffness -- as determined by the number, location, and orientation of resisting elements -- and by the plan-wise distribution of strength -- as characterized by the overstrength factor and relative values of strength and stiffness eccentricities. In particular, several systems are investigated with the objective of establishing how the response is influenced by (1) the presence of resisting elements oriented perpendicular to the direction of ground motion; (2) the relative contribution of these perpendicular resisting elements to the torsional stiffness; (3) the translational stiffness of the system along the perpendicular direction relative to the stiffness along the direction of ground motion; (4) the number of resisting elements along the direction of ground motion; (5) the overstrength factor; (6) the relative values of the strength and stiffness eccentricities; and (7) whether the asymmetry of the system is due to eccentricity in stiffness or in mass. Based on these response results, the adequacy of the system parameters, identified in Chapter 3, in characterizing the inelastic response of asymmetric-plan system is evaluated.

In Chapter 5, the effects of various system parameters -- uncoupled lateral vibration period, uncoupled torsional-to-lateral frequency ratio, stiffness eccentricity, relative values of the strength and stiffness eccentricity, and yield factor -- on the response of asymmetric-plan systems are investigated. Furthermore, the influence of yielding on the response of asymmetric-plan systems is examined to determine whether the well known relationship between the response of yielding and elastic SDF systems is also applicable to asymmetric-plan systems. Based on the results of Chapter 4, a system that is simple and yet exhibits the behavior of many asymmetric-plan buildings is selected to ensure wide applicability of results.

Chapter 6 has the objective of identifying how the structural response is affected by plan-asymmetry and how these effects differ between elastic and inelastic systems. For this purpose, the dynamic responses of an asymmetric-plan and the corresponding symmetric-plan systems are compared for a wide range of system parameters -- uncoupled lateral vibration period, uncoupled torsional-to-lateral frequency ratio, stiffness eccentricity, and yield factor. Elastic as well as inelastic systems are studied; for the latter, two values of the strength eccentricity are considered: equal to the stiffness eccentricity and zero; the latter is representative of code-designed buildings.

The main objective of Chapter 7 is to investigate the effects of plan-asymmetry on the earthquake response of code-designed systems and to determine how well these effects are represented by torsional provisions in building codes. For this purpose, the influence of the design provisions in various codes on the element design forces, strength eccentricity, and overstrength factor is investigated first. Subsequently, the deformation and ductility demands on resisting elements of asymmetric-plan systems are compared with the values if the system plan were symmetric. Based on these results, deficiencies in code provisions are identified and improvements suggested.

Finally, the conclusions of this investigation on the earthquake response of one-story, asymmetric-plan systems are presented in Chapter 8.

2. SYSTEM AND GROUND MOTIONS

2.1 One-Story System

Consider the idealized one-story building (Figure 2.1), consisting of a rigid deck of mass m. Resisting elements are frames or walls having strength and stiffness in their planes only. The force-deformation relationship of each element is assumed to be elastic-perfectly-plastic (EPP).

Let k_{ix} and k_{jy} represent the initial, elastic lateral stiffnesses of i^{th} and j^{th} resisting elements oriented along the principal axes X and Y, respectively. Then

$$K_x = \sum_i k_{ix} \quad \text{and} \quad K_y = \sum_j k_{jy} \tag{2.1}$$

are the lateral stiffnesses of the structure in the X- and Y-directions, respectively. With the origin at the center of mass (CM), let x_j and y_i define the locations of j^{th} element oriented along the Y-direction and i^{th} element oriented along the X-direction, respectively (Figure 2.1). Then

$$K_\theta = \sum_i k_{ix} y_i^2 + \sum_j k_{jy} x_j^2 \tag{2.2}$$

is the initial, elastic torsional stiffness of the structure about the CM.

The center of rigidity (CR) of the linearly elastic one-story system is the point on the deck through which application of a static horizontal force in any direction causes no rotation of the deck. For such a system the CR coincides with the center of stiffness (CS), which is the point in the plane of the deck about which the first moment of the resisting element stiffnesses becomes zero. For a system with discrete resisting elements, all of which remain linearly elastic, the coordinates of the CS, e_{sx} and e_{sy}, measured from the CM along the X- and Y-axes, respectively, are given as:

$$e_{sx} = \frac{1}{K_y} \sum_j x_j k_{jy} \quad \text{and} \quad e_{sy} = \frac{1}{K_x} \sum_i y_i k_{ix} \tag{2.3}$$

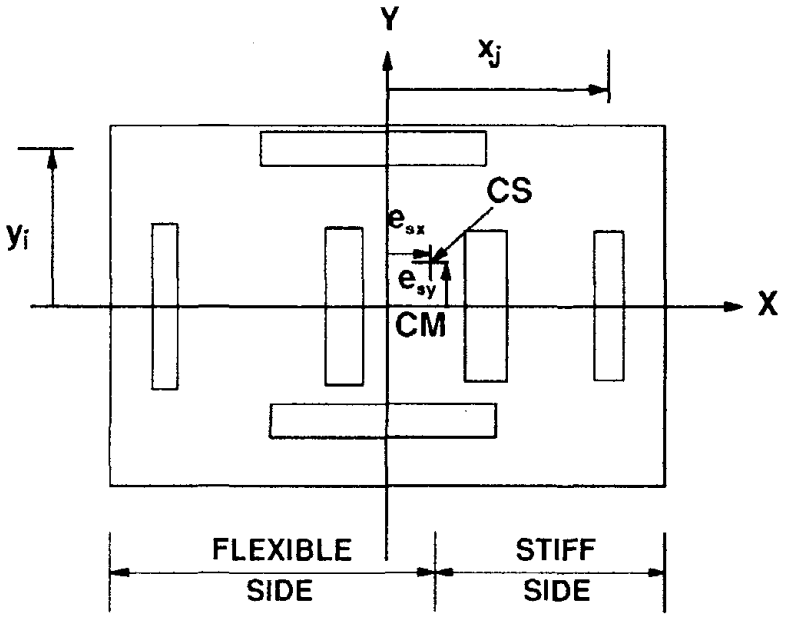

Figure 2.1 Idealized one-story system.

The stiffness eccentricity is defined as the distance between the CM and the CS. Therefore, e_{sx} and e_{sy} are the X and Y components of the stiffness eccentricity. Equation (2.3) implies that the stiffness eccentricity can be zero for many combinations of plan-geometry and stiffness distribution. In particular, e_{sx} and e_{sy} are zero if resisting elements are located symmetrically about the CM and each symmetric element pair has the same stiffness.

In the inelastic range of behavior, the location of the instantaneous CS, which varies with time, is determined by replacing the element elastic stiffnesses in equations (2.1) and (2.3) with the element tangent stiffnesses. Note that for EPP force-deformation relationship of resisting elements, the location of the CS becomes indeterminate when all the elements are yielding because the numerator and denominator in equation (2.3) become zero. However, if the elements are assumed to strain harden after reaching their yield deformation, the CS can still be located uniquely.

Let V_{ixp} and V_{jyp} represent the strength or yield force of the i^{th} and j^{th} resisting elements oriented along the X- and Y-directions, respectively. Then

$$V_{xp} = \sum_i V_{ixp} = \sum_i k_{ix} u_{yi} \quad \text{and} \quad V_{yp} = \sum_j V_{jyp} = \sum_j k_{jy} u_{yj} \tag{2.4}$$

are the fully plastic shears for the system. In equation (2.4), u_{yi} and u_{yj} are the yield deformations of the i^{th} and j^{th} elements, respectively.

The plastic center (or center of strength) is defined as the location of the resultant of yield forces of the resisting elements [31]. For a system with discrete resisting elements, the coordinates of the center of strength, e_{px} and e_{py}, measured from the CM along the X- and Y-axes, respectively, are found by taking the first moment of the yield forces and are given by:

$$e_{px} = \frac{1}{V_{yp}} \sum_j x_j V_{jyp} \quad \text{and} \quad e_{py} = \frac{1}{V_{xp}} \sum_i y_i V_{ixp} \tag{2.5}$$

The strength eccentricity is defined as the distance between the CM and the center of strength. Therefore, e_{px} and e_{py} are the X and Y components of the strength eccentricity.

The strength eccentricity of an asymmetric-plan system can be shown (from equations (2.5), (2.1) and (2.3)) to equal its stiffness eccentricity, i.e.,

$$e_{px} = e_{sx} \quad \text{and} \quad e_{py} = e_{sy} \tag{2.6}$$

if all the resisting elements oriented along each of the principal directions have same yield deformation, i.e., $u_{yi}=u_{yj}$. Furthermore, if $u_{yi}=u_{yj}=u_y$, where u_y is the yield deformation of the corresponding symmetric-plan system, the element yield forces are same in the two systems. Thus, in particular the strength and stiffness eccentricities of an asymmetric-plan system are the same if the element yield forces are the same as in the corresponding symmetric-plan system.

However, the two eccentricities need not be the same; in particular, stiffness-eccentric systems, i.e., $e_s \neq 0$, may not be eccentric in strength, i.e., $e_p=0$. Consider a system with all the resisting elements having equal yield forces, i.e., $V_{jyp}=V_{ixp}$. Then equation (2.5) reduces to

$$e_{px} = \frac{1}{n_y}\sum_j x_j \quad \text{and} \quad e_{py} = \frac{1}{n_x}\sum_i y_i \tag{2.7}$$

in which n_x and n_y are the number of resisting elements along the X- and Y- directions, respectively. Equation (2.7) implies that the center of strength is located at the centroid of element locations. For such a system, the strength eccentricity is zero if the elements are located symmetrically about the CM.

This investigation is restricted to systems with the mass, stiffness, and strength properties symmetric about the X-axis; i.e., $e_{sy}=e_{py}=0$. The translational motions of such a system in the X-direction may be considered separately as they are not coupled with the torsional motions. However, the system would undergo coupled lateral-torsional motions when subjected to ground acceleration $a_g(t)$ in the Y-direction.

2.2 Ground Motions

2.2.1 Simple Input

The first ground motion selected is a half-cycle displacement pulse, having the displacement, velocity, and acceleration histories with peak values of u_{go}, v_{go}, and a_{go}, respectively shown in Figure 2.2. The elastic response spectrum of the ground motion is shown in Figure 2.3, plotted against T/t_1 and ft_1, where T and f are the system period and frequency, respectively and t_1 is the half-duration of the ground motion. The half-cycle displacement pulse is selected because there is a close relationship between the response of systems to such a simple ground motion and actual earthquake ground motion [38], and it has the desirable property of a smooth response spectrum.

Various frequency regions of the spectrum for the half-cycle displacement pulse have been identified previously [38], and are shown in Figure 2.3, separated by points a, b, c, and d. The region to the right of point b ($ft_1<0.55$) is defined as the low-frequency region of the spectrum, the region between points b and c ($0.55 \leq ft_1 \leq 0.76$) as the medium-frequency region, and the portion to the left of point c ($ft_1>0.76$) as the high-frequency region. It is sometimes desirable to subdivide the low-frequency region at point a into an extremely-low-frequency sub-region for which peak displacements S_d are equal to or less than the maximum ground displacement u_{go} and a moderately-low-frequency sub-region for which S_d are greater than u_{go}. The high-frequency region is similarly subdivided at point d into a moderately-high-frequency sub-region for which the spectral pseudo-accelerations S_a are greater than the maximum ground acceleration a_{go}, and an extremely-high-frequency sub-region for which S_a are for all practical purposes equal to a_{go}.

The extremely-high-frequency sub-region, the medium-frequency region, and the extremely-low-frequency sub-regions may also be referred to as the acceleration-sensitive, velocity-sensitive, and displacement-sensitive regions. The moderately-high-frequency sub-region provides a transition from the acceleration-sensitive to the velocity-sensitive region

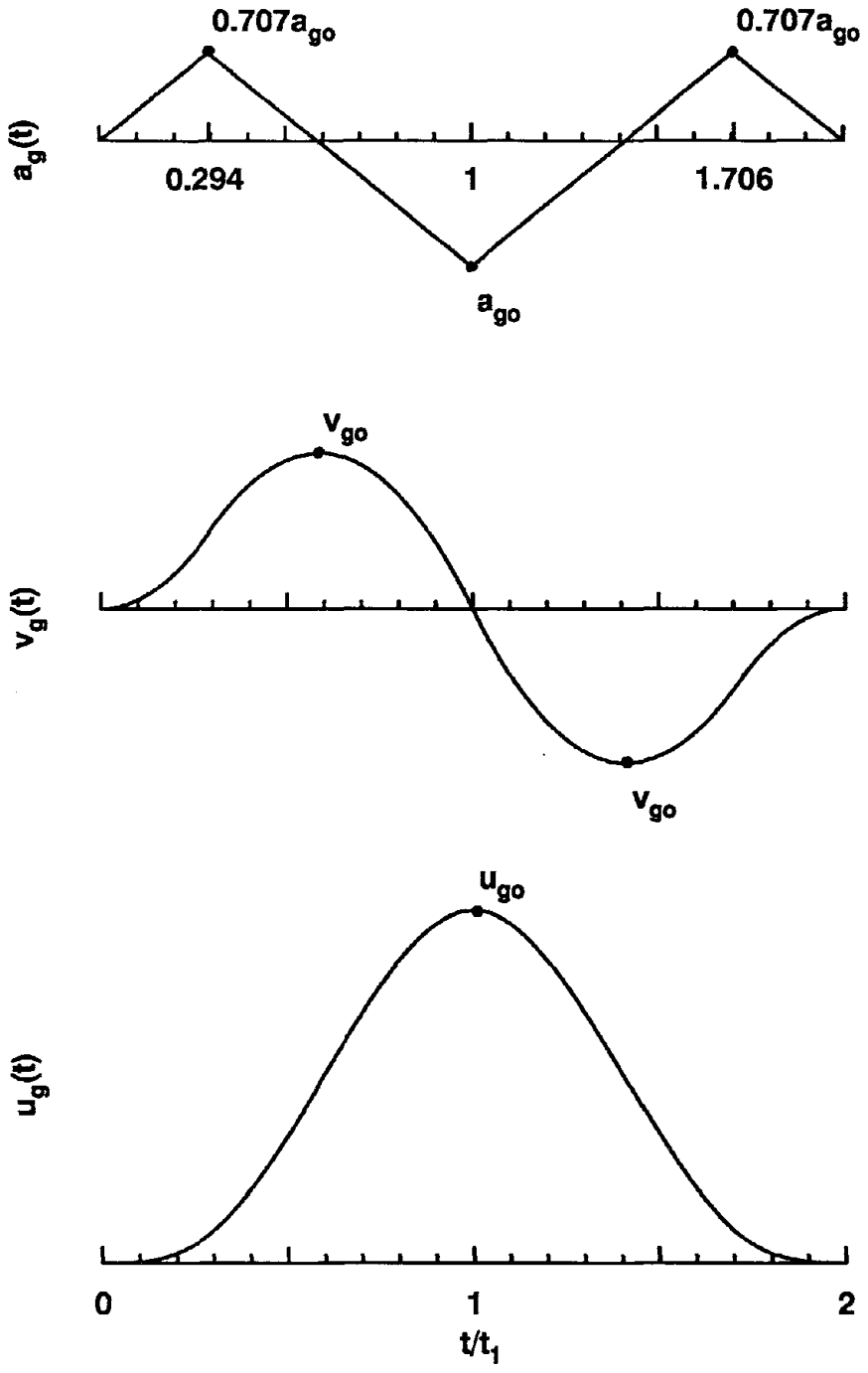

Figure 2.2 Time-histories of deformation, velocity, and acceleration for half-cycle displacement ground motion.

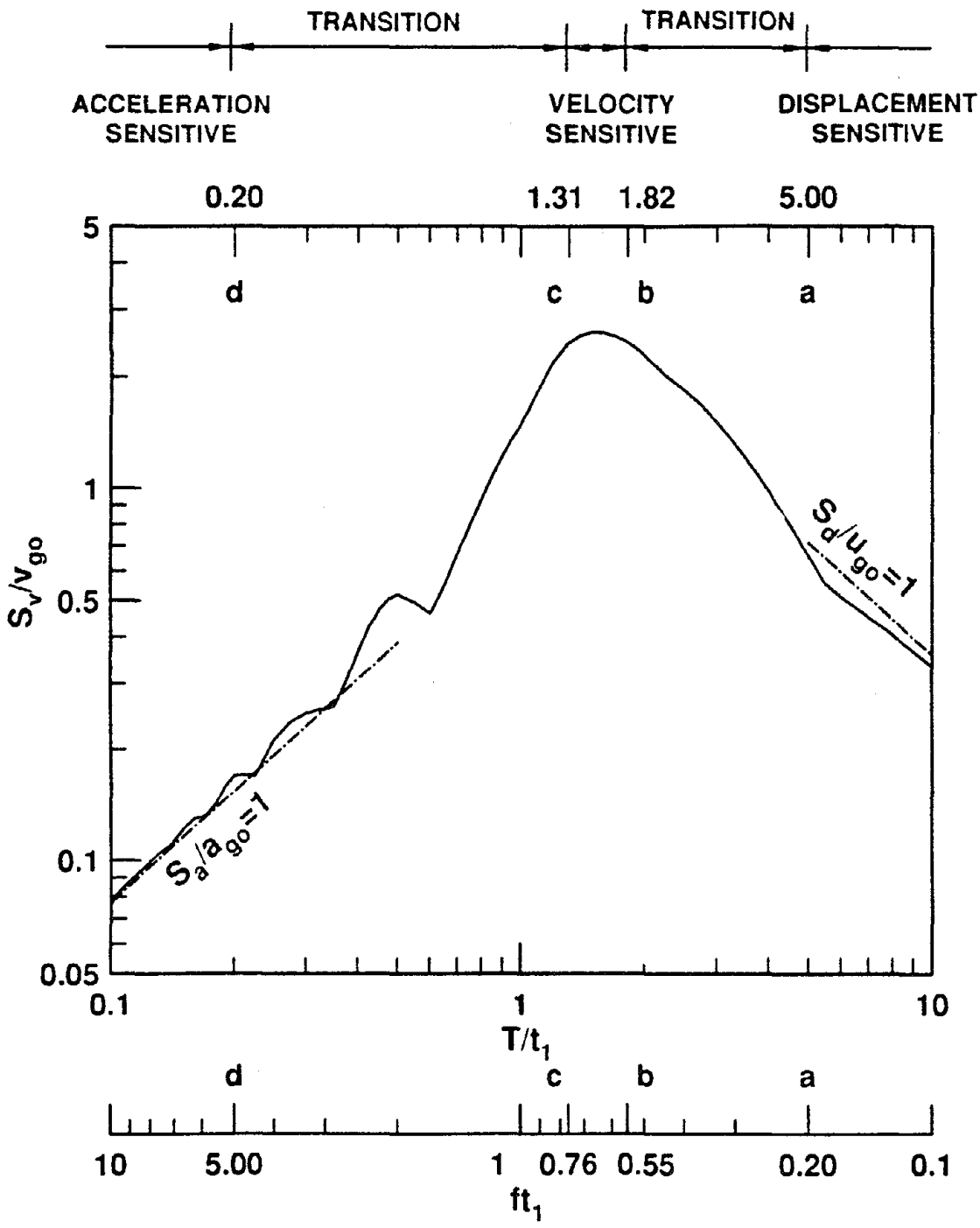

Figure 2.3 Response spectrum for half-cycle displacement ground motion with spectral regions identified.

and the moderately-low-frequency sub-region is a transition from the velocity-sensitive to the displacement-sensitive region. The observations of structural response behavior in each of these spectral regions for the simple input (Figure 2.3) generally carry over to the corresponding regions for actual earthquake ground motions [37,38].

2.2.2 El Centro Ground Motion

The second ground motion selected is the first 6.3 seconds of the S00E component of the El Centro record obtained during the Imperial Valley earthquake of May 18, 1940. The displacement, velocity, and acceleration histories of this earthquake with peak values of 8.28 inches, 14 inches/second, and 0.3125 g (g is the acceleration due to gravity), respectively are shown in Figure 2.4. The elastic response spectrum of the ground motion is shown in Figure 2.5, plotted against the system period T. Various frequency regions in the response spectrum for this excitation have also been identified previously [38] and are shown in Figure 2.5 separated by points a, b, c, and d.

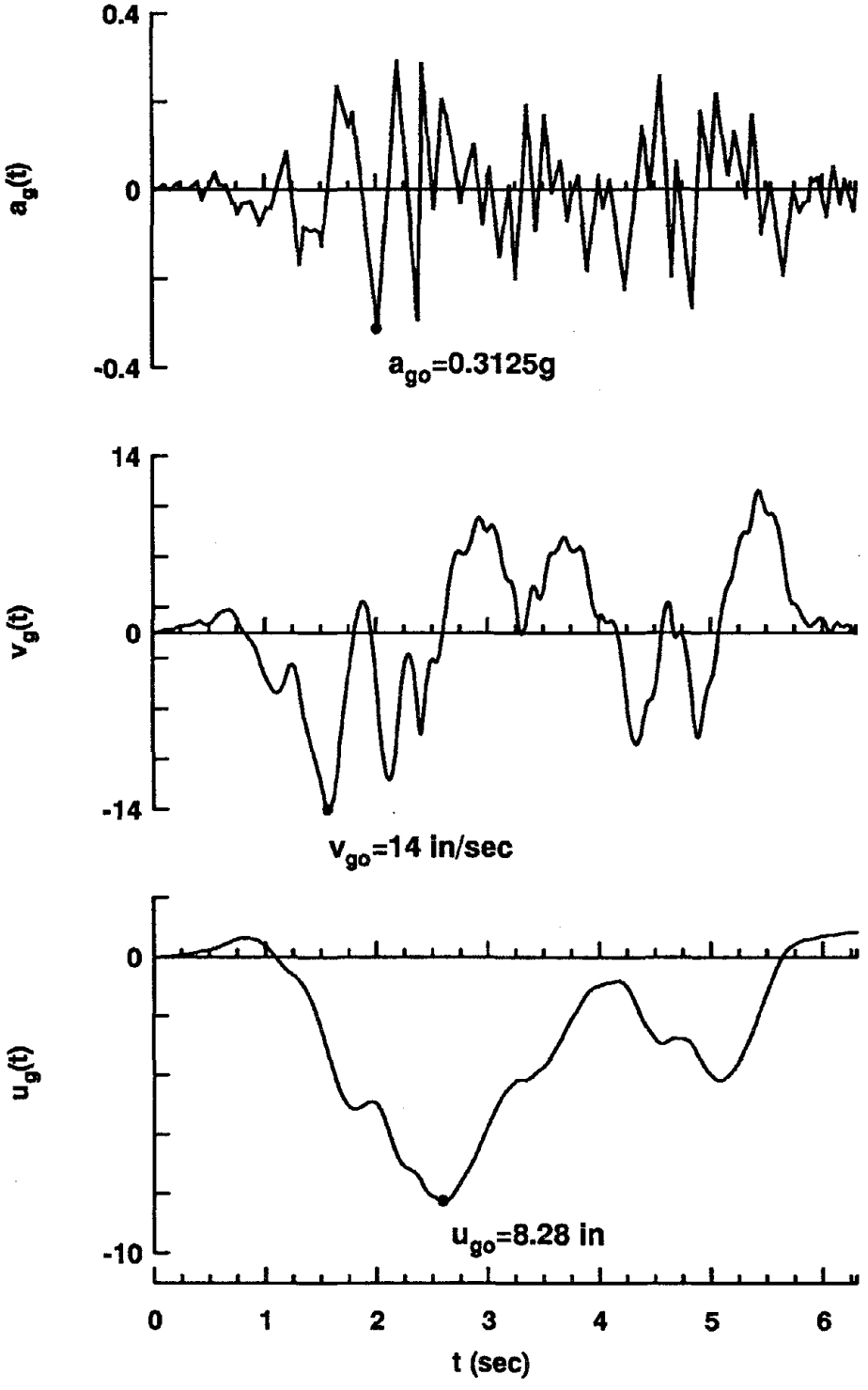

Figure 2.4 Time-histories of deformation, velocity, and acceleration for El Centro ground motion.

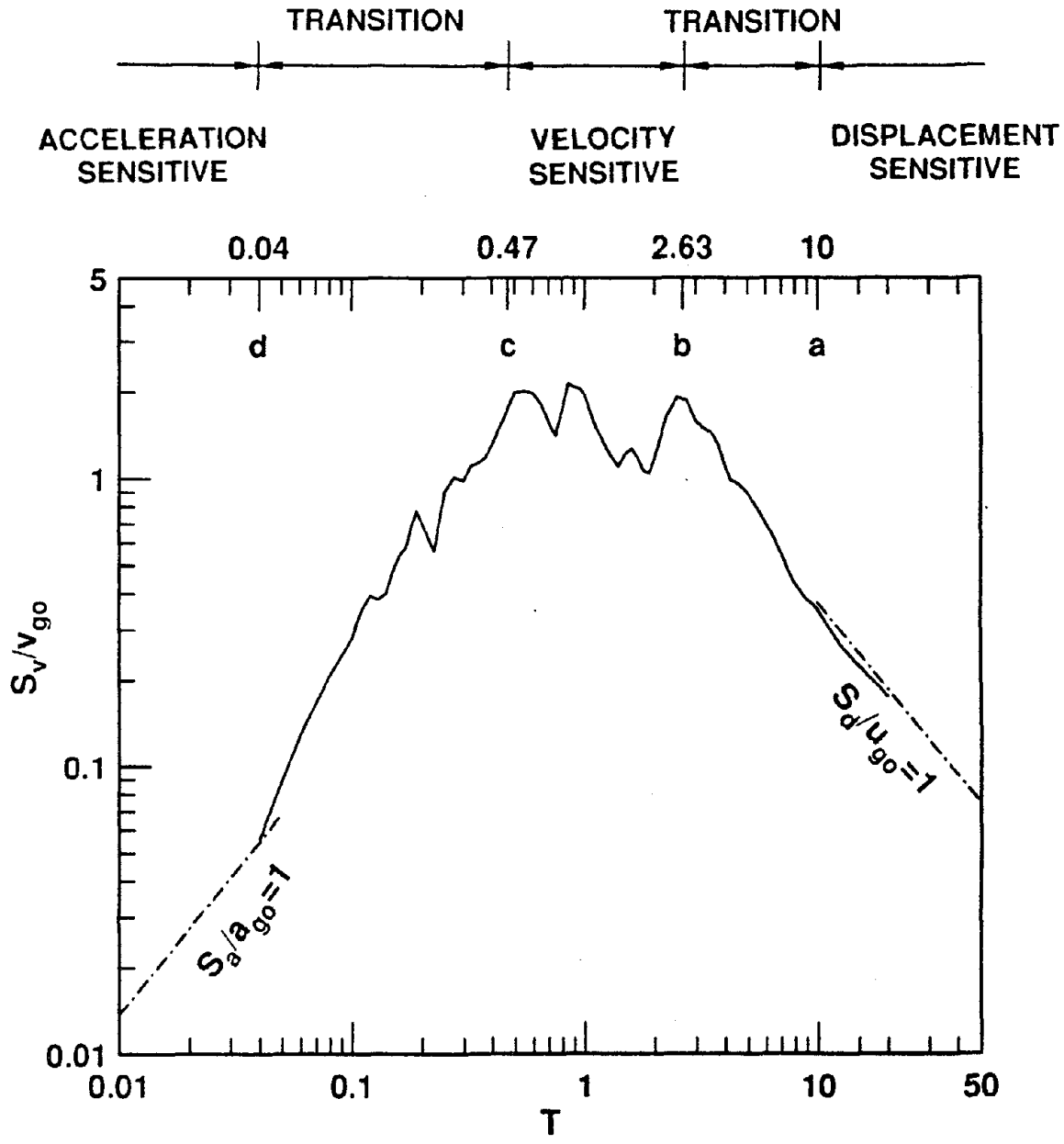

Figure 2.5 Response spectrum for El Centro ground motion with spectral regions identified.

3. EQUATIONS OF MOTION AND METHOD OF ANALYSIS

3.1 Introduction

The governing equations of motion for an undamped, one-story system, symmetric in mass, stiffness, and strength about the X-axis, subjected to the ground motion along the Y-axis are presented in this chapter. Subsequently, the parameters that are believed to be the most important in characterizing the inelastic response are identified. Finally, the numerical technique to solve the equations of motion is briefly described.

3.2 Equations of Motion

The equations of motion for an undamped, one-story system governing the lateral displacement u at the CM and torsional displacement u_θ are:

$$\begin{Bmatrix} \ddot{u}(t) \\ r\ddot{u}_\theta(t) \end{Bmatrix} + \mathbf{F}(t) = - \begin{Bmatrix} 1 \\ 0 \end{Bmatrix} a_g(t) \tag{3.1}$$

where $\mathbf{F}$ is the vector of restoring forces corresponding to the degrees of freedom $\mathbf{u}^T = \langle u, ru_\theta \rangle$.

In the linearly elastic range, equation (3.1) becomes [19,20]

$$\begin{Bmatrix} \ddot{u}(t) \\ r\ddot{u}_\theta(t) \end{Bmatrix} + \omega^2 \begin{bmatrix} 1 & e_s/r \\ e_s/r & \Omega_\theta^2 + (e_s/r)^2 \end{bmatrix} \begin{Bmatrix} u(t) \\ ru_\theta(t) \end{Bmatrix} = - \begin{Bmatrix} 1 \\ 0 \end{Bmatrix} a_g(t) \tag{3.2}$$

in which $e_s = e_{sx}$ is the stiffness eccentricity, r is the radius of gyration of the deck about the CM,

$$\Omega_\theta = \omega_\theta / \omega \tag{3.3}$$

where ω and ω_θ are the natural vibration frequencies of the corresponding symmetric-plan (or torsionally uncoupled) elastic system, a system with $e_s = 0$ but m, K_y, $K_{\theta s}$, and the element stiffnesses k_{jy} same as in the coupled system:

$$\omega = \sqrt{K_y/m} \quad \text{and} \quad \omega_\theta = \sqrt{K_{\theta s}/mr^2} \tag{3.4}$$

where $K_{\theta s} = K_\theta - e_s^2 K_y$ is the torsional stiffness of the structure about the CS. The linearly elastic response of the system is characterized by the following system parameters: ω, Ω_θ, the normalized stiffness eccentricity e_s/r, and the damping ratio ξ assumed to be same in each mode of vibration.

However, the inelastic response of the system is affected by the location, stiffness, and yield deformation of each of the resisting elements as well as their number. Thus, 3N parameters are necessary to completely define a system with N resisting elements for the purpose of characterizing its inelastic response. Obviously it is unmanageable to conduct a parametric study with 3N parameters and almost impossible to identify in a meaningful manner the influence of each parameter on the inelastic response. Most of the previous investigations have avoided this difficulty by restricting to a particular system with a specified number, location, stiffness, and yield deformation of the resisting elements. Thus, the results of these investigations are not valid in general, but are restricted to the particular system and underlying modeling assumptions. In order to develop more generally applicable results, a limited number of additional parameters that are believed to be the most important in characterizing the response are introduced. The inelastic response of various systems with identical values of these parameters is approximately the same even though the number, location, stiffness, and yield deformation of the resisting elements are not identical among the systems.

The first two of the additional parameters depend on the stiffness properties and locations of the resisting elements oriented perpendicular to the ground motion: (1) ω_x/ω, the ratio of the uncoupled translational vibration frequencies, where $\omega_x = \sqrt{K_x/m}$, the vibration frequency in X-translation (note that $\omega_x/\omega = K_x/K_y$); and (2) γ_x, the relative torsional stiffness parameter, defined as the torsional stiffness of the system arising from the resisting elements oriented perpendicular to the ground motion divided by the total torsional stiffness

of the system. For the systems considered in this investigation, which are symmetric about the X-axis, γ_x is given by:

$$\gamma_x = \frac{\sum_i k_{ix} y_i^2}{K_{\theta s}} \tag{3.5}$$

For a system without perpendicular elements, γ_x=0.

In a system with fixed values of ω, Ω_θ, and e_s/r, the additional parameters, γ_x and ω_x/ω, may or may not be independent. If the lateral load resisting elements of the system are restricted to the edges of the deck, the two parameters are inter-related and only one of them may be varied independently (Appendix A). However, the two parameters are independent if the resisting elements are not restricted to the plan edges (Appendix A). The latter type of systems are considered in this investigation, and the parameters, γ_x and ω_x/ω are varied independently.

Three additional parameters are introduced that are related to the yield strengths (or yield deformations) of resisting elements along the direction of ground motion: (1) the strength eccentricity e_p=e_{px} given by equation (2.5); (2) the overstrength factor O_s defined as the ratio of the strengths of the asymmetric-plan and symmetric-plan systems; and (3) the yield deformation u_y of the corresponding symmetric-plan system. It is convenient to define u_y through the dimensionless yield factor c as:

$$u_y = cu_o \tag{3.6}$$

where u_o is the peak deformation of the corresponding symmetric-plan (SDF) system if it were to remain elastic during the selected ground motion. The yield force then is c times the peak force in the elastic system.

Thus, the inelastic response of asymmetric-plan systems is characterized in this investigation by the relative torsional stiffness parameter, γ_x, the ratio of the uncoupled vibration frequencies, ω_x/ω, the strength eccentricity, e_p, the overstrength factor, O_s, and the yield

factor, c, in addition to all the parameters -- ω, Ω_θ, e_s/r, and ξ -- characterizing the elastic response. Since these parameters are not sufficient to uniquely define the locations, stiffnesses, and yield deformations of resisting elements of systems considered in this investigation, additional restrictions on the system properties are necessary. These restrictions are identified in Appendix B, where procedures to determine the locations and stiffnesses of resisting elements in a system characterized by the above-listed parameters are presented, and in Appendix C, where procedures to compute the yield deformations of resisting elements are developed. It will be shown in the following chapter that the inelastic response of many asymmetric-plan systems may be characterized to a useful degree of accuracy by considering only the above-listed parameters.

3.3 Method of Analysis

The response of the system to the selected ground motion is determined by solving the equations of motion (equation (3.1)) by a numerical, step-by-step integration procedure [21]. The time scale is discretized into equal intervals of no more than a small fraction (1/50th) of the lateral vibration period of the corresponding torsionally uncoupled elastic system. Within each time interval, the lateral and torsional accelerations of the deck are assumed to remain constant. For the time interval during which stiffness of any of the resisting elements changes, the tangent stiffness matrix is re-evaluated and the force unbalance created by the numerical approximation is reduced to an acceptably small value by an iterative procedure.

4. EFFECTS OF STIFFNESS AND STRENGTH DISTRIBUTION

4.1 Introduction

The effects of plan-wise distribution of stiffness -- as determined by the number, location, and orientation of resisting elements -- and of the plan-wise distribution of strength -- as characterized by the overstrength factor and relative values of strength and stiffness eccentricities -- on the inelastic response of systems are investigated in this chapter. Subsequently, the adequacy of the system parameters identified in Chapter 3 in characterizing the inelastic response is evaluated. The response results are presented for the simple excitation defined in Chapter 2.

4.2 Systems Considered

Several systems are investigated with the objective of establishing how the response is influenced by (1) the presence of resisting elements oriented perpendicular to the direction of ground motion (Figure 4.1); (2) the relative contribution of these perpendicular resisting elements to the torsional stiffness; (3) the translational stiffness of the system along the perpendicular direction relative to the stiffness along the direction of ground motion; (4) the number of resisting elements along the direction of ground motion (Figure 4.2); (5) the overstrength typical of code-designed buildings; (6) the property typical of code-designed buildings that strength eccentricity is much smaller than stiffness eccentricity; and (7) whether the asymmetry of the system is due to eccentricity in stiffness or in mass (Figure 4.3). The stiffness and location of resisting elements in the systems of Figures 4.1 to 4.3 are determined by procedure presented in Appendix B and their yield deformations by procedures presented in Appendix C. Also examined are some of the systems considered in earlier studies, described in Chapter 1, in order to resolve any differences in conclusions.

Response results are presented for a wide range of values of the uncoupled lateral vibration period $T=2\pi/\omega$. Since in the linear elastic range of behavior the torsional response is most prominent for close uncoupled torsional and lateral frequencies, Ω_0 is chosen to be unity. The selected stiffness eccentricity ratio, $e_s/r=0.5$, represents significant

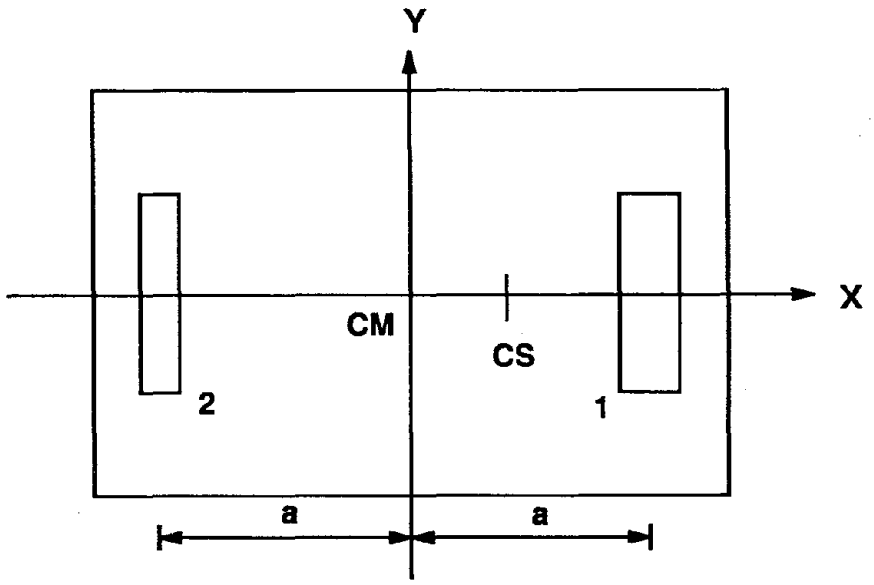

(a) System without perpendicular resisting elements

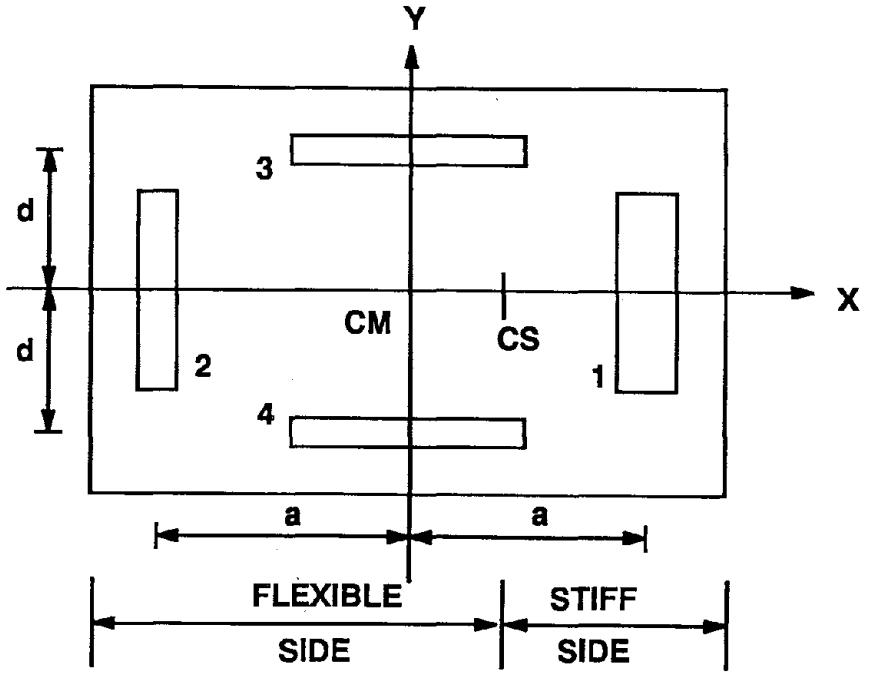

(b) System with perpendicular resisting elements

Figure 4.1 Systems with and without resisting elements perpendicular to ground motion.

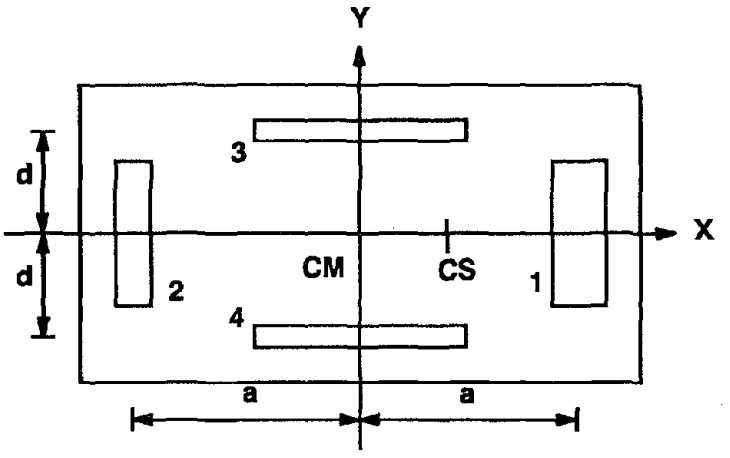

(a) Two elements along Y-direction

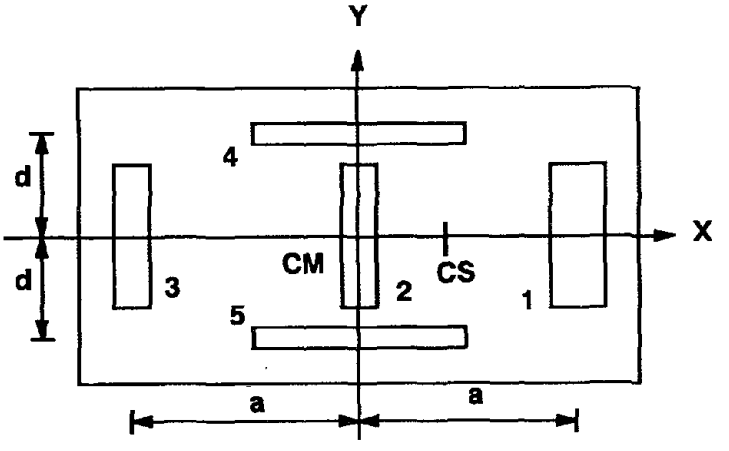

(b) Three elements along Y-direction

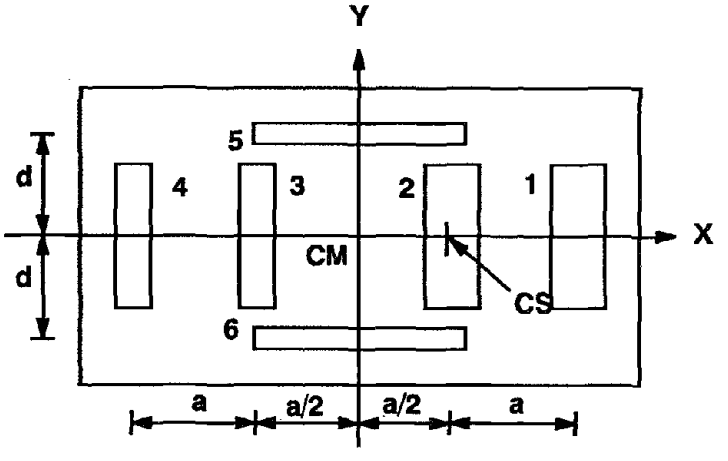

(c) Four elements along Y-direction

Figure 4.2 Systems with two, three, and four resisting elements along the direction of ground motion (Y-direction).

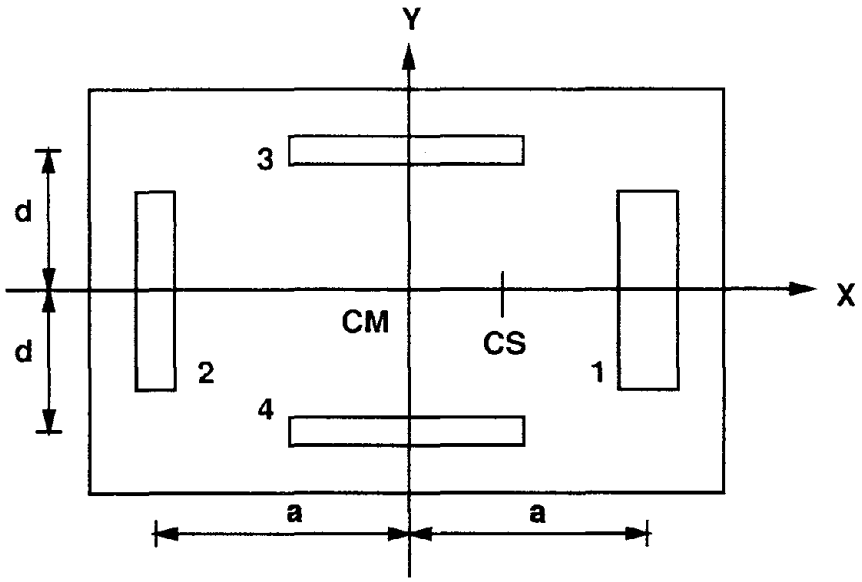

(a) Stiffness-eccentric system

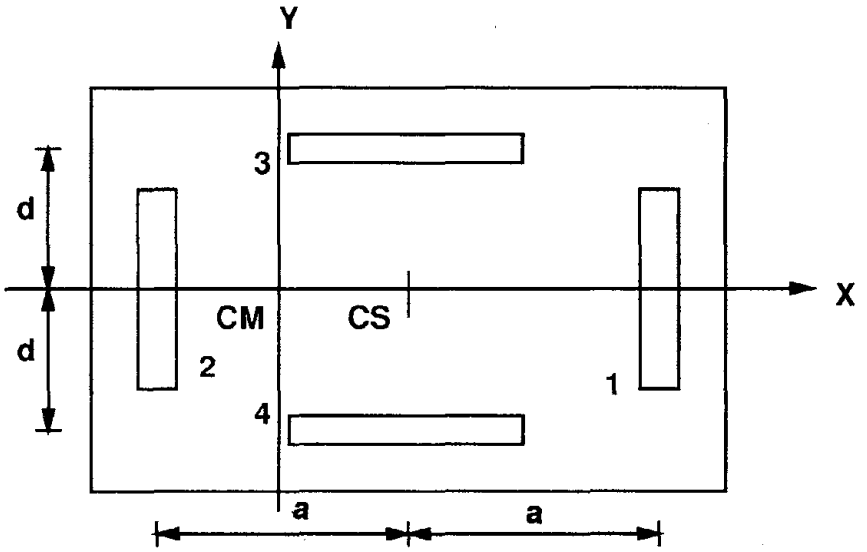

(b) Mass-eccentric system

Figure 4.3 Systems with eccentricity due to uneven distribution of stiffness and of mass.

eccentricity between centers of mass and stiffness; for a rectangular building plan, it is equivalent to an eccentricity of approximately 30% of the dimension perpendicular to the direction of ground motion. Four values are chosen for the strength eccentricity: $e_p=e_s$, $e_s/2$, $e_s/4$, and zero; the first implies, for example, a system with element yield forces same as for the corresponding symmetric-plan system, and the last represents a system with strength properties symmetric about the CM. The intermediate values of $e_p=e_s/2$ and $e_s/4$ are included to cover the range of e_p values representative of systems designed according to various building codes. Four values are chosen for the overstrength factor: $O_s=1$, 1.1, 1.2, and 1.3. The first represents an asymmetric-plan system with combined design strength of all resisting elements equal to the value for the corresponding symmetric-plan system. The latter three cover the range of overstrength values for code-designed buildings. Since the strength of code-designed systems is a small fraction of that required for the system to remain elastic, the yield factor c is chosen to be 0.25. The damping ratio ξ is assigned a value of 5% which is reasonable for many buildings.

Figure 4.4 shows the yield deformations of the outermost elements on the flexible and stiff sides of the system, determined by procedures presented in Appendix C. It is apparent that for asymmetric-plan systems with no overstrength ($O_s=1$) and $e_p=e_s$, the yield deformations of all the resisting elements are identical and equal to the yield deformation, u_y, of the symmetric-plan system. However, for asymmetric-plan systems with $e_p<e_s$, the yield deformations of resisting elements differ from each other and from u_y. The yield deformations of flexible-side elements are higher whereas those of the stiff-side elements are lower (Figure 4.4) compared to u_y. The element yield forces and hence yield deformations obviously increase with increasing values of O_s (Figure 4.4c).

The relative increase or decrease in yield deformations of these elements depends on the number, location, and orientation of resisting elements in plan. The yield deformation of a flexible-side element is increased more, and that of a stiff-side element is decreased more in systems with perpendicular elements compared to systems with elements only along

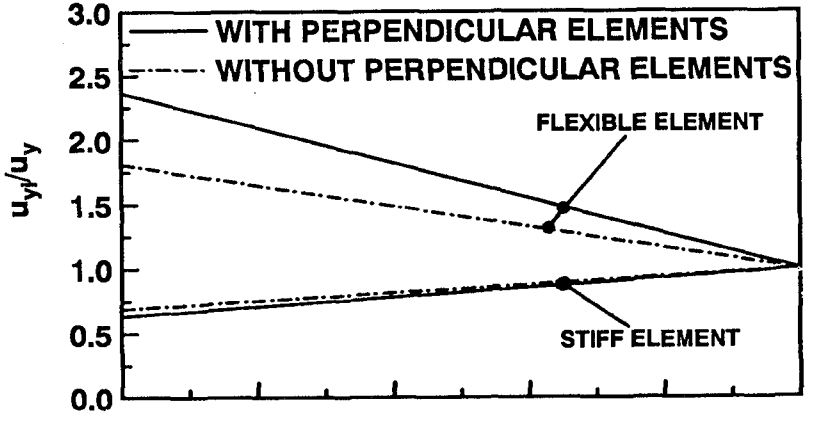

(a) Systems with and without perpendicular resisting elements

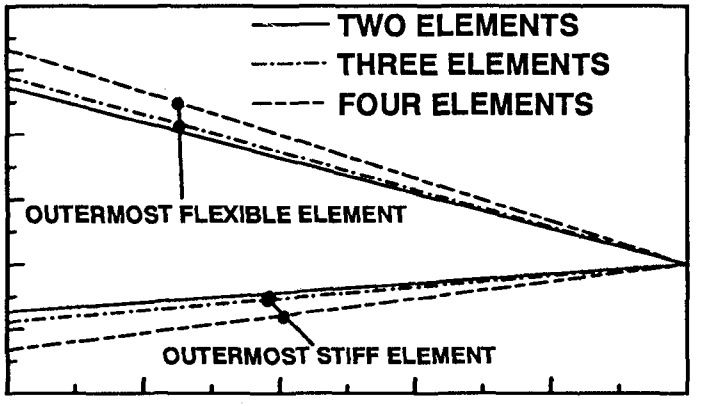

(b) Systems with two, three, and four resisting elements along Y-direction

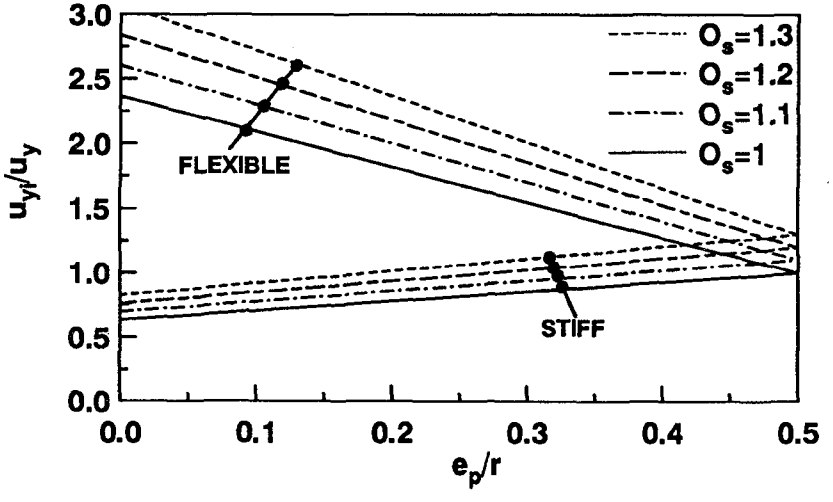

(c) Systems with O_s=1, 1.1, 1.2, and 1.3

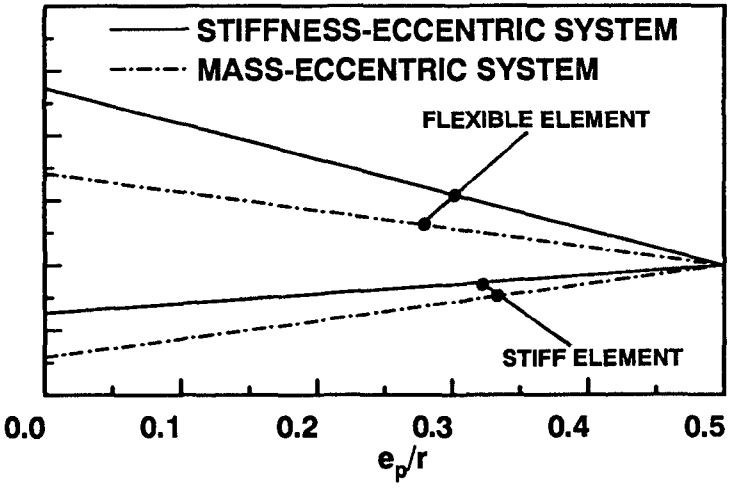

(d) Stiffness- and mass-eccentric systems

Figure 4.4 Yield deformations of outermost flexible and stiff element of systems with e_s/r=0.5, and Ω_θ=1.

the ground motion direction (Figure 4.4a); also in systems with larger number of resisting elements compared to systems with fewer elements (Figure 4.4b). The yield deformation of a flexible-side element in a stiffness-eccentric system is increased more and that of the stiff-side element is decreased less compared to the corresponding elements of a mass-eccentric system (Figure 4.4d).

4.3 Response Characteristics

Figure 4.5 shows response histories for the asymmetric-plan system of Figure 4.1b and its corresponding symmetric-plan system, each analyzed for two different assumptions of force-deformation behavior: linearly elastic and inelastic. Whereas symmetric-plan systems respond only in translation, asymmetric-plan systems undergo translational as well as torsional motions. This torsional-coupling generally has the effect of reducing lateral deformations compared to the symmetric-plan system, an observation made many times before [7,20]. The torsional component of response [7] causes larger deformations in elements located on flexible side of the CS and smaller deformations in those located on the stiff side, compared to deformations of elements in a symmetric-plan system (Figure 4.5c).

It is also apparent that whereas, elastic systems oscillate about the initial equilibrium position, the response of inelastic systems is characterized by increments in the plastic part of the deformation, each causing a shift in the equilibrium position about which the system oscillates until the next increment occurs. This characteristic of inelastic systems has been identified earlier for symmetric-plan, SDF systems [37]. As is well known, the ductility demand for SDF systems with same c generally increases for decreasing values of T [37] and, as will be seen later, the same trend holds for asymmetric-plan systems.

The responses of the inelastic system are replotted in Figure 4.6, together with the history of yielding in the various resisting elements. Elements oriented perpendicular to the ground motion yield, unload, or re-yield simultaneously; when the element on one side of the CS experiences positive yielding, the other element undergoes negative yielding, and vice versa. On the other hand, elements oriented along the ground motion direction yield,

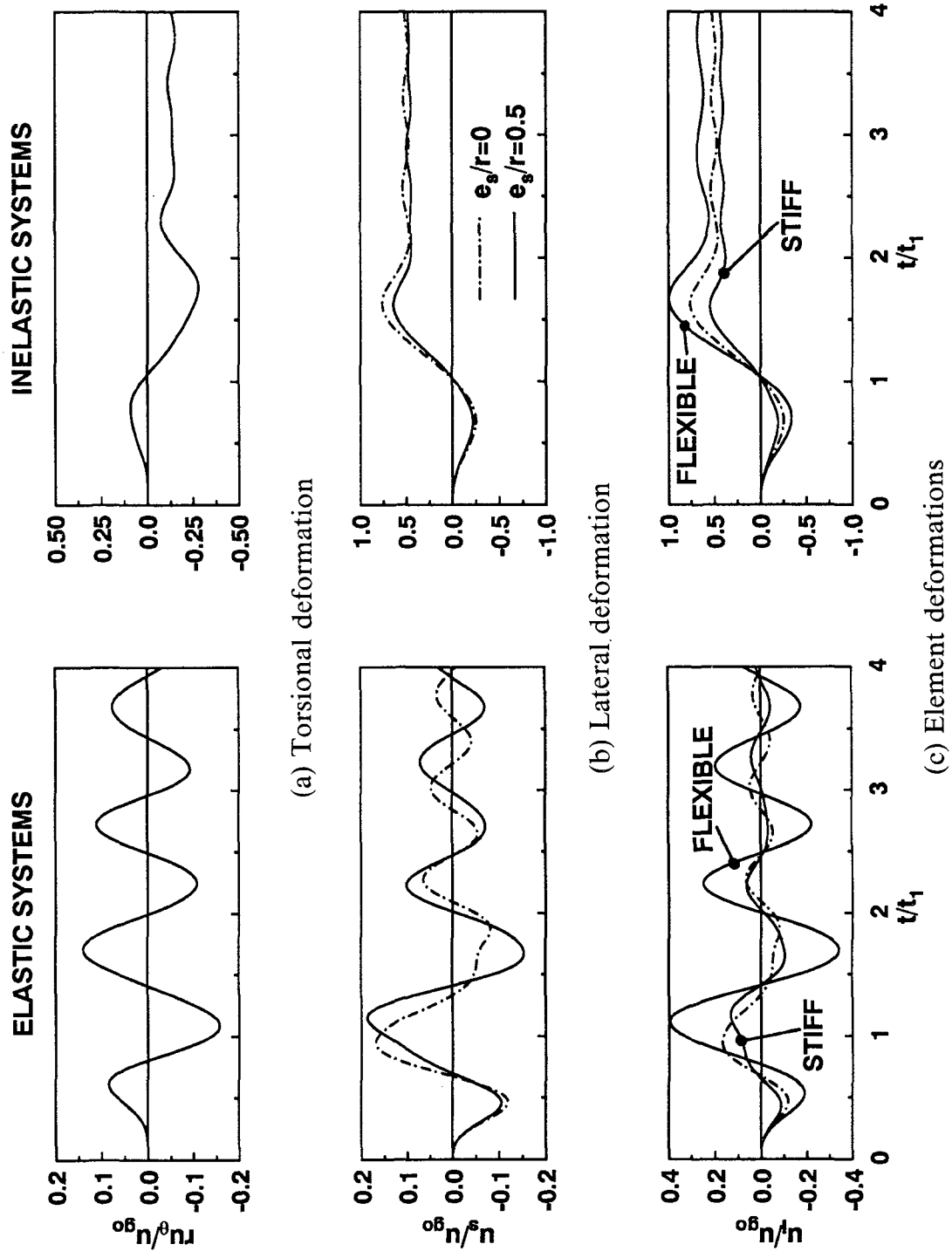

(a) Torsional deformation

(b) Lateral deformation

(c) Element deformations

Figure 4.5 Response histories of elastic and inelastic (c=0.25, $e_p=e_s$, and O_s=1) systems due to simple input; T/t_1=0.75, e_s/r=0.5, Ω_θ=1, γ_x=0.5, ω_x/ω=1, and ξ=5%.

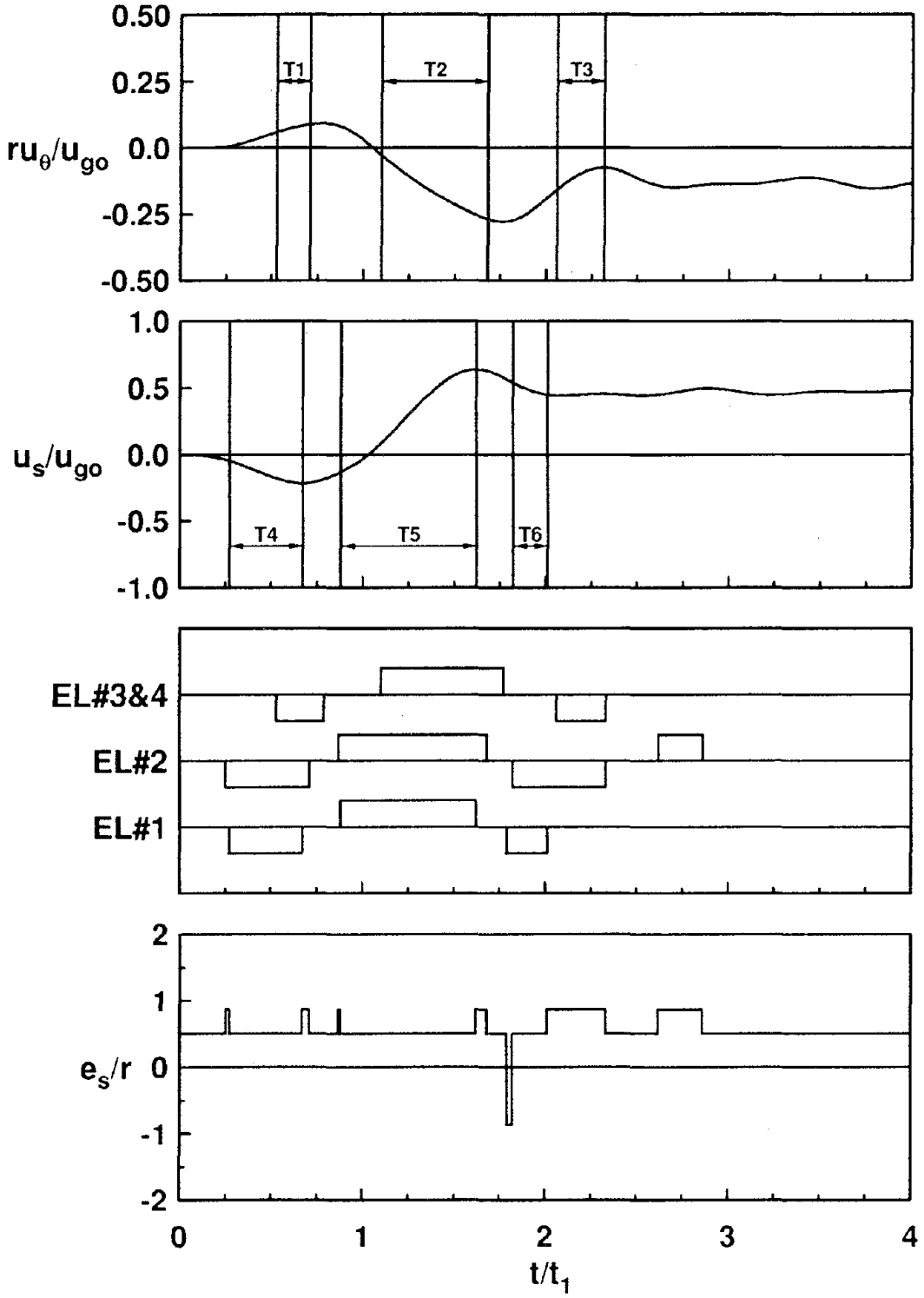

Figure 4.6 Response histories of the four-element system due to simple input; T/t_1=0.75, e_s/r=0.5, Ω_θ=1.0, γ_x=0.5, ω_x/ω=1, c=0.25, e_p=e_s, O_s=1, and ξ=5%.

unload, or re-yield with a time lag. The system has no torsional stiffness about the instantaneous CS during the time durations when all elements oriented perpendicular to the ground motion yield together with all, or all but one, of the elements oriented along the ground motion direction. Such time durations are identified as T1, T2, and T3. The lateral stiffness of the system is zero during the time durations when all the elements oriented along the ground motion direction yield; and these durations are identified as T4, T5, and T6. The system undergoes significant plastic torsional deformation during the time durations when the torsional stiffness is zero, especially during T2 which is the longest of all these durations. Similarly, the system experiences significant plastic lateral deformation during the time durations when the lateral stiffness is zero, especially T5. As a result of these plastic deformations, the system has a tendency to undergo larger total deformations. These observations made from Figure 4.6 are typical of short-period systems in which significant inelastic action occurs.

In a yielding system the location of the CS varies with time. In the four-element system of Figure 4.1b, the CS abruptly shifts from its initial position (e_s/r=0.5) to the location of element 1 when element 2 is yielding and to the location of element 2 when element 1 is yielding (Figure 4.6). For systems with more than two resisting elements in the direction of ground motion (Figure 4.2c), yielding of one element has smaller effect and the stiffness eccentricity changes more gradually (Figure 4.7). Because the one-element system of Figure 1.1a, described in Chapter 1, does not permit migration of the CS, it may not be able to accurately predict the inelastic response of buildings with lateral load resisting system consisting of several elements, especially if the system undergoes significant yielding.

The ductility demands in all the resisting elements oriented along the direction of ground motion are not the same because of torsional response. As shown for the four-element system (Figure 4.1b), the higher ductility demand occurs in the stiff-side element (μ_1) for systems with e_p=0 but generally in the flexible-side element (μ_2) for systems with e_p=e_s; in the latter case, for some T/t_1 values the ductility demand in the stiff-side element

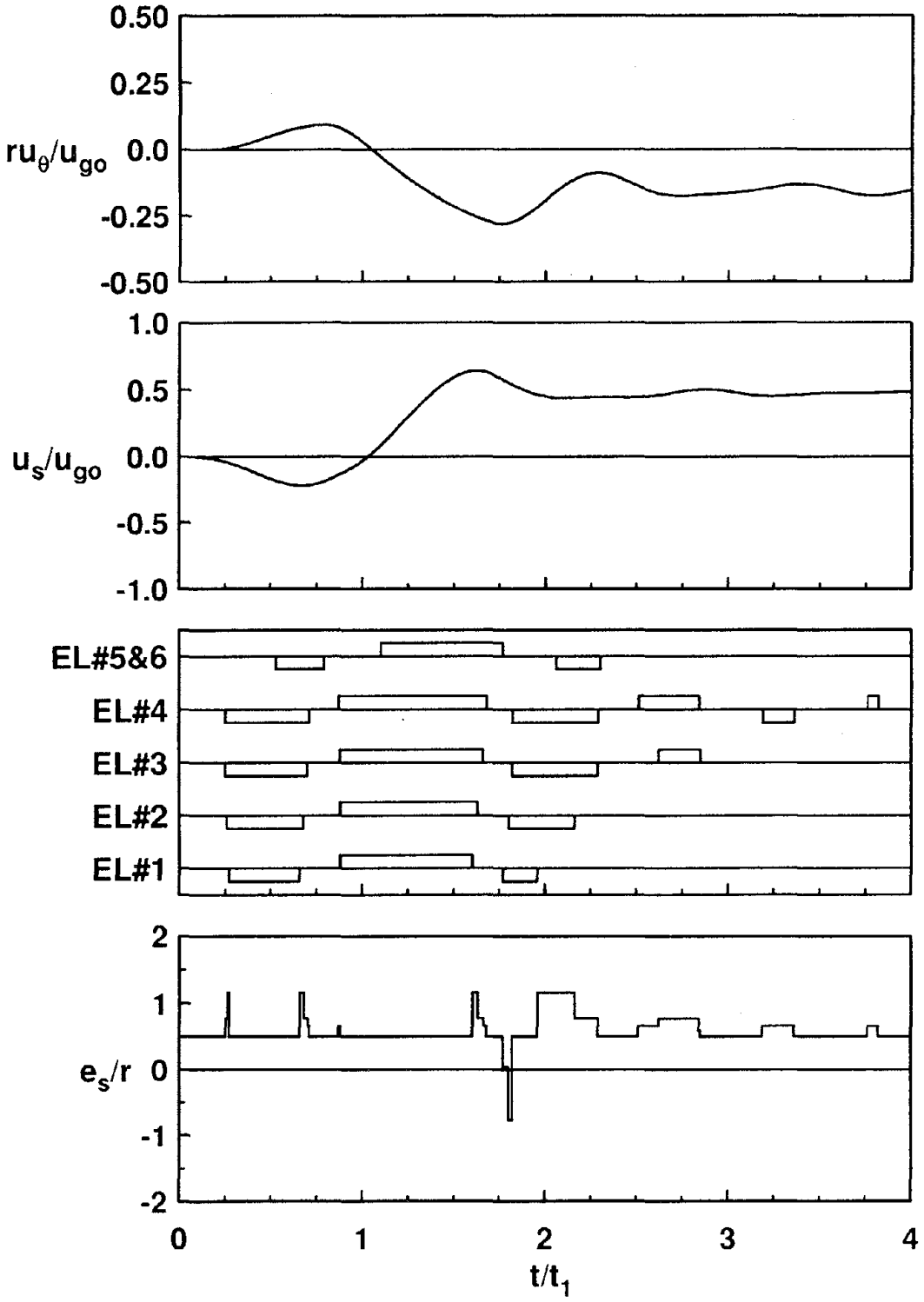

Figure 4.7 Response histories of the six-element system due to simple input; T/t_1=0.75, e_s/r=0.5, Ω_θ=1.0, γ_x=0.5, ω_x/ω=1, c=0.25, e_p=e_s, O_s=1, and ξ=5%.

may be higher (Table 4.1 and Figure 4.8). This is primarily due to the differences in the yield deformations of resisting elements in the two types of systems. In systems with $e_p=e_s$, the higher deformation generally occurs in the flexible-side element [36], all the resisting elements have identical yield deformation, and therefore the higher ductility demand also occurs in this element. On the other hand, in systems with $e_p=0$, the yield deformation of the stiff-side element is much lower than that of the flexible-side element (Figure 4.4), which results in the former element generally experiencing higher ductility demand even if the larger deformation occurs in the latter element.

4.4 Influence of Torsional Stiffness Distribution

Idealized systems considered in this investigation include: (1) systems with torsional stiffness provided only by resisting elements oriented along the direction of ground motion (Figure 4.1a), and (2) systems with torsional stiffness provided by elements oriented along both the principal directions (Figure 4.1b). In the system of Figure 4.1b, resisting elements oriented along the two principal direction are selected to contribute equally to the torsional stiffness of the system, i.e., $\gamma_x=0.5$; and the translational stiffness along the two principal directions is identical, i.e., $\omega_x/\omega=1$. But for this difference, the properties of the two systems are taken to be same in comparing their responses. In particular, the uncoupled lateral vibration period T, the normalized stiffness eccentricity e_s/r, and the uncoupled torsional-to-lateral frequency ratio Ω_θ are identical. Note that in order to keep the same value of Ω_θ, the resisting elements need to located farther from the CS in the first system compared to the second. Moreover, the yield factor c, the overstrength factor O_s, and the strength eccentricity e_p are the same in the two systems. Thus, the elastic response at the CS of the two systems is identical, and the differences in the inelastic response result from differences in the torsional stiffness distribution.

Figure 4.9 shows time-histories of the torsional deformations and element yield patterns of systems with and without resisting elements perpendicular to the direction of ground motion. It is apparent that the torsional stiffness in the system without

Table 4.1 Ductility demand in resisting elements of four-element system due to simple input; $e_s/r=0.5$, $\Omega_\theta=1$, $\gamma_x=0.5$, $\omega_x/\omega=1$, $c=0.25$, $O_s=1$, and $\xi=5\%$.

T/t_1	$e_p=e_s$		$e_p=0$	
	μ_1	μ_2	μ_1	μ_2
.1	315.532	**421.647**	**564.808**	151.151
0.15	201.226	**245.352**	**351.375**	94.1092
0.2	135.353	**161.457**	**233.813**	62.4743
0.25	101.123	**126.678**	**178.544**	48.0487
0.3	81.3332	**102.032**	**144.334**	38.6379
0.35	75.4044	**98.7459**	**136.169**	36.1259
0.4	48.6423	**63.299**	**87.0761**	23.454
0.45	33.3241	**45.7615**	**61.1287**	16.7553
0.5	28.281	**41.4251**	**53.9012**	14.8673
0.55	29.0679	**43.6203**	**56.6972**	15.4781
0.6	29.7591	**44.794**	**58.7235**	15.8181
0.65	23.2447	**36.5327**	**47.8726**	12.7011
0.7	17.378	**29.1873**	**38.3264**	9.94042
0.75	13.07	**23.8034**	**31.3989**	7.97841
0.8	9.84748	**19.7515**	**26.1234**	6.58318
0.85	7.44507	**16.6826**	**22.0263**	5.60371
0.9	5.76104	**14.444**	**18.9062**	4.94131
0.95	4.63778	**12.8295**	**16.5128**	4.48745
1	3.91341	**11.6439**	**14.64**	4.1631
1.5	2.80418	**5.58387**	**5.43897**	2.18273
2	3.29834	**4.41056**	**5.24111**	1.95558
2.5	3.25403	**3.44748**	**5.17473**	1.851
3	**2.94291**	2.6823	**4.66672**	1.58764
3.5	2.61571	**2.79212**	**4.01823**	1.3419
4	2.71902	**3.15727**	**3.86775**	1.1534
4.5	3.15932	**3.55135**	**4.50696**	1.30726
5	3.59734	**3.94785**	**5.18025**	1.47422
5.5	4.02676	**4.34531**	**5.51303**	1.55902
6	4.07654	**4.35413**	**5.84706**	1.64358
6.5	4.06446	**4.3079**	**6.5063**	1.81211
7	4.05294	**4.26898**	**6.56035**	1.81977
7.5	4.04345	**4.23662**	**6.52181**	1.80351
8	4.03761	**4.21044**	**6.4915**	1.7896
8.5	4.03315	**4.18898**	**6.46604**	1.77796
9	4.02968	**4.17108**	**6.44606**	1.76854
9.5	4.02563	**4.15472**	**6.43004**	1.7608
10	4.02182	**4.14027**	**6.41708**	1.75435

Note: Bold-faced numbers are the maximum ductility demand in the system.

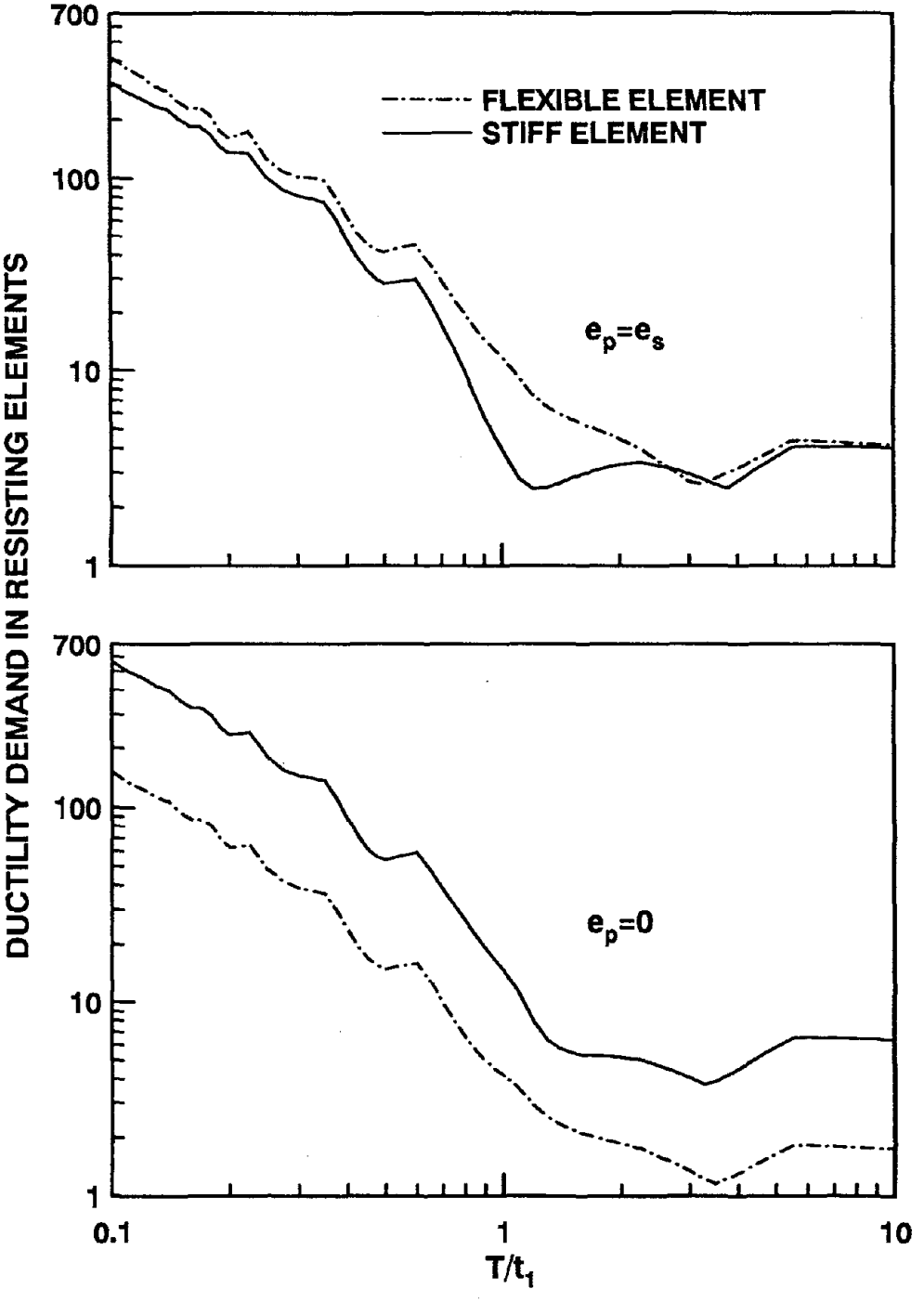

Figure 4.8 Ductility demand in resisting elements of four-element system due to simple input; $e_s/r=0.5$, $\Omega_\theta=1.0$, $\gamma_x=0.5$, $\omega_x/\omega=1$, $c=0.25$, $O_s=1$, and $\xi=5\%$.

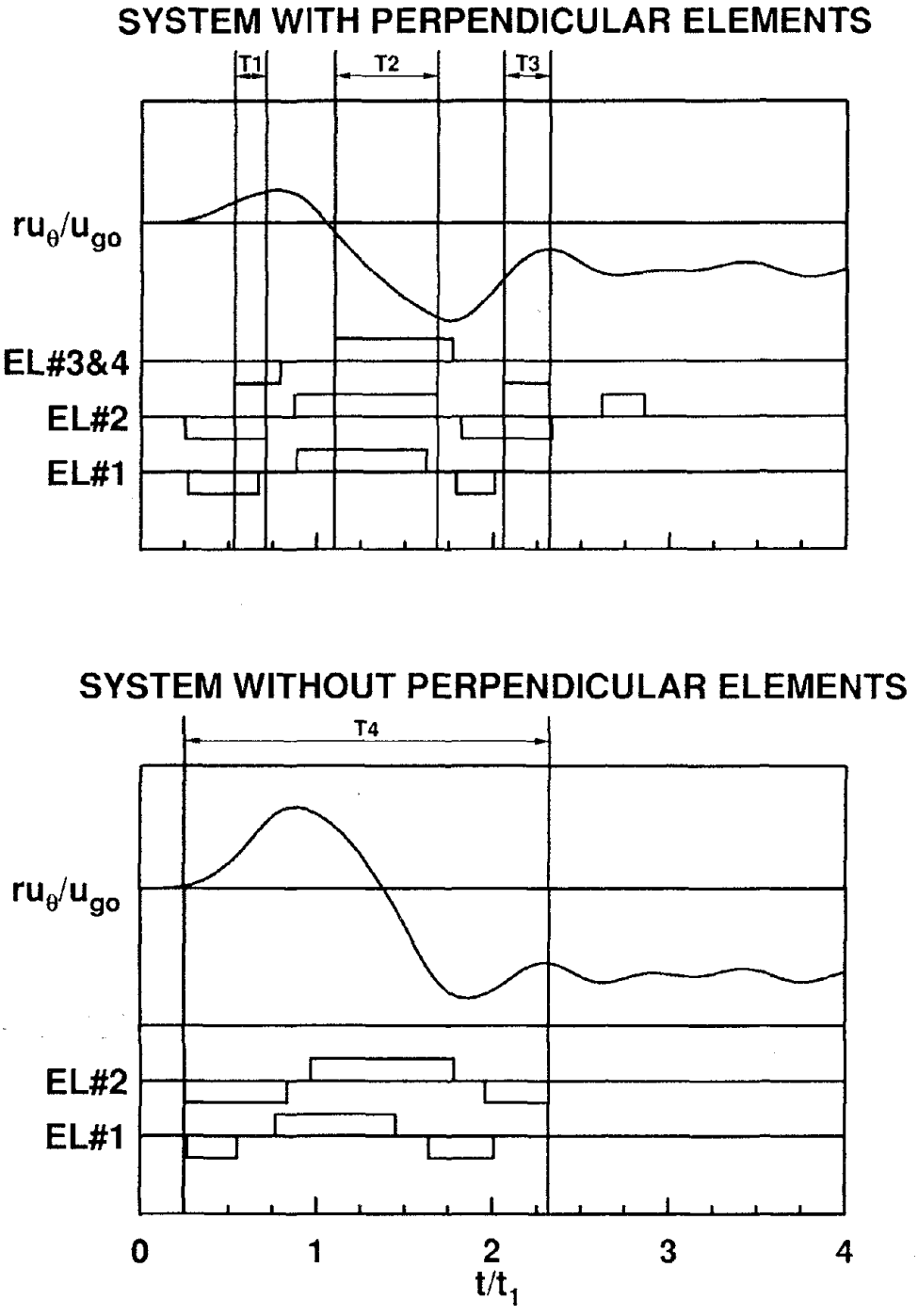

Figure 4.9 Torsional deformations and element yielding patterns of systems with and without perpendicular resisting elements due to simple input; T/t_1=0.75, e_s/r=0.5, Ω_θ=1.0, γ_x=0.5, ω_x/ω=1, c=0.25, e_p=e_s, O_s=1, and ξ=5%. T1, T2, and T3 identify time durations when torsional stiffness is zero and T4 identifies time duration when lateral stiffness is zero.

perpendicular elements becomes zero for longer durations of time compared to the system with perpendicular elements, resulting in larger torsional deformations in the first case.

The peak values of the responses of the two systems are presented as a function of period ratio T/t_1 for two values of e_p and for fixed values of Ω_θ, e_s/r, c, O_s, and ξ in Figures 4.10 and 4.11. Such response spectra are presented for: the normalized lateral and torsional displacements at the CS, u_s/u_{go} and ru_θ/u_{go}; the normalized element deformations, u_i/u_{go}; and the maximum ductility demand in the system $\mu_{\max}$. The peak responses of short-period, acceleration-sensitive systems are influenced significantly by the contribution to the torsional stiffness from the resisting elements perpendicular to the direction of ground motion. If such elements do not exist, the effects of torsional coupling are larger, leading to greater increase in torsional response and greater decrease in the lateral response. The torsional response is affected more than the lateral response. Thus, in the system without perpendicular elements, the flexible-side element experiences larger deformations and the stiff-side element undergoes smaller deformations compared to the system with perpendicular elements.

While these observations are valid for systems with equal strength and stiffness eccentricities (e_p=e_s) as well as 'strength-symmetric' systems (e_p=0), the differences in these two systems influence the largest ductility demand among all elements. For systems with e_p=e_s, the largest ductility demand generally occurs in the flexible-side element (Figure 4.8), which is smaller in systems with perpendicular elements because this element experiences smaller deformations. On the other hand, for systems with e_p=0, the largest ductility demand generally occurs in the stiff-side element (Figure 4.8), which is smaller in systems without perpendicular elements because this element experiences smaller deformations and its yield deformation is higher.

It is apparent from the preceding results that the torsional deformation, element deformations, and maximum ductility demand for systems in the short-period, acceleration-sensitive region of the spectrum are significantly affected by the contribution to the torsional stiffness from the resisting elements perpendicular to the direction of ground motion. These

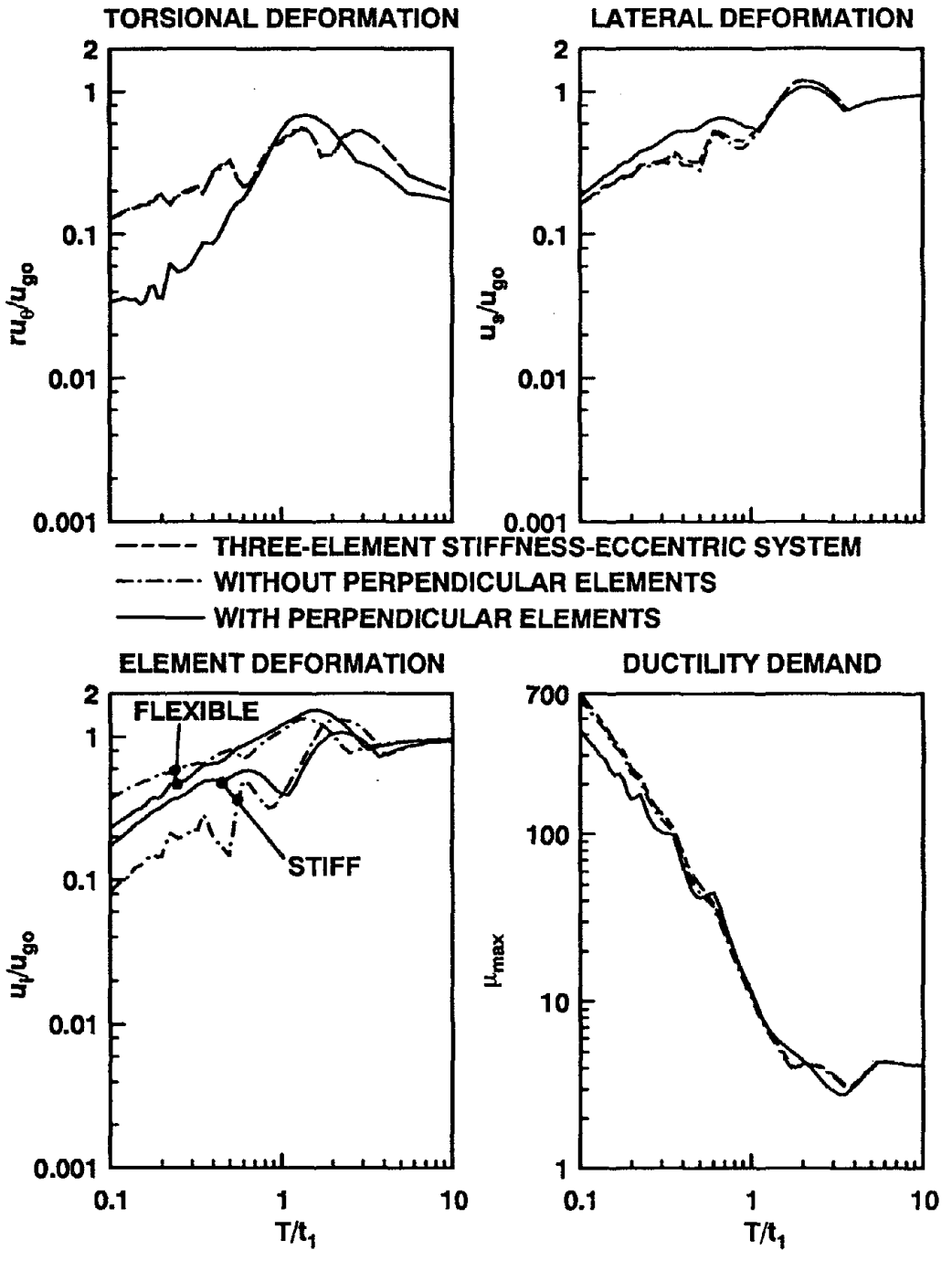

Figure 4.10 Response spectra for systems with and without perpendicular resisting elements due to simple input; $e_s/r=0.5$, $\Omega_\theta=1.0$, $\gamma_x=0.1$, $\omega_x/\omega=1$, $c=0.25$, $e_p=e_s$, $O_s=1$, and $\xi=5\%$.

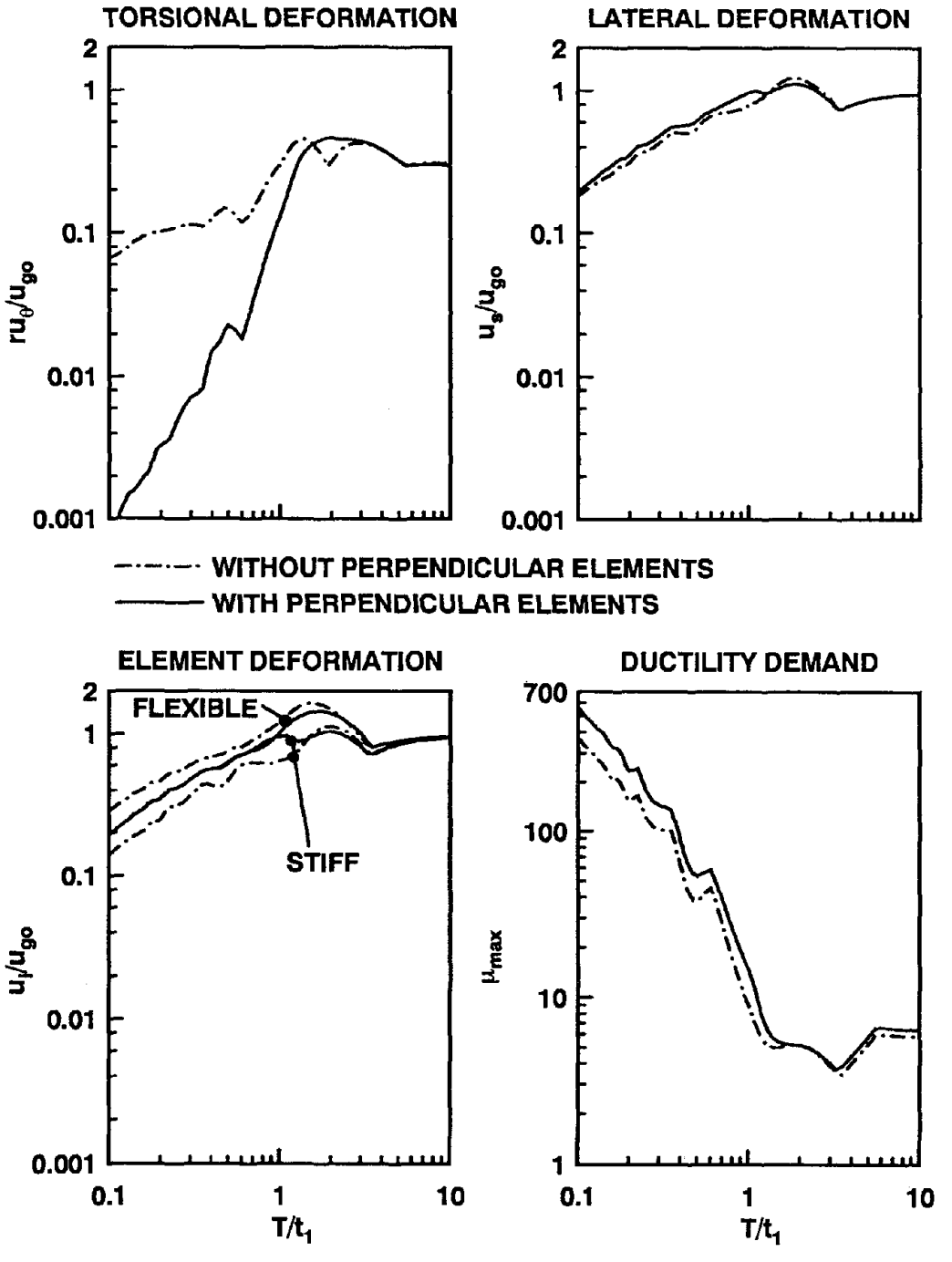

Figure 4.11 Response spectra for systems with and without perpendicular resisting elements due to simple input; $e_s/r=0.5$, $\Omega_\theta=1.0$, $\gamma_x=0.5$, $\omega_x/\omega=1$, $c=0.25$, $e_p=0$, $O_s=1$, and $\xi=5\%$.

elements have no influence on the elastic response because the overall properties: ω, Ω_θ, e_s/r, and ξ of the two systems -- with and without such elements -- are chosen to be identical. Thus the differences in the responses of the two systems presented in Figures 4.10 and 4.11 are the result of differences in their yielding behavior presented in the preceding section. Because acceleration-sensitive systems usually undergo much yielding, the system response is significantly affected by the perpendicular elements. However, these elements have smaller influence in the medium-period, velocity-sensitive and the long-period, displacement-sensitive regions of the design spectrum because such systems typically experience less yielding (Figures 4.10 and 4.11).

The system of Figure 1.1c with all three resisting elements in the direction of ground motion has been the subject of extensive investigation [1,30,35,36]. It was concluded from responses of acceleration-sensitive systems that considerable torsional motions occur that can lead to ductility demand in an asymmetric-plan system that may be two to three times larger than in a symmetric-plan system, and the edge displacements are larger by a factor of two to six [1,35]. These conclusions were contrary to those reached in References [7,20] from responses of systems with resisting elements providing resistance in both plan directions. In order to investigate the reasons underlying these apparent contradictions, the response spectrum for the system of Figure 1.1c is also presented in Figure 4.10 where it is seen to be essentially identical to the response of the two-element system with the same overall properties. Thus, the conclusions of References [1,35], while applicable to the system of Figure 1.1c, are not valid for systems with resisting elements in both directions considered in References [7,20]. More importantly, they are not applicable to most actual buildings which invariably include resisting elements in both lateral directions to provide resistance to both horizontal components of ground motion. In particular, the large increases in ductility demand and edge displacements due to plan-asymmetry, observed in References [1,35], are overly excessive for the design of most buildings.

After having examined the extreme case of γ_x=0, i.e, no torsional stiffness from perpendicular elements, the influence of γ_x within a practical range is examined next. The peak responses of systems with γ_x=0.25, 0.5, and 0.75 are presented in Figures 4.12 and 4.13 as a function of period ratio T/t_1 for two values of e_p: e_p=e_s and e_p=0; and for fixed values of Ω_θ, e_s/r, ω_x/ω, c, O_s, and ξ. A value of γ_x=0.25 implies that the perpendicular elements contribute 25 percent to the total torsional stiffness whereas elements oriented in the direction of ground motion contribute 75 percent.

The peak responses of short-period, acceleration-sensitive systems with e_p=e_s are significantly affected by the parameter γ_x (Figure 4.12). As γ_x increases, i.e, the relative contribution of the torsional stiffness due to perpendicular elements increases, the torsional deformation decreases and the lateral deformation increases. Because the torsional response is affected more than the lateral response, the flexible-side element deformation decreases and the stiff-side element deformation increases with increasing γ_x. Furthermore, the largest ductility demand decreases with increasing γ_x. The response of medium-period, velocity-sensitive and long-period, displacement-sensitive systems is essentially unaffected by γ_x, i.e., the relative contribution of perpendicular elements to the torsional stiffness (Figures 4.12).

The response of 'strength-symmetric' (e_p=0) systems is affected very little (Figure 4.13) by the parameter γ_x compared to systems with e_p=e_s (Figure 4.12). In particular, the decrease in torsional deformation, increase in the lateral deformation, and modifications in largest ductility demand and in deformations of flexible-side and stiff-side elements are small in 'strength-symmetric' (e_p=0) systems.

It is apparent from the preceding results that the inelastic response of short-period, acceleration-sensitive systems with e_p=e_s is significantly influenced by the relative contribution of perpendicular elements to the torsional stiffness of the system, but the response of medium-period, velocity-sensitive and long-period, displacement-sensitive systems is affected little in the parameter range considered. However, the response of 'strength-symmetric'

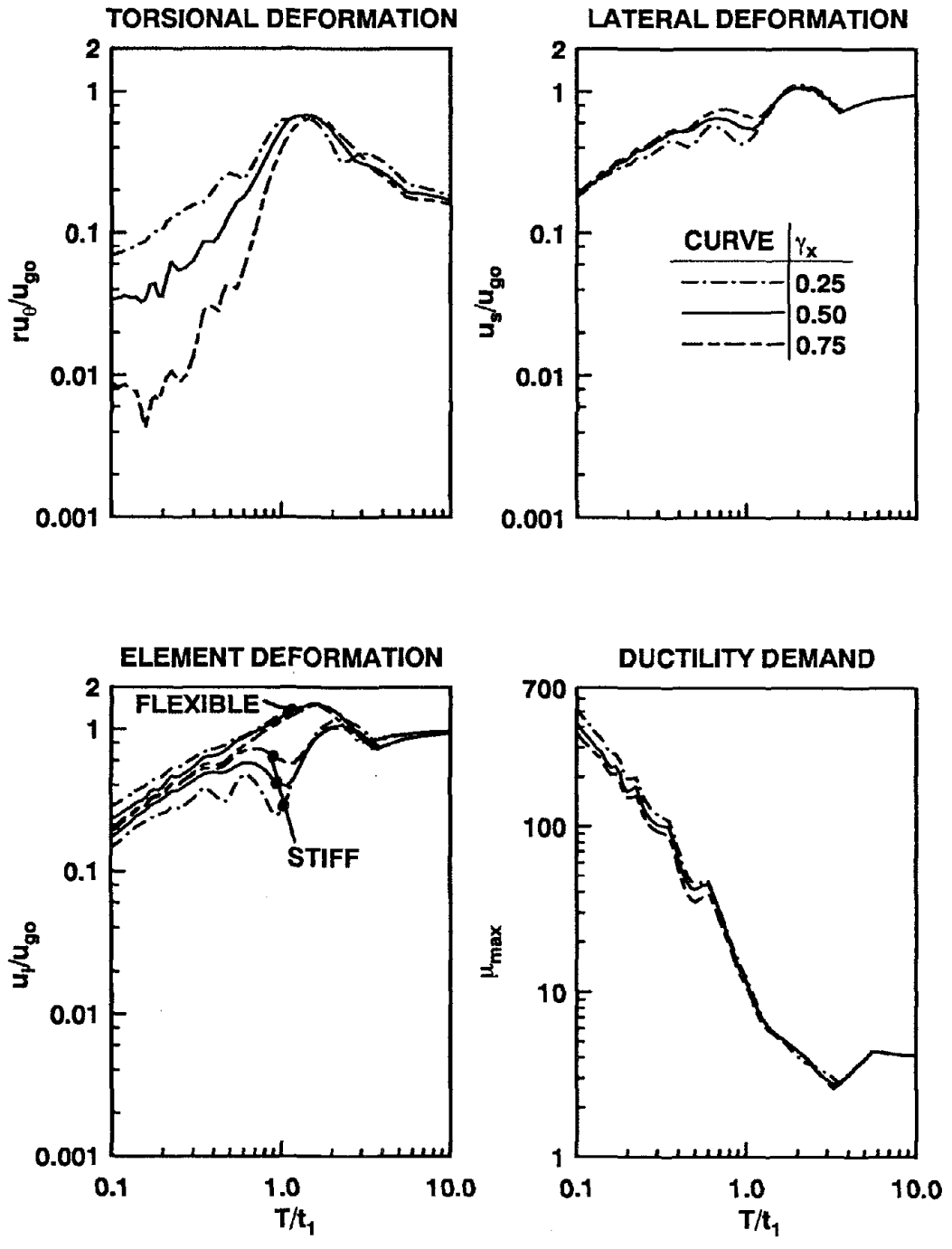

Figure 4.12 Response spectra for systems with γ_x=0.25, 0.5, and 0.75 due to simple input; e_s/r=0.5, Ω_θ=1.0, ω_x/ω=1, c=0.25, e_p=e_s, O_s=1, and ξ=5%.

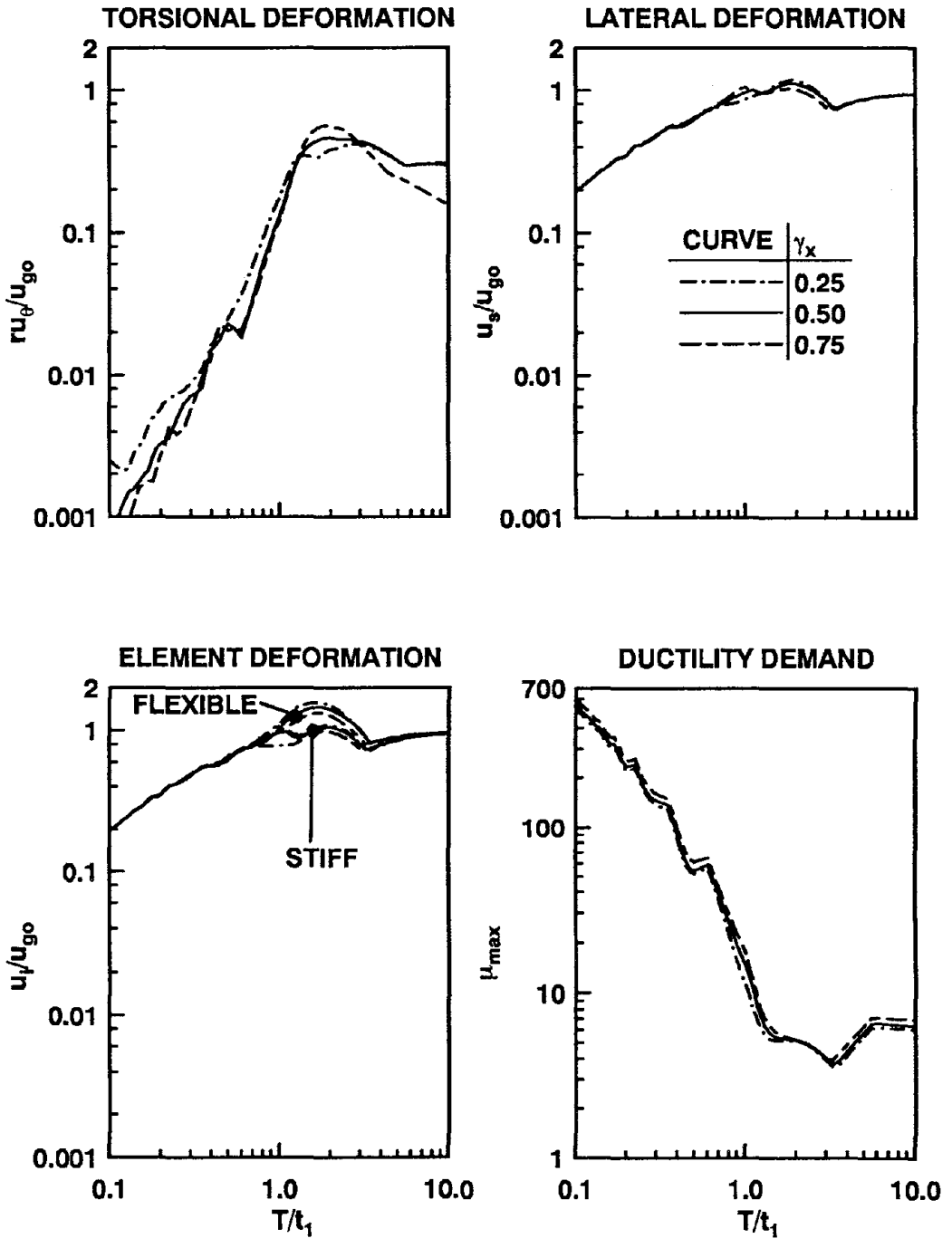

Figure 4.13 Response spectra for systems with γ_x=0.25, 0.5, and 0.75 due to simple input; e_s/r=0.5, Ω_θ=1.0, ω_x/ω=1, c=0.25, e_p=0, O_s=1, and ξ=5%.

(e_p=0) systems is affected very little by γ_x over the entire period range. It will be shown in Chapter 7 that many asymmetric-plan buildings designed according to building codes possess strength eccentricity much smaller than the stiffness eccentricity, and hence respond like 'strength-symmetric' (e_p=0) systems. The above results indicate that the response of such systems would be essentially unaffected by γ_x. Therefore, the parameter γ_x is fixed in the rest of this investigation at γ_x=0.5, a value representative of many actual buildings.

4.5 Influence of Translational Stiffness in Perpendicular Direction

As mentioned earlier, the linearly elastic response of the system of Figure 4.1b to ground motion in the Y-direction is characterized by system parameters, ω, Ω_θ, e_s/r, and ξ. In particular, the response does not depend separately on the translational stiffness of the system in the direction perpendicular to the direction of ground motion. However, such is not the case after the system yields because the perpendicular elements may also yield because of torsional deformation, thus affecting the instantaneous value of Ω_θ. Thus, the influence of the relative translational stiffness in the perpendicular direction, as characterized by the frequency ratio ω_x/ω (which is equal to K_x/K_y) on the inelastic response of systems is examined next. For this purpose, the peak response of systems having ω_x/ω=0.8, 1, and 1.25 are presented in Figures 4.14 and 4.15 as a function of period ratio T/t_1 for two values of e_p: e_p=e_s and e_p=0; and for fixed values of Ω_θ, e_s/r, γ_x, c, O_s, and ξ. The values of ω_x/ω considered represent a practical range for many asymmetric-plan buildings [10].

The peak response of short-period, acceleration-sensitive systems with e_p=e_s is significantly influenced by ω_x/ω or K_x/K_y (Figure 4.14). As the relative stiffness along the perpendicular direction increases, i.e., as ω_x/ω increases, the effects of torsional coupling decrease. In particular, the system undergoes smaller torsional deformation and larger lateral deformation (Figure 4.14). Since these effects are larger in torsional deformation compared to lateral deformation, the deformation of flexible-side element decreases and that of the stiff-side element increases with increasing ω_x/ω. Furthermore, the largest ductility demand

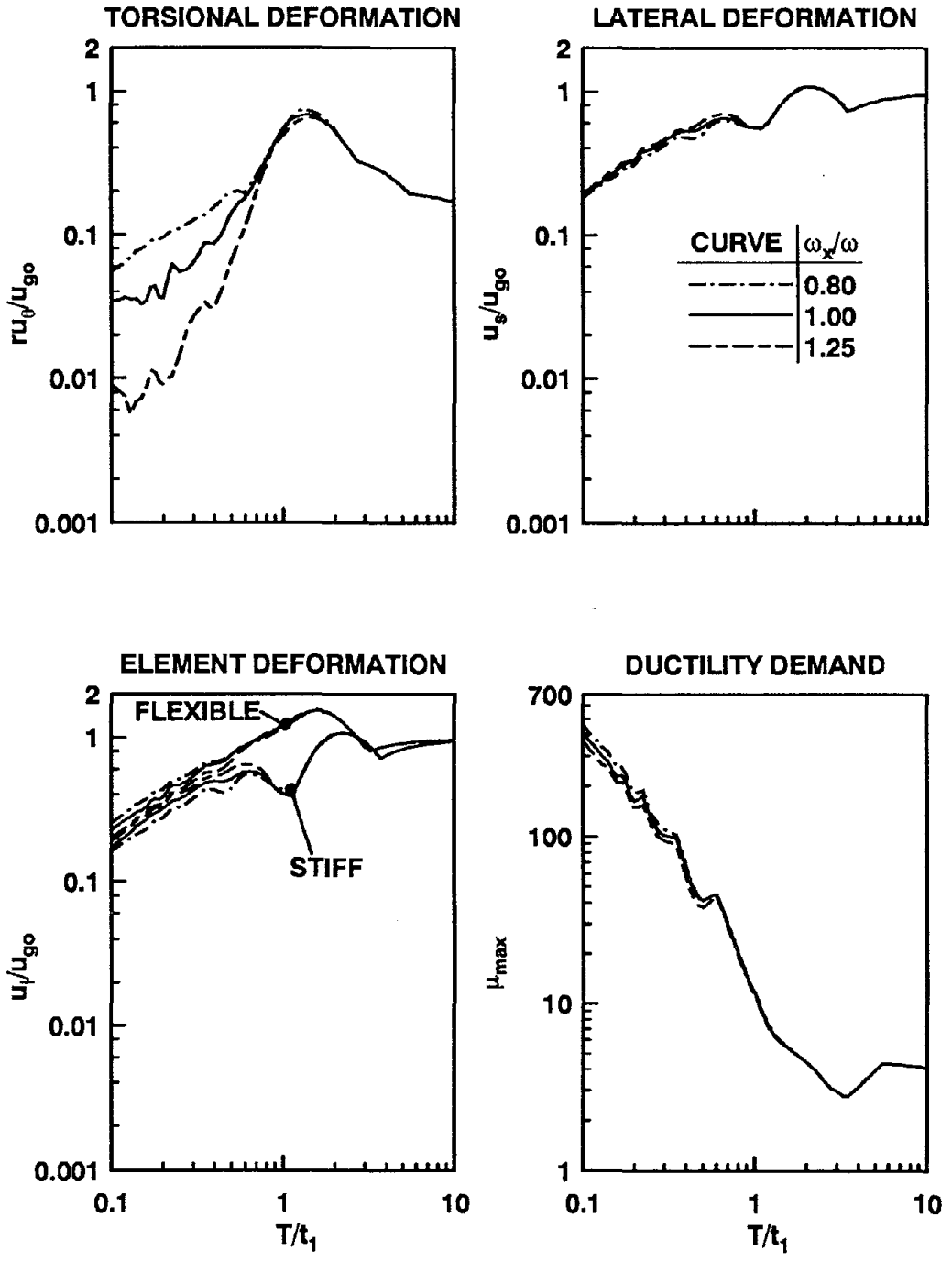

Figure 4.14 Response spectra for systems with ω_x/ω=0.8, 1, and 1.25 due to simple input; e_s/r=0.5, Ω_θ=1.0, γ_x=0.5, c=0.25, e_p=e_s, O_s=1, and ξ=5%.

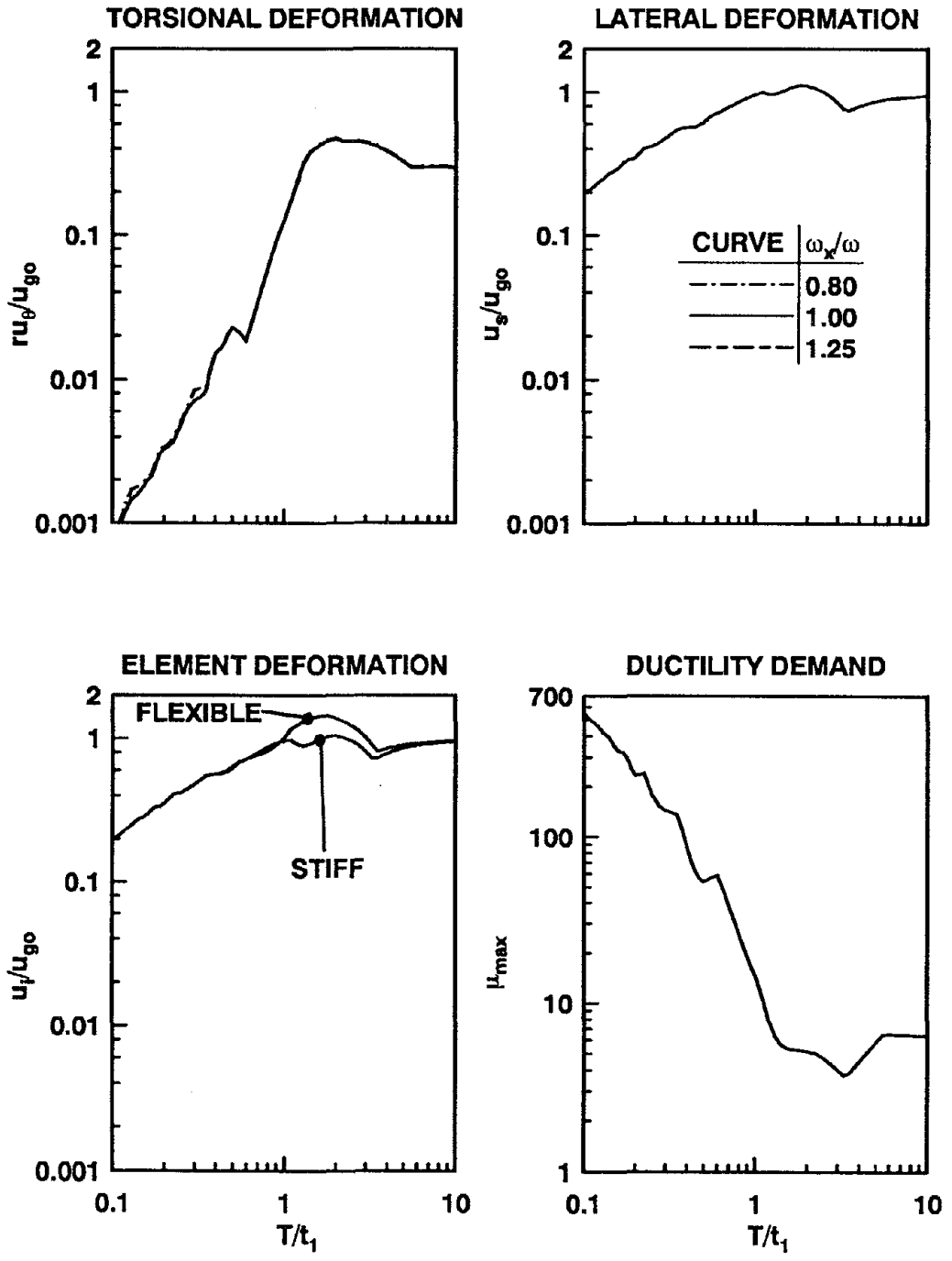

Figure 4.15 Response spectra for systems with ω_x/ω=0.8, 1, and 1.25 due to simple input; e_s/r=0.5, Ω_θ=1.0, γ_x=0.5, c=0.25, e_p=0, O_s=1, and ξ=5%.

decreases with increasing ω_x/ω. The response of medium-period, velocity-sensitive and long-period, displacement-sensitive systems is essentially unaffected by ω_x/ω or K_x/K_y.

The response of 'strength-symmetric' (e_p=0) systems is essentially independent of ω_x/ω or K_x/K_y over the entire range of period values (Figure 4.15).

The preceding results indicate that the inelastic response of short-period, acceleration-sensitive systems with $e_p=e_s$ is significantly influenced by K_x/K_y, the translational stiffness along the perpendicular direction relative to the translational stiffness along the ground motion direction; but the responses of medium-period, velocity-sensitive and long-period, displacements-sensitive systems are essentially unaffected. However, the response of 'strength-symmetric' (e_p=0) systems is essentially independent of ω_x/ω in the parameter range considered over the entire range of period values. As will be shown in Chapter 7, many asymmetric-plan buildings designed according to building codes possess strength eccentricity much smaller than the stiffness eccentricity, and hence respond like 'strength-symmetric' (e_p=0) systems. The above results indicate that the response of such systems would be essentially unaffected by ω_x/ω. Furthermore, ω_x/ω is close to one for many buildings [10]. Thus, ω_x/ω is fixed at ω_x/ω=1 in the rest of the investigation.

4.6 Influence of Number of Resisting Elements

The lateral and torsional deformations of linearly elastic systems depend only on the uncoupled lateral period T, the normalized stiffness eccentricity e_s/r, the uncoupled torsional-to-lateral frequency ratio Ω_θ, and the damping ratio ξ, but not independently on the number and location of the resisting elements. However, the number, location, and yield properties of resisting elements affect the instantaneous values of T, e_s/r, and Ω_θ and may therefore influence the inelastic response of systems. This question is examined next by comparing the response of systems shown in Figures 4.2a, 4.2b, and 4.2c, having the same values for the elastic parameters T, Ω_θ, and e_s/r, and the overall inelastic parameters c, O_s, and e_p. Thus, the differences in the responses of the three systems will be due to the number of

elements influencing the yielding behavior. Note that in order to keep the same value of Ω_θ, the outermost element in a system with larger number of resisting elements needs to be located farther from the CS compared to the resisting element in a system with fewer elements. The peak responses of systems shown in Figure 4.2 are presented in Figures 4.16 and 4.17 as a function of period ratio T/t_1 for two values of e_p: $e_p=e_s$ and $e_p=0$; and for fixed values of Ω_θ, e_s/r, γ_x, ω_x/ω, c, O_s, and ξ.

The number of resisting elements in the direction of ground motion has very little effect on the response of systems with equal stiffness and strength eccentricities ($e_p=e_s$) (Figure 4.16). The lateral as well as torsional deformations at the CS are essentially unaffected, the deformations of resisting elements are affected for some values of T/t_1, and the maximum ductility demand is essentially unaffected. The element deformations, although affected little by the number of elements, are affected more than the other response quantities. The deformation of the outermost element on the flexible side tends to increase with increasing number of elements whereas that of the element on the stiff side tends to decrease. Such is the case because the outermost elements on the flexible and stiff sides in a system with larger number of elements are located farther from the CS compared to those in a system with fewer elements, and they experience greater effects of torsional coupling even if the lateral and torsional displacements at the CS are the same.

The response of 'strength-symmetric' systems ($e_p=0$) is affected more (Figure 4.17) by the number of resisting elements compared to systems with $e_p=e_s$ (Figure 4.16); however, the effects are still small over a wide range of lateral vibration periods. The lateral and torsional displacements at the CS as well as the element deformations are essentially independent of the number of resisting elements. However, the maximum ductility demand, which occurs in the outermost element on the stiff side of such systems (Table 4.1), increases with the number of elements because the yield deformation of this element in systems with $e_p=0$ decreases with increasing number of resisting elements (Figure 4.4b).

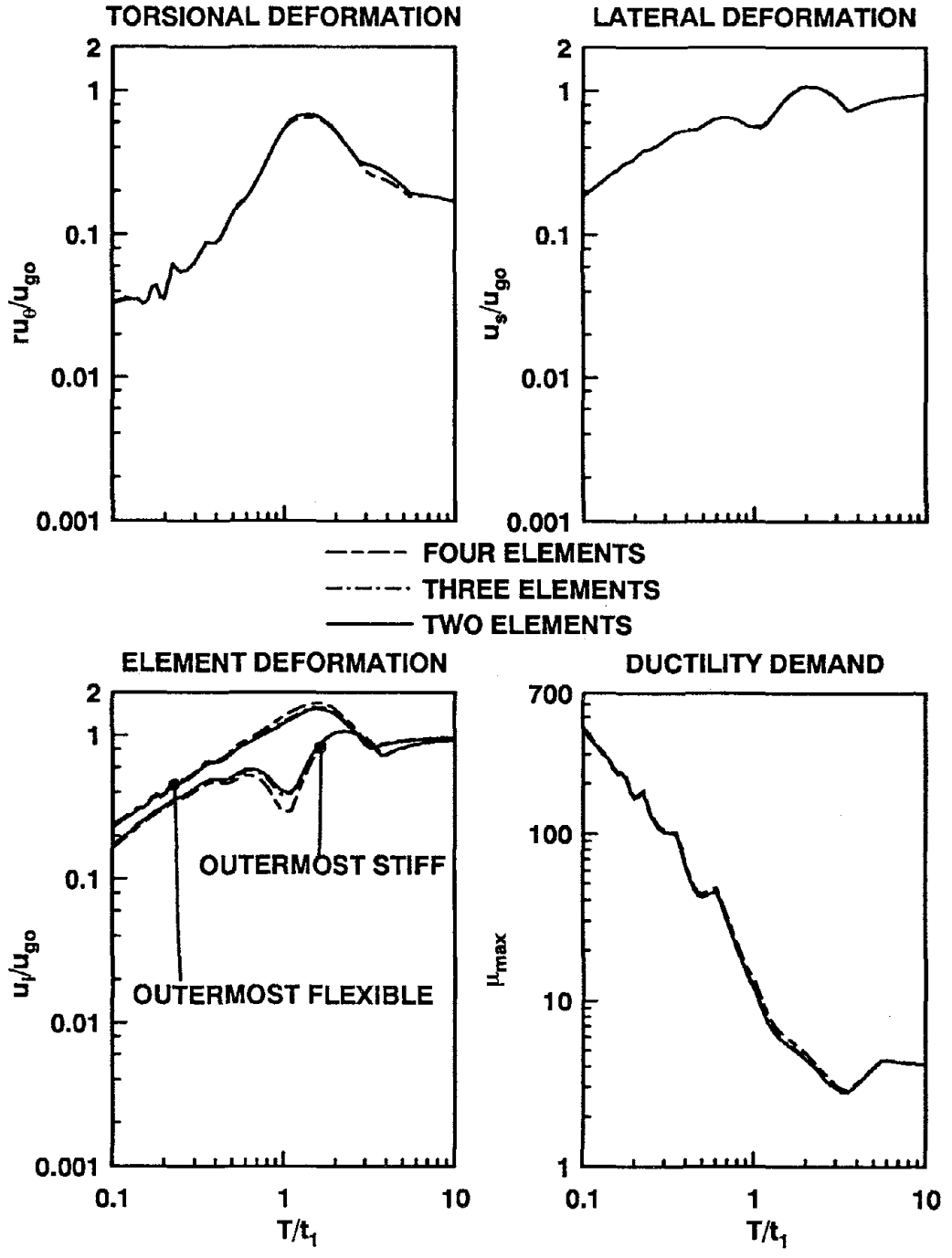

Figure 4.16 Response spectra for systems with two, three, and four resisting elements along the direction of ground motion due to simple input; $e_s/r=0.5$, $\Omega_\theta=1.0$, $\gamma_x=0.5$, $\omega_x/\omega=1$, $c=0.25$, $e_p=e_s$, $O_s=1$, and $\xi=5\%$.

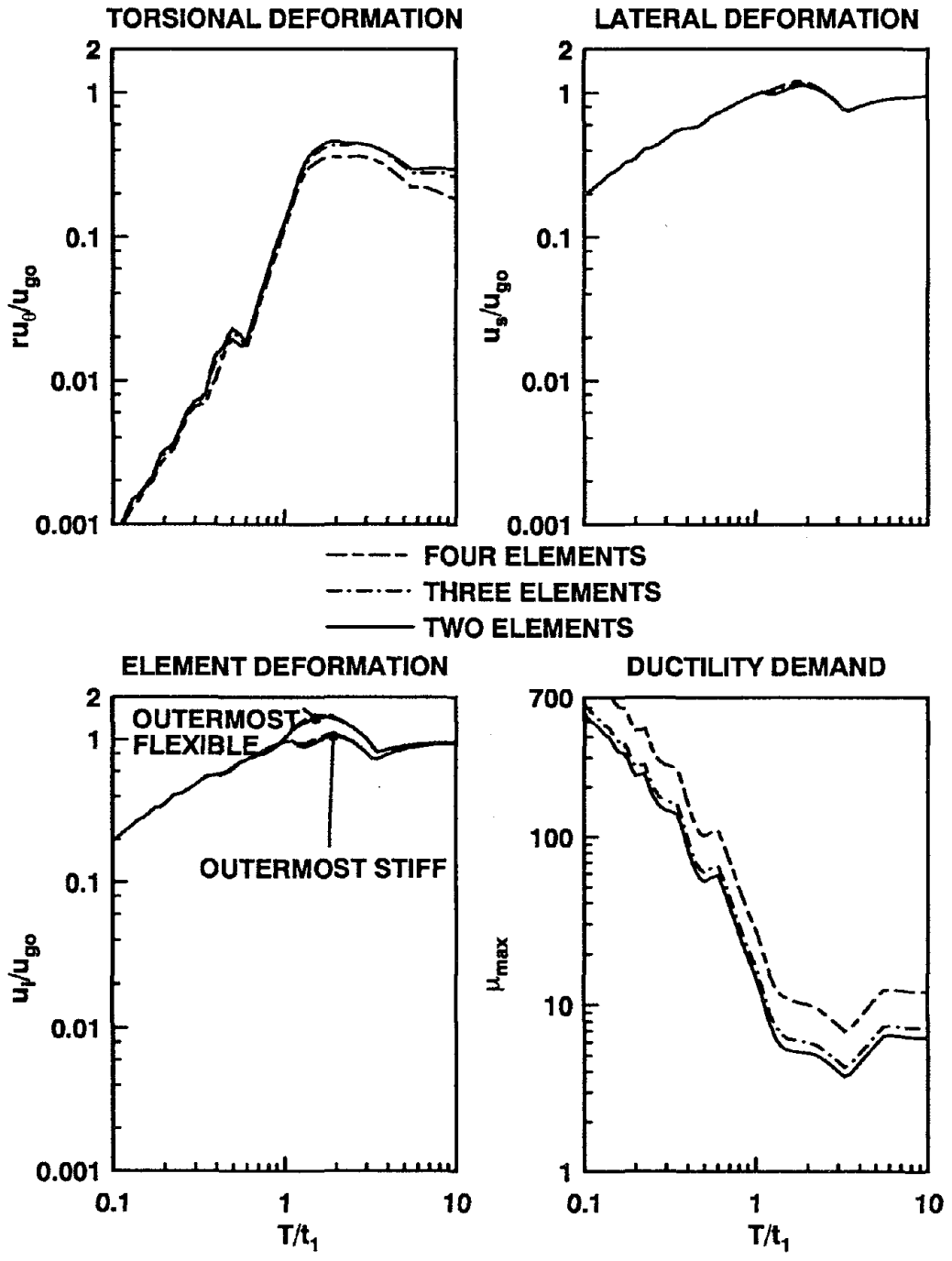

Figure 4.17 Response spectra for systems with two, three, and four resisting elements along the direction of ground motion due to simple input; $e_s/r=0.5$, $\Omega_\theta=1.0$, $\gamma_x=0.5$, $\omega_x/\omega=1$, $c=0.25$, $e_p=0$, $O_s=1$, and $\xi=5\%$.

It is apparent from the preceding results that the number of resisting elements oriented along the direction of ground motion has little influence on the overall (ru_θ and u_s) as well as the local (u_i and μ_{max}) responses of systems with e_p=e_s. Thus, a system with only two resisting elements along the direction of ground motion should provide a satisfactory estimate of the inelastic response of a system with larger number of resisting elements provided the parameters T, e_s/r, Ω_θ, γ_x, ω_x/ω, e_p, c, O_s, and ξ are the same for the two systems. Therefore, using a three-element system [1,35] over a two-element system [17], or a sixteen-element system [7] over a four-element system [7] is of little benefit in research studies.

Although the number of resisting elements has very little influence on the lateral and torsional displacements at the CS, and element deformations of systems with e_p=0, it has significant influence on the maximum ductility demand. Therefore, for such structures, a system with actual number of elements should be used to accurately predict the ductility demand from the other response quantities; the latter may be determined from dynamic analysis of a system with two elements.

4.7 Mass-Eccentric and Stiffness-Eccentric Systems

In some earlier studies, mass-eccentric and stiffness-eccentric systems have been used interchangeably to study the inelastic response of asymmetric-plan systems. While the elastic response of these two systems at the CS is identical provided that the elastic parameters, T, Ω_θ, e_s/r, and ξ are the same for both systems, the inelastic response is not the same [35]. The factors contributing to these differences are examined in this section.

The inelastic response of mass- and stiffness-eccentric systems (Figures 4.3a and 4.3b) having the same values for T, Ω_θ, e_s/r, γ_x, ω_x/ω, and ξ as well as c, O_s, and e_p are compared in Figures 4.18 and 4.19. The torsional and lateral displacements at the CS are essentially identical for mass- and stiffness-eccentric systems with e_p=e_s but the the elements on the flexible as well as stiff sides of the system undergo smaller deformations in the mass-eccentric system (Figure 4.18). Such is the case because the flexible-side element is located

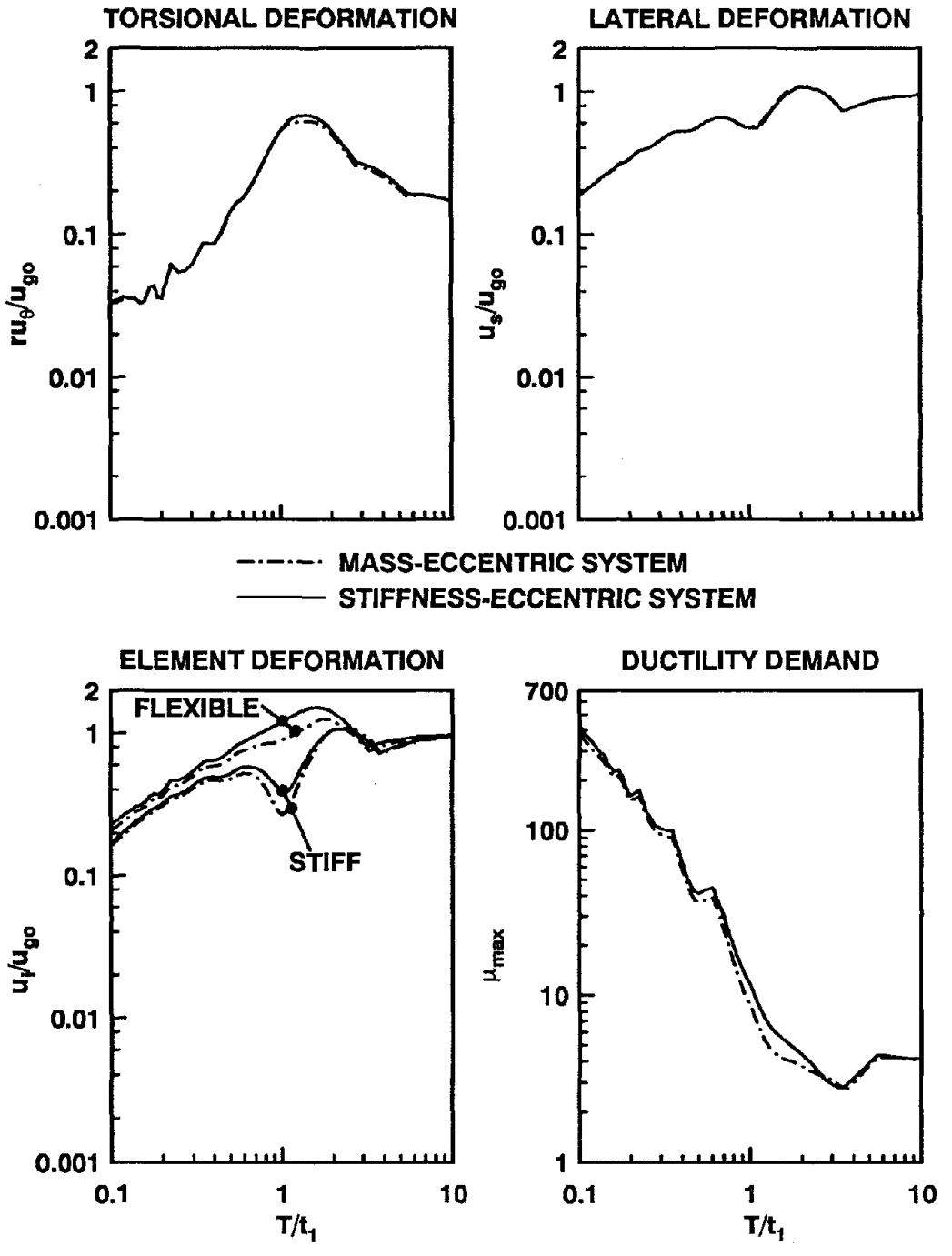

Figure 4.18 Response spectra for stiffness- and mass-eccentric systems due to simple input; $e_s/r=0.5$, $\Omega_\theta=1.0$, $\gamma_x=0.5$, $\omega_x/\omega=1$, $c=0.25$, $e_p=e_s$, $O_s=1$, and $\xi=5\%$.

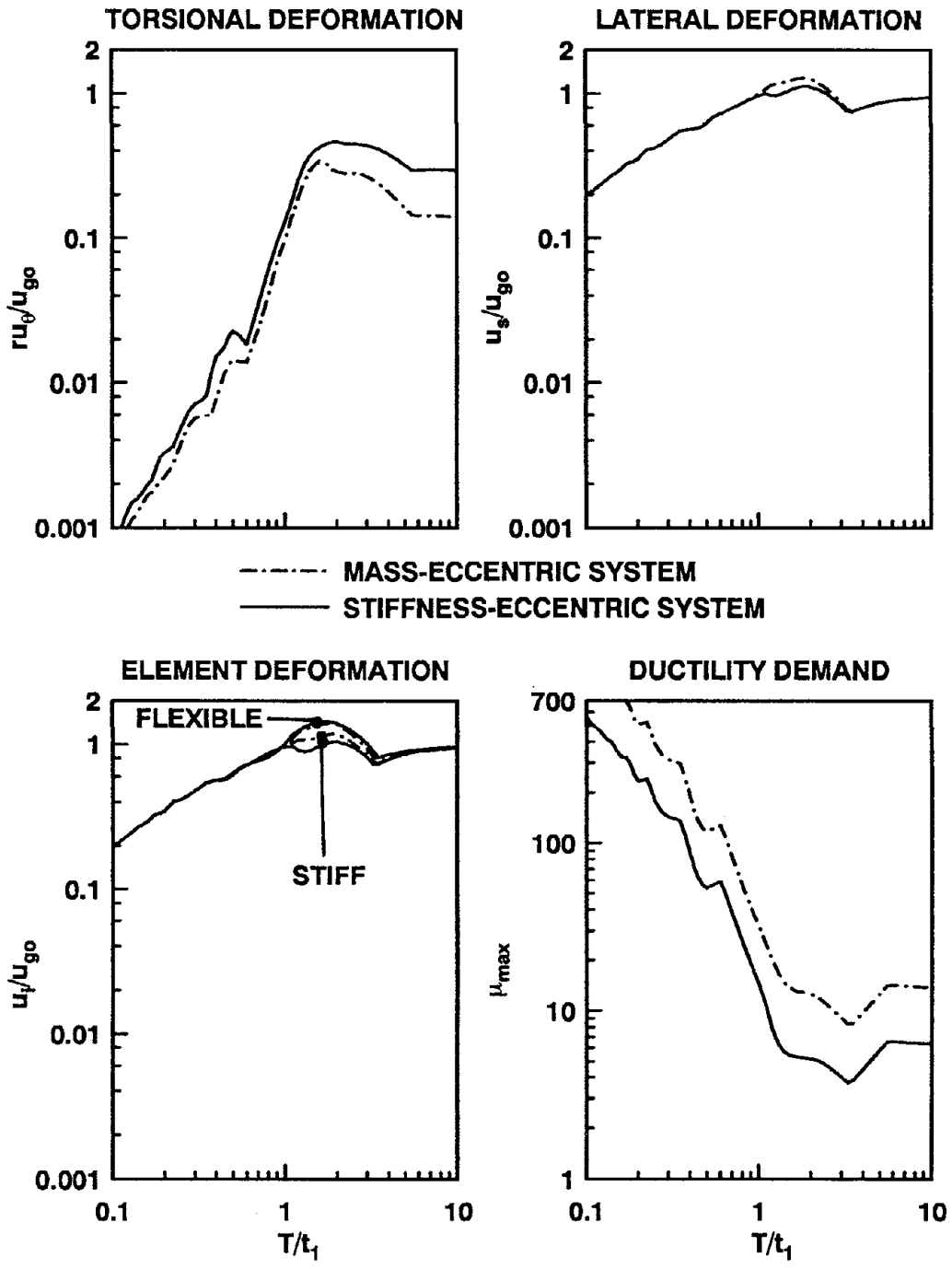

Figure 4.19 Response spectra for stiffness- and mass-eccentric systems due to simple input; $e_s/r=0.5$, $\Omega_\theta=1.0$, $\gamma_x=0.5$, $\omega_x/\omega=1$, $c=0.25$, $e_p=0$, $O_s=1$, and $\xi=5\%$.

closer to the CS, and the stiff-side element is located farther from the CS, in the mass-eccentric system compared to the stiffness-eccentric system, both having the same values of Ω_θ. Therefore, the effects of torsional coupling are smaller for the flexible-side element and larger for the stiff-side element in a mass-eccentric system, although the lateral and torsional displacements at the CS are about the same as in the corresponding stiffness-eccentric system. Because the maximum ductility demand, μ_{max}, in systems with $e_p=e_s$ generally occurs in the outermost element on the flexible side (Figure 4.8), and this element experiences smaller deformations in a mass-eccentric system, μ_{max} is also slightly smaller.

The above observations help explain why two earlier investigations, both considering systems with $e_p=e_s$, resulted in contradictory conclusions. The additional ductility demand in an asymmetric-plan system over that for the corresponding symmetric-plan, SDF system was observed to be generally below 30 percent in one case [17] which is much smaller than the factor of two to three observed in other studies [1,35]. In order to identify the reasons for the apparent contradiction, the ratio of ductility demands in asymmetric-plan and symmetric-plan, SDF systems is presented in Figure 4.20 for the stiffness-eccentric system (Figure 1.1c) used in References [1,35] and the mass-eccentric system (Figure 1.1f) of Reference [17]. In the acceleration- and velocity-sensitive regions of the spectrum, the increase in ductility demand due to plan-asymmetry is much larger for stiffness-eccentric systems. Thus, it is apparent that the differences in conclusions between the two investigations result from the use of different systems in the two investigations.

For 'strength-symmetric' systems ($e_p=0$), all the response quantities can be significantly different for the two systems (Figure 4.19). The torsional displacement of the mass-eccentric system is lower, whereas the lateral displacement at the CS is unaffected over a wide range of T/t_1 values, except in the velocity-sensitive region where it tends to be larger. This combination results in lower deformation in the flexible-side element and higher deformation in the stiff-side element of mass-eccentric systems for medium-period, velocity-sensitive systems. For other spectral regions, the element deformations are similar for the two types of

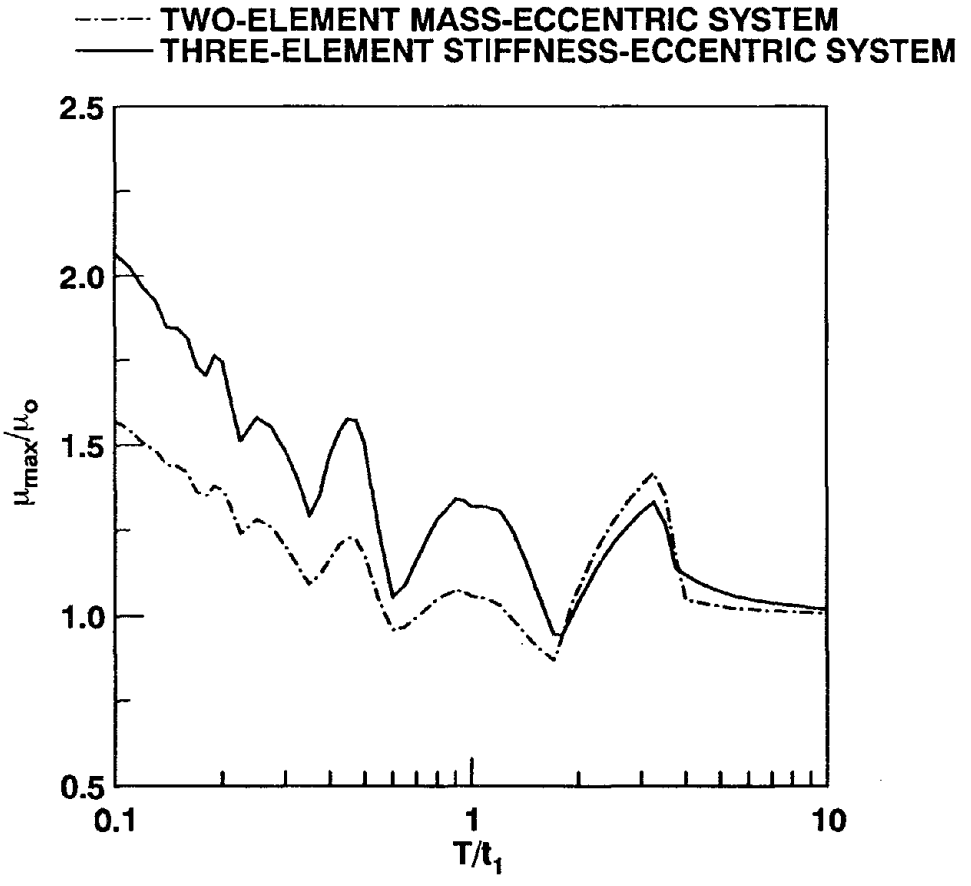

Figure 4.20 Normalized ductility demand of three-element stiffness-eccentric and two-element mass-eccentric systems due to simple input; $e_s/r=0.5$, $\Omega_\theta=1.0$, $\gamma_x=0$, $c=0.25$, $e_p=e_s$, $O_s=1$, and $\xi=5\%$.

systems.

The maximum ductility demand in mass-eccentric systems with e_p=0 is up to two to three times that for stiffness-eccentric systems. As shown previously, the maximum ductility demand for systems with e_p=0 occurs in the stiff-side element (Table 4.1 and Figure 4.8), the yield deformation of this element is significantly smaller for mass-eccentric systems (Figure 4.4d), and the maximum deformation of the stiff-side element tends to be larger for mass-eccentric systems. Consequently, the maximum ductility demand in mass-eccentric systems is much larger.

These results indicate that for systems with identical values of strength and stiffness eccentricities (e_p=e_s), mass-eccentric and stiffness-eccentric systems may be used interchangeably to estimate the deformations at the CS but not for predicting the maximum ductility demand. For 'strength-symmetric' systems (e_p=0), however, these two systems can not be used interchangeably at all because responses, overall as well as local, can be significantly different for the two systems. Since the plan-asymmetry in most buildings arises from distribution of stiffness and not of mass, the mass-eccentric system should not be used in inelastic response studies of such buildings. In particular, the imposition of a minimum value of the strength eccentricity in the recent Mexico Federal District Code [9] in order to reduce the ductility demand may be unnecessary for most buildings because this restriction is based on the response studies of mass-eccentric systems.

4.8 Influence of Overstrength Factor

Figure 4.21 shows time-histories for the asymmetric-plan system of Figure 4.1b with two values of the overstrength factor: O_s=1 and O_s=1.2. The increase in strength has the effect of reducing slightly the time durations T4, T5, and T6 when the system has no lateral stiffness; and increasing slightly the time durations T1, T2, and T3 of no torsional stiffness. Consequently, the system with overstrength experiences smaller lateral deformation and larger torsional deformation. These observations made from Figure 4.21 are typical of short-period systems which undergo significant inelastic action.

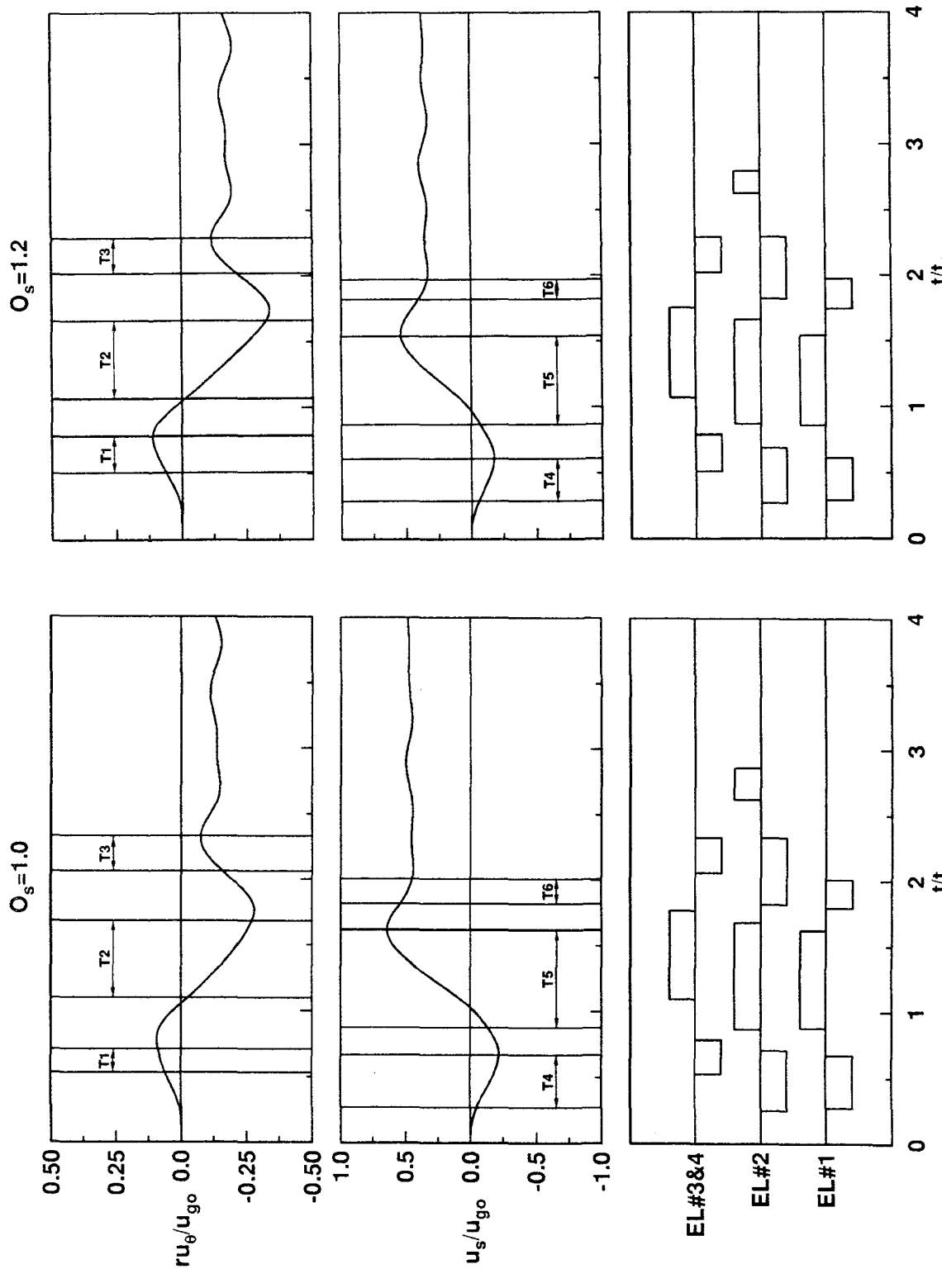

Figure 4.21 Response histories of the four-element system due to simple input; T/t_1=0.75, e_s/r=0.5, Ω_θ=1.0, γ_x=0.5, ω_x/ω=1, c=0.25, e_p=e_s, and ξ=5%. T1, T2, and T3 identify time-durations when torsional stiffness is zero and T4, T5, and T6 are time-durations when lateral stiffness is zero.

The peak values of responses of systems with different strengths, as characterized by overstrength factor O_s=1, 1.1, 1.2, and 1.3 are presented in the form of response spectra in Figures 4.22 and 4.23 for two values of the strength eccentricity: e_p=e_s and e_p=0. The influence of overstrength on the system response varies with the response quantity of interest and the spectral region. With increase in strength, the lateral deformation decreases in the acceleration-sensitive region, may increase for some values of T/t_1 in the velocity-sensitive region, and remains unaffected in the displacement-sensitive region. These effects of increased strength on the lateral deformation of asymmetric-plan systems are consistent with earlier results for SDF systems [38]. The torsional deformation increases slightly for all but a few T/t_1 values. Deformations of the elements on the flexible and stiff sides follow the same trends as the lateral deformation because the contribution of the torsional deformation, which increases slightly with overstrength, to the element deformations is small compared to that of the lateral deformation. Since the element deformations generally decrease, and the element yield deformations increase (Figure 4.4c), the maximum ductility demand μ_{max} is smaller in systems with overstrength. The above observations are valid for systems with e_p=e_s as well as systems with e_p=0. However, the effects are slightly smaller in the latter systems compared to the former.

In most of the earlier investigations [1,7,17,20,24,35], the combined strength of all the resisting elements in an asymmetric-plan system has been assumed to be equal to that of the corresponding symmetric-plan system. However, as would be demonstrated in Chapter 7, code-designed asymmetric-plan systems are generally stronger than corresponding symmetric-plan systems. Thus the conclusions from most earlier studies are not directly applicable to code-designed buildings. Such overstrength may lead to significant reduction in the response, e.g., the maximum ductility demands for acceleration-sensitive systems with 30% overstrength, which is not unusual in code-designed buildings, may decrease by more than 33%. Such reductions in ductility demand may merit consideration in the design process.

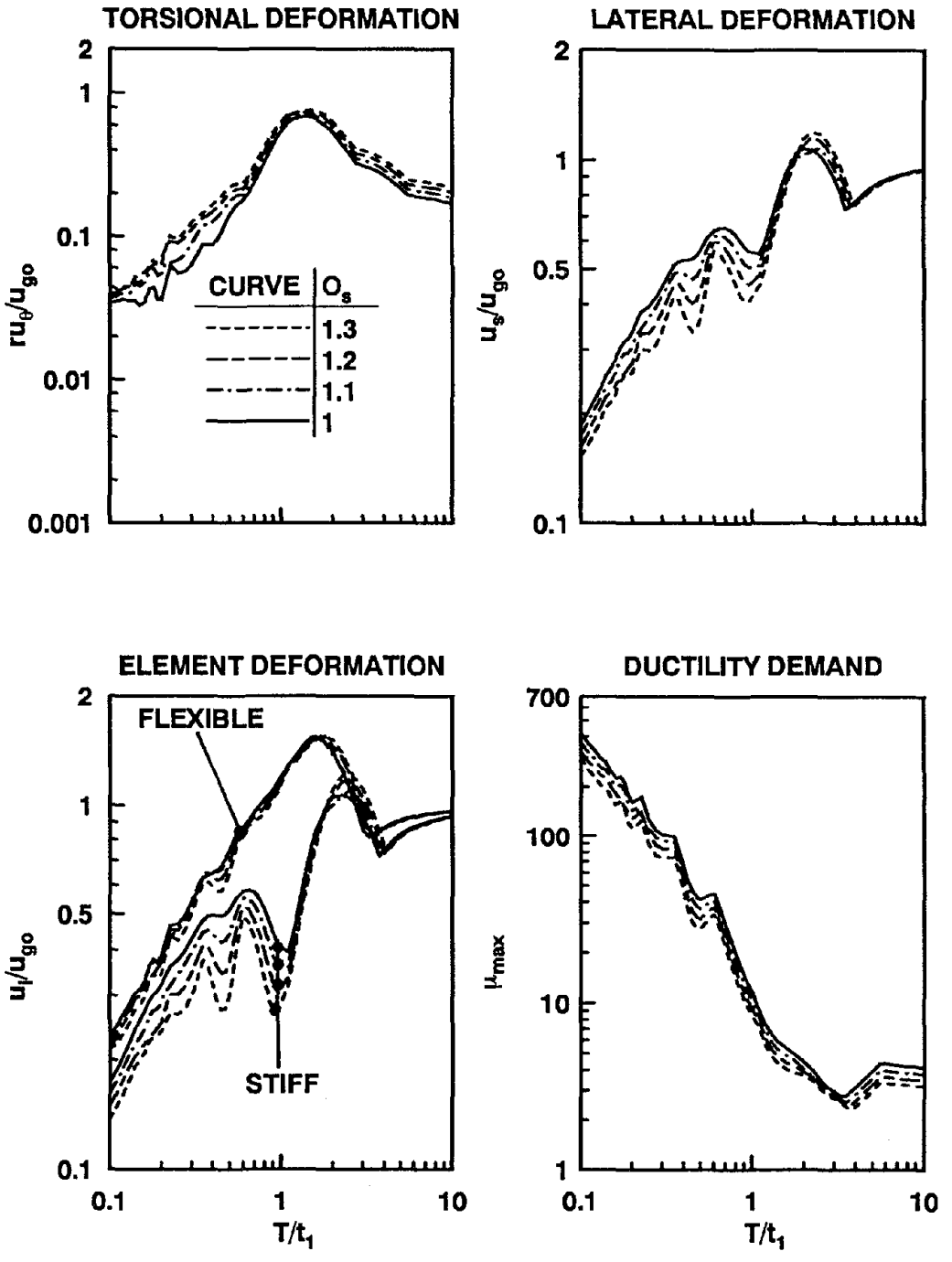

Figure 4.22 Response spectra of systems with O_s=1, 1.1, 1.2, and 1.3 due to simple input; e_s/r=0.5, Ω_θ=1.0, γ_x=0.5, ω_x/ω=1, c=0.25, e_p=e_s, and ξ=5%.

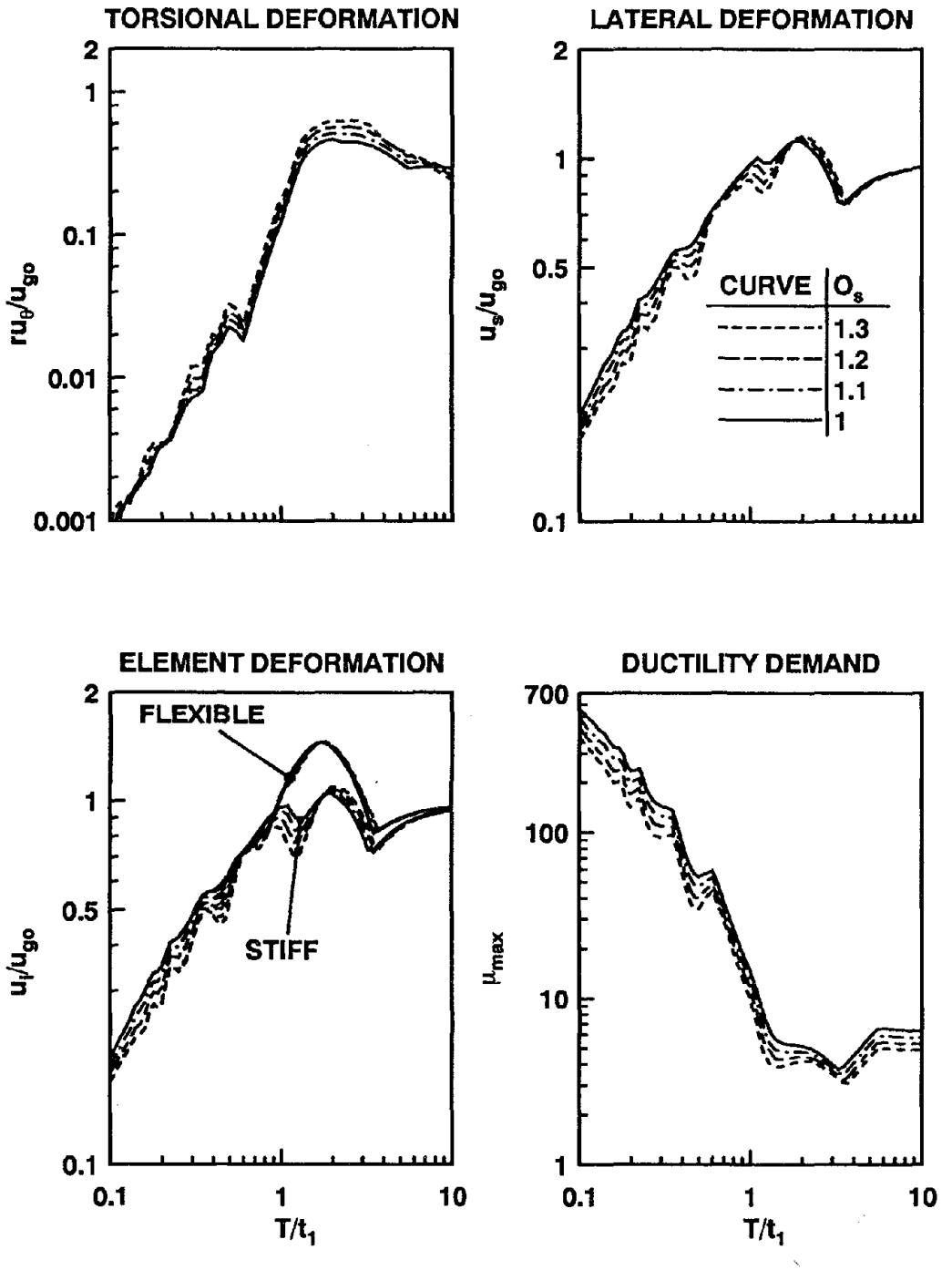

Figure 4.23 Response spectra of systems with O_s=1, 1.1, 1.2, and 1.3 due to simple input; e_s/r=0.5, Ω_θ=1.0, γ_x=0.5, ω_x/ω=1, c=0.25, e_p=0, and ξ=5%.

4.9 Influence of Strength Eccentricity

It is apparent from the preceding sections that the relative values of the strength eccentricity and stiffness eccentricity can significantly influence the response behavior of asymmetric-plan systems. For example, among systems having equal strength and stiffness eccentricities, those without perpendicular resisting elements experience larger ductility demands compared to systems with perpendicular elements; the opposite trend is observed in 'strength-symmetric' systems (e_p=0). Similarly, mass-eccentric systems undergo smaller ductility demand compared to stiffness-eccentric systems if e_p=e_s, whereas the opposite occurs for systems with e_p=0. The influence of the strength eccentricity value is further examined by considering two additional values, e_p=e_s/2 and e_s/4, to cover a range of values typical of code-designed buildings.

Figure 4.24 shows time-histories of deformations and element yielding for the inelastic system of Figure 4.1b for two values of the strength eccentricity: e_p=e_s and e_p=0. The stiff-side element of the system with e_p=0 yields for longer durations and the flexible-side element for shorter durations compared to systems with e_p=e_s. Such is the case because, among the two systems, the yield deformation of the stiff-side element is smaller and that of the flexible-side element is larger in systems with e_p=0 (Figure 4.4). Furthermore, the perpendicular elements do not yield at all in the system with e_p=0, whereas they yield for significant time-durations in the system with e_p=e_s. As a result, the torsional stiffness of the system with e_p=0 becomes zero for much shorter durations (in this particular case the duration is zero) compared to the system with e_p=e_s. Thus, the system with e_p=0 undergoes much smaller torsional deformation. Although, both systems, e_p=e_s and e_p=0, have no lateral stiffness for similar time-durations, the stiff-side element of the system with e_p=0 yields for longer time durations resulting in smaller lateral stiffness and hence larger lateral deformation. These observations made from Figure 4.24 are typical of short-period systems in which significant inelastic action occur.

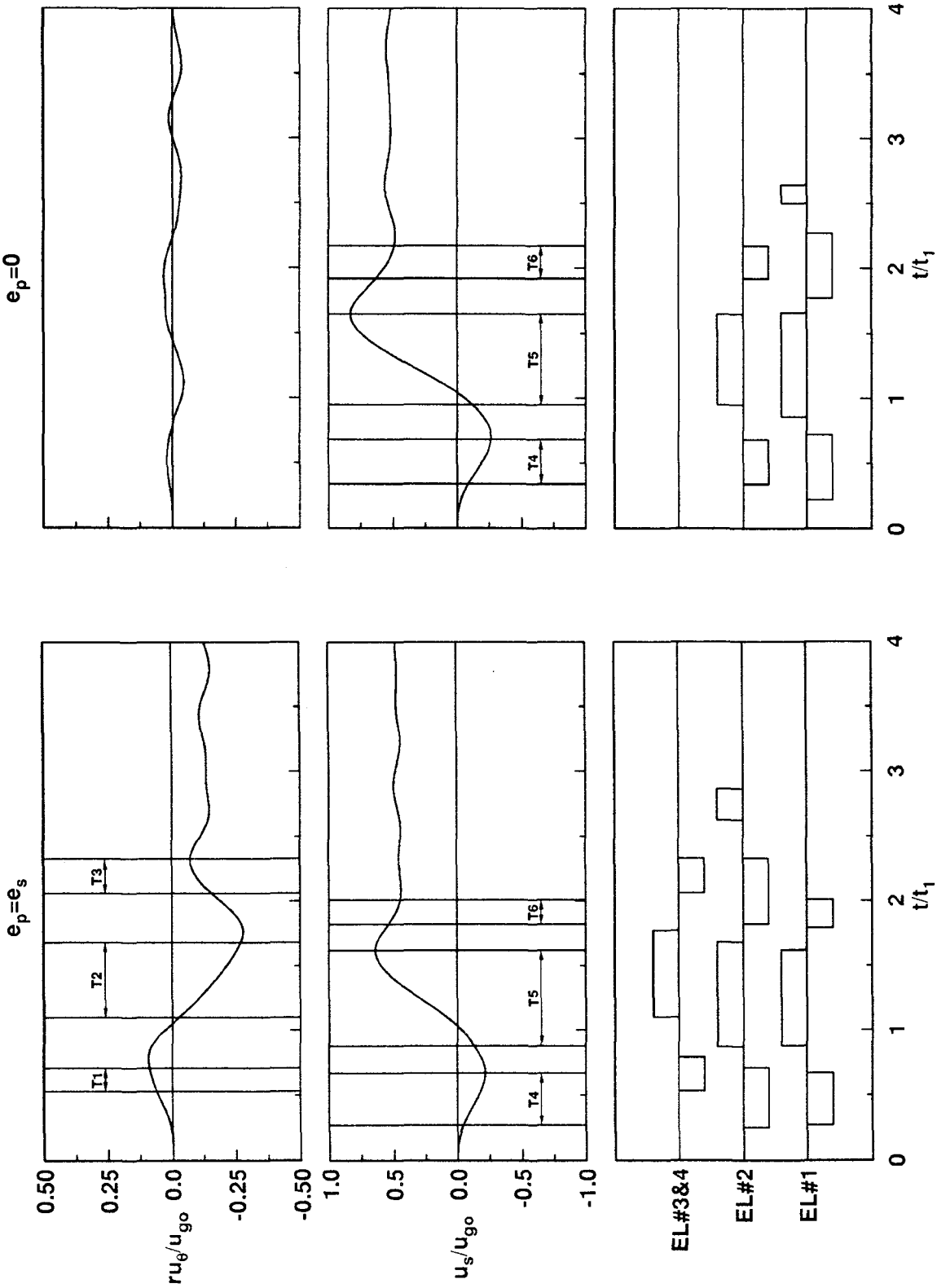

Figure 4.24 Response histories of the four-element system due to simple input; $T/t_1=0.75$, $e_s/r=0.5$, $\Omega_\theta=1.0$, $\gamma_\chi=0.5$, $\omega_\chi/\omega=1$, $c=0.25$, $O_s=1$, and $\xi=5\%$. T1, T2, and T3 identify time-durations when torsional stiffness is zero and T4, T5, and T6 are time-durations when lateral stiffness is zero.

The peak values of responses of systems with $e_p = e_s$, $e_s/2$, $e_s/4$, and zero are presented in Figure 4.25 in the form of response spectra for fixed values of Ω_θ, e_s/r, γ_x, ω_x/ω, c, O_s, and ξ. Because the overall elastic parameters: ω, Ω_θ, e_s/r, and ξ and the inelastic parameters c, and O_s are chosen to be identical, the differences in the responses of these systems are the result of differences in their yielding behavior arising from differences in the e_p values. As acceleration-sensitive systems typically undergo much yielding, their response is affected more by the strength eccentricity compared to velocity- and displacement-sensitive systems which typically experience less yielding.

The torsional deformation and element deformations of short-period, acceleration-sensitive systems are significantly affected by the strength eccentricity (Figure 4.25). The torsional response of systems with $e_p < e_s$ ($e_p = e_s/2$, $e_s/4$, and zero) is much smaller compared to the systems with $e_p = e_s$, whereas the lateral response of the former systems is slightly larger than the latter, indicating that systems with $e_p < e_s$ experience smaller effects of torsional coupling due to plan-asymmetry. The lateral and torsional deformations combine to produce smaller deformation in flexible-side elements, and larger deformations in stiff-side elements, of systems with $e_p < e_s$ compared to systems with $e_p = e_s$.

Because the yield deformations of the resisting elements are different in systems with $e_p < e_s$ compared to the systems with $e_p = e_s$ (Figure 4.4), the largest of ductility demands among all elements is affected in all the spectral regions by the strength eccentricity although the element deformations are affected primarily in the acceleration-sensitive spectral region. As shown in Figure 4.8, for systems with $e_p = e_s$ the largest ductility demand generally occurs in the flexible-side element; it occurs in the stiff-side element for systems with $e_p = 0$. Because the deformation of the stiff-side element generally increases with reduction in the strength eccentricity (Figure 4.25) and its yield deformation decreases (Figure 4.4), the maximum ductility demand, μ_{max}, generally increases. The effect of e_p value on the μ_{max} is not large, and it may be reversed for a few T/t_1 values compared to the general trend.

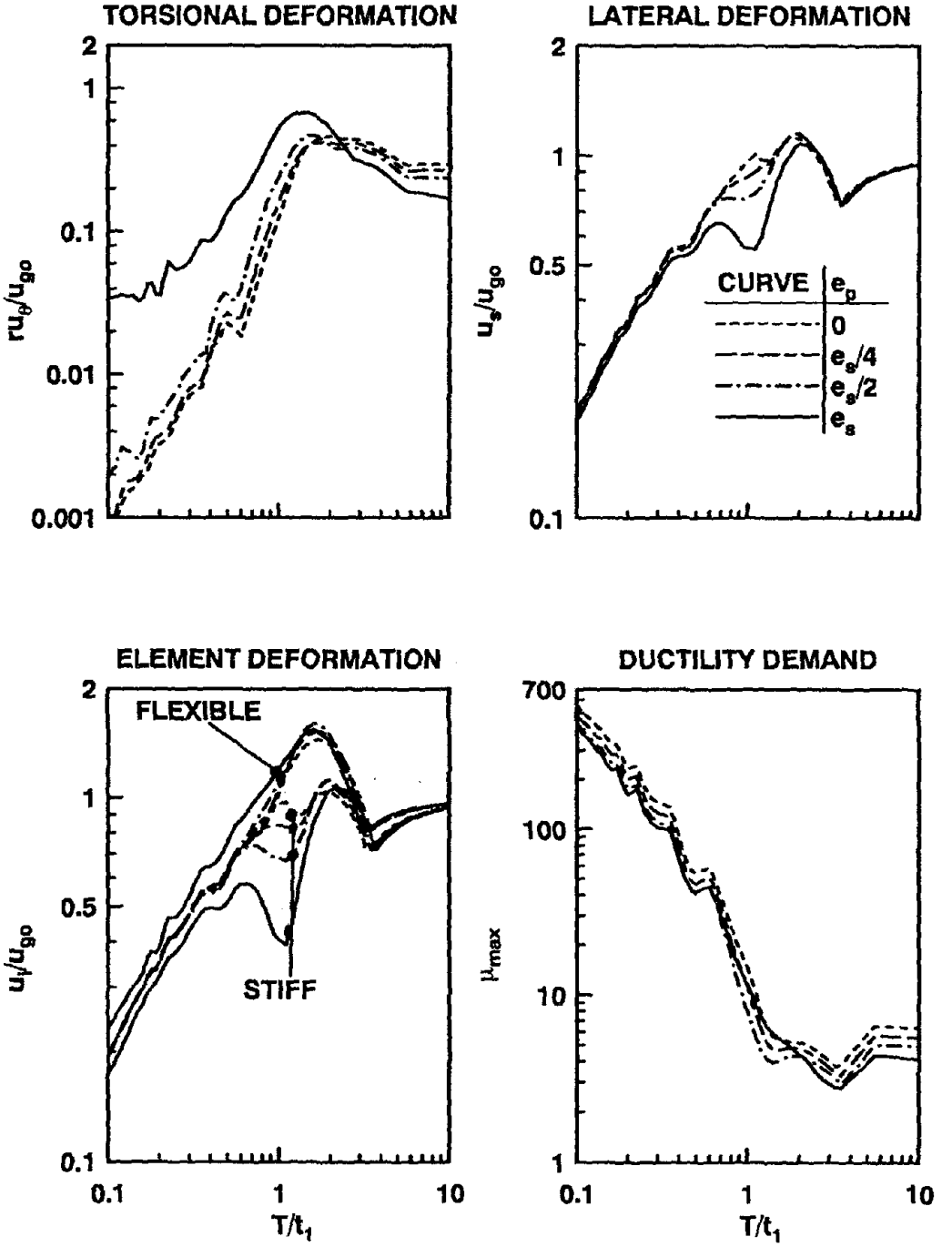

Figure 4.25 Response spectra of systems with $e_p=e_s$, $e_s/2$, $e_s/4$, and zero due to simple input; $e_s/r=0.5$, $\Omega_\theta=1.0$, $\gamma_x=0.5$, $\omega_x/\omega=1$, $c=0.25$, $O_s=1$, and $\xi=5\%$.

It was recently concluded from the response of three-element mass-eccentric systems (Figure 1.1f) that systems with strength eccentricity much smaller than their stiffness-eccentricity would experience excessive ductility demand due to torsional coupling [8]. However, another investigation arrived at the opposite conclusion for stiffness-eccentric systems (Figure 1.1c) in that torsional coupling leads only to a little additional ductility demand in systems with $e_p << e_s$ [36]. Two reasons explain this apparent contradiction. Firstly, the assumption of Reference [36] that the largest ductility demand occurs in the flexible-side element even for systems with $e_p << e_s$ is not supported by Figure 4.26. These results indicate that, whereas this assumption is generally appropriate for system with $e_p = e_s$, it is not so for systems with $e_p = 0$. The largest ductility demand in the former class of systems generally occurs in element 3, which is the outermost element on the flexible side; in the latter class of systems however, it occurs in element 1, the outermost element on the stiff side. The assumption of Reference [36] therefore led to underestimation of the ductility demand and hence to the contradictory conclusion. Secondly, as shown in Figure 4.27, the increase in ductility demand resulting from plan-asymmetry is much smaller for stiffness-eccentric systems (Figure 1.1c) of Reference [36] compared to mass-eccentric systems (Figure 1.1f) of Reference [8], both with $e_p = 0$.

4.10 Adequacy of System Parameters

As mentioned in Chapter 3, 3N parameters are required to fully characterize the inelastic response of a one-story system with N resisting elements. Most of the previous investigations have avoided the difficulty in dealing with many parameters by restricting to a particular system with a specified number, location, stiffness, and yield deformation of the resisting elements. In order to develop more generally applicable results, inelastic systems in this investigation have been characterized by the following parameters: ω, Ω_θ, e_s/r, γ_x, ω_x/ω, e_p, O_s, c, and ξ. In order to evaluate whether these parameters are sufficient to characterize the inelastic response of asymmetric-plan systems to a useful degree of accuracy, the results of preceding sections are re-examined next.

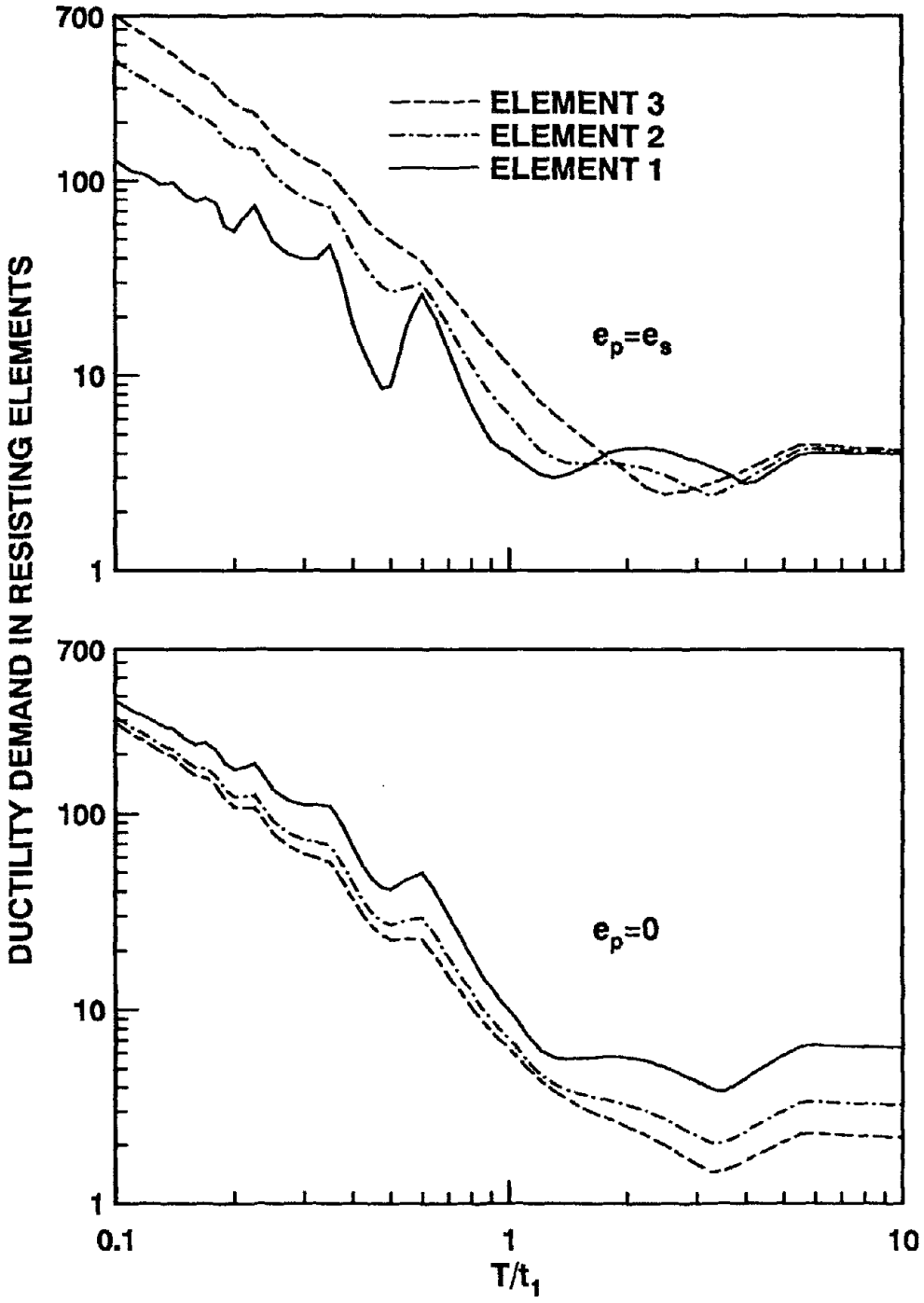

Figure 4.26 Ductility demands in resisting elements of three-element stiffness-eccentric systems due to simple input; $e_s/r=0.5$, $\Omega_\theta=1.0$, $\gamma_x=0$, $c=0.25$, $O_s=1$, and $\xi=5\%$.

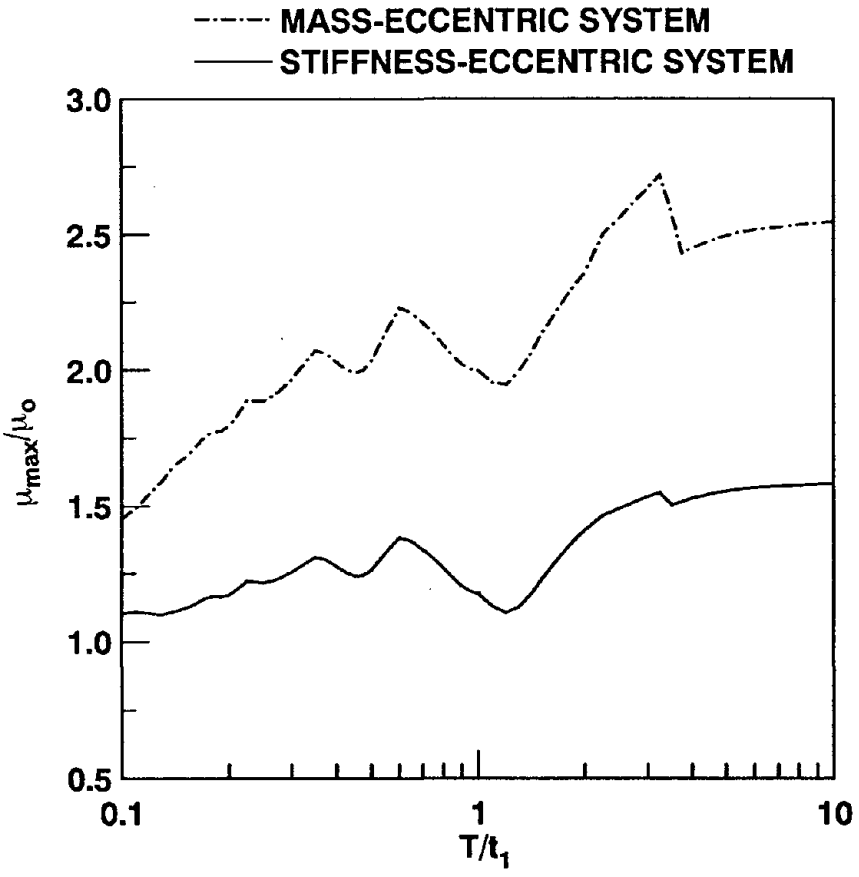

Figure 4.27 Normalized ductility demand of three-element stiffness-eccentric and three-element mass-eccentric systems due to simple input; $e_s/r=0.5$, $\Omega_\theta=1.0$, $\gamma_x=0$, $c=0.25$, $e_p=0$, $O_s=1$, and $\xi=5\%$.

The inelastic responses of stiffness-eccentric systems having two, three, and four resisting elements along the direction of ground motion (Figures 4.2a, 4.2b, and 4.2c) were compared in a preceding section. The above-listed parameters were kept the same for the three systems, although the location, stiffness, and yield deformation of individual resisting elements differed significantly in these systems. However, it was shown that the overall lateral and torsional deformations at the CS of these systems are almost identical (Figures 4.16 and 4.17). This indicates that the overall inelastic responses of different stiffness-eccentric systems would be essentially the same if the above-listed parameters are identical in these systems.

The inelastic response of mass-eccentric and stiffness-eccentric systems (Figures 4.3a and 4.3b), both with two resisting elements along the direction of ground motion and identical values of the above-listed parameters were compared in another section. Clearly the locations, stiffnesses, and yield deformations of both the resisting elements differ significantly in the two systems. It was shown that the overall responses of these two systems are essentially identical if $e_p=e_s$ (Figure 4.18), but they may differ significantly for 'strength-symmetric' ($e_p=0$) systems (Figure 4.19). Thus, the system parameters considered in this investigation are not able to distinguish between the response behavior of mass-eccentric and stiffness-eccentric systems if the strength eccentricity of these systems is much smaller than the stiffness eccentricity.

The preceding discussion indicates that the overall inelastic response of many asymmetric-plan buildings may be characterized to a useful degree of accuracy by only a few parameters -- γ_x, ω_x/ω, e_p, O_s, c -- in addition to those necessary to characterize linearly elastic systems -- ω, Ω_0, e_s/r, and ξ. Thus, the overall inelastic response of an asymmetric-plan system may be estimated by analyzing a simpler system with fewer resisting elements but having the same values of the above-mentioned system parameters as in the actual system. However, a mass-eccentric system should not be used to estimate the response of a stiffness-eccentric system and vice-versa, especially if the strength eccentricity of the system

is much smaller than the stiffness eccentricity.

5. EFFECTS OF SYSTEM PARAMETERS AND YIELDING

5.1 Introduction

The inelastic responses of one-story, asymmetric-plan systems with plan-wise distribution of stiffness and strength chosen in accordance with the conclusios of Chapter 4 to ensure wide applicability of results are presented and analyzed with the objective of identifying the influence of system parameters: uncoupled lateral vibration period, uncoupled torsional-to-lateral frequency ratio, stiffness eccentricity, relative values of the strength and stiffness eccentricities, and yield factor. Furthermore, the influence of yielding on the response of asymmetric-plan systems is examined. In particular, we determine whether the well known relationship between the response of yielding and elastic SDF systems are also applicable to asymmetric-plan systems.

5.2 System Considered

Consider the idealized one-story building of Figure 5.1, which includes resisting elements oriented along the direction of ground motion as well as perpendicular to the ground motion; the latter are included to ensure widely applicable results (Chapter 4). Because the system response is not sensitive to the number of elements along the direction of ground motion, two elements are sufficient (Chapter 4).

As shown in Chapter 4, parameters γ_x and ω_x/ω affect the inelastic response of short-period, acceleration-sensitive systems with e_p=e_s to a significant degree; but the response of medium-period, velocity-sensitive and long-period, displacement-sensitive systems is affected very little. However, the response of 'strength-symmetric' (e_p=0) systems is essentially unaffected by these parameters over the entire range of period values. Because many asymmetric-plan buildings designed according to building codes possess strength eccentricity much smaller than the stiffness eccentricity [36], and respond like 'strength-symmetric' (e_p=0) systems (Chapter 7), the response of such buildings would also be essentially independent of γ_x and ω_x/ω. Thus, in the present chapter and subsequent chapters these parameters

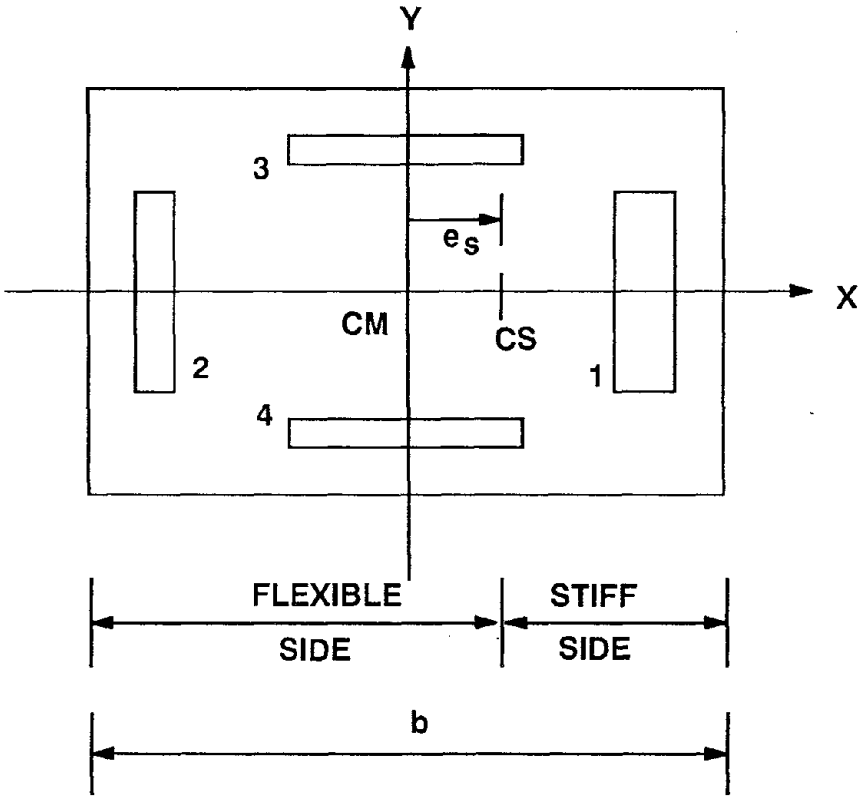

Figure 5.1 Selected one-story asymmetric-plan system; elements 1 and 2 are located equidistant from the CM, and system parameters γ_x and ω_x/ω are fixed at 0.5 and 1 respectively.

have been fixed at values that are representative of many actual buildings: γ_x=0.5 and ω_x/ω=1.

Consequently, the inelastic response of the system of Figure 5.1 is characterized by the strength eccentricity, e_p, and the yield factor, c, in addition to all the parameters -- ω, Ω_θ, e_s/r, and ξ -- characterizing the elastic system; note that O_s is selected as one.

5.3 Response Characteristics

Figures 5.2 to 5.6 show response histories for the asymmetric-plan ($e_s \neq 0$) system of Figure 5.1 and its corresponding symmetric-plan (e_s=0) system -- a SDF system -- subjected to the simple input. Such response histories are presented for elastic systems and inelastic systems with four values of c=0.75, 0.5, 0.25, and 0.1. Also included in these figures for inelastic systems are the histories of yielding in resisting elements and histories of instantaneous values of the system parameters Ω_θ and e_s/r.

In symmetric-plan (e_s/r=0) systems, which respond as SDF systems, all the elements oriented along the direction of ground motion yield simultaneously and elements oriented perpendicular to the ground motion do not undergo any deformation and thus they experience no yielding. On the other hand, in asymmetric-plan ($e_s/r \neq 0$) systems, elements 1 and 2 oriented along the ground motion direction yield, unload, or re-yield with a time lag. Moreover, the torsional component of the response produces deformation in elements 3 and 4, causing these elements to yield, unload, or re-yield simultaneously; when the element on one side of the CS experiences positive yielding, the other element undergoes negative yielding, and vice versa. The duration of yielding in asymmetric-plan as well as symmetric-plan systems increases as the yield factor, c, reduces, i.e., as the strength of the system decreases and it is excited more and more into the inelastic range.

The response histories for inelastic systems (Figures 5.3 to 5.6) show that as the yield factor decreases, the torsional deformation decreases significantly and the lateral deformation history of the asymmetric-plan system becomes increasingly similar to that of the

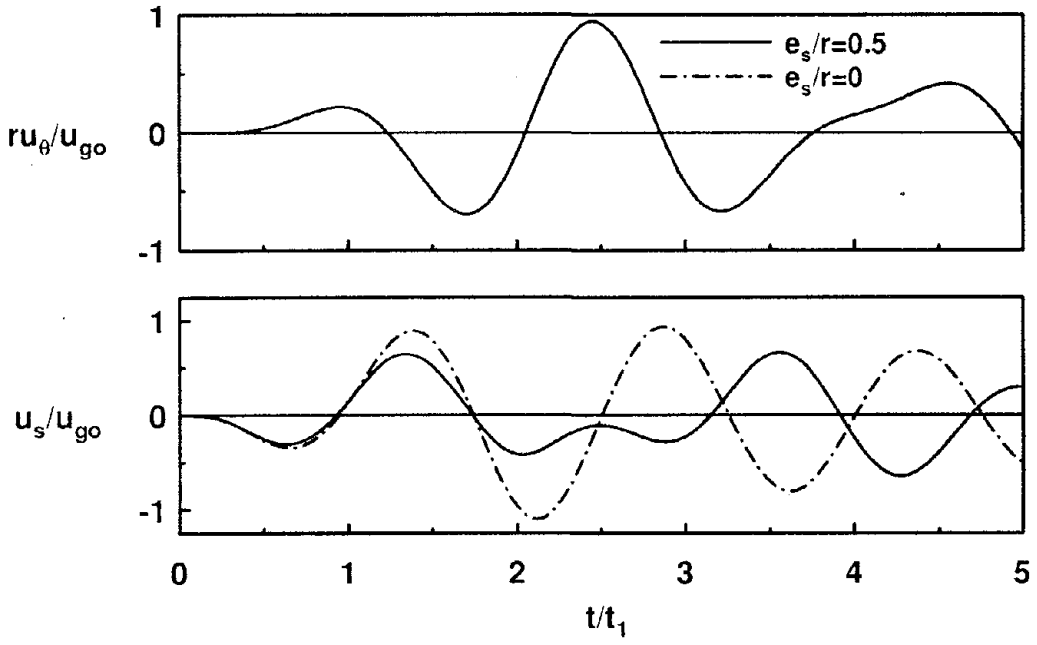

Figure 5.2 Time variation of torsional and lateral deformations of elastic system due to simple input; $T/t_1 = 1.5$, $e_s/r = 0.5$, $\Omega_\theta = 1$, and $\xi = 5\%$.

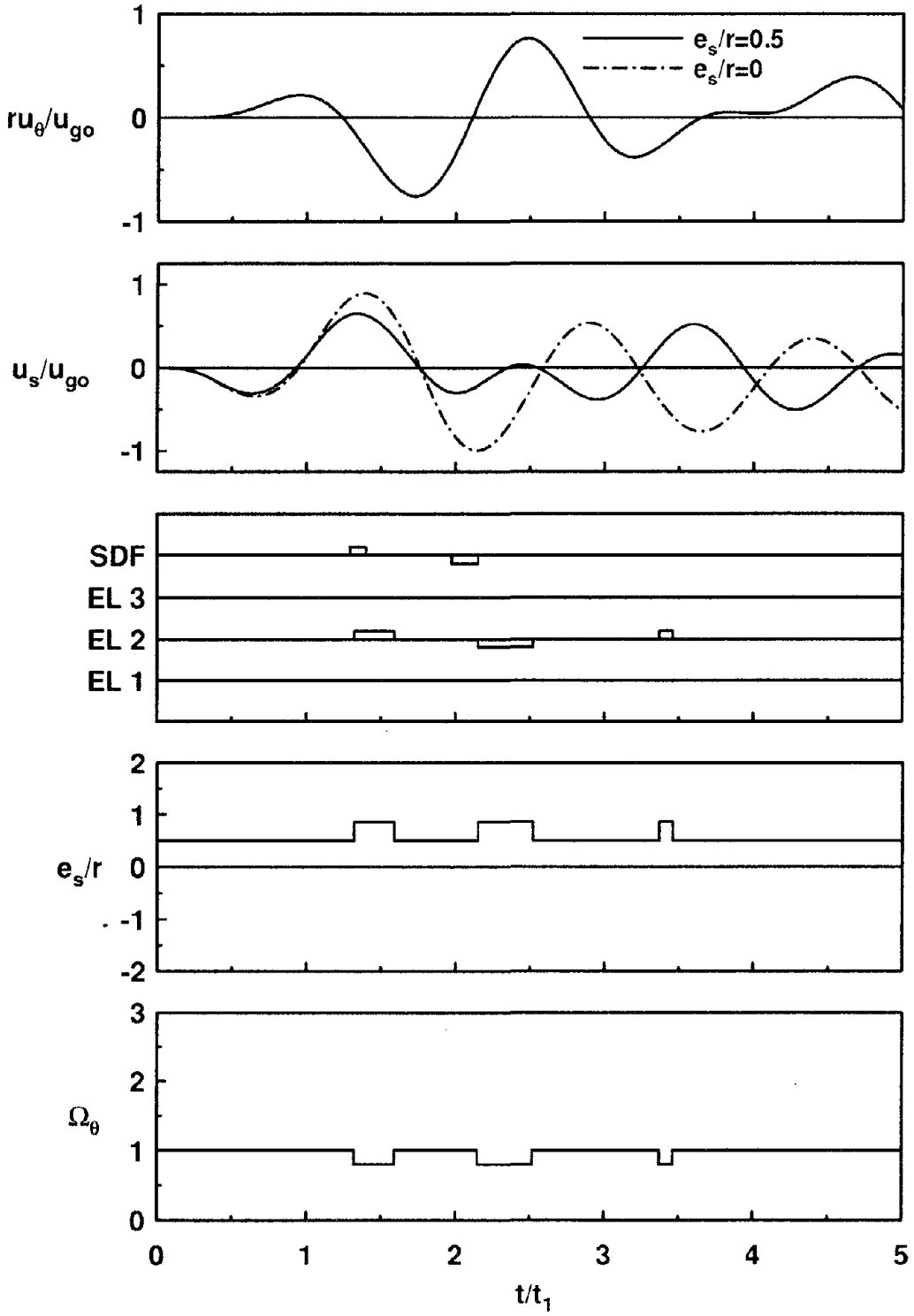

Figure 5.3 Time variation of torsional and lateral deformations, element yielding, stiffness eccentricity, and frequency ratio of inelastic system due to simple input; $T/t_1 = 1.5$, e_p=e_s, $c = 0.75$, $e_s/r = 0.5$, $\Omega_\theta = 1$, and $\xi = 5\%$.

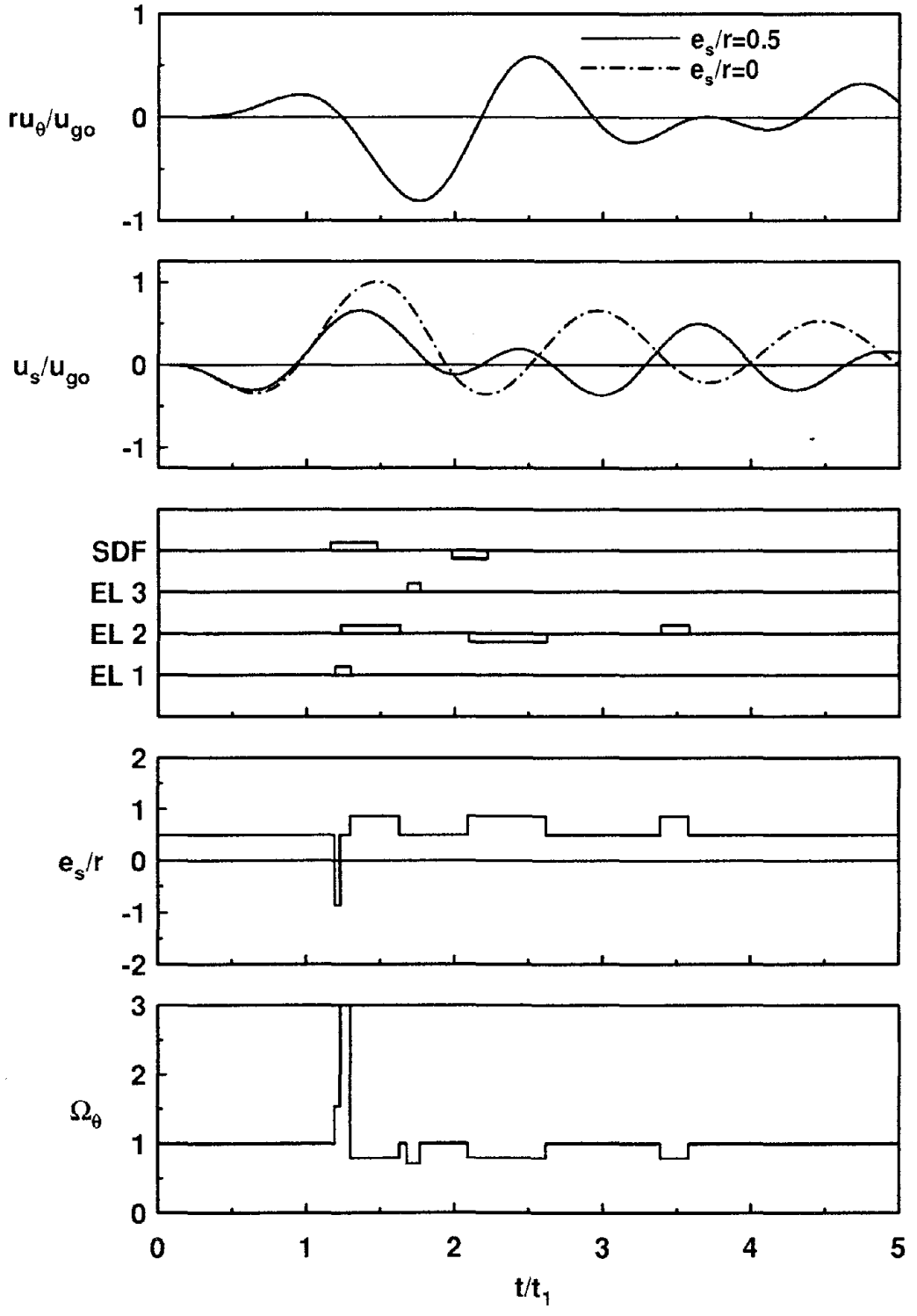

Figure 5.4 Time variation of torsional and lateral deformations, element yielding, stiffness eccentricity, and frequency ratio of inelastic system due to simple input; $T/t_1 = 1.5$, $e_p=e_s$, $c = 0.5$, $e_s/r = 0.5$, $\Omega_\theta = 1$, and $\xi = 5\%$.

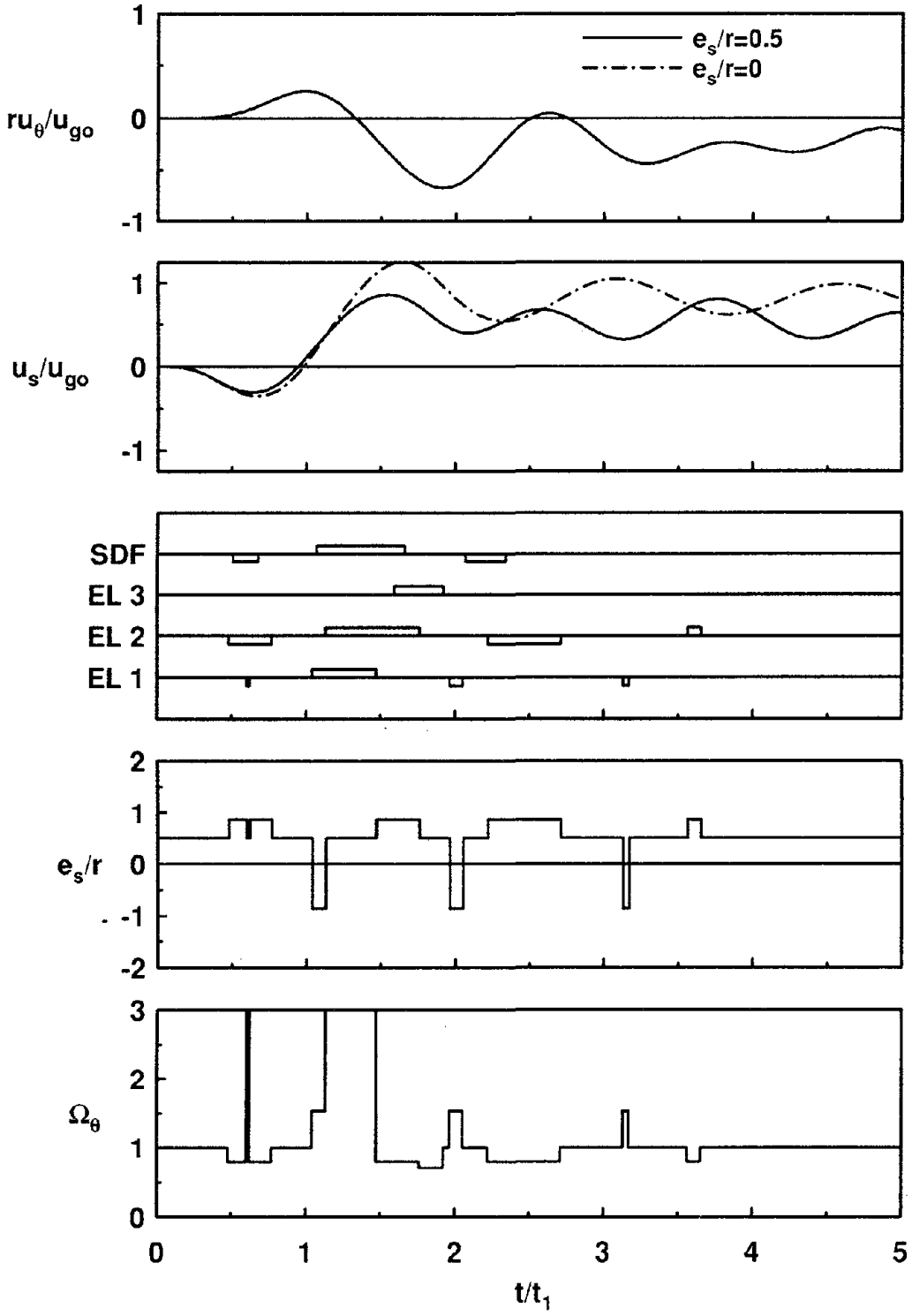

Figure 5.5 Time variation of torsional and lateral deformations, element yielding, stiffness eccentricity, and frequency ratio of inelastic system due to simple input; $T/t_1 = 1.5$, $e_p=e_s$, $c = 0.25$, $e_s/r = 0.5$, $\Omega_\theta = 1$, and $\xi = 5\%$.

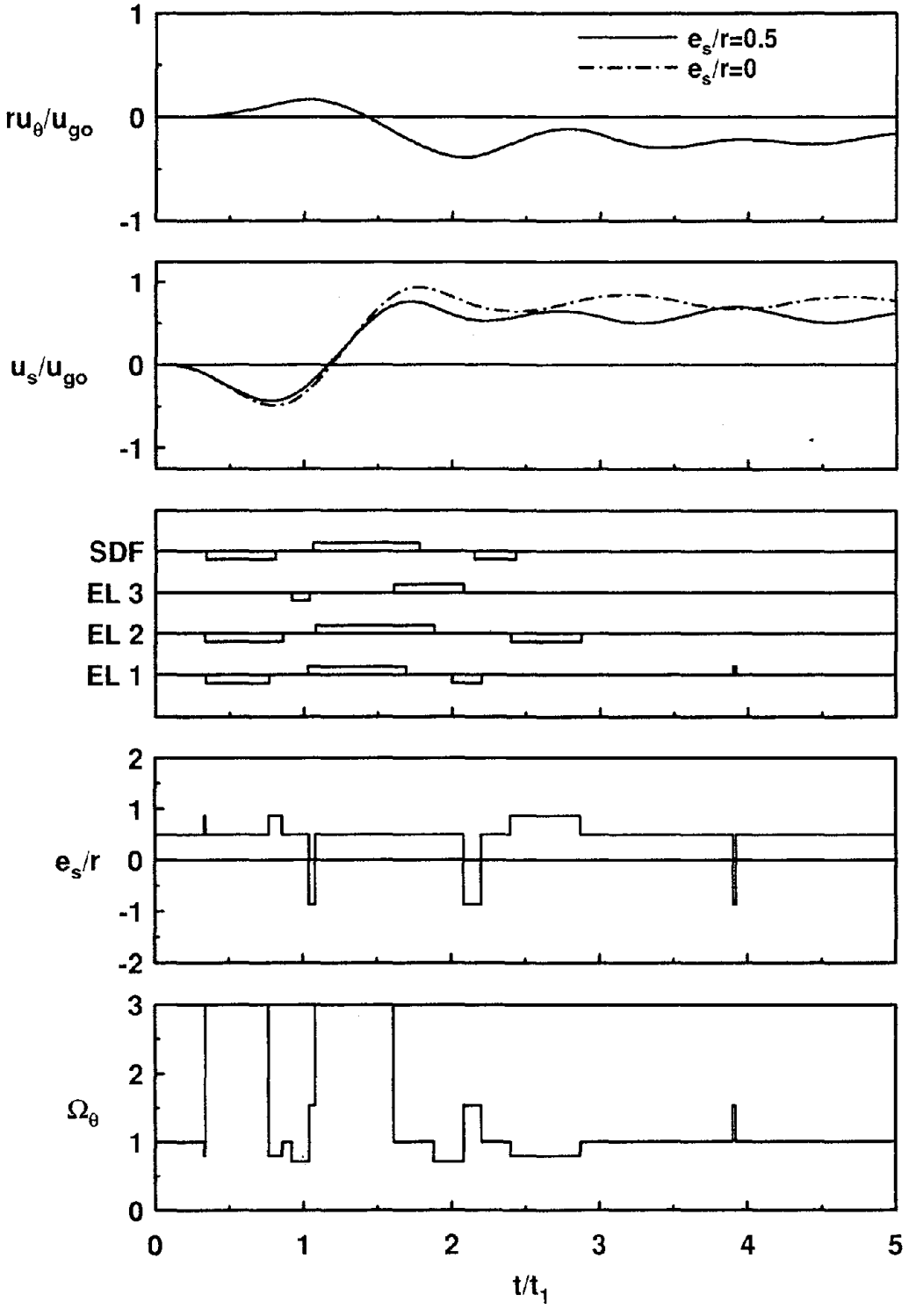

Figure 5.6 Time variation of torsional and lateral deformations, element yielding, stiffness eccentricity, and frequency ratio of inelastic system due to simple input; $T/t_1 = 1.5$, e_p=e_s, $c = 0.1$, $e_s/r = 0.5$, $\Omega_\theta = 1$, and $\xi = 5\%$.

corresponding symmetric-plan system. This indicates that as the asymmetric-plan system is excited increasingly into the inelastic range, it behaves more and more like the corresponding symmetric-plan system. While this statement has been made before [7,19,20], the plot of Figure 5.6 provides an especially clear demonstration. Several factors possibly contribute to this behavior, the more significant of which are mentioned next.

In a yielding system, instantaneous values of the stiffness eccentricity, e_s, and the uncoupled torsional-to-lateral frequency ratio, Ω_θ, which have been shown to affect significantly the response of elastic systems [19,20], vary with time. In the four-element system of Figure 5.1, the CS abruptly shifts from its initial position (e_s/r=0.5) to the location of element 1 when the element 2 is yielding and to the location of the element 2 when element 1 is yielding. Thus, the instantaneous CS may move farther away from the CM or abruptly shift to the opposite side, leading to cancellation of some of the effects of increased stiffness eccentricity. The instantaneous value of Ω_θ becomes infinite during time-durations when the lateral stiffness is zero while the system still has some torsional stiffness, and the system behaves as if it is laterally very flexible or torsionally rigid. With decreasing yield factor, the system tends to behave as torsionally-rigid for longer time durations (Figures 5.3 to 5.6), and the above-mentioned cancellation of stiffness eccentricity effects become increasingly significant. As a result, the torsional deformation decreases as the system is excited more and more into the inelastic range (Figures 5.3 to 5.6).

Figures 5.3 to 5.6 show that the instantaneous value of the frequency ratio, Ω_θ, may become smaller or larger compared to its initial elastic value, which implies that the yielding system may become torsionally-flexible or torsionally-stiff compared to the initial elastic system. As a result, the uncoupled torsional and lateral frequencies which are identical in a system with initial elastic value of Ω_θ =1 may temporarily become separated (Figures 5.3 to 5.6); similarly it seems possible for the uncoupled torsional and lateral frequencies of a system with $\Omega_\theta \neq 1$ to become close for short time-durations. Therefore, as will be demonstrated in Chapter 6, the large effects of torsional coupling in elastic systems with Ω_θ=1 are reduced

by inelastic behavior.

The observations of this section are based on the response of medium-period, velocity-sensitive systems with equal torsional and lateral vibration frequencies and resisting elements in both lateral directions. They are also expected to apply to systems with much different torsional and lateral frequencies, because their torsional response is smaller in the elastic range and inelastic behavior is likely to reduce it further. However, these observations generally would not apply to the following situations: (1) systems with resisting elements only along the direction of ground motion because such systems undergo larger torsional deformation (Chapter 4), and even with strongly inelastic behavior, the lateral deformation history may not become similar to that of the corresponding symmetric-plan system [35]; (2) short-period, acceleration-sensitive systems with larger eccentricities which tend to undergo larger torsional deformations because their torsional stiffness may become zero for extended time durations (Chapter 4); and (3) long-period, displacement-sensitive systems because, as will be demonstrated later, the lateral deformation of such systems is affected very little by yielding or plan-asymmetry; although, the torsional deformation of such systems is reduced by yielding in a manner similar to medium-period, velocity-sensitive systems.

5.4 Effects of System Parameters

5.4.1 Stiffness eccentricity

Presented in the form of response spectra are the peak values of three response quantities: the normalized lateral and torsional displacements at the CS, u_s/u_{go} and ru_θ/u_{go}; and the normalized value of the largest of peak deformations among all resisting elements, $u_{\max}/u_{go}$. Such response spectra are presented in Figures 5.7 to 5.10 for e_s/r=0, 0.05, 0.2, and 0.5 with fixed values of Ω_θ and c. For inelastic systems, two values of strength eccentricity, e_p, are considered: e_p=e_s and e_p=0. The results are presented for the half-cycle displacement pulse (or simple input) and the El Centro ground motion. The general trends gleaned from the responses to the simple input are described first followed by the differences

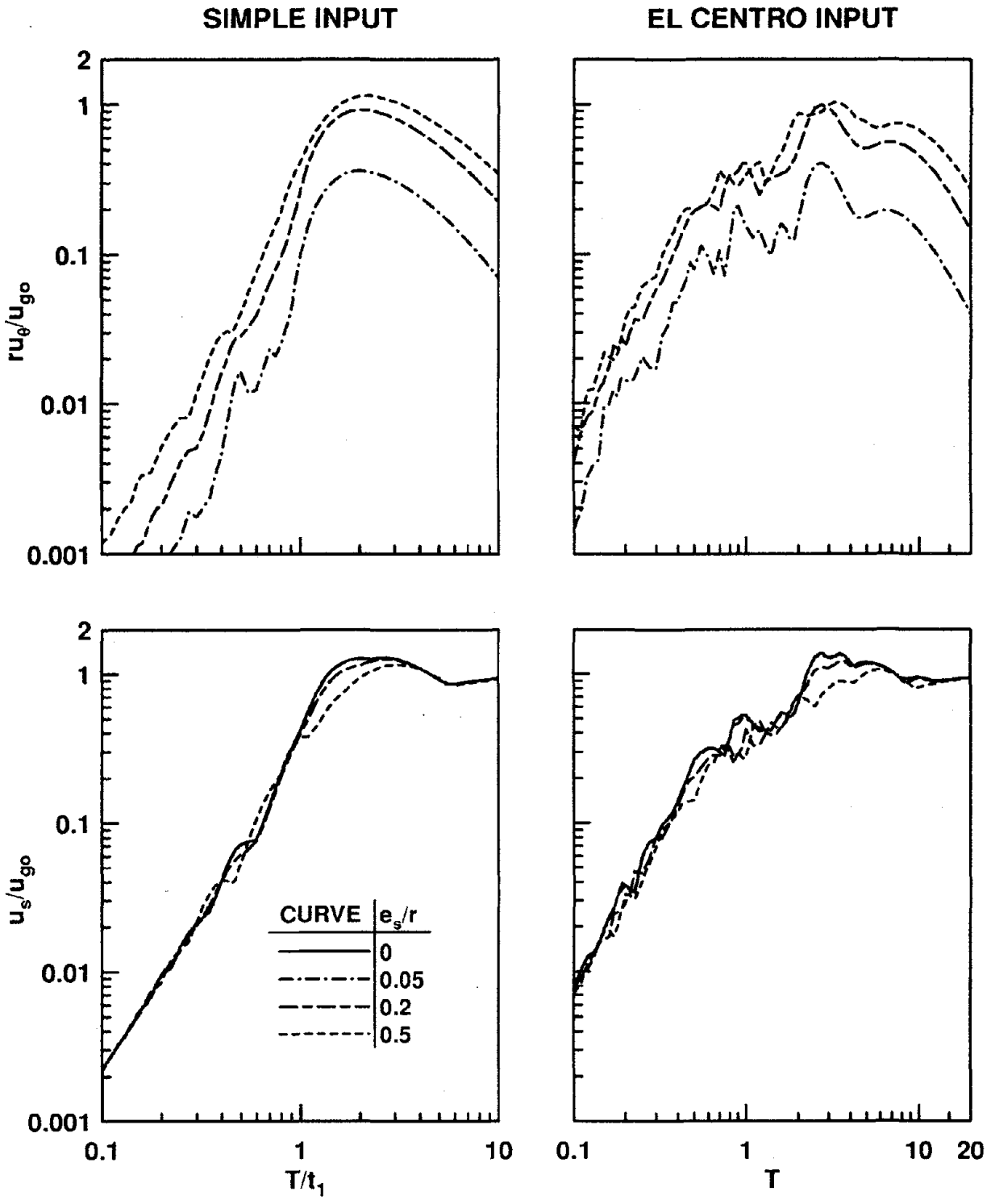

Figure 5.7 Peak lateral and torsional deformations of elastic systems with e_s/r = 0, 0.05, 0.2, and 0.5; Ω_θ = 1 and ξ = 5%.

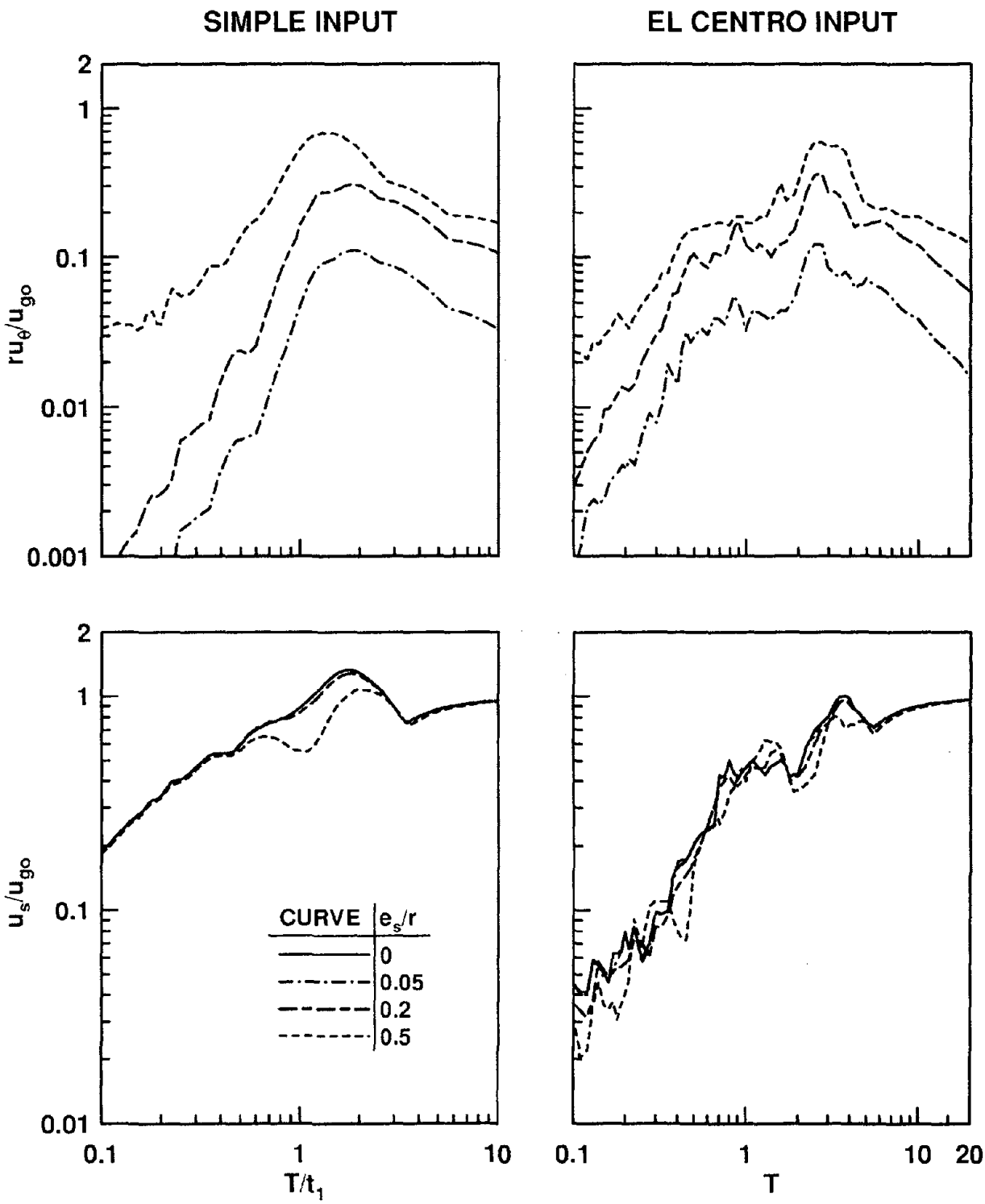

Figure 5.8 Peak lateral and torsional deformations of inelastic systems with e_p=e_s and c = 0.25; e_s/r = 0, 0.05, 0.2, and 0.5; Ω_θ = 1 and ξ = 5%.

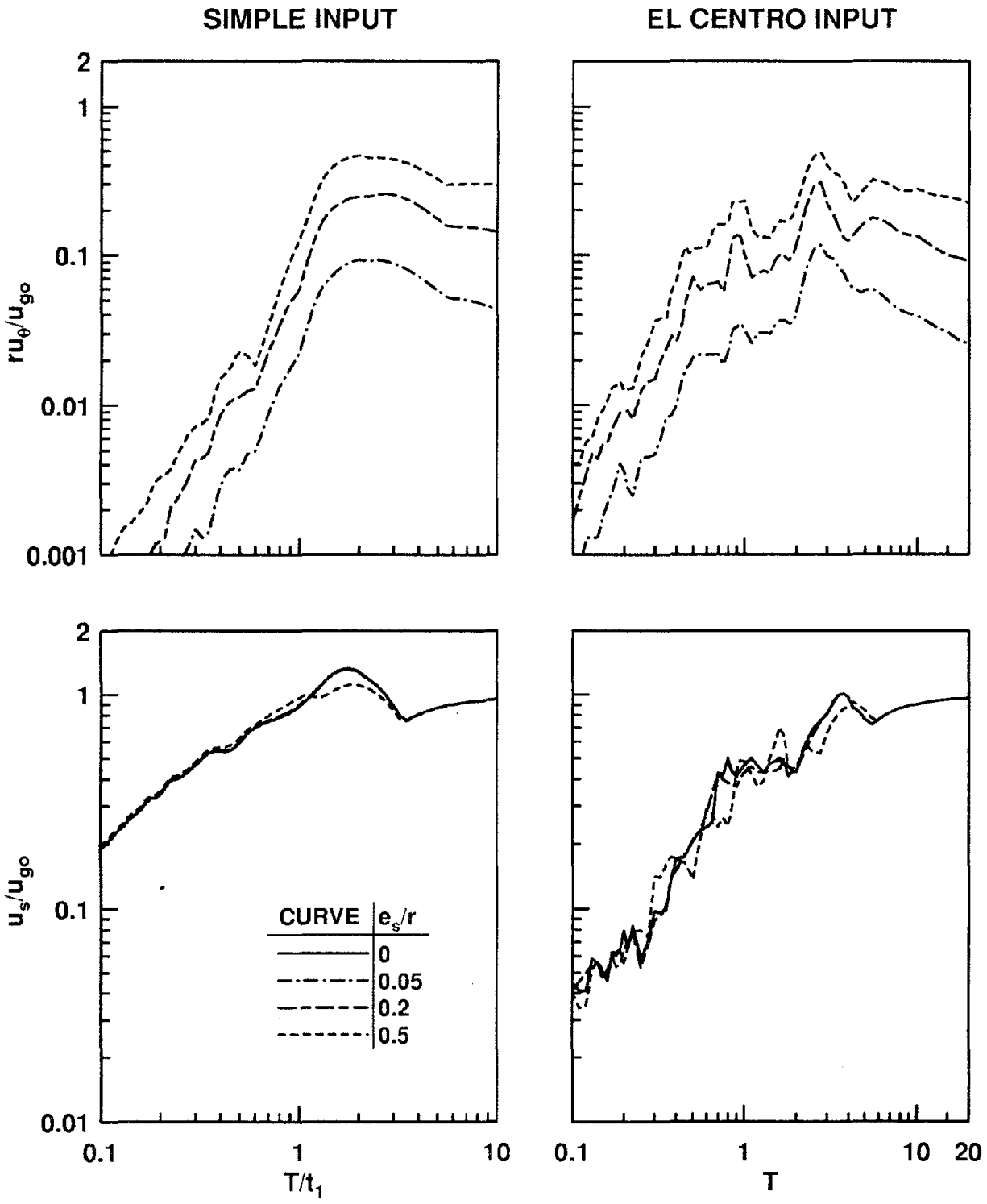

Figure 5.9 Peak lateral and torsional deformations of inelastic systems with e_p=0 and c = 0.25; e_s/r = 0, 0.05, 0.2, and 0.5; Ω_θ = 1 and ξ = 5%.

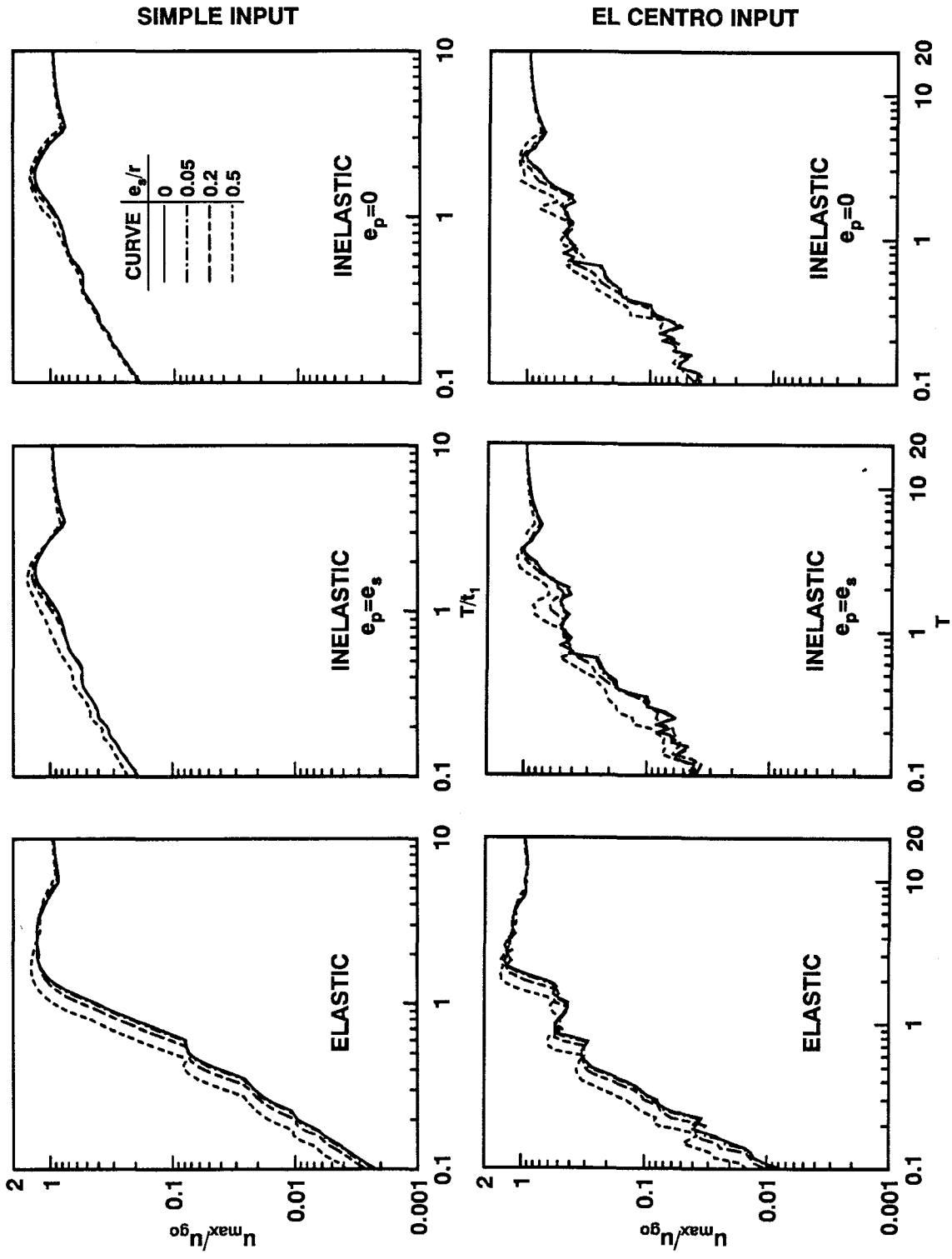

Figure 5.10 Largest of peak element deformations of elastic systems and inelastic systems (c = 0.25; e_p = 0 and e_s); e_s/r = 0, 0.05, 0.2, and 0.5; Ω_θ = 1 and ξ = 5%.

arising from the complexity of actual earthquake motions.

The system response to the simple excitation indicates that the peak deformation response of elastic as well as inelastic asymmetric-plan systems may be significantly influenced by the stiffness eccentricity, e_s/r (Figures 5.7 to 5.10). The torsional deformation increases with increasing stiffness eccentricity for a wide range of structural vibration periods. For very-short-period, acceleration-controlled, elastic systems the torsional deformation increases linearly with e_s/r (Appendix D); inelastic systems in the same period range may experience significantly larger increase in torsional deformation (Figure 5.8), especially for larger e_s/r, because the torsional stiffness of such systems may become zero for extended time-durations (Chapter 4). The torsional deformation of very-long-period, displacement-sensitive, elastic systems tends to zero regardless of the e_s/r value (Appendix D); however, such may not be the case for inelastic systems as indicated by the flattening of the curves in Figures 5.8 and 5.9. Furthermore, for systems with small values of eccentricities, the largest increase in the torsional deformation with increasing e_s/r occurs in the medium-period, velocity-sensitive spectral region compared to other spectral regions; this becomes apparent by comparing the torsional deformations of systems with e_s/r=0.05 with the zero torsional deformation for symmetric-plan (e_s/r=0) systems (Figures 5.7 to 5.9). However, as the stiffness eccentricity becomes large, short-period, acceleration-sensitive systems may experience larger increase in the torsional deformation with increasing e_s/r compared to systems in other spectral regions (Figure 5.8). Among inelastic systems, the increase in torsional deformation with increasing e_s/r tends to be smaller for 'strength-symmetric' (e_p=0) systems (Figure 5.9) compared to systems with equal strength and stiffness eccentricities (e_p=e_s) (Figure 5.8), with this difference between the two types of systems being most pronounced in the acceleration-sensitive spectral region.

The lateral deformation is affected primarily in the velocity-sensitive region of the spectrum where it generally decreases with increase in the stiffness eccentricity (Figures 5.7 to 5.9). In particular, significant decrease in the response occurs only for very large values of

stiffness eccentricities (e_s/r=0.5); response of systems with small e_s/r values (e_s/r=0.05, and 0.2) is essentially identical to that of the symmetric-plan system (e_s/r=0). The stiffness eccentricity affects the response of elastic and inelastic systems with equal strength and stiffness eccentricities (e_p=e_s) in a similar manner (Figures 5.7 and 5.8); however, the response of 'strength-symmetric' (e_p=0) systems is affected to a much smaller degree (Figure 5.9). In the acceleration-sensitive and displacement-sensitive spectral regions the lateral deformation is essentially unaffected by the stiffness eccentricity (Figures 5.7 to 5.9). In the limit, as the vibration period becomes very short or very long, it can be analytically demonstrated that the lateral deformation of an elastic system is independent of the stiffness eccentricity; the limiting value for long periods is the same as the peak ground displacement and that for short periods is zero (Appendix D). For inelastic systems, the same limiting value is valid for long periods; but it tends to be larger for short periods (Figures 5.8 and 5.9). The observation about the lateral deformation being independent of the stiffness eccentricity carries over to inelastic systems in the acceleration- and displacement-sensitive spectral regions (Figures 5.8 and 5.9). In the transition regions of the spectrum, the lateral deformation depends on the stiffness eccentricity in a complex manner, increasing for some period values and decreasing for others; however, the dependence is small.

These observations of how stiffness eccentricity influences structural response in the various spectral regions of the simple input generally carry over to the corresponding spectral regions of the El Centro excitation. However, the detailed trends are more complicated because the response spectrum of an actual ground motion is irregular compared to the relatively smooth shape for the simple input. Because of this irregularity, the response is affected more by the differences in the natural vibration periods, T_1 and T_2, of the asymmetric-plan system compared to the vibration period, T, of the corresponding symmetric-plan system. Depending on the variation of the response spectrum in the neighborhood of T, the spectral ordinates associated with the periods T_1 and T_2 may increase or decrease by varying degrees. Thus, it is possible that the lateral deformation of an elastic, asymmetric-plan

system may even become slightly larger than that of the corresponding symmetric-plan system (Figure 5.7). This tendency is even greater for inelastic systems (Figures 5.8 and 5.9) for reasons that are not apparent. The resulting complications in the trends show up more strongly, as will be seen later, when the response spectra are plotted for different values of Ω_θ. Such is the case because the uncoupled torsional-to-lateral frequency ratio, Ω_θ, affects the coupled vibration periods to a larger degree compared to the stiffness eccentricity ratio, e_s/r.

The deformation of a resisting element arises from the combined effects of lateral deformation, u_s, at the CS and the torsional deformation, u_θ, the peaks of which generally do not occur at the same time instant. The increase in torsional deformation with increasing stiffness eccentricity combined with decrease in lateral deformation results in increased u_{max}, the largest of peak deformations among all elements, because of plan-asymmetry (Figure 5.10). This increase in u_{max} is observed for systems over a wide range of vibration periods with isolated exceptions -- few for the simple input and more for the El Centro input. The increase in u_{max} with increasing e_s/r is larger for elastic systems compared to inelastic systems, being especially small for 'strength-symmetric' (e_p=0) systems relative to systems with equal strength and stiffness eccentricities (e_p=e_s) (Figure 5.10). How significant in design application is the increase in element deformation due to plan-asymmetry is an issue that remains to be addressed. Among the various spectral regions, the increase in u_{max} is generally more significant in the acceleration- and velocity-sensitive regions of the spectrum, whereas it is negligible for displacement-sensitive systems; in the latter case the u_{max} is essentially equal to the peak ground displacement. All of the aforementioned trends regarding increased element deformation in asymmetric-plan systems are closely tied to how the torsional deformation is affected by the stiffness eccentricity in various regions of the spectrum (Figures 5.7 to 5.9).

5.4.2 Frequency Ratio

Another key parameter that influences the response of asymmetric-plan systems is Ω_θ, the uncoupled torsional-to-lateral frequency ratio. This is apparent from Figures 5.11 to 5.14 where the response quantities are presented in the form of response spectra for several values of Ω_θ=0.8, 1, 1.25, and 2 but e_s/r and c are kept fixed. System responses to the simple input and El Centro excitation were computed for the same set of system parameters; however, when required for clarity, some of the curves have been omitted from the figures associated with the El Centro excitation.

The computed responses to the simple excitation show that, as Ω_θ decreases, implying that the system becomes increasingly flexible in torsion, the torsional deformation tends to increase over a wide range of structural vibration periods, with this effect being largest for acceleration-sensitive systems, smaller for velocity-sensitive and even more so for displacement-sensitive systems (except for inelastic systems with e_p=0) (Figures 5.11 to 5.13). The torsional deformation of very-short-period, acceleration-sensitive, elastic systems is proportional to the factor $1/\Omega_\theta^2$ (Appendix D). Thus, the torsional deformation of elastic systems increases at this ratio as Ω_θ decreases (Figure 5.11); however, inelastic systems may experience significantly larger increase in deformation with decreasing Ω_θ (Figures 5.12 and 5.13). The torsional deformation of very-long-period, displacement-sensitive, elastic systems tends to zero regardless of the Ω_θ value (Appendix D); however, such may not be the case for inelastic systems as indicated by flattening of curves in Figures 5.12 and 5.13. Among inelastic systems, the increase in torsional deformation of 'strength-symmetric' (e_p=0) systems (Figure 5.13) is generally smaller compared to systems with e_p=e_s (Figure 5.12).

The results for the simple input show that the lateral deformation of medium-period, velocity-sensitive systems tends to decrease, with a few exceptions, as Ω_θ decreases (Figures 5.11 to 5.13). Furthermore, as mentioned previously, the lateral deformation of acceleration-sensitive and displacement-sensitive systems is essentially unaffected by Ω_θ. In

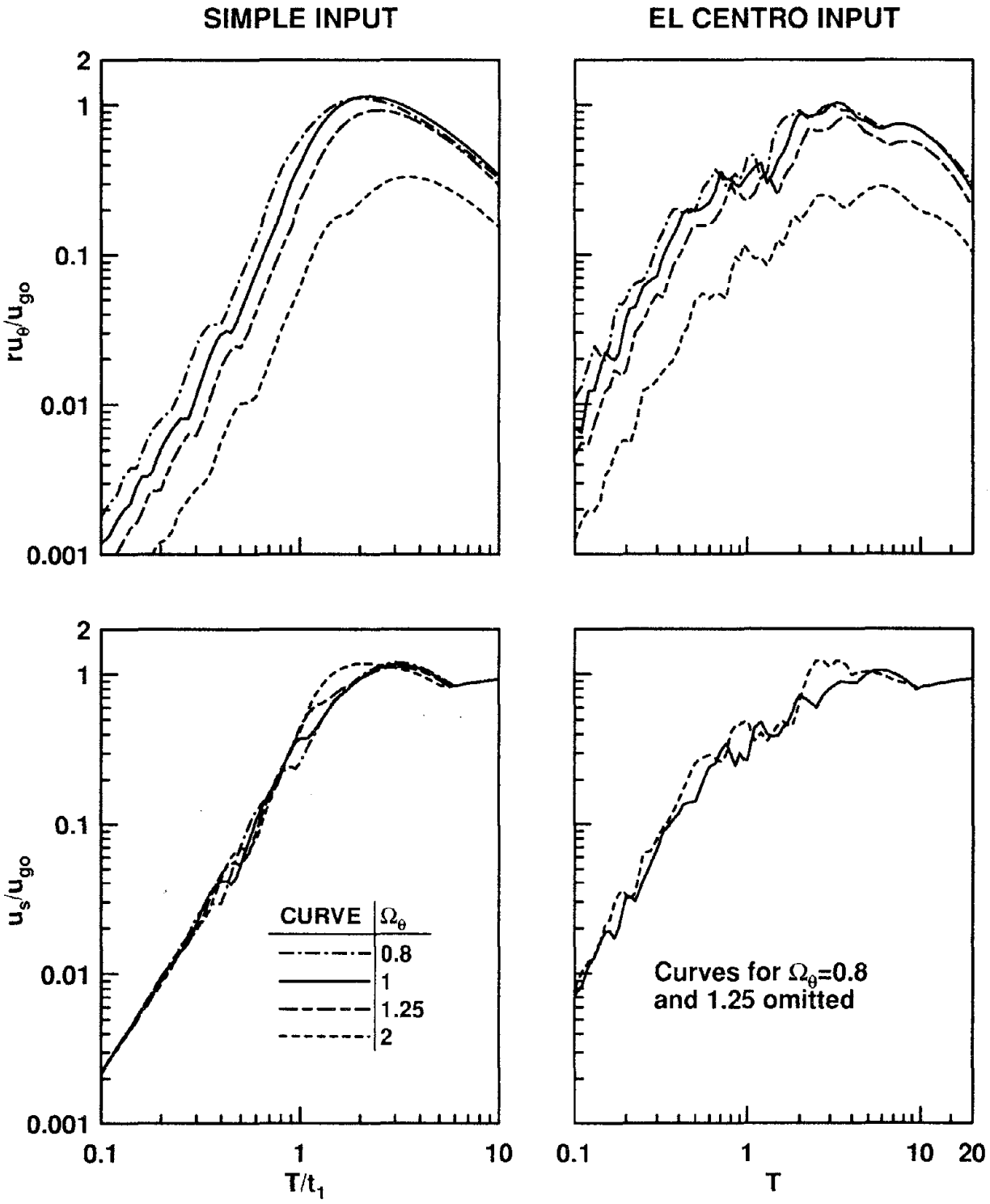

Figure 5.11 Peak lateral and torsional deformations of elastic systems with Ω_θ = 0.8, 1, 1.25, and 2; e_s/r = 0.5 and ξ = 5%.

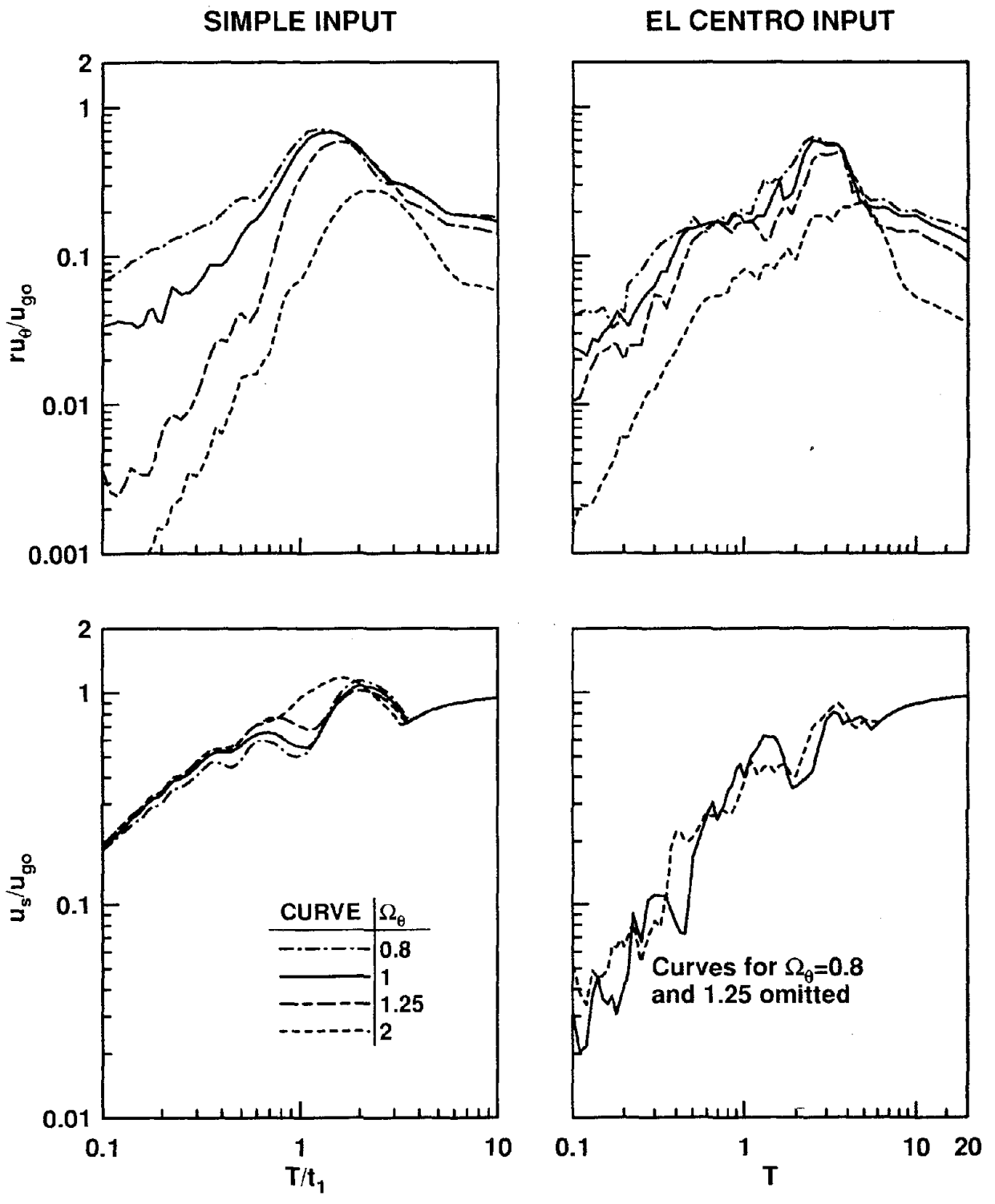

Figure 5.12 Peak lateral and torsional deformations of inelastic systems with e_p=e_s and c = 0.25; Ω_θ = 0.8, 1, 1.25, and 2; e_s/r = 0.5 and ξ = 5%.

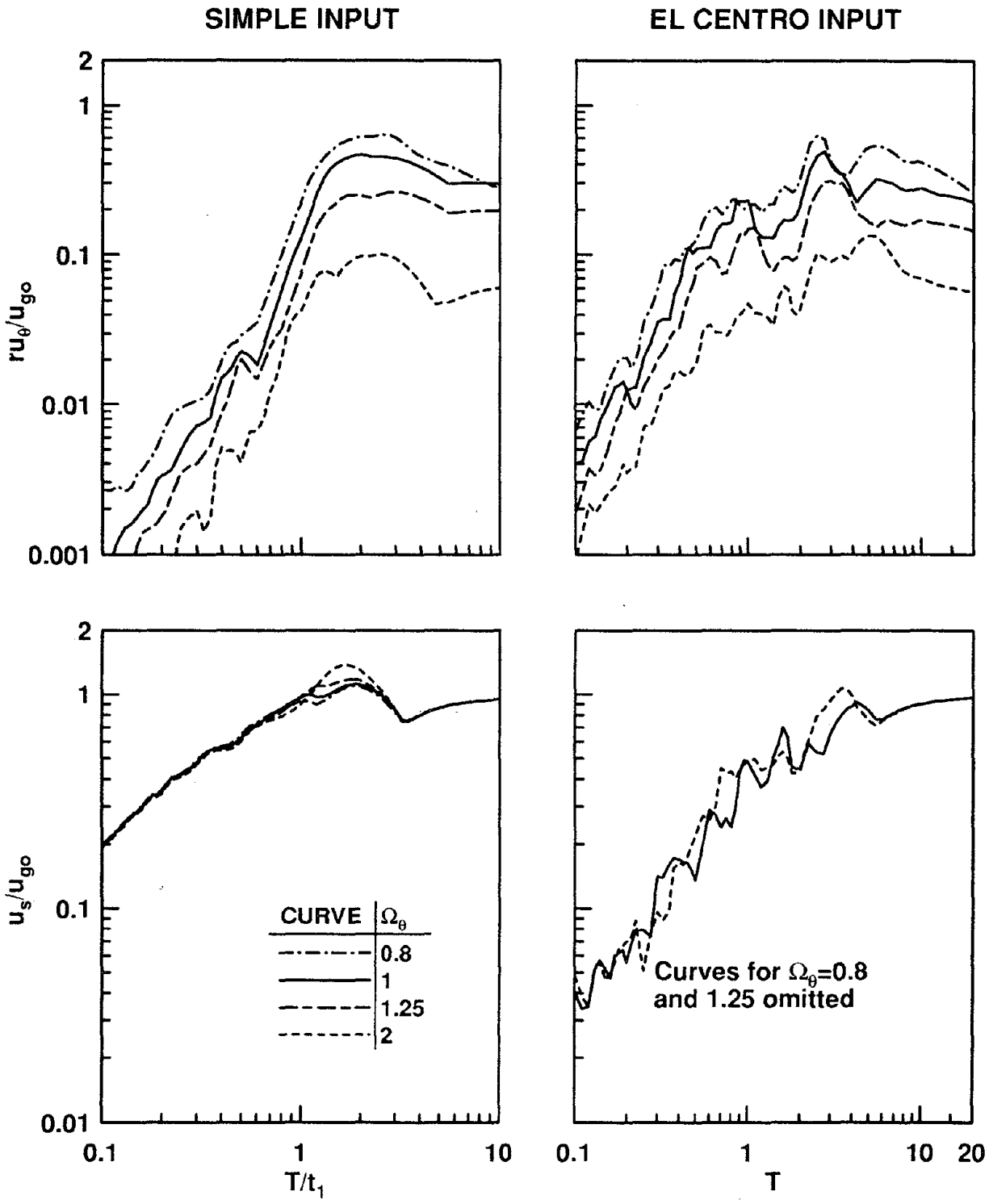

Figure 5.13 Peak lateral and torsional deformations of inelastic systems with e_p=0 and c = 0.25; Ω_θ = 0.8, 1, 1.25, and 2; e_s/r = 0.5 and ξ = 5%.

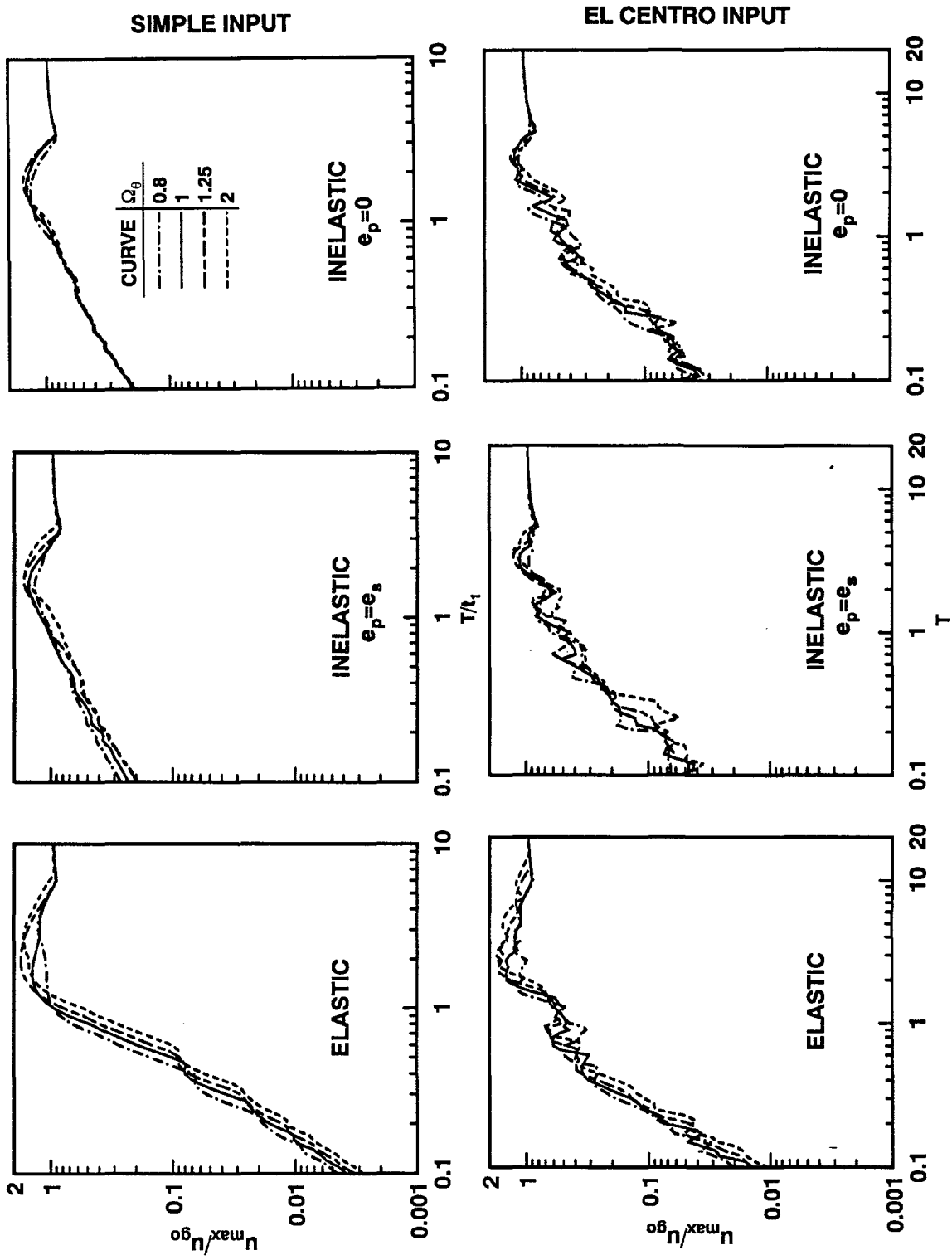

Figure 5.14 Largest of peak element deformations of elastic systems and inelastic systems (c = 0.25; e_p = 0 and e_s); Ω_θ = 0.8, 1, 1.25, and 2; e_s/r = 0.5, and ξ = 5%.

the limit, as the vibration period becomes very short or very long it has been analytically shown that the lateral deformation of elastic systems is independent of Ω_θ (Appendix D); the limiting value is equal to the peak ground displacement for very long periods and zero for very short periods. In the transition regions of the spectrum, the lateral deformation depends on Ω_θ in a complex manner, increasing for some period values and decreasing for others; however, the dependence is small. These effects of Ω_θ on the lateral deformation of inelastic systems with equal strength and stiffness eccentricities (e_p=e_s) (Figure 5.12) are generally similar to those for elastic systems (Figure 5.11); however, the lateral deformation of 'strength-symmetric' (e_p=0) systems (Figure 5.13) is affected to a much smaller degree.

The above mentioned trends in the lateral and torsional deformations of systems combine to produce increasing element deformation, u_{max}, with decreasing Ω_θ for systems in the acceleration-sensitive region of the spectrum (Figure 5.14). For systems in the velocity-sensitive and its associated transition regions, however, these trends may be reversed primarily because of reduction in the lateral deformation. Furthermore, in the displacement-sensitive region, u_{max} is affected very little by Ω_θ. The maximum element deformations of inelastic systems are affected by Ω_θ much less compared to elastic systems, especially in case of the simple input (Figure 5.14). Between the two types of inelastic systems, 'strength-symmetric' (e_p=0) systems are affected by Ω_θ to a much smaller degree, especially in the acceleration-sensitive spectral region, compared to systems with equal strength and stiffness eccentricities (e_p=e_s). Such is the case because Ω_θ generally has smaller effect on the lateral and torsional deformations of the former type of inelastic systems (Figure 5.13) compared to the latter (Figure 5.12).

These observations of how the frequency ratio Ω_θ influences structural response in the various spectral regions of the simple input also apply in an overall sense to the corresponding spectral regions of the El Centro excitation. However, the detailed trends are more complicated for reasons mentioned in the preceding section. Furthermore, the complications in the trends are more pronounced in Figures 5.11 to 5.14 compared to Figures 5.7 to 5.10

because the frequency ratio, Ω_θ, affects the coupled vibration periods of the system to a larger degree compared to the stiffness eccentricity ratio, e_s/r.

5.5 Effects of Yielding

5.5.1 Response of Asymmetric-Plan Systems

The effects of yielding on the lateral and torsional deformations, u_s/u_{go} and ru_θ/u_{go}, and the largest of peak deformations among all resisting elements, $u_{\max}/u_{go}$, are examined next. For this purpose, these response quantities are presented in the form of response spectra in Figures 5.15 to 5.23 for elastic systems and inelastic systems with yield factor, c=0.25 and 0.5. The value of Ω_θ=1 is chosen to emphasize the large effects of plan-asymmetry in elastic systems. Three values of stiffness eccentricity are considered: e_s/r= 0.05, 0.2, and 0.5; and two values of strength eccentricity are included: e_p=e_s and e_p=0. System responses to the simple input and El Centro excitation were determined for the same set of system parameters; however, when required for clarity, some of the curves have been omitted from the figures associated with the El Centro excitation.

It is apparent from response of asymmetric-plan systems to the simple input (Figures 5.15 to 5.20) that effects of yielding on the lateral deformation, u_s/u_{go}, at the CS depend on the vibration period of the system. In the short-period, acceleration-sensitive spectral region, the lateral deformation is greatly increased by yielding. In the medium-period, velocity-sensitive region, and the neighboring transition regions, depending on the lateral period T, yielding may increase or decrease the lateral deformation. These effects of yielding in the short- and medium-period systems increase as the yield factor decreases, i.e., the system is excited increasingly into the inelastic range; because short-period, acceleration-sensitive systems are known to experience generally the largest ductility demand, the effects of yielding are largest for such systems. In the long-period, displacement-sensitive region, lateral deformation is controlled by the ground displacement, and is unaffected by the inelastic behavior, regardless of the yield factor. The above-noted effects of yielding on the lateral

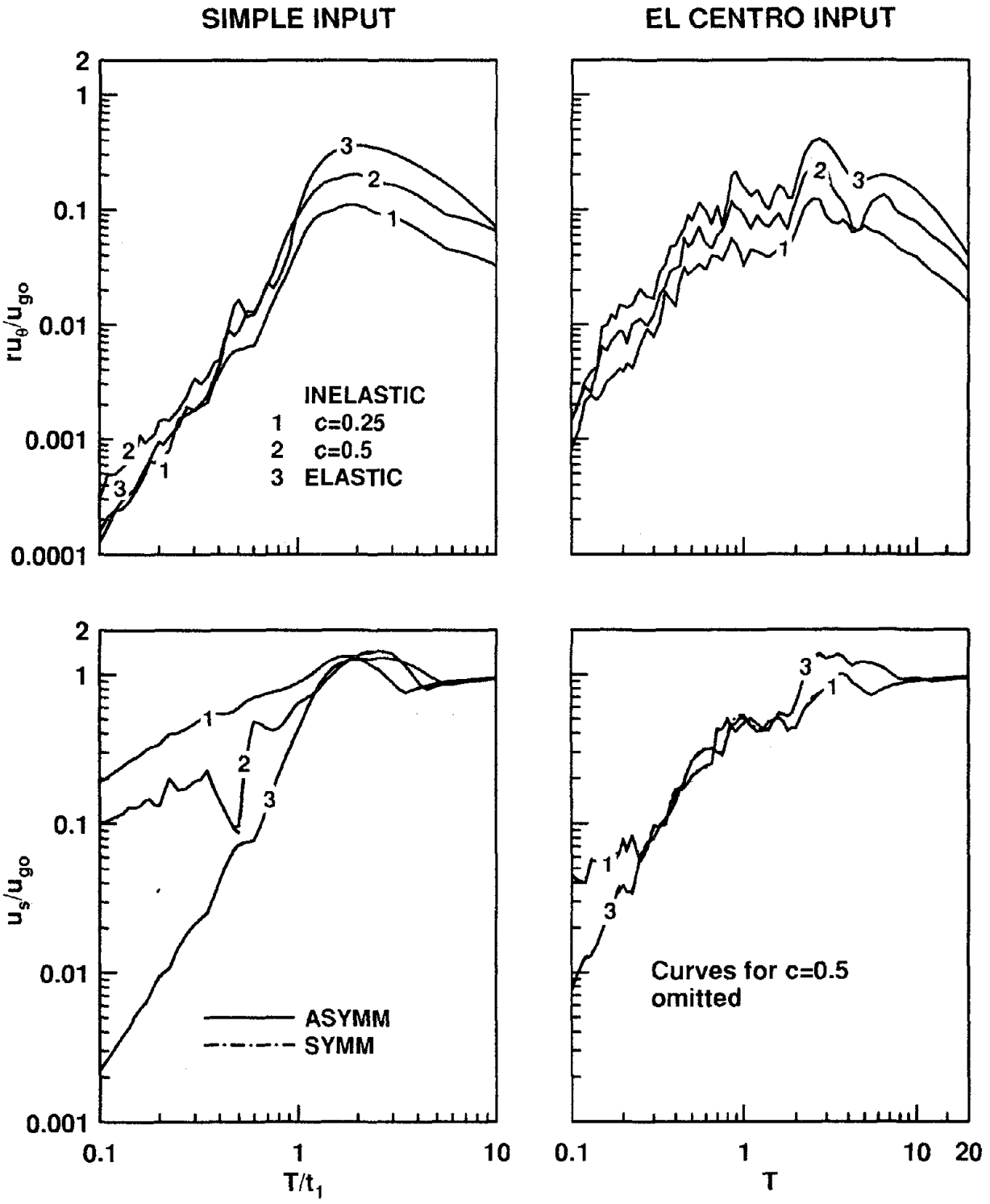

Figure 5.15 Peak lateral and torsional deformations of elastic and inelastic systems (e_p=e_s, c = 0.25 and 0.5). Results are presented for asymmetric-plan (e_s/r = 0.05, Ω_θ =1) and symmetric-plan systems; ξ = 5%.

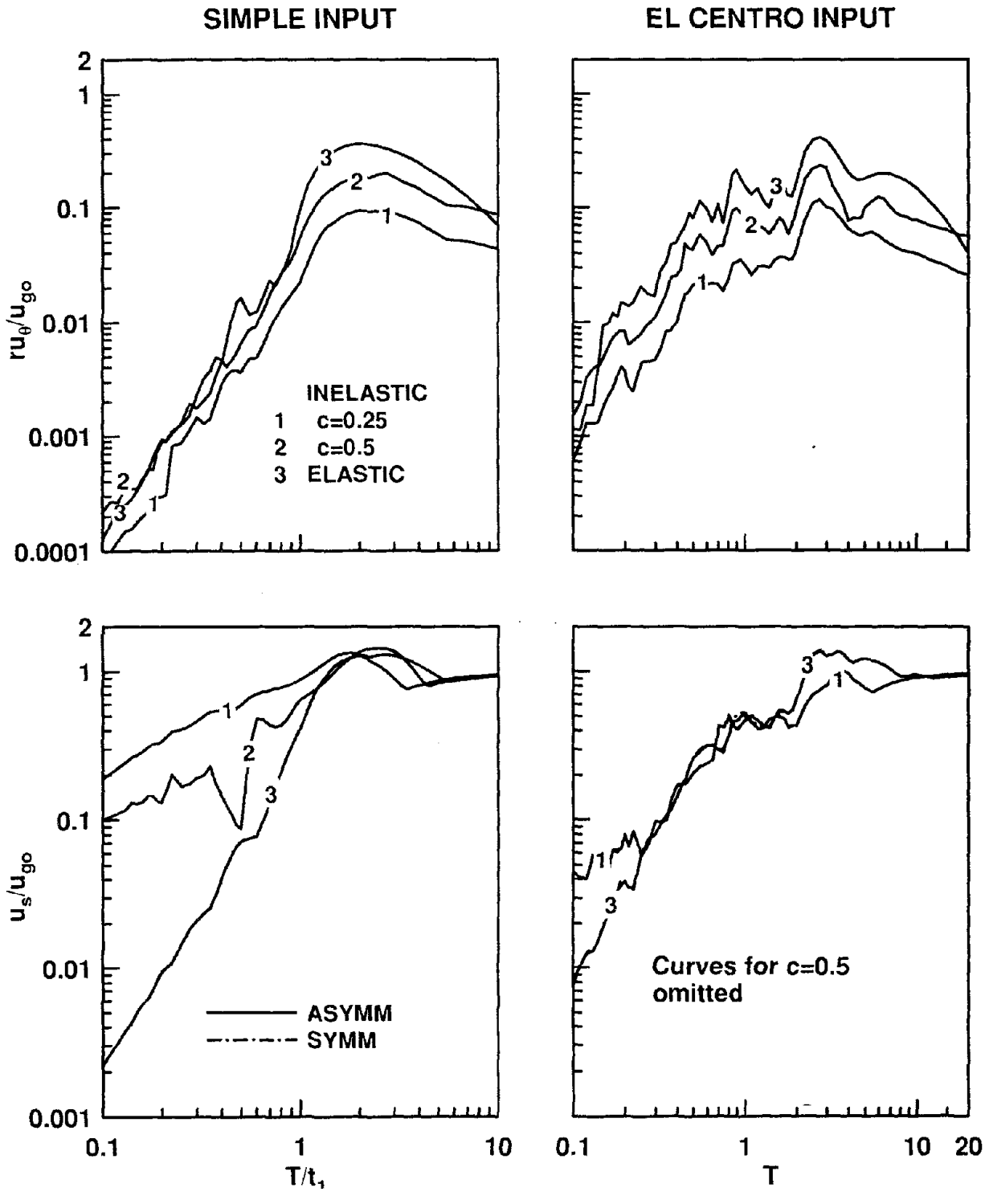

Figure 5.16 Peak lateral and torsional deformations of elastic and inelastic systems (e_p=0, c = 0.25 and 0.5). Results are presented for asymmetric-plan (e_s/r = 0.05, Ω_θ =1) and symmetric-plan systems; ξ = 5%.

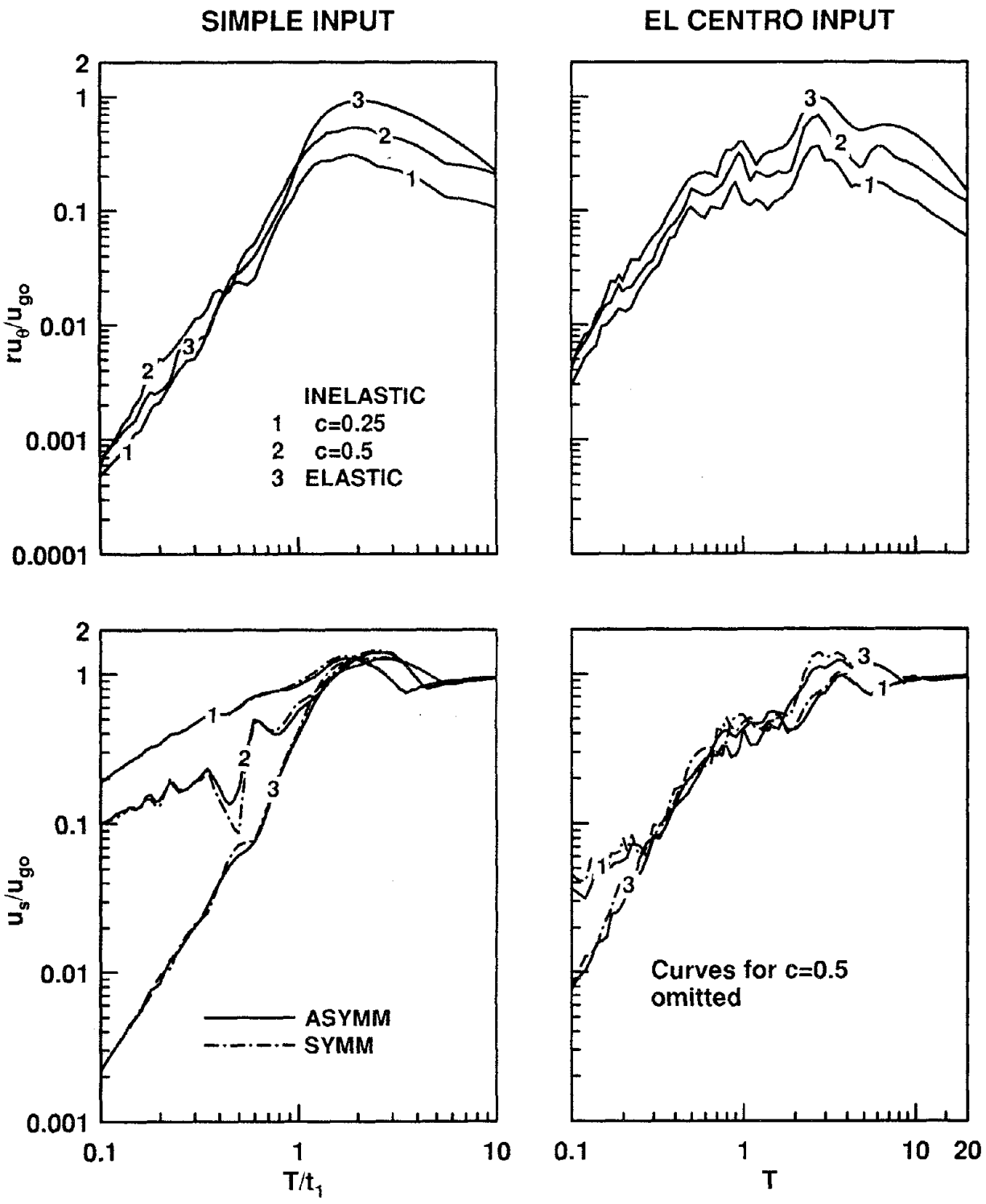

Figure 5.17 Peak lateral and torsional deformations of elastic and inelastic systems (e_p=e_s, c = 0.25 and 0.5). Results are presented for asymmetric-plan (e_s/r = 0.2, Ω_θ =1) and symmetric-plan systems; ξ = 5%.

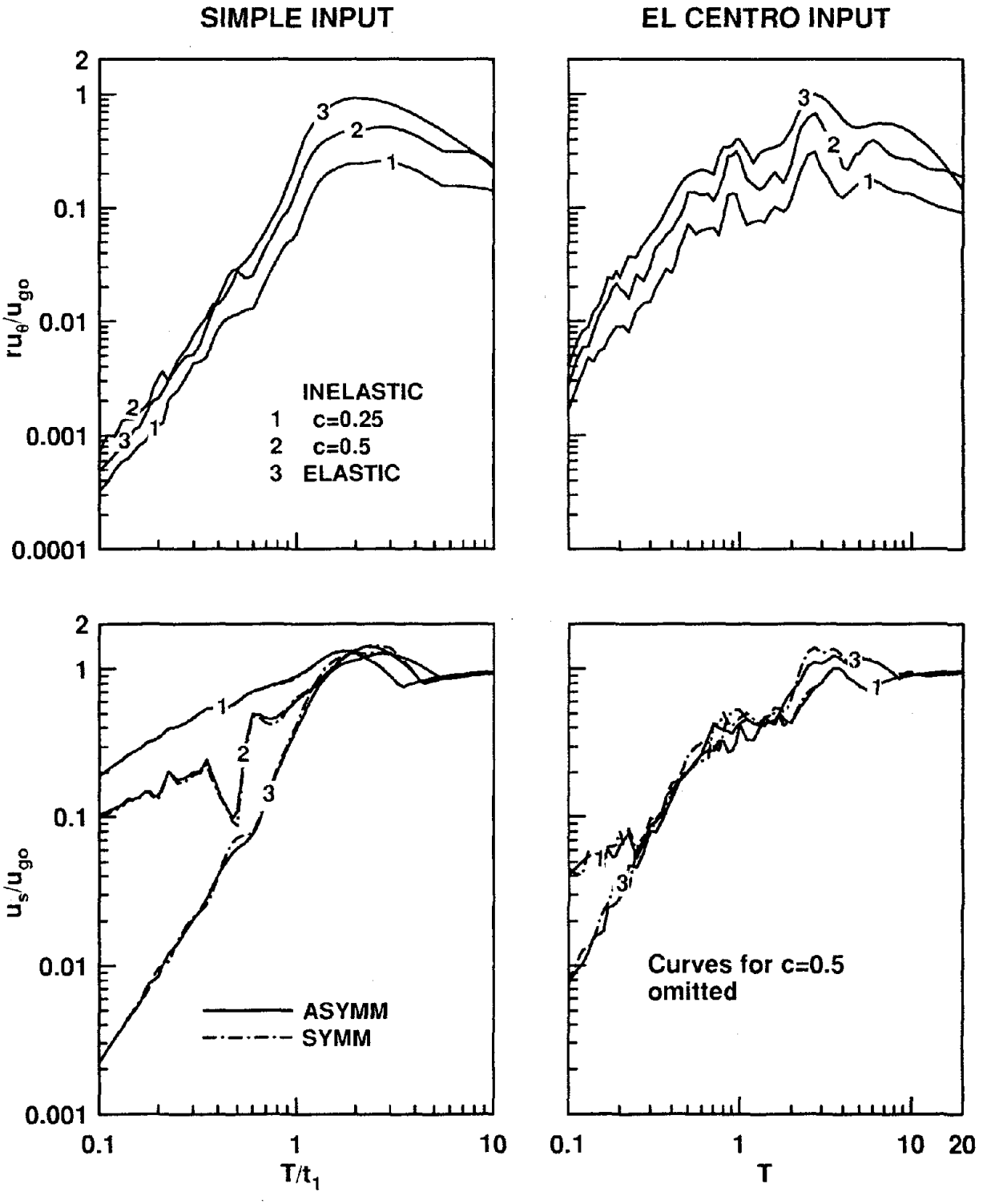

Figure 5.18 Peak lateral and torsional deformations of elastic and inelastic systems (e_p=0, c = 0.25 and 0.5). Results are presented for asymmetric-plan (e_s/r = 0.2, Ω_θ =1) and symmetric-plan systems; ξ = 5%.

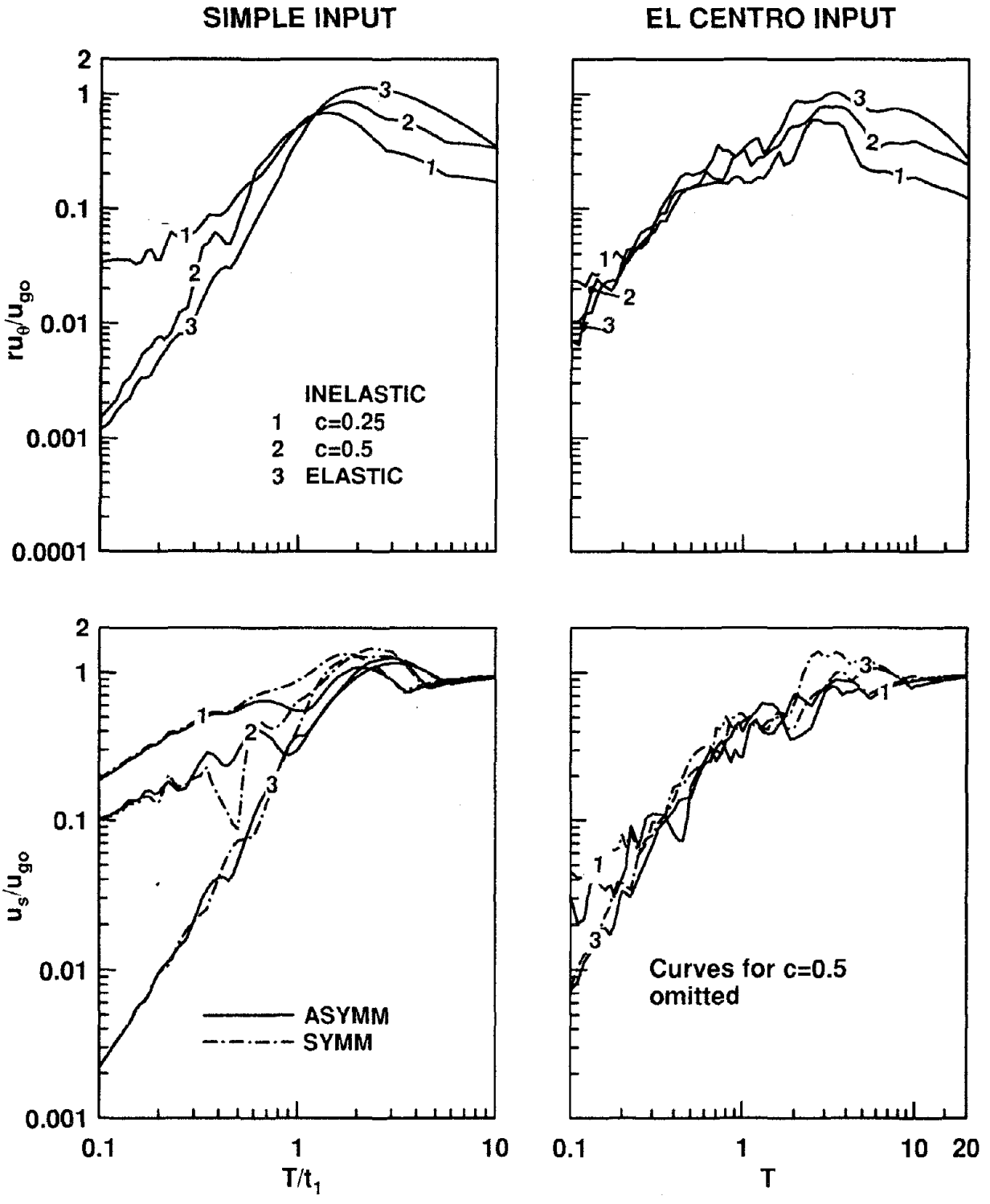

Figure 5.19 Peak lateral and torsional deformations of elastic and inelastic systems (e_p=e_s, c = 0.25 and 0.5). Results are presented for asymmetric-plan (e_s/r = 0.5, Ω_θ =1) and symmetric-plan systems; ξ = 5%.

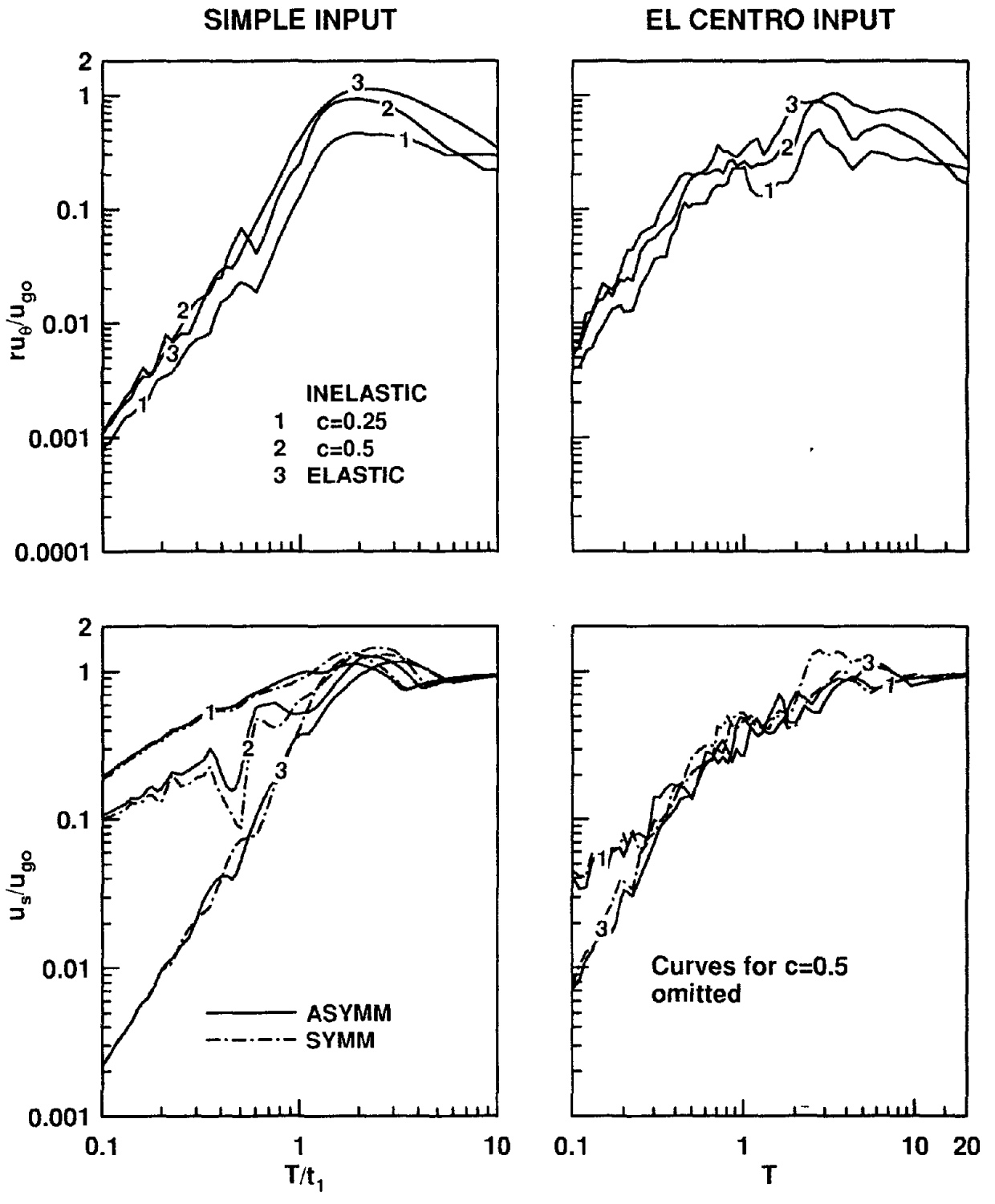

Figure 5.20 Peak lateral and torsional deformations of elastic and inelastic systems (e_p=0, c = 0.25 and 0.5). Results are presented for asymmetric-plan (e_s/r = 0.5, Ω_θ =1) and symmetric-plan systems; ξ = 5%.

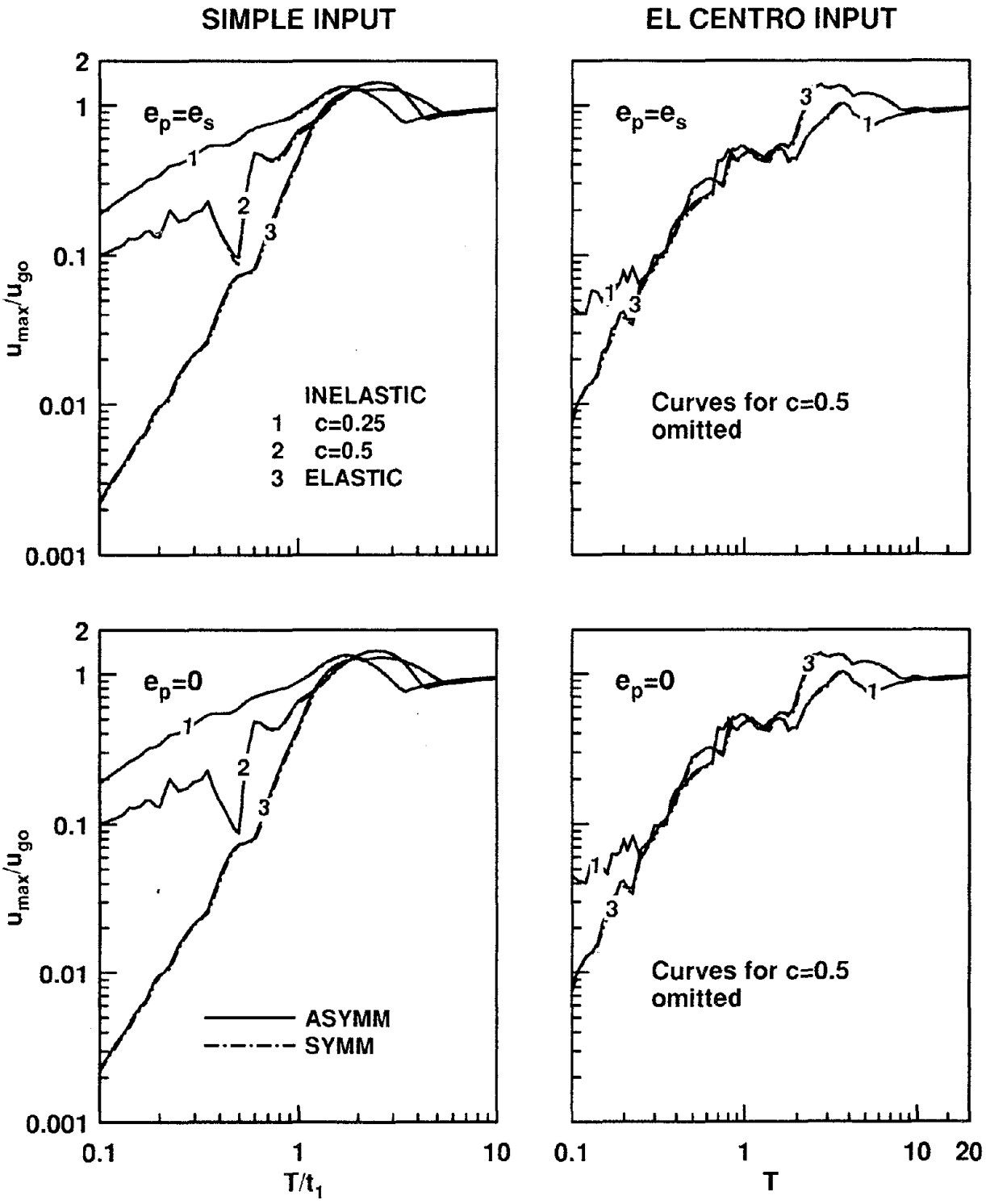

Figure 5.21 Largest of peak element deformations of elastic and inelastic systems (e_p=e_s and e_p=0, c = 0.25 and 0.5). Results are presented for asymmetric-plan (e_s/r = 0.05, Ω_θ =1) and symmetric-plan systems; ξ = 5%.

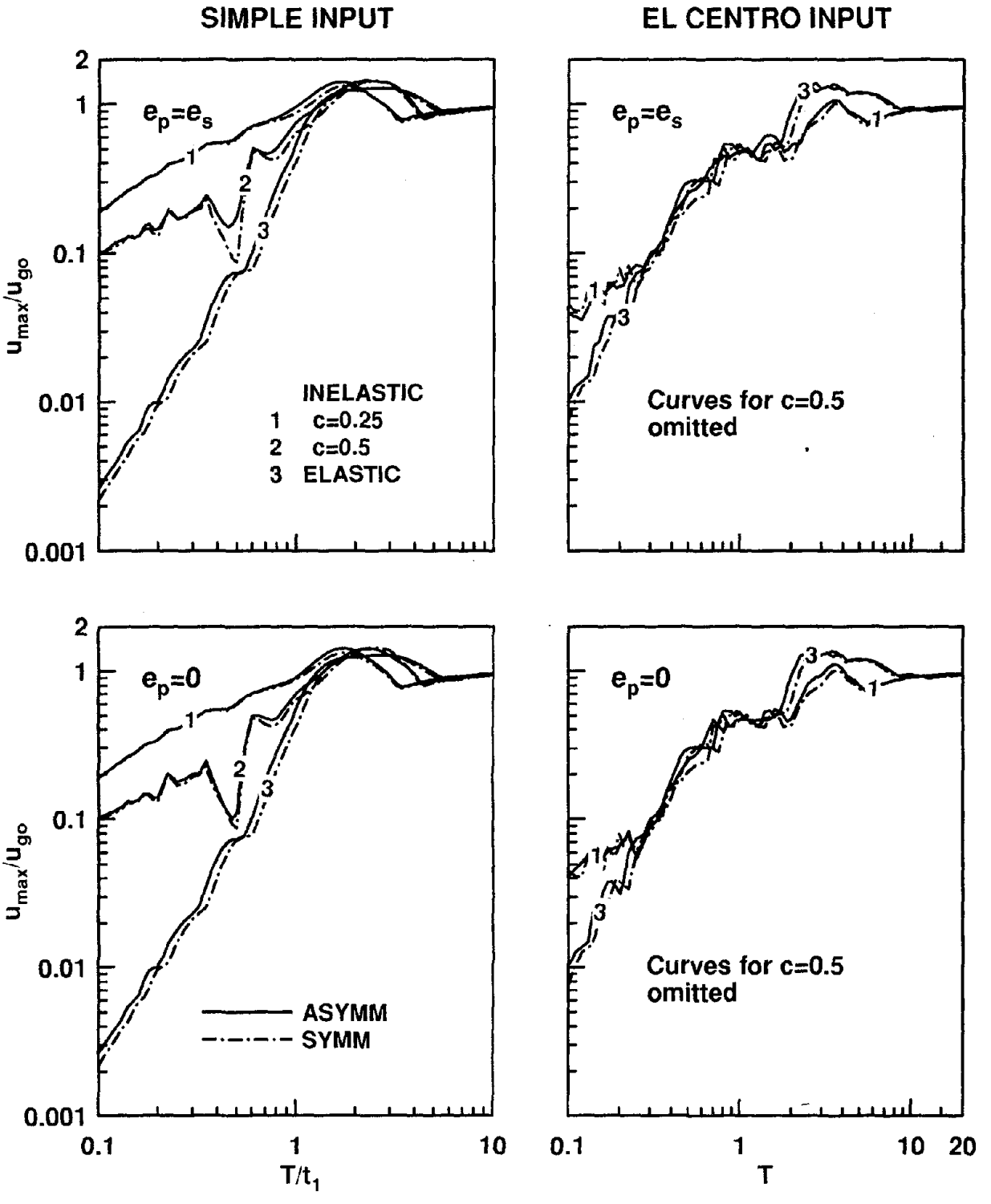

Figure 5.22 Largest of peak element deformations of elastic and inelastic systems ($e_p=e_s$ and $e_p=0$, c = 0.25 and 0.5). Results are presented for asymmetric-plan (e_s/r = 0.2, Ω_θ =1) and symmetric-plan systems; ξ = 5%.

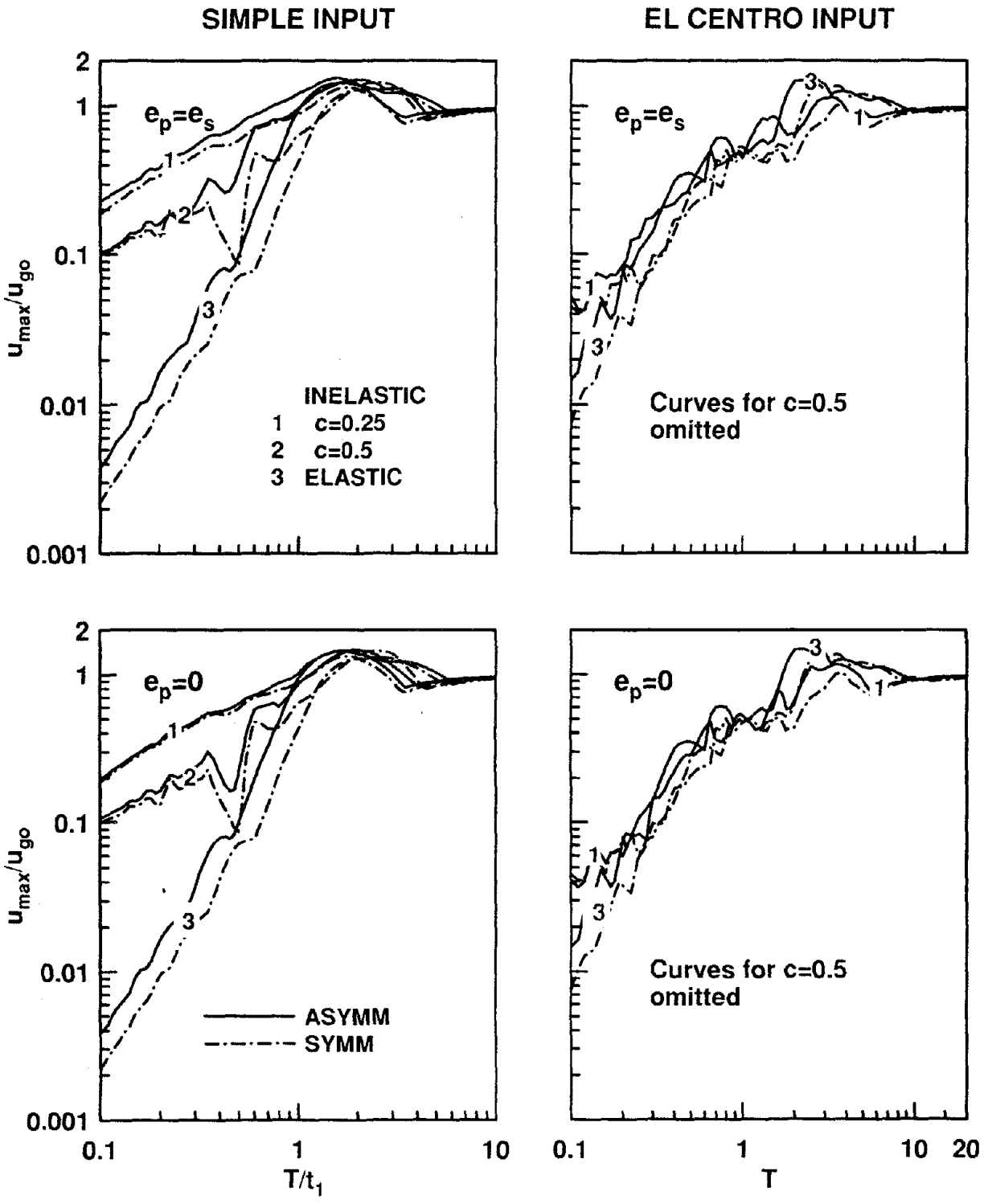

Figure 5.23 Largest of peak element deformations of elastic and inelastic systems (e_p=e_s and e_p=0, c = 0.25 and 0.5). Results are presented for asymmetric-plan (e_s/r = 0.5, Ω_θ =1) and symmetric-plan systems; ξ = 5%.

deformation of asymmetric-plan systems in the various spectral regions are seen in Figures 5.15 to 5.20 to be generally similar to symmetric-plan, SDF systems; the latter have been extensively investigated [e.g. 38].

The effects of yielding on the torsional deformation depend on the lateral vibration period, T, and on the stiffness and strength eccentricities of the asymmetric-plan system. For short-period, acceleration-sensitive systems with yield strength about one-half of that required for the system to remain elastic (c=½), yielding has the effect of slightly increasing the torsional deformation. However, if the yield strength is much smaller, the torsional deformation may increase or decrease depending on the values of strength and stiffness eccentricities. For systems with equal strength and stiffness eccentricities (e_p=e_s) and large stiffness eccentricity, the torsional deformation of short-period systems is increased by yielding (Figure 5.19); such is the case because the torsional stiffness of such systems becomes zero for extended time durations (Chapter 4). On the other hand, if the stiffness eccentricity of the system is smaller, the torsional deformation of inelastic systems with e_p=e_s tends to be smaller compared to elastic systems (Figures 5.15 and 5.17). The torsional deformation of 'strength-symmetric' (e_p=0) inelastic systems with very small yield strength is smaller than that of the elastic system even for larger stiffness eccentricity (Figure 5.20). Such is the case because, for reasons identified in Chapter 4, 'strength-symmetric' (e_p=0) systems experience smaller torsional deformation compared to systems with e_p=e_s.

The torsional deformation of medium-period, velocity-sensitive and long-period, displacement-sensitive systems decreases as the yield factor decreases, i.e., as the system is excited more and more into the inelastic range, regardless of the stiffness eccentricity (Figures 5.15 to 5.20). This is the case because, as mentioned in a preceding section, such systems tend to behave as torsionally-rigid for extended time-durations and inelastic action causes the stiffness eccentricity to vary -- increase or decrease -- with time, leading to cancellation of some of the effects of increased eccentricity.

Inelastic action influences the largest of peak deformations among all resisting elements, u_{max}, of systems in various spectral regions in generally a similar manner as it influences the lateral deformation, u_s (Figures 5.21 to 5.23). Such is the case because u_{max} for inelastic systems is dominated by u_s with the contribution of torsional deformation decreasing with increasing inelastic action, i.e., decreasing c.

The observations presented in the preceding paragraphs of how yielding influences structural responses in the various spectral regions of the simple input also apply in an overall sense to the corresponding spectral regions of the El Centro excitation. However, the detailed trends are more complicated for reasons mentioned earlier. Furthermore, the effects of yielding on the lateral deformation of acceleration-sensitive systems due to El Centro excitation seem to be less pronounced, in part because the spectra do not extend to periods as extremely-short as in the case of the simple input.

5.5.2 Effects of Plan-Asymmetry

It is of obvious interest to know how the deformation responses of an asymmetric-plan system differ from that of the corresponding symmetric-plan system. These effects of plan-asymmetry are investigated in detail in Chapter 6; only the principal effects are identified here. By comparing the lateral deformations of asymmetric-plan and corresponding symmetric-plan (SDF) systems due to the simple input (Figures 5.15 to 5.20), the following observations can be made.

The lateral deformations of the asymmetric-plan and SDF systems are essentially identical in the short-period, acceleration-sensitive and long-period, displacement-sensitive spectral regions. This observation applies to elastic as well inelastic systems. In the medium-period, velocity-sensitive region, however, the lateral deformation of the asymmetric-plan system tends to be smaller than that of the SDF system. Among the two types of inelastic systems considered, 'strength-symmetric' (e_p=0) systems experience smaller reduction. As the system yield strength decreases and the system is excited more and more into the inelastic range, the reduction in the lateral deformation becomes small, resulting in essentially

identical deformations of the asymmetric-plan and symmetric-plan systems.

Due to the contribution of the torsional deformation, the element deformation, u_{max}, tends to be larger in asymmetric-plan systems compared to symmetric-plan systems, especially in the short-period, acceleration-sensitive spectral region (Figures 5.21 to 5.23). However, if the system is excited well into the inelastic range (small c), the difference between the element deformation of the two systems decreases; this difference becomes especially small for 'strength-symmetric' systems (e_p=0).

The above-noted differences between responses of asymmetric-plan and symmetric-plan (SDF) systems are apparent only for systems with larger stiffness eccentricities (Figures 5.19, 5.20, and 5.23). For systems with small stiffness eccentricities, as seen in a preceding section, these differences are small for elastic systems and become even smaller as the yield strength decreases (Figures 5.15 to 5.18, 5.21 and 5.22).

5.5.3 Ratio of Inelastic and Elastic Responses

In the 1960's, there was much interest in relating the earthquake response of yielding, SDF systems to that of associated linearly elastic systems. This relationship was shown to vary with the spectral region and general trends for the various spectral regions were identified [38]. From a design point of view it would be useful to know whether the relationships well known for SDF systems are also applicable to asymmetric-plan systems. For this purpose, the response spectral plots of Figures 5.15 to 5.23 for lateral deformation, u_s, and the element deformation, u_{max}, are presented in a different form. Figures 5.24 to 5.29 show peak deformations of the inelastic system divided by the value for the associated elastic system.

This deformation ratio for asymmetric-plan systems is about the same as for SDF (symmetric-plan) systems when the effects of plan-asymmetry on lateral deformation are small (Figures 5.24 and 5.25). As indicated by the results of the preceding sections, plan-asymmetry effects are small for short-period, acceleration-sensitive systems; long-period, displacement-sensitive systems; systems with small stiffness eccentricity; and systems with

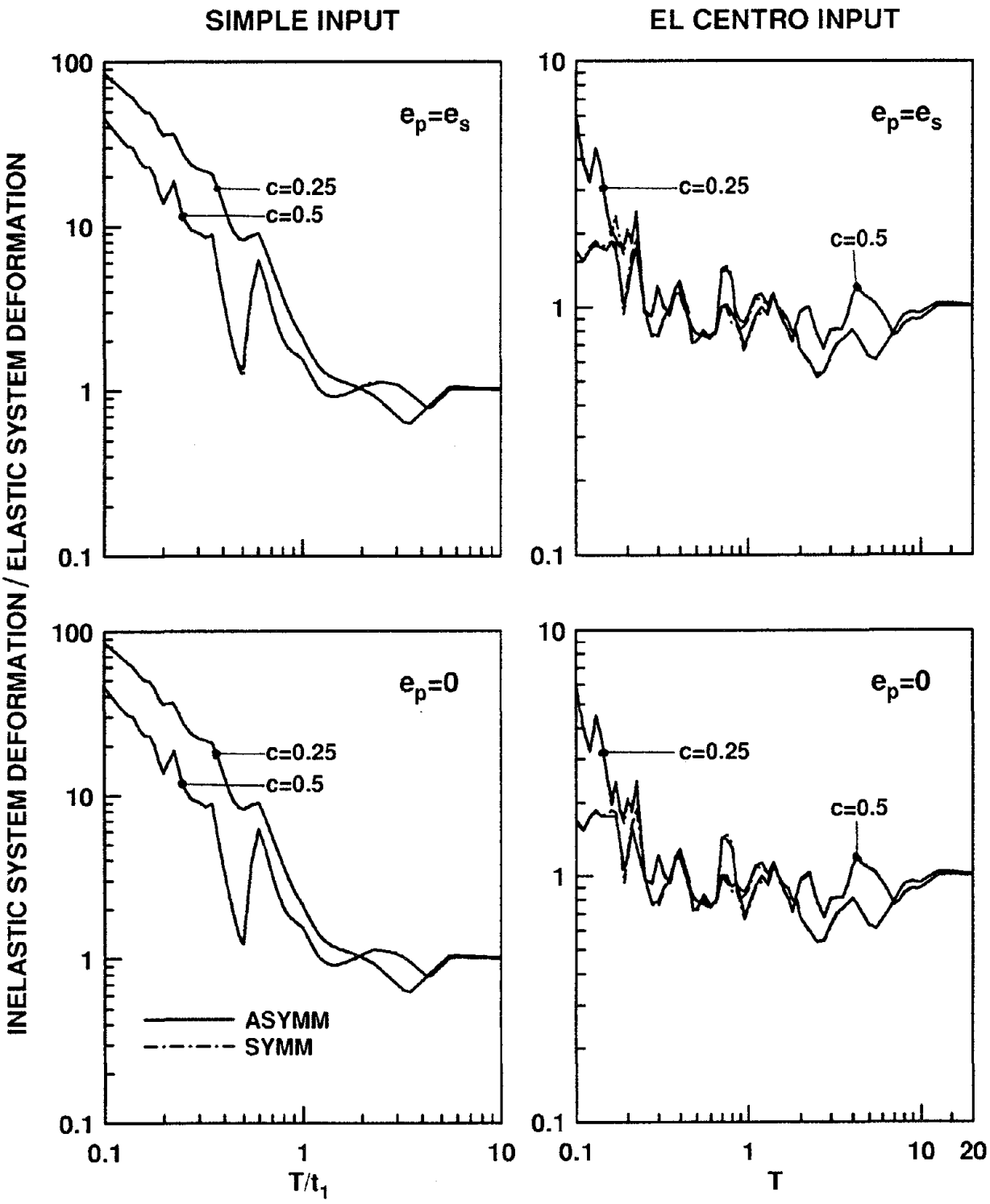

Figure 5.24 Ratio of peak lateral deformations of inelastic ($e_p=e_s$ and $e_p=0$, c = 0.25 and 0.5) and elastic systems. Results are presented for asymmetric-plan (e_s/r = 0.05, Ω_θ =1) and symmetric-plan systems; ξ = 5%.

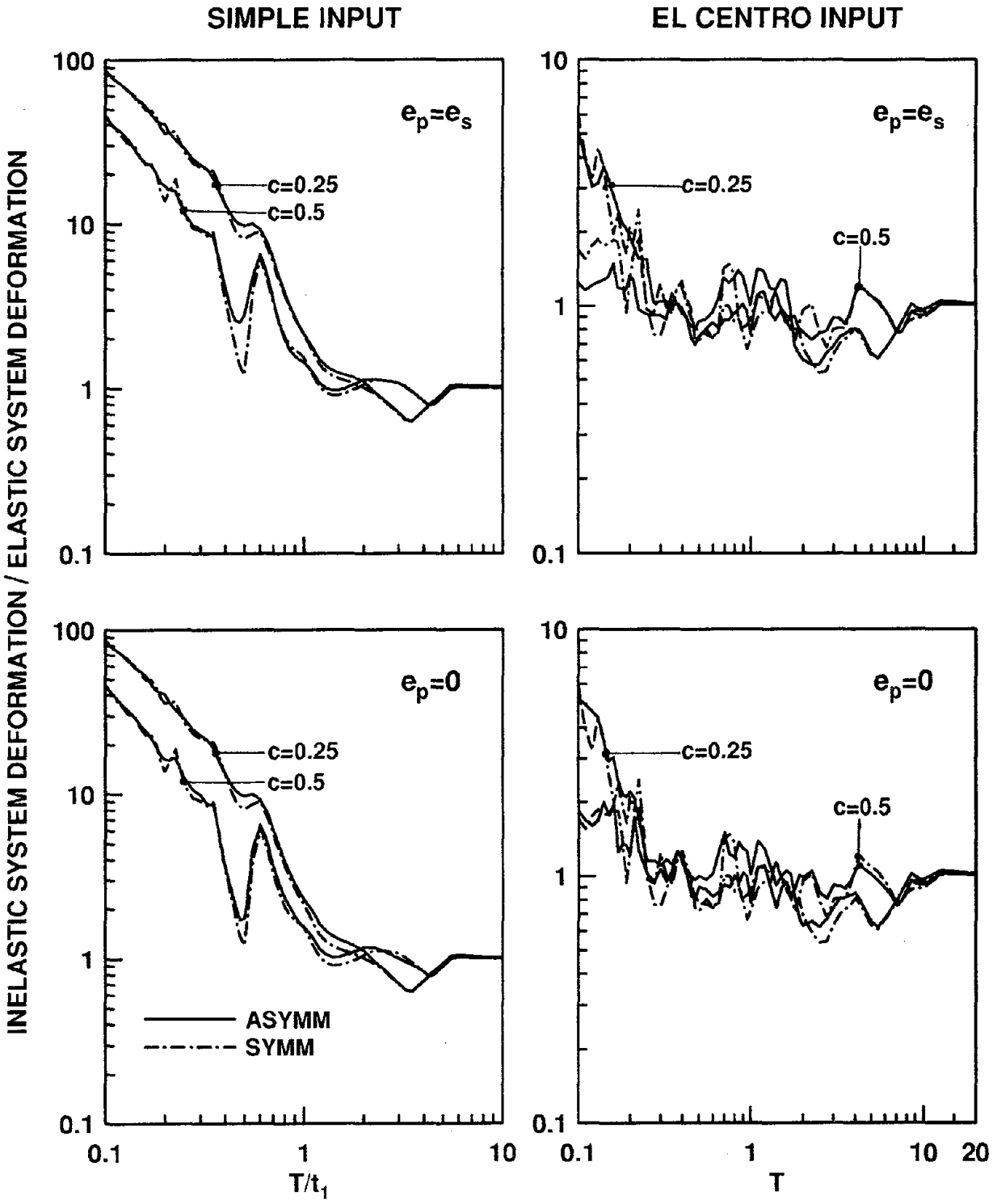

Figure 5.25 Ratio of peak lateral deformations of inelastic ($e_p=e_s$ and $e_p=0$, c = 0.25 and 0.5) and elastic systems. Results are presented for asymmetric-plan (e_s/r = 0.2, Ω_θ =1) and symmetric-plan systems; ξ = 5%.

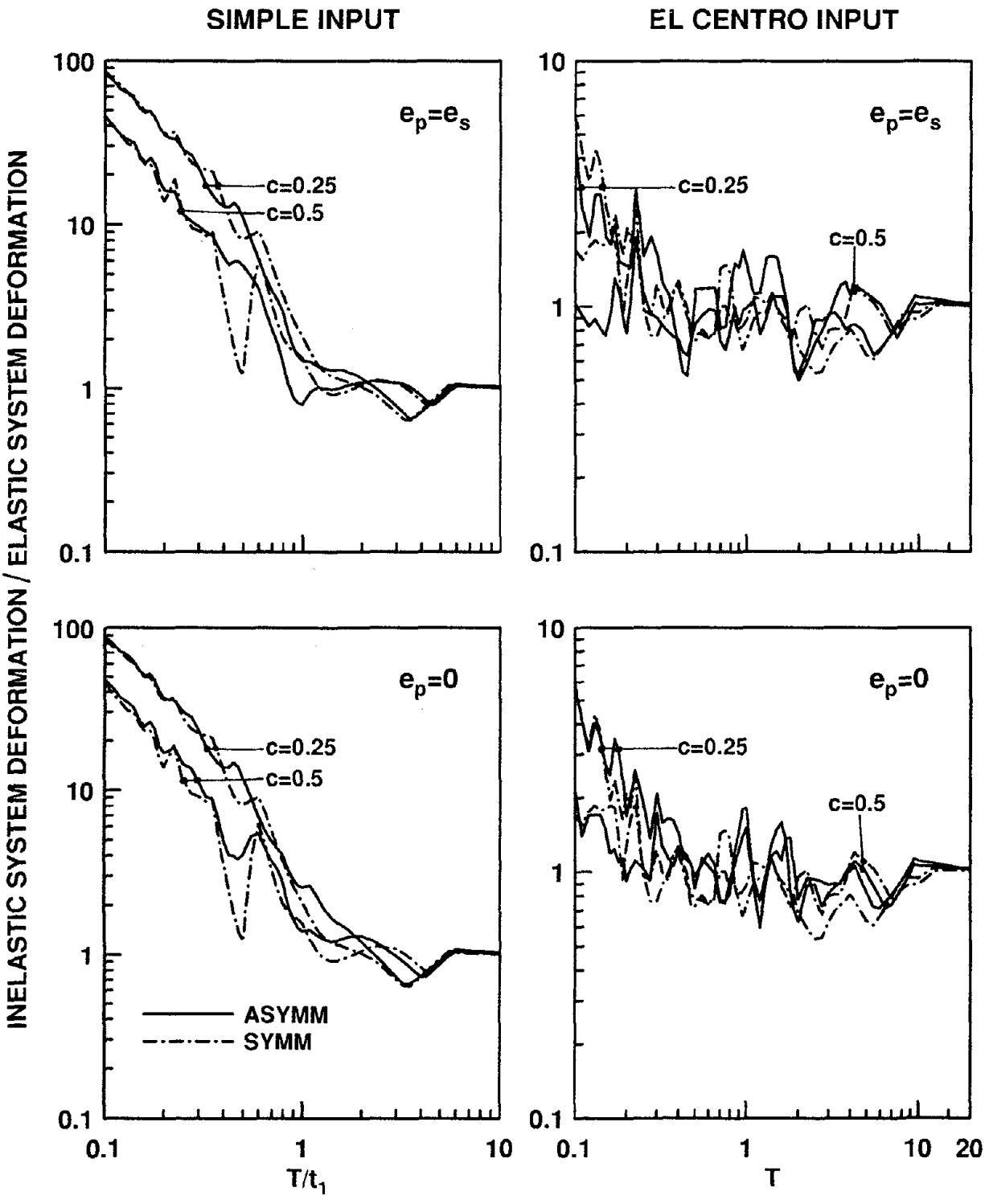

Figure 5.26 Ratio of peak lateral deformations of inelastic ($e_p=e_s$ and $e_p=0$, c = 0.25 and 0.5) and elastic systems. Results are presented for asymmetric-plan (e_s/r = 0.5, Ω_θ = 1) and symmetric-plan systems; ξ = 5%.

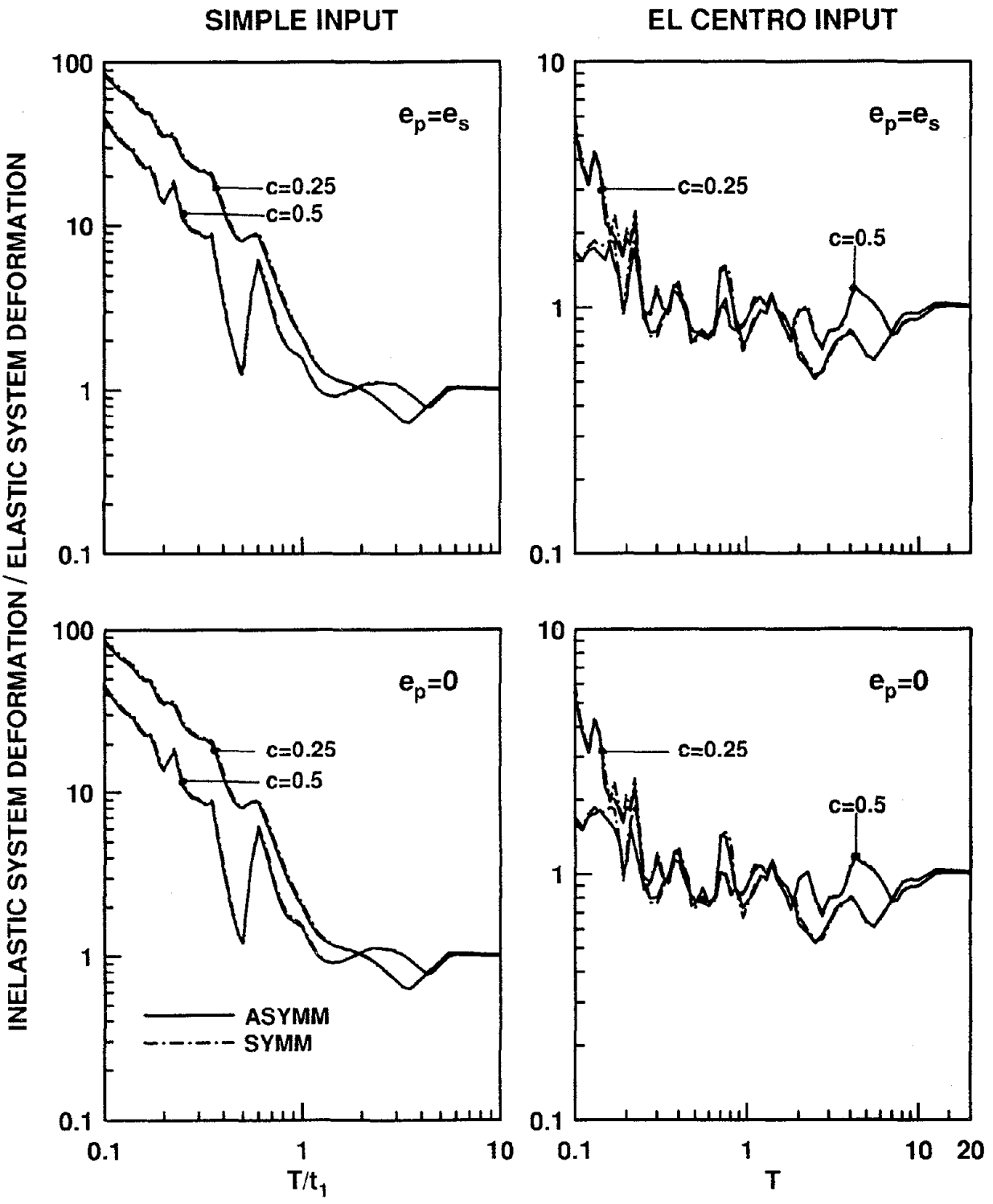

Figure 5.27 Ratio of largest of peak element deformations of inelastic ($e_p=e_s$ and $e_p=0$, c = 0.25 and 0.5) and elastic systems. Results are presented for asymmetric-plan (e_s/r = 0.05, Ω_θ =1) and symmetric-plan systems; ξ = 5%.

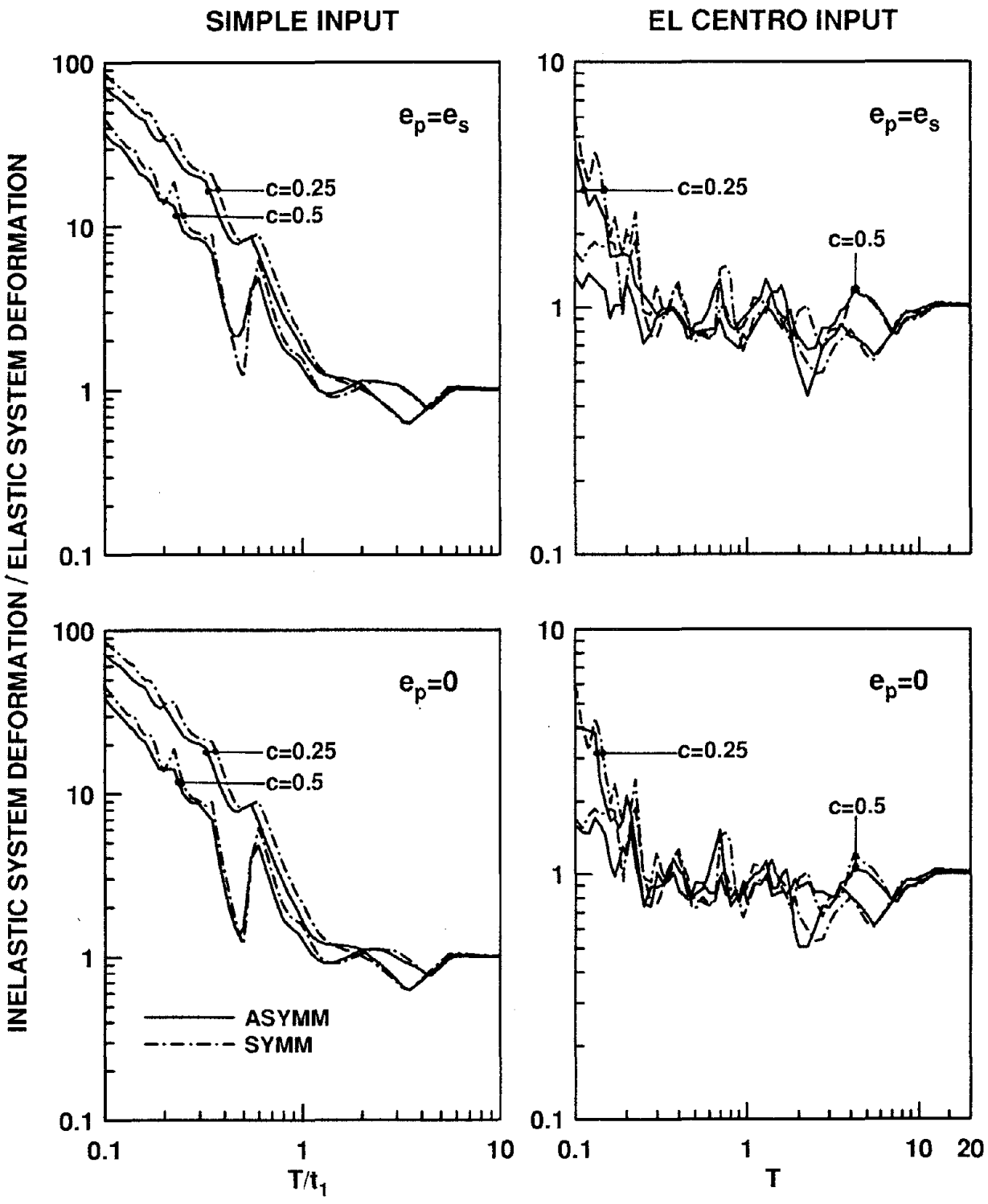

Figure 5.28 Ratio of largest of peak element deformations of inelastic ($e_p=e_s$ and $e_p=0$, c = 0.25 and 0.5) and elastic systems. Results are presented for asymmetric-plan (e_s/r = 0.2, Ω_θ = 1) and symmetric-plan systems; ξ = 5%.

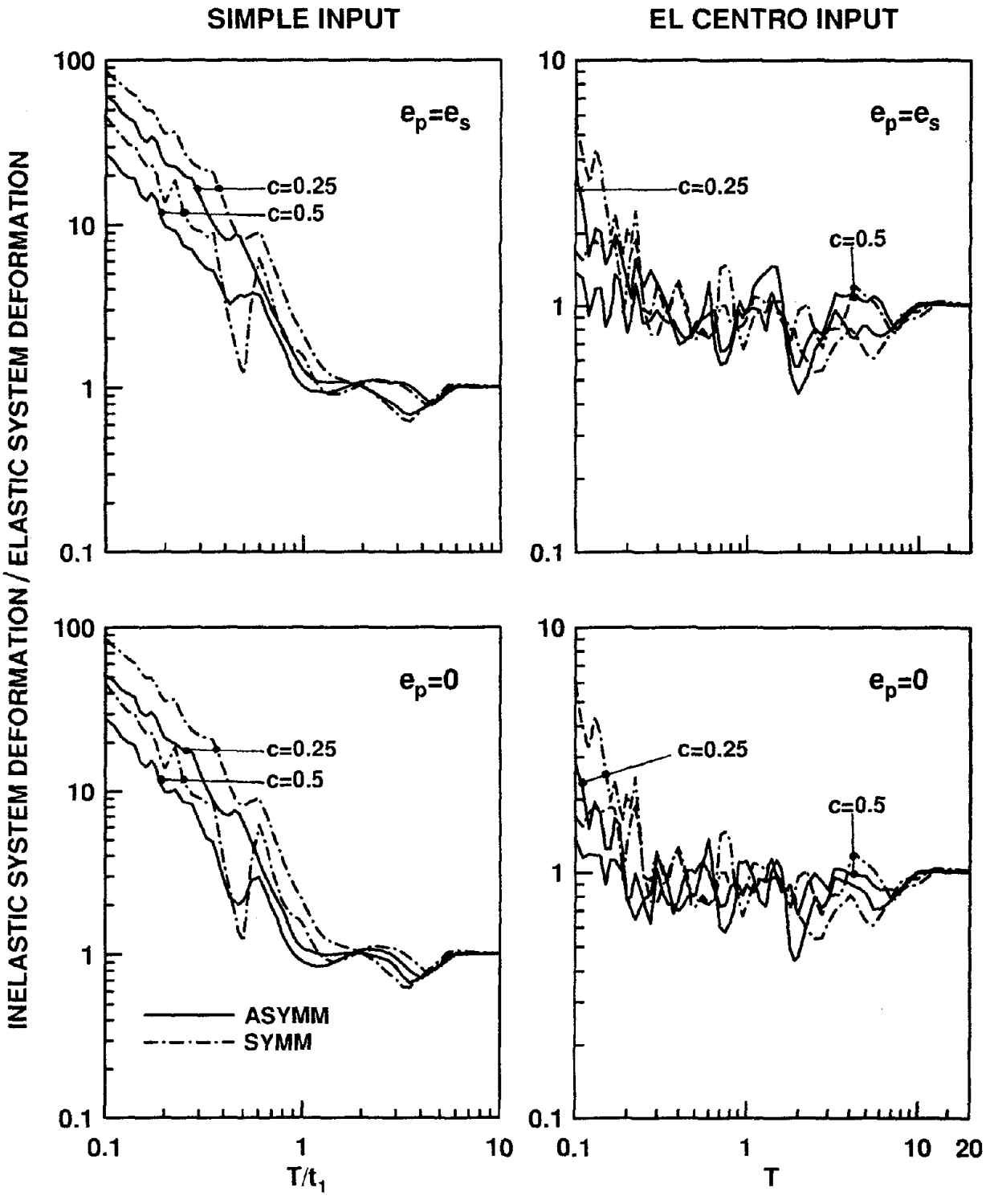

Figure 5.29 Ratio of largest of peak element deformations of inelastic ($e_p=e_s$ and $e_p=0$, c = 0.25 and 0.5) and elastic systems. Results are presented for asymmetric-plan (e_s/r = 0.5, Ω_θ = 1) and symmetric-plan systems; ξ = 5%.

small yield factors that undergo much yielding. For a system that falls into any of these categories, the ratio of deformations for inelastic and elastic systems is affected little by plan-asymmetry and tends to be slightly higher. As a corollary, the deformation ratio may be affected significantly by plan-asymmetry, being smaller or larger compared to SDF systems, for systems with lateral vibration period in the velocity-sensitive spectral region, large stiffness eccentricity, or yield factor close to one -- implying essentially elastic behavior (Figure 5.26).

Because of the contribution of torsional deformation, plan-asymmetry has greater influence on u_{max}, the maximum among the peak deformations of all the resisting elements, compared to u_s, the lateral deformation at the CS. Consequently, the ratio of element deformations for inelastic and elastic systems, while affected by plan-asymmetry in a manner generally similar to the lateral deformation at the CS (Figures 5.24 to 5.26) is affected to a greater degree (Figures 5.27 to 5.29). When significantly different, the ratio is generally smaller for asymmetric-plan systems compared to symmetric-plan systems (Figure 5.29).

6. EFFECTS OF PLAN-ASYMMETRY

6.1 Introduction

From a design point of view, it would also be useful to know how the response of an asymmetric-plan system differs from the response of the corresponding symmetric-plan system, and how these effects of plan-asymmetry differ between elastic and inelastic systems. With this objective, the dynamic response of an asymmetric-plan system and the corresponding symmetric-plan system is compared in this chapter for a wide range of system parameters -- uncoupled lateral vibration period, uncoupled torsional-to-lateral frequency ratio, stiffness eccentricity, and yield factor; elastic as well inelastic systems are studied. The system analyzed is shown in Figure 5.1, which includes resisting elements oriented along the direction of ground motion as well as in the perpendicular direction to ensure wide applicability of results (Chapter 4).

6.2 Response Quantities

The earthquake responses of an asymmetric-plan system and the corresponding symmetric-plan system are compared with the objective of identifying how structural response is affected by the coupling of lateral and torsional motions arising from plan-asymmetry. For this purpose, the peak lateral displacement, u_s, of the asymmetric-plan system at its CS is compared with the peak lateral deformation, u_o, of the corresponding symmetric-plan system which is an elastic or inelastic system consistent with the asymmetric-plan systems. Therefore, in contrast to equation (3.6), the meaning of u_o in rest of this investigation is not restricted to elastic systems. From a design point of view it would be useful to know how much the design deformation for a resisting element increases because of plan-asymmetry. For this purpose, $u_{\max}$, the largest of peak deformations among all resisting elements is also compared with the peak element deformation in the corresponding symmetric-plan system, u_o.

The torsional response of the one-story asymmetric-plan system may be usefully characterized by the dynamic eccentricity, e_d. Suppose that the ground motion produces peak lateral deformation, u_s, peak base shear, V_s, at the CS, peak torsional deformation, u_θ, and the peak base torque, $T_{\theta s}$ in the asymmetric-plan system. The same excitation causes peak deformation, u_o, and the base shear, V_o, in the corresponding symmetric-plan system. At least two different definitions of e_d have been introduced previously for linearly elastic systems: (1) e_d is the distance from the CS at which static application of the force V_o produces the base torque $T_{\theta s}$ [11], and (2) e_d is the distance from the CS at which V_o should be applied to produce the torsional deformation u_θ [7]. The two definitions are conceptually different in that the static and dynamic values of the torque are matched in the first case, in contrast to the torsional deformation in the second case. Needed in this study is a definition for e_d which also applies to inelastic systems. In this case, the first definition based on matching of torque is not meaningful because the peak values of torque and base shear are restricted to their yield values. Therefore, the definition based on matching of deformations is selected, i.e.,

$$e_d = \frac{K_{\theta s} u_\theta}{V_o} = \frac{K_{\theta s} u_\theta}{K_y u_o} \tag{6.1}$$

The effects of plan-asymmetry, or lateral-torsional coupling, are measured by the deviations of u_s/u_o and $u_{\max}/u_o$ from unity and e_d from zero. The dynamic amplification of torsional deformation is measured by the increase of e_d/e_s above unity, which implies that the peak torsional deformation exceeds its value due to static application of the lateral force (or base shear V_o) at a distance e_s from the CS. How the effects of plan-asymmetry vary with the uncoupled lateral vibration period, T, the uncoupled torsional-to-lateral frequency ratio, Ω_θ, and the stiffness eccentricity ratio, e_s/r, is investigated in the subsequent sections.

6.3 Influence of Uncoupled Lateral Vibration Period

The variation of u_s/u_o and e_d/e_s against the vibration period, T, are presented for elastic systems; and two types of inelastic systems: systems with equal strength and stiffness eccentricities ($e_p=e_s$), and 'strength-symmetric' ($e_p=0$) systems. Such plots are presented in Figures 6.1 to 6.3 for three values of $e_s/r=0.05$, 0.2, and 0.5; a fixed value of $\Omega_\theta=1$; and for inelastic systems, a single value of $c=0.25$. Similar plots are presented in Figures 6.4 and 6.5 for each of the two types of inelastic systems, for two values of the yield factor, $c=0.25$ and 0.5, and compared with elastic systems; e_s/r is fixed at 0.2 and Ω_θ at 1. In Figures 6.6 and 6.7, $u_{\max}/u_o$ is plotted against T for these inelastic systems and compared with elastic systems for two values of $e_s/r=0.2$ and 0.5, and a fixed value of $\Omega_\theta=1$. The frequency ratio is chosen as unity to emphasize the effects of plan-asymmetry in the response of elastic systems. System responses to the simple input and El Centro excitation were computed for the same set of system parameters; however, when required for clarity, some of the curves have been omitted from the figures associated with the El Centro excitation.

Plan-asymmetry causes torsional deformation, as indicated by $e_d>0$ in Figures 6.1 to 6.3, which does not occur in the corresponding symmetric-plan system; and modifies the lateral deformation, u_o, experienced by the corresponding symmetric-plan system resulting in a smaller or larger deformation, u_s, depending on the lateral vibration period, T. In contrast, plan-asymmetry was shown to reduce the lateral deformation of a system no matter what its vibration period when the structural response was calculated by response spectrum analysis of elastic systems with the ground motion characterized by smooth spectra [11,12,18]. Thus, it is apparent that the effects of plan-asymmetry in the time-history response of elastic systems vary with period, T, especially for realistic excitations, such as the El Centro ground motion. As e_s/r increases, i.e., as structural plan becomes more asymmetric, the variation of u_s/u_o for elastic systems with respect to the period T increases, implying that the effects of plan-asymmetry become increasingly sensitive to the period T. In contrast, the ratio e_d/e_s is most sensitive to the period for elastic systems with small

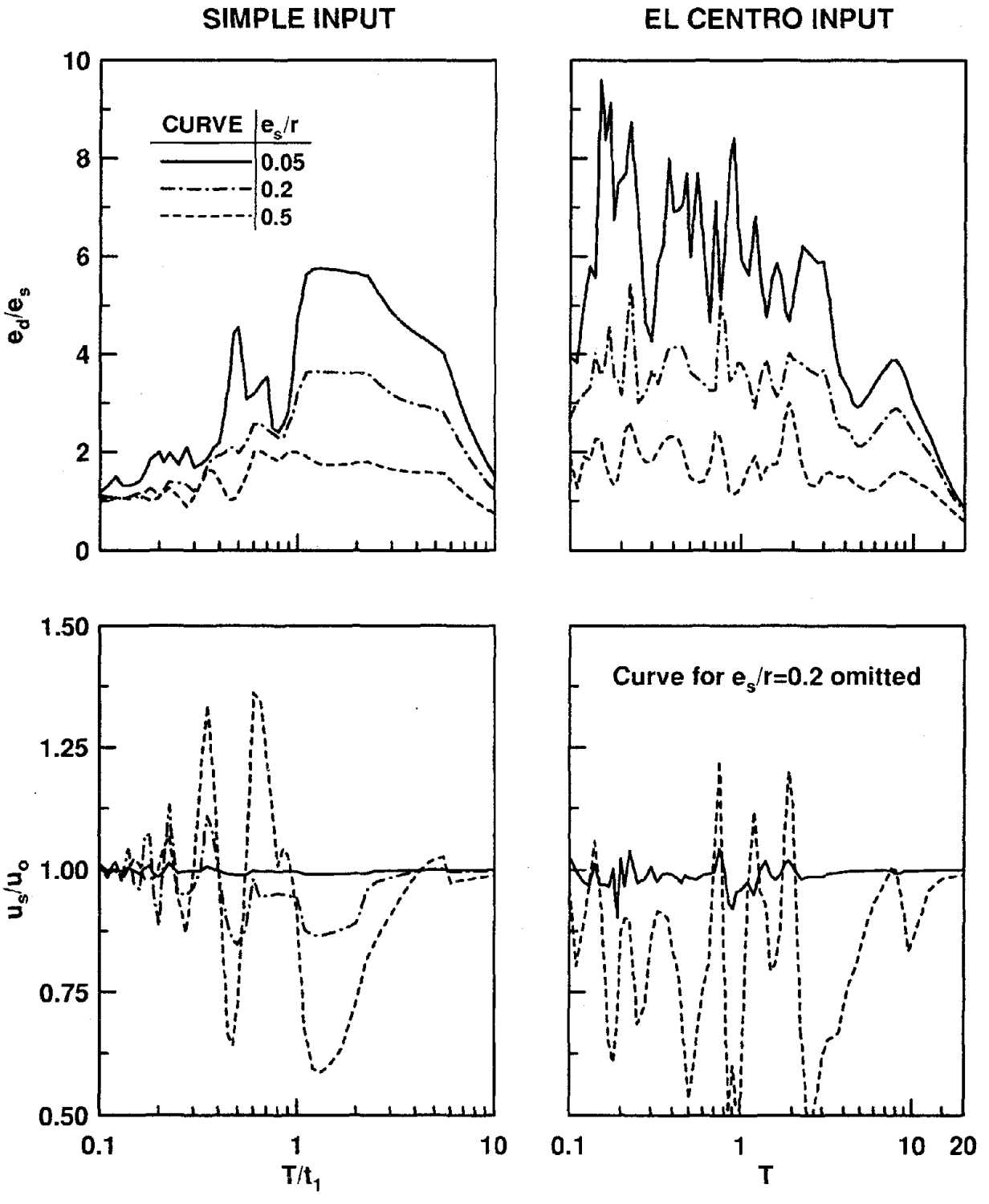

Figure 6.1 Ratio of peak lateral deformations of asymmetric- and symmetric-plan systems, u_s/u_o, and ratio of dynamic and static eccentricities, e_d/e_s, for elastic systems; e_s/r = 0.05, 0.2, and 0.5; Ω_θ = 1, and ξ = 5%.

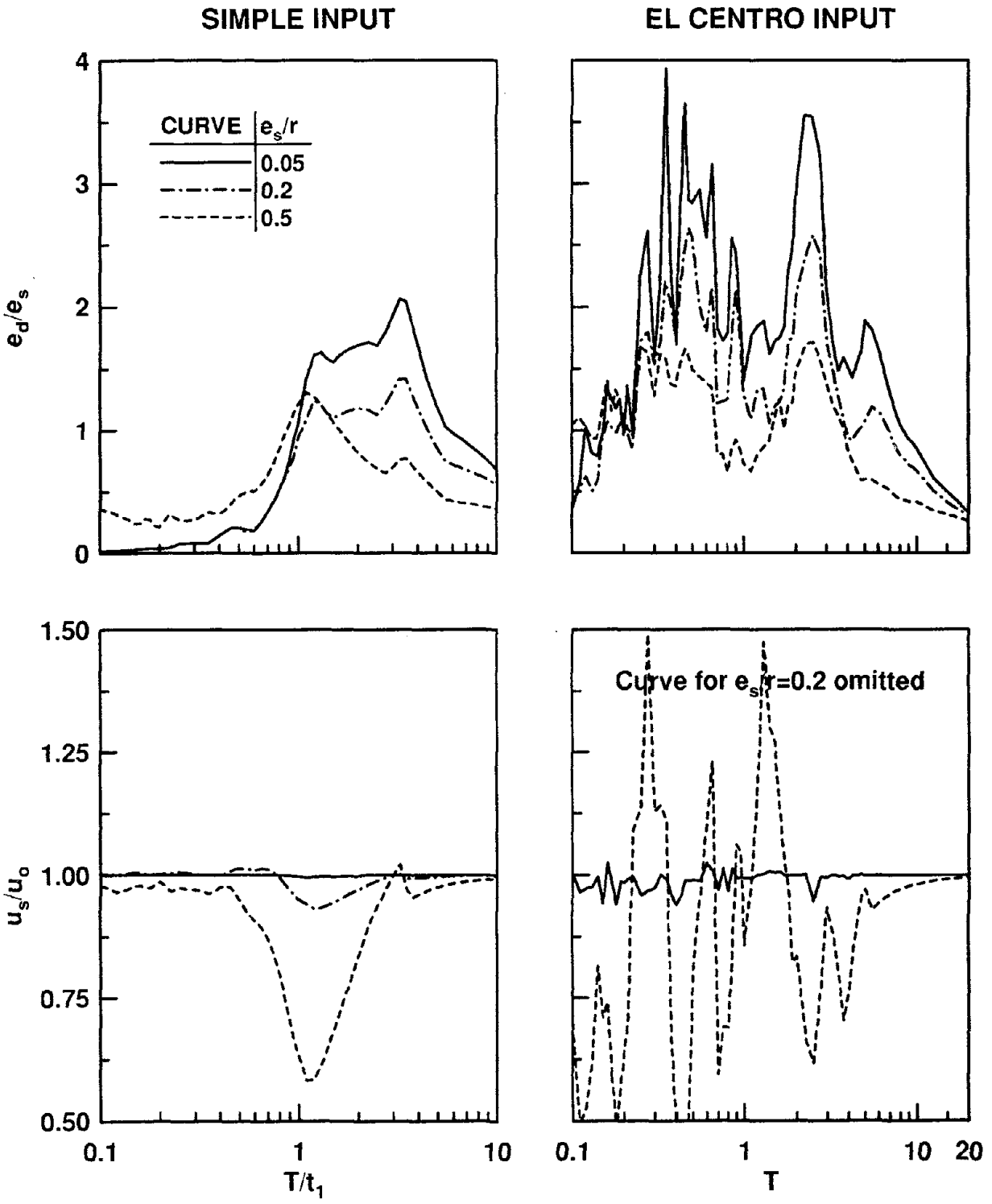

Figure 6.2 Ratio of peak lateral deformations of asymmetric- and symmetric-plan systems, u_s/u_o, and ratio of dynamic and static eccentricities, e_d/e_s, for inelastic systems with e_p=e_s and c = 0.25; e_s/r = 0.05, 0.2, and 0.5; Ω_0 = 1, and ξ = 5%.

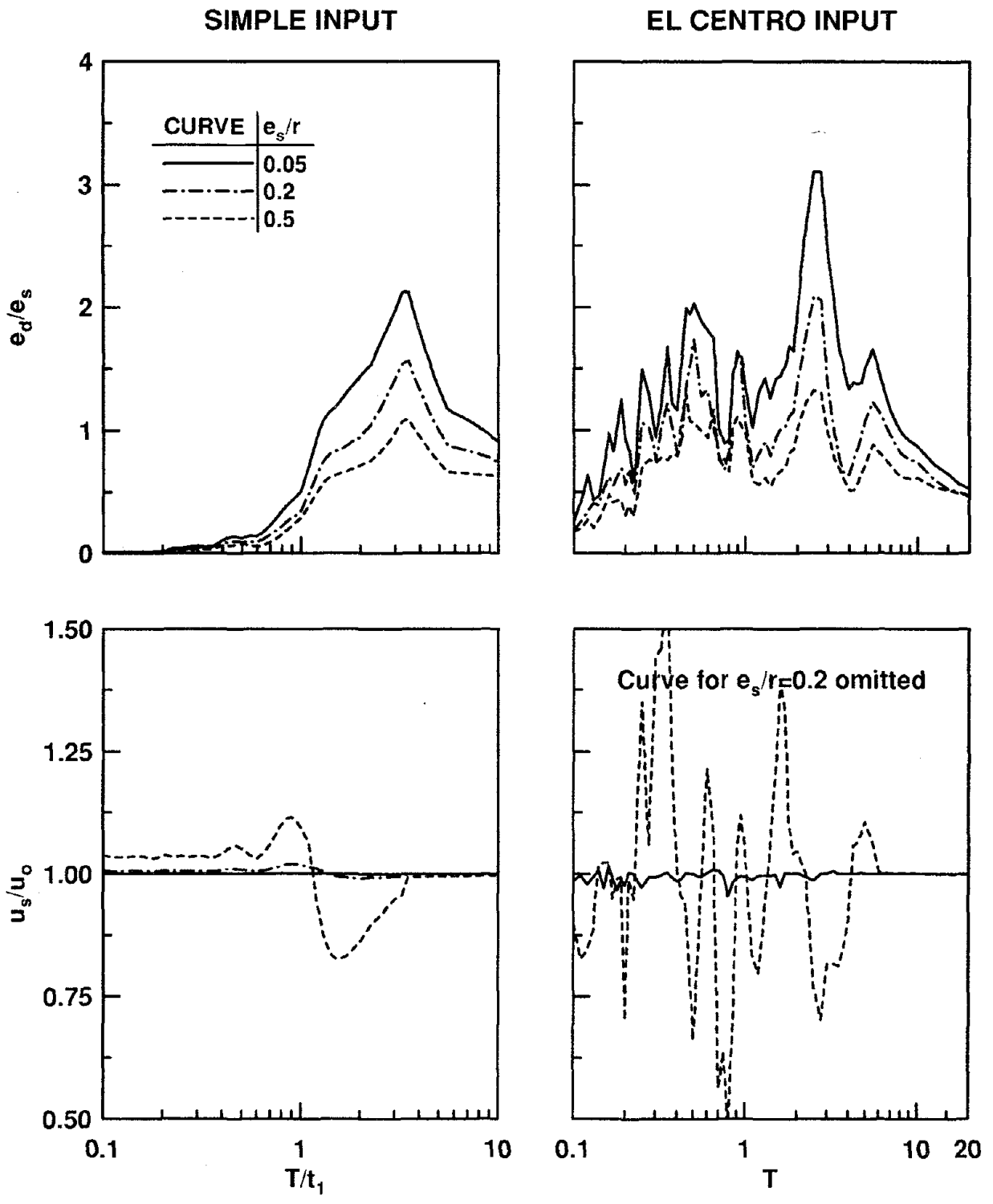

Figure 6.3 Ratio of peak lateral deformations of asymmetric- and symmetric-plan systems, u_s/u_o, and ratio of dynamic and static eccentricities, e_d/e_s, for inelastic systems with e_p=0 and c = 0.25; e_s/r = 0.05, 0.2, and 0.5; Ω_θ = 1, and ξ = 5%.

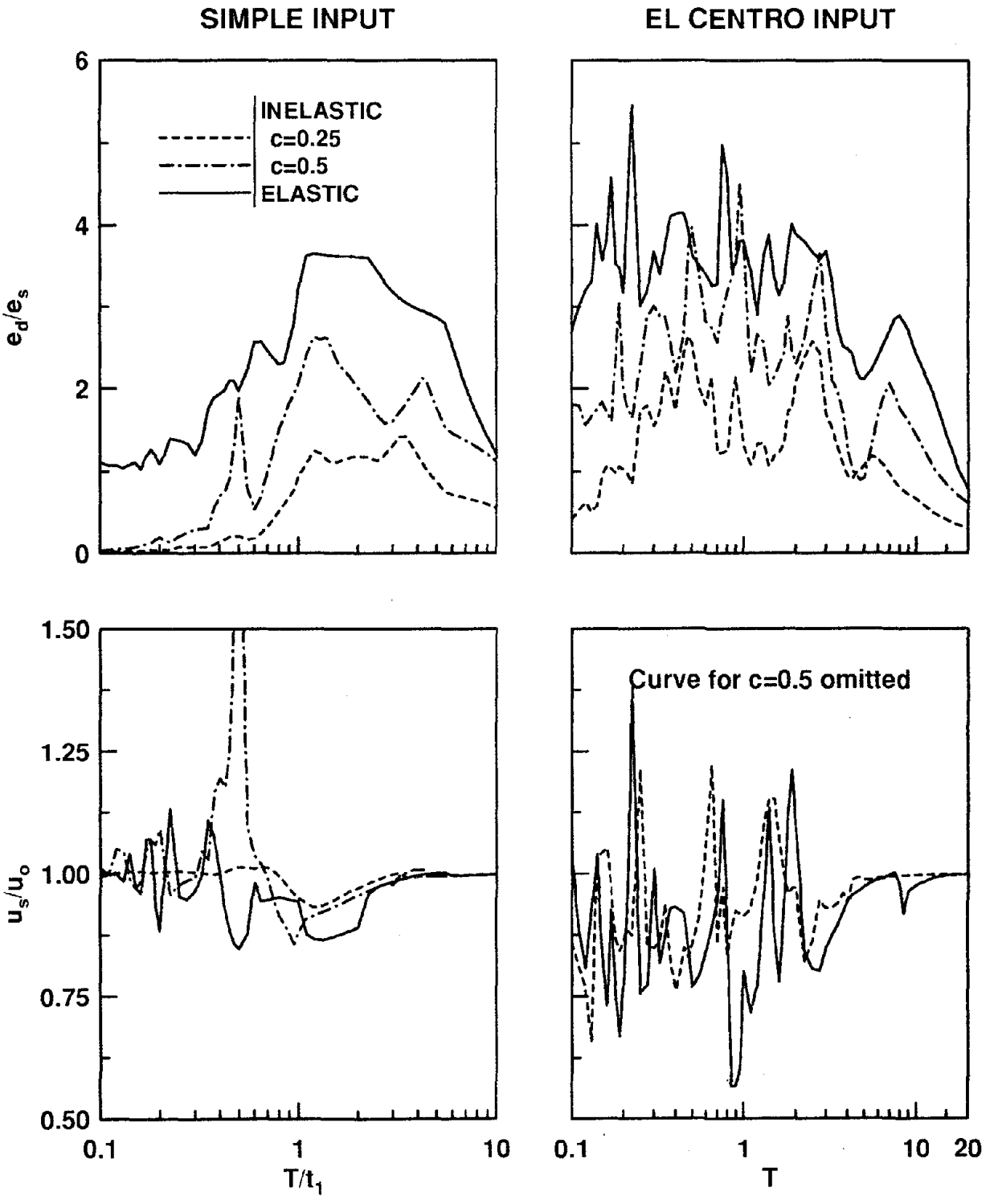

Figure 6.4 Ratio of peak lateral deformations of asymmetric- and symmetric-plan systems, u_s/u_o, and ratio of dynamic and static eccentricities, e_d/e_s, for elastic systems and inelastic systems (e_p=e_s; c = 0.25 and 0.5); e_s/r = 0.2, Ω_θ = 1, and ξ = 5%.

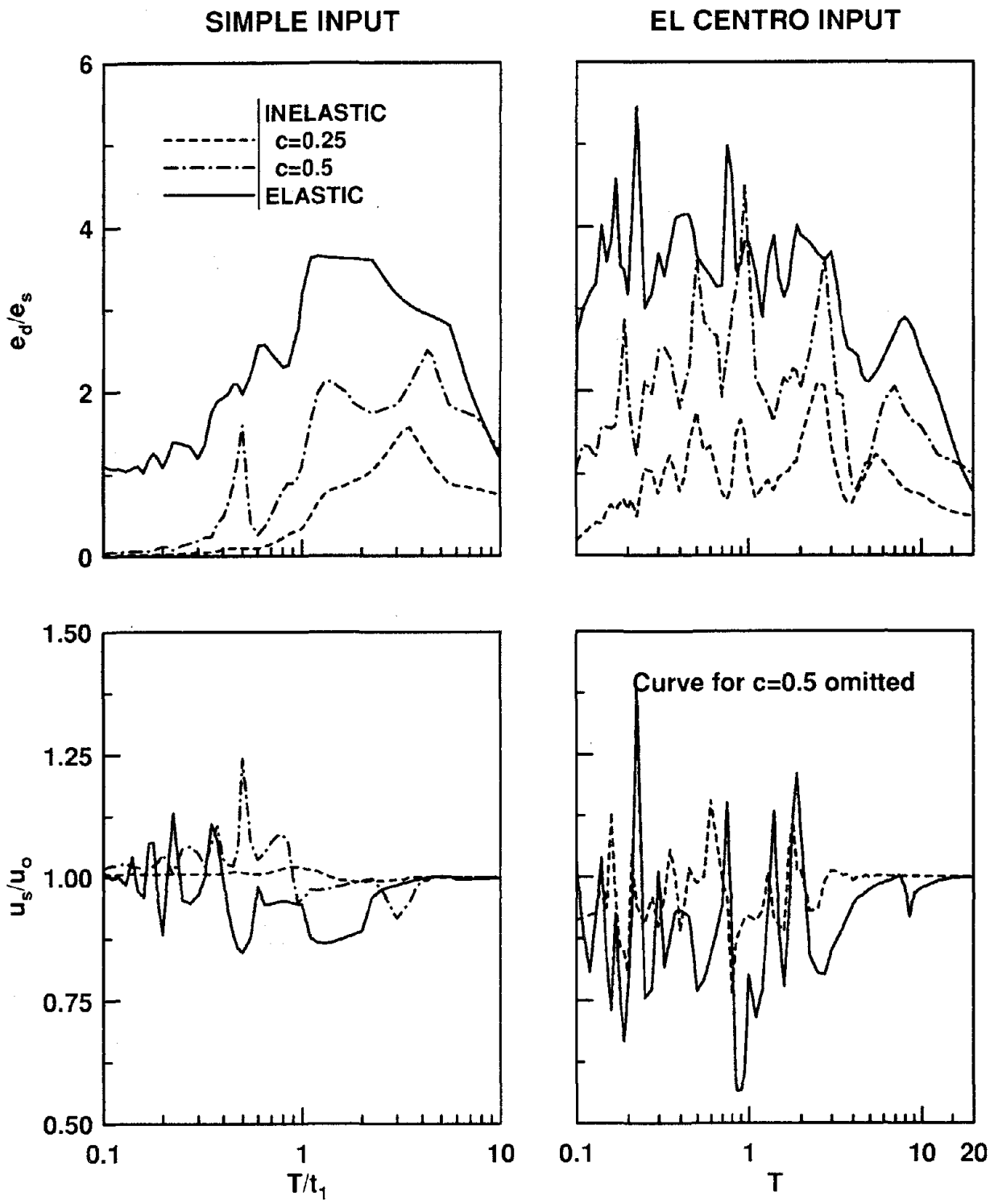

Figure 6.5 Ratio of peak lateral deformations of asymmetric- and symmetric-plan systems, u_s/u_o, and ratio of dynamic and static eccentricities, e_d/e_s, for elastic systems and inelastic systems (e_p=0; c = 0.25 and 0.5); e_s/r = 0.2, Ω_θ = 1, and ξ = 5%.

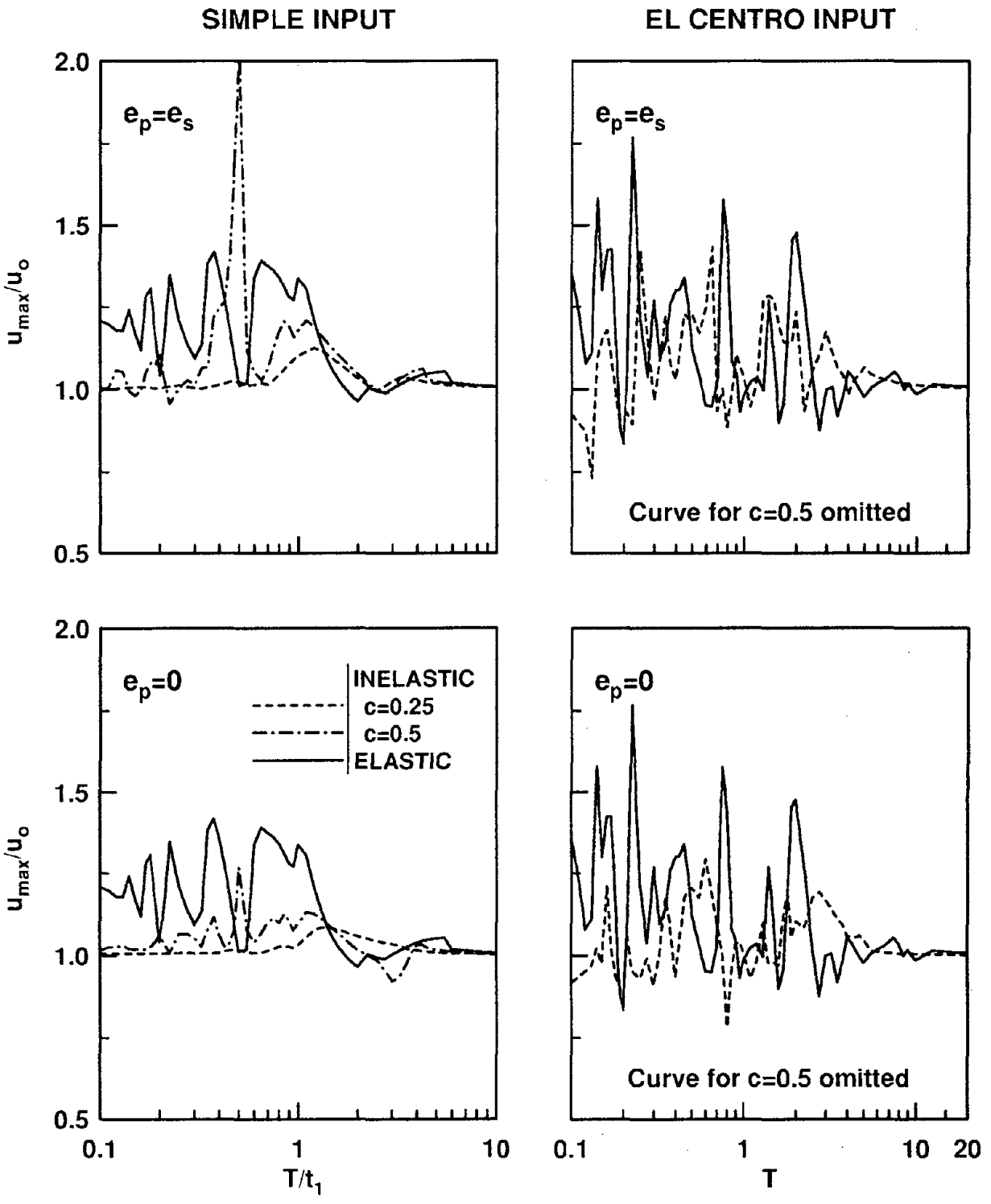

Figure 6.6 Ratio of peak element deformations of asymmetric- and symmetric-plan systems, u_{max}/u_o, for elastic systems and inelastic systems (e_p = 0 and e_s; c = 0.25 and 0.5); e_s/r = 0.2, Ω_θ = 1, and ξ = 5%.

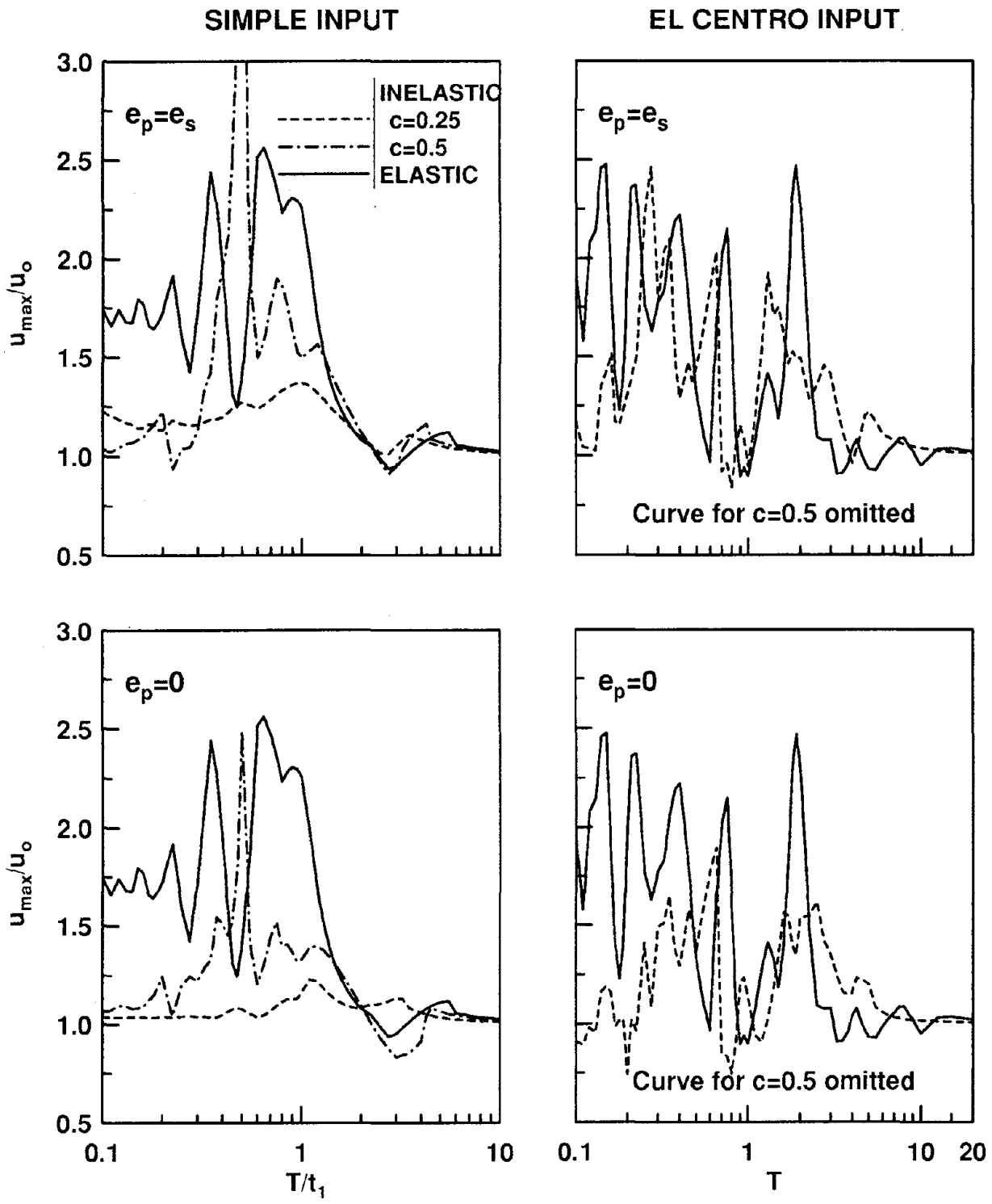

Figure 6.7 Ratio of peak element deformations of asymmetric- and symmetric-plan systems, u_{max}/u_o, for elastic systems and inelastic systems (e_p= 0 and e_s; c = 0.25 and 0.5); e_s/r = 0.5, Ω_θ = 1, and ξ = 5%.

eccentricity. However, the period dependence of the effects of plan-asymmetry tends to be less pronounced for inelastic systems and decreases with increasing inelastic action (decreasing c) (Figures 6.4 and 6.5).

The plan-asymmetry effects are especially significant for medium-period systems in the velocity-sensitive and neighboring transition regions of the spectrum, where these effects are sensitive to the stiffness eccentricity (Figures 6.1 to 6.3) and to the yield factor (Figures 6.4 and 6.5). The ratio e_d/e_s of dynamic eccentricity to its static value tends to reach its largest value for medium-period, velocity-sensitive systems. This dynamic amplification of torsional deformation is largest for elastic systems with the smallest e_s/r (Figure 6.1) but is smaller for inelastic systems (Figures 6.2 and 6.3). As the yield factor c decreases, implying reduction in yield strength and increasing inelastic action, the e_d/e_s value becomes smaller (Figures 6.4 and 6.5). The dynamic eccentricity is generally larger in case of El Centro excitation compared to the simple input.

The lateral deformation, u_s, of velocity-sensitive, asymmetric-plan systems can be significantly different -- larger or smaller -- than u_o of the symmetric-plan system (Figures 6.1 to 6.3). With increasing inelastic action (decreasing c), this difference tends to decrease and the deformation of the asymmetric-plan system becomes closer to that of the symmetric-plan system (Figures 6.4 and 6.5).

The ratio, u_s/u_o, of lateral deformations of the asymmetric-plan and the corresponding symmetric-plan systems is affected very little by plan-asymmetry (Figures 6.1 to 6.3) or by inelastic behavior (Figures 6.4 and 6.5) in the short-period, acceleration-sensitive and long-period, displacement-sensitive spectral regions of both excitations. In the limit, as T becomes very short or very long, it can be shown analytically that the lateral deformation of an asymmetric-plan system is the same as that of the corresponding symmetric-plan system (Appendix D). From earlier studies on SDF systems, it is known that inelastic behavior has smaller influence on the response of long-period, displacement-sensitive systems. Because plan-asymmetry also has little influence on the response of such systems, the ratio u_s/u_o for

inelastic systems also approaches one regardless of the yield strength (Figures 6.2 to 6.5). However, it is not entirely clear why the ratio u_s/u_o for short-period, acceleration-sensitive, inelastic systems also becomes close to one.

The dynamic amplification of torsional deformation, characterized by e_d/e_s, in the acceleration-sensitive spectral region is quite different between elastic and inelastic systems. As T becomes very short, e_d/e_s for elastic systems approaches one (Figure 6.1), indicating that the torsional deformation is equal to that resulting from static application of the lateral force (or base shear) V_o at a distance e_s from the CS (Appendix D). However, e_d/e_s for inelastic systems tends to zero as the period becomes very short, implying very little torsional deformation (Figures 6.2 to 6.5). As seen in Figure 6.2 there are exceptions to this trend because the torsional stiffness of systems with large stiffness eccentricity and small yield strength may become zero for extended time-durations leading to increased torsional deformation (Chapter 4).

The values of e_d/e_s in the long-period, displacement-sensitive spectral region tend to be smaller for inelastic systems compared to elastic systems (Figures 6.4 and 6.5). In the limit, as T becomes very long, e_d/e_s for elastic systems can be shown to approach zero, implying very little torsional deformation (Appendix D). It is not known whether this limiting value of e_d/e_s is also valid for inelastic systems, but e_d/e_s for such systems decreases as T becomes long (Figures 6.2 to 6.5).

The above mentioned observations on the effects of plan-asymmetry on the earthquake response of one-story systems, and how these effects are influenced by inelastic action, are more easily discernible from the response results for the various spectral regions of the simple input. They also apply in a rough overall sense to the corresponding spectral regions of the El Centro excitation although the trends are much more irregular and complicated. They would tend to smooth out if the responses were averaged over several earthquake excitations.

The normalized element deformation, u_{max}/u_o, is plotted against the vibration period, T, in Figures 6.6 and 6.7 for the simple and El Centro excitations. Over a wide range of T values in the acceleration- and velocity-sensitive spectral regions of both excitations, but for a few exceptions, the element deformation is increased by asymmetry of plan; in the displacement-sensitive region, the element deformation is affected very little by plan-asymmetry (Figures 6.6 and 6.7). The increase in element deformation due to plan-asymmetry is generally smaller for inelastic systems, especially for 'strength-symmetric' (e_p=0) systems, compared to elastic systems. With increasing inelastic action, i.e., decreasing c, u_{max}/u_o tends to become closer to one implying that, with some exceptions, the element deformation is affected less by plan-asymmetry (Figure 6.6 and 6.7). These effects of inelastic behavior are more pronounced in the acceleration- and velocity-sensitive regions of the spectrum but are negligible in the displacement-sensitive spectral region. The increase in element deformation of elastic systems due to plan-asymmetry is about the same for the two excitations but for inelastic systems, the increase is larger in case of the El Centro excitation.

6.4 Influence of Frequency Ratio and Stiffness Eccentricity

Separately for elastic systems, inelastic systems with $e_p=e_s$, and 'strength-symmetric' (e_p=0) inelastic systems, u_s/u_o and e_d/e_s are plotted in Figures 6.8 to 6.10 against the uncoupled torsional-to-lateral frequency ratio, Ω_θ, for three values of e_s/r, and in Figures 6.11 to 6.13 against the normalized eccentricity, e_s/r, for several values of Ω_θ. Subsequently, the responses of the two inelastic systems, each for two values of c=0.25 and 0.5, are compared with the elastic system, in Figures 6.14 to 6.20. Since the effects of plan-asymmetry were shown earlier to be most pronounced in the medium-period, velocity-sensitive spectral region, a lateral vibration period value representative of this region is chosen: T/t_1=1.5 with the simple input and T=1 in case of the El Centro input.

For elastic systems, the lateral deformation u_s of the asymmetric-plan system is smaller than the deformation u_o of the corresponding symmetric-plan system; and over a wide range

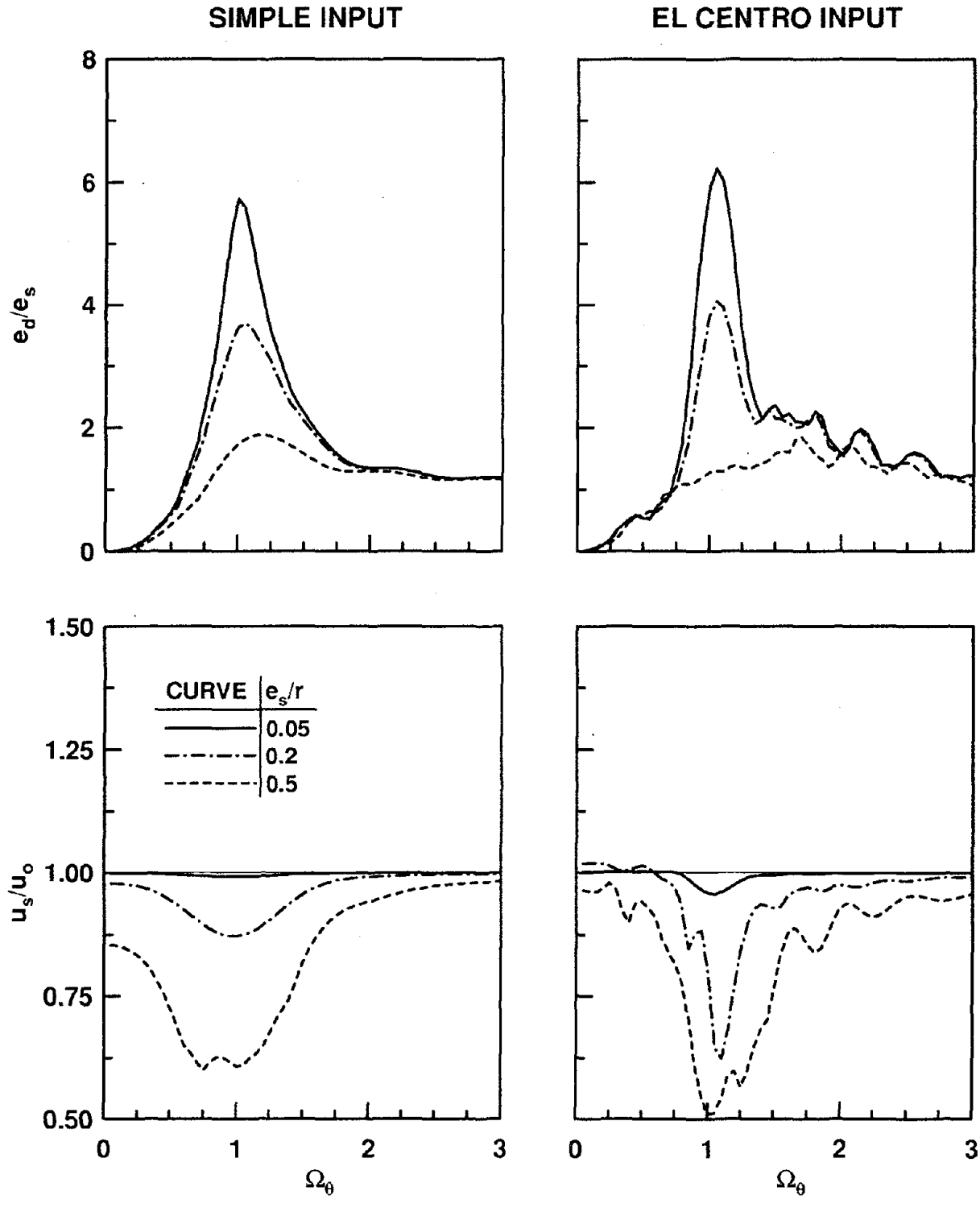

Figure 6.8 Ratio of peak lateral deformations of asymmetric- and symmetric-plan systems, u_s/u_o, and ratio of dynamic and static eccentricities, e_d/e_s, for elastic systems; $T/t_1 = 1.5$ for simple input and $T = 1$ for El Centro input; $e_s/r = 0.05$, 0.2, and 0.5; $\xi = 5\%$.

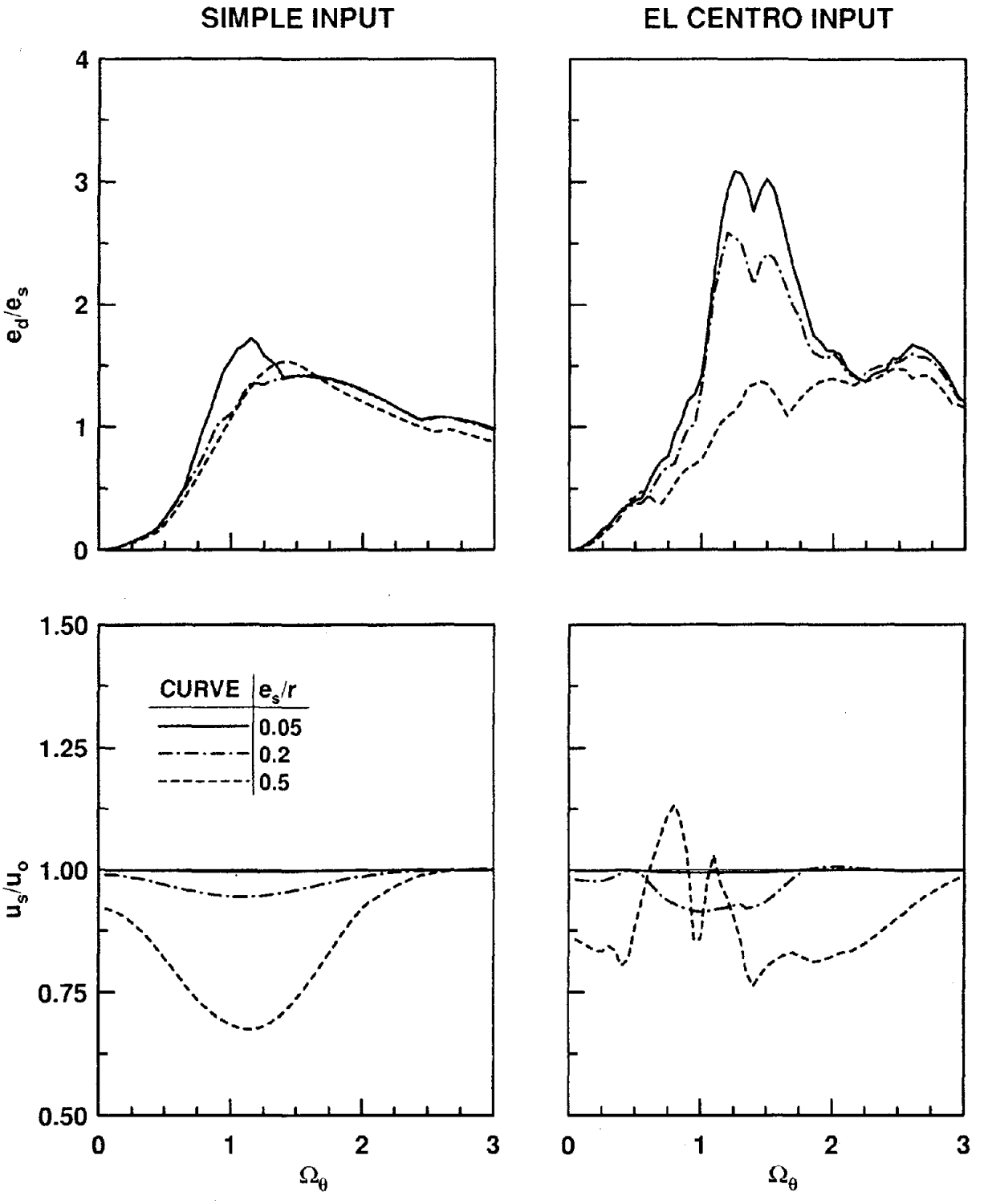

Figure 6.9 Ratio of peak lateral deformations of asymmetric- and symmetric-plan systems, u_s/u_o, and ratio of dynamic and static eccentricities, e_d/e_s, for inelastic systems with e_p=e_s and c = 0.25; T/t_1 = 1.5 for simple input and T = 1 for El Centro input; e_s/r = 0.05, 0.2, and 0.5; ξ = 5%.

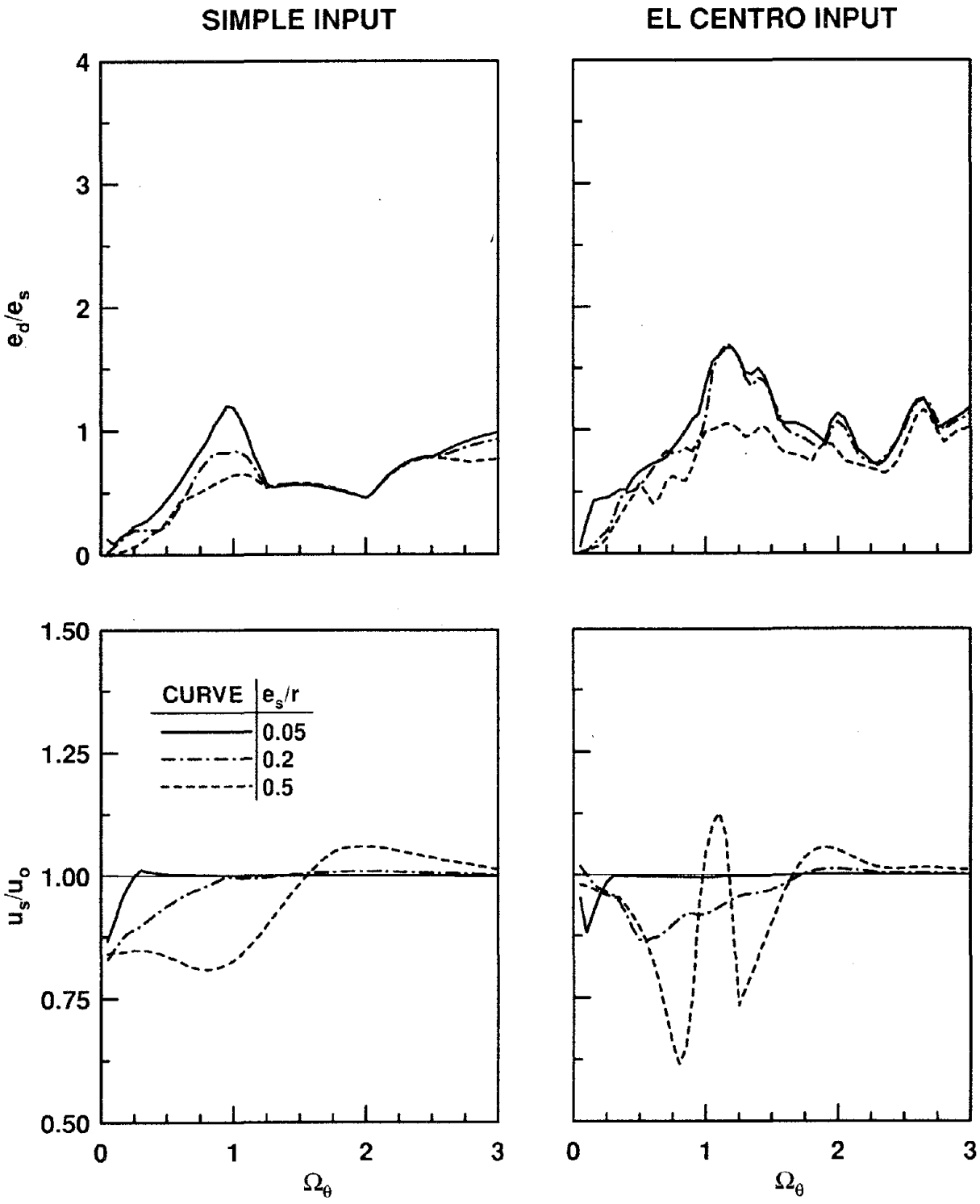

Figure 6.10 Ratio of peak lateral deformations of asymmetric- and symmetric-plan systems, u_s/u_o, and ratio of dynamic and static eccentricities, e_d/e_s, for inelastic systems with e_p=0 and c = 0.25; T/t_1 = 1.5 for simple input and T = 1 for El Centro input; e_s/r = 0.05, 0.2, and 0.5; ξ = 5%.

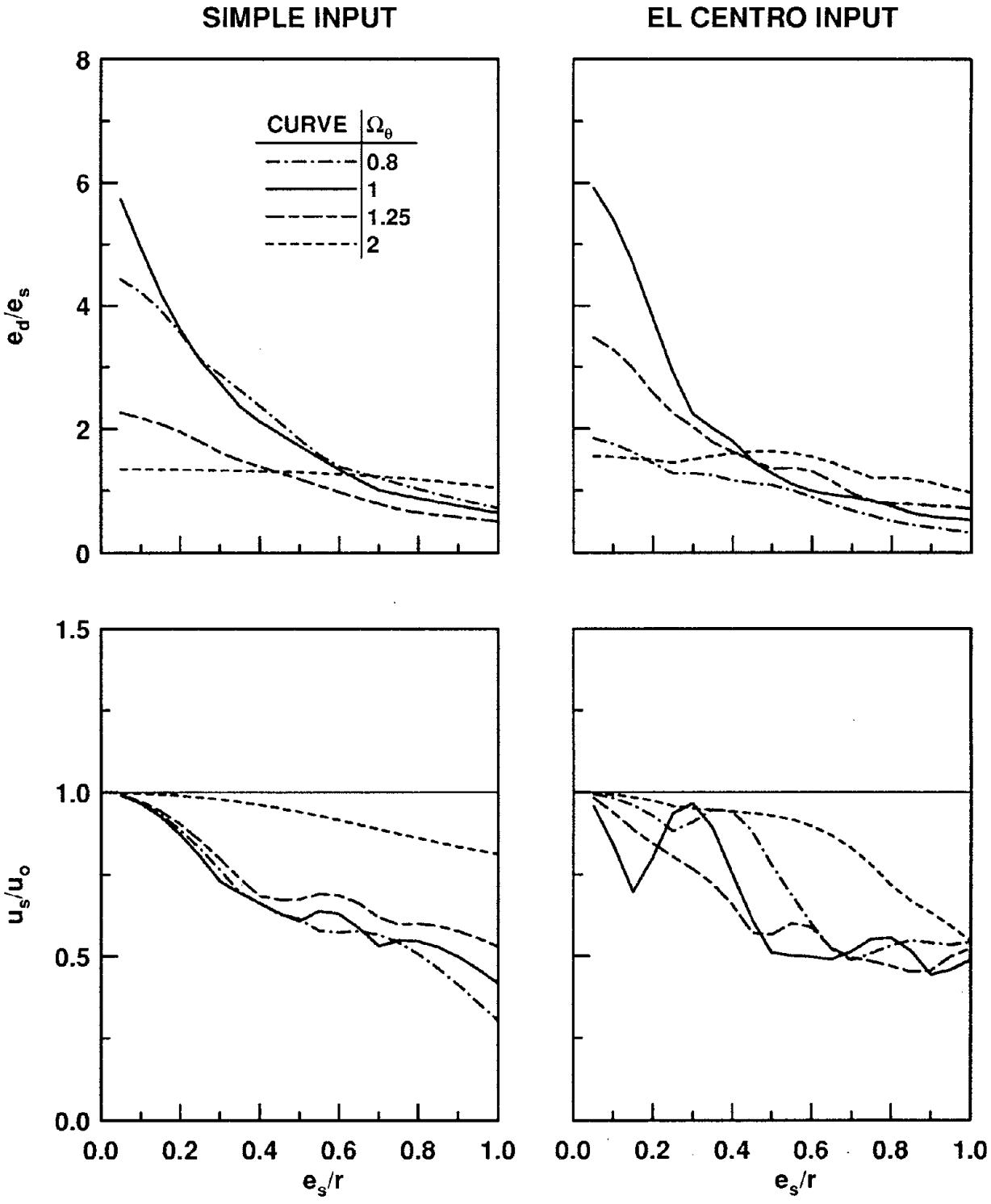

Figure 6.11 Ratio of peak lateral deformations of asymmetric- and symmetric-plan systems, u_s/u_o, and ratio of dynamic and static eccentricities, e_d/e_s, for elastic systems; $T/t_1 = 1.5$ for simple input and $T = 1$ for El Centro input; $\Omega_0 = 0.8$, 1, 1.25, and 2; $\xi = 5\%$.

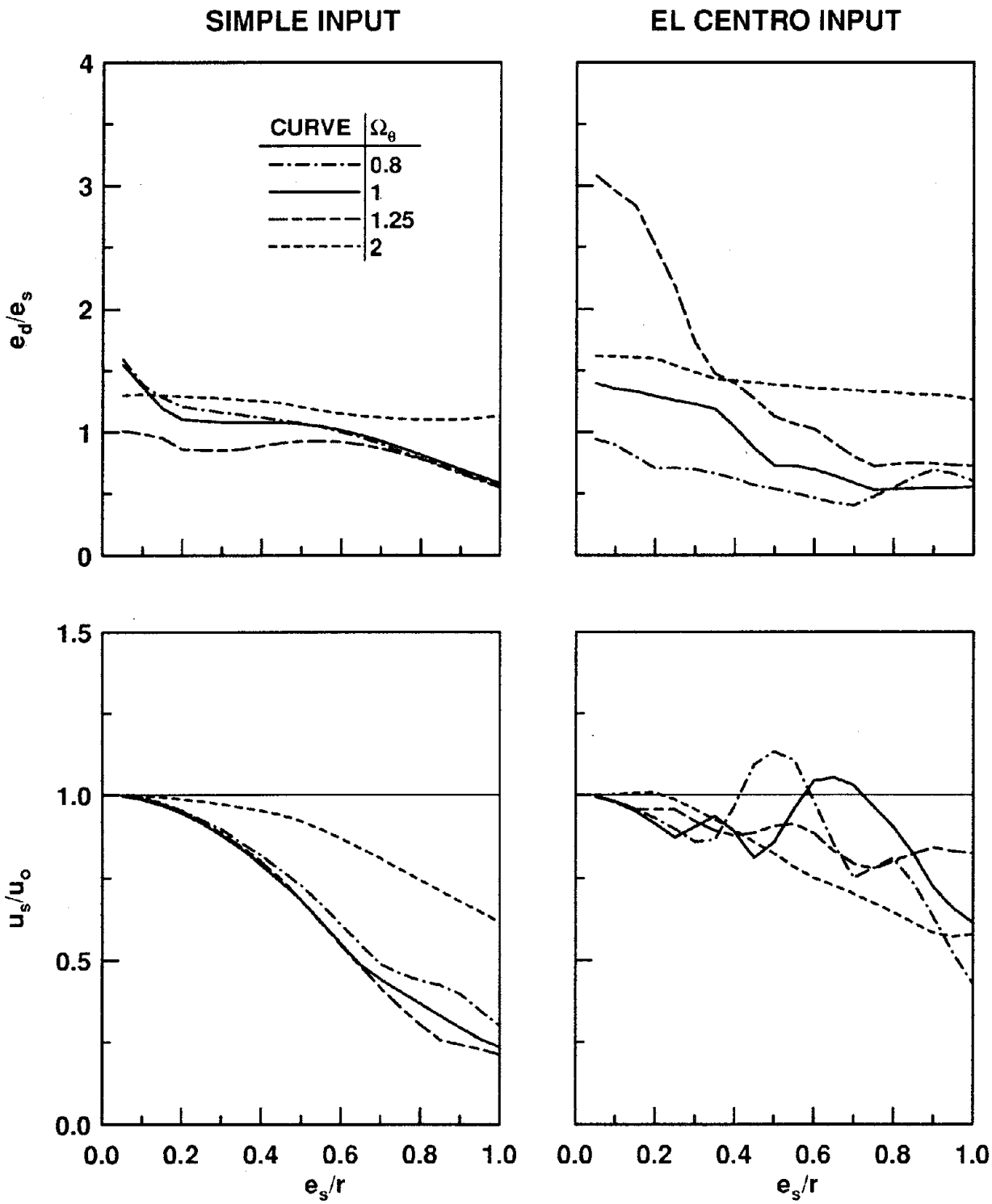

Figure 6.12 Ratio of peak lateral deformations of asymmetric- and symmetric-plan systems, u_s/u_o, and ratio of dynamic and static eccentricities, e_d/e_s, for inelastic systems with e_p=e_s and c = 0.25; T/t_1 = 1.5 for simple input and T = 1 for El Centro input; Ω_θ = 0.8, 1, 1.25, and 2; ξ = 5%.

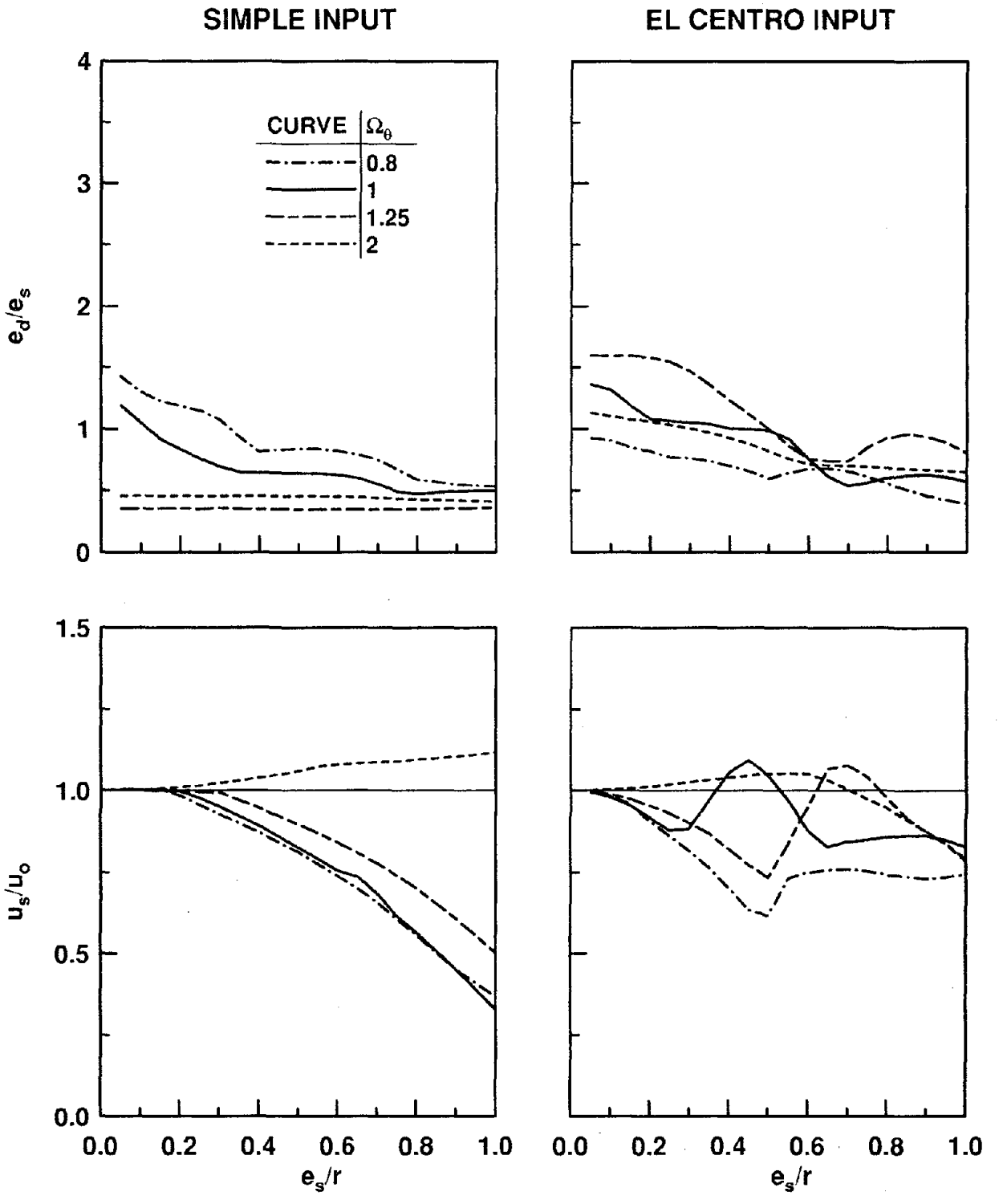

Figure 6.13 Ratio of peak lateral deformations of asymmetric- and symmetric-plan systems, u_s/u_o, and ratio of dynamic and static eccentricities, e_d/e_s, for inelastic systems with e_p=0 and c = 0.25; T/t_1 = 1.5 for simple input and T = 1 for El Centro input; Ω_θ = 0.8, 1, 1.25, and 2; ξ = 5%.

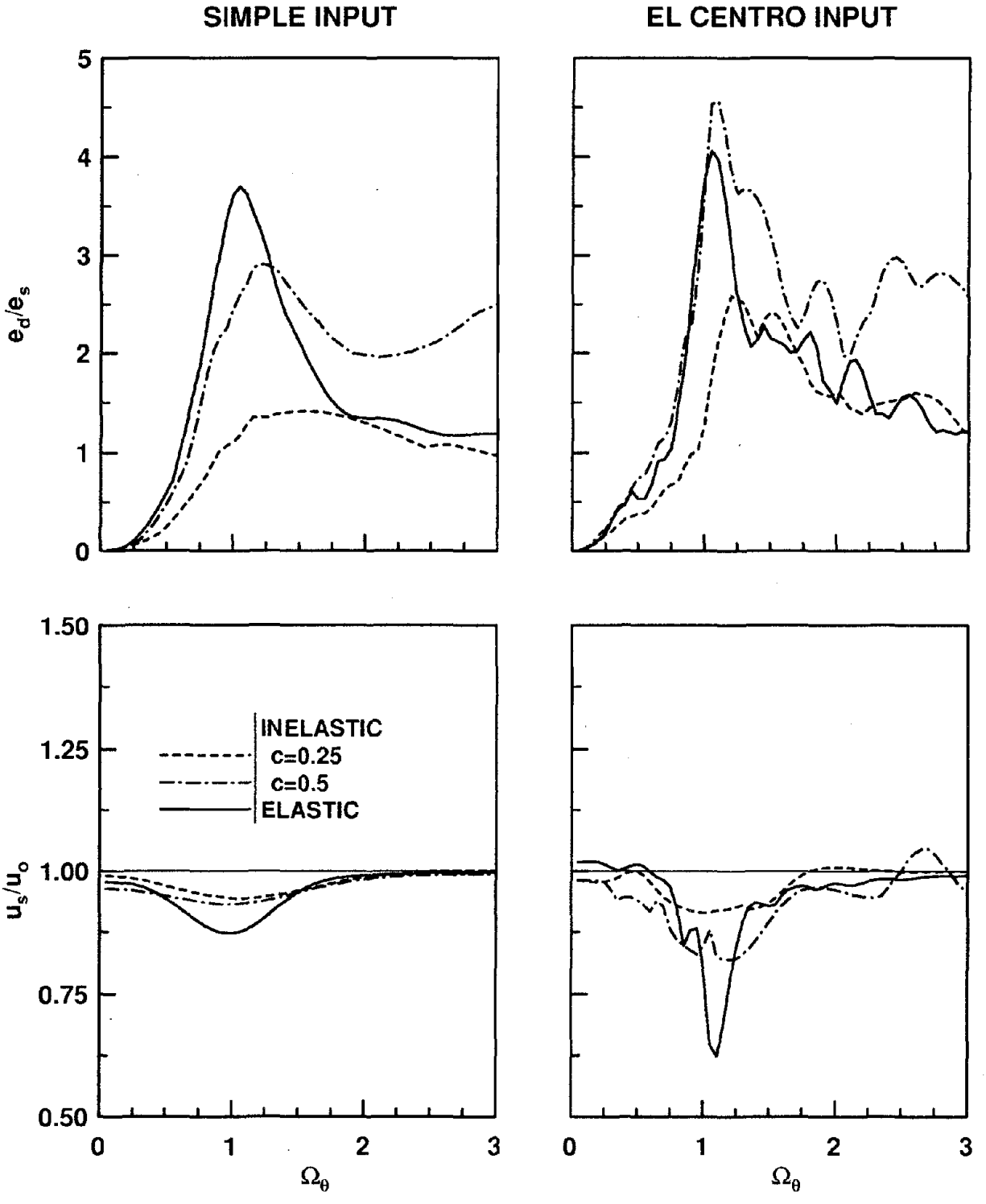

Figure 6.14 Ratio of peak lateral deformations of asymmetric- and symmetric-plan systems, u_s/u_o, and ratio of dynamic and static eccentricities, e_d/e_s, for elastic systems and inelastic systems (e_p=e_s; c = 0.25 and 0.5); T/t_1 = 1.5 for simple input and T = 1 for El Centro input; e_s/r = 0.2 and ξ = 5%.

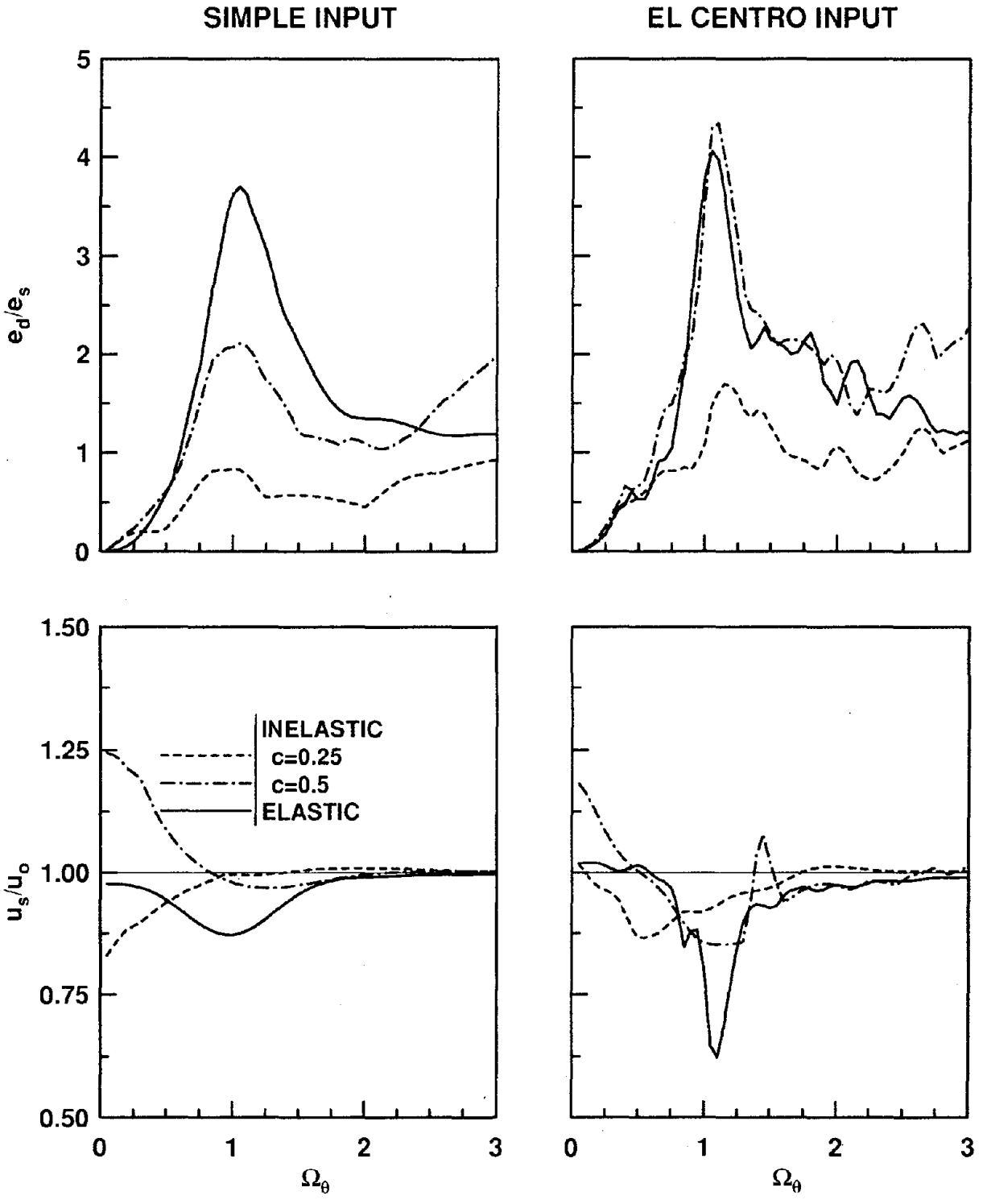

Figure 6.15 Ratio of peak lateral deformations of asymmetric- and symmetric-plan systems, u_s/u_o, and ratio of dynamic and static eccentricities, e_d/e_s, for elastic systems and inelastic systems (e_p=0; c = 0.25 and 0.5); T/t_1 = 1.5 for simple input and T = 1 for El Centro input; e_s/r = 0.2 and ξ = 5%.

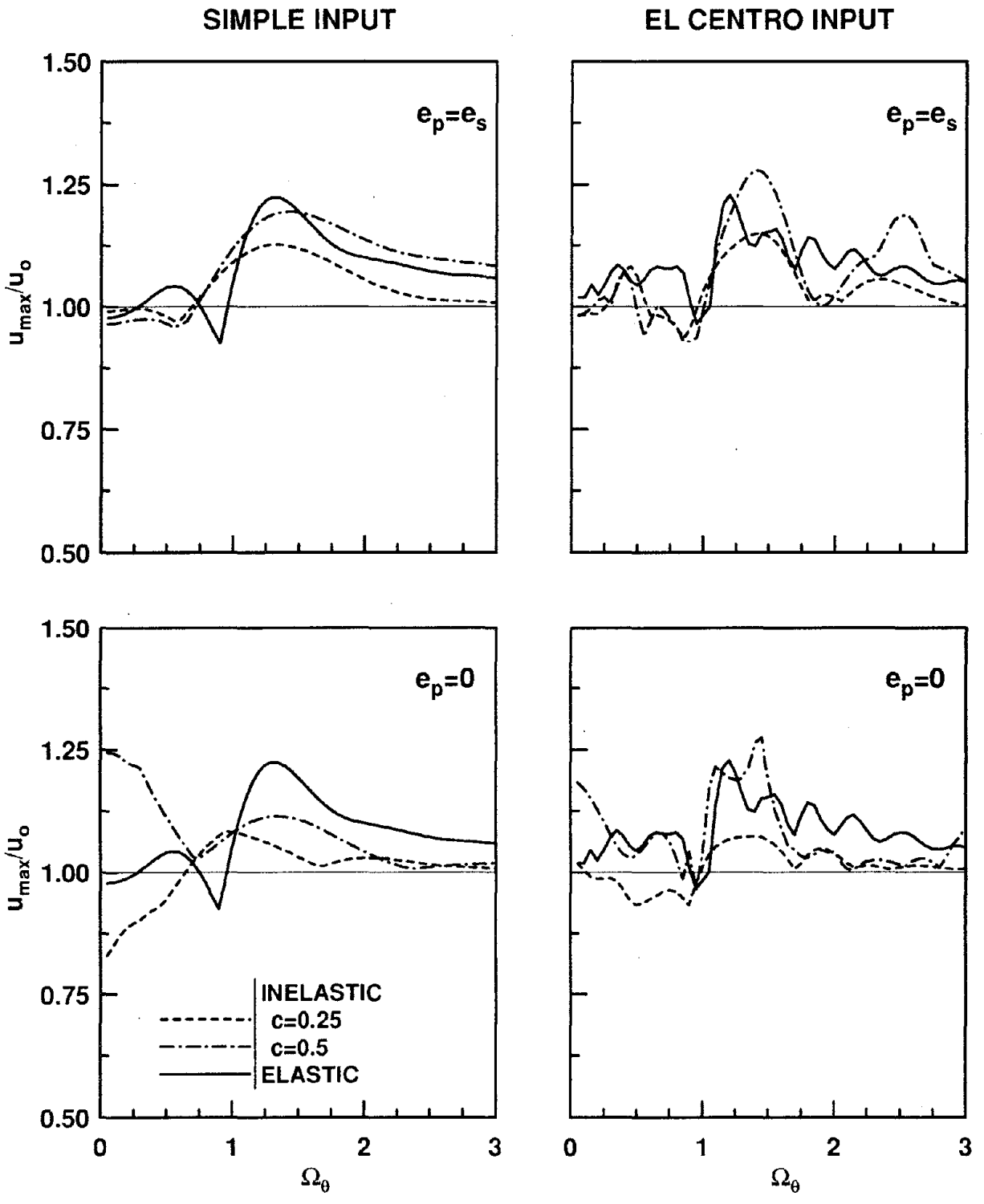

Figure 6.16 Ratio of peak element deformations of asymmetric- and symmetric-plan systems, u_{max}/u_o, for elastic systems and inelastic systems (e_p=0 and e_s; c = 0.25 and 0.5); T/t_1 = 1.5 for simple input and T = 1 for El Centro input; e_s/r = 0.2 and ξ = 5%.

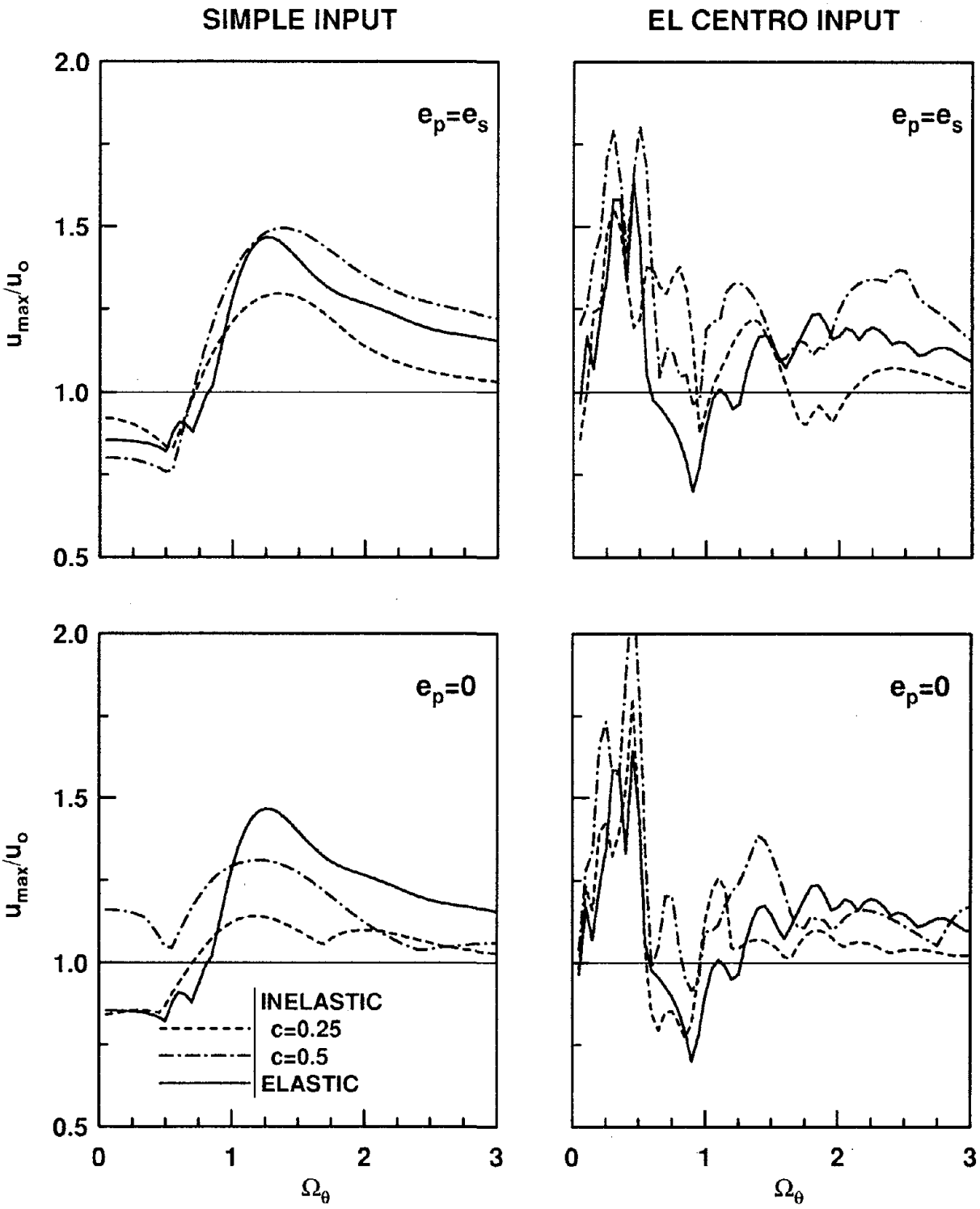

Figure 6.17 Ratio of peak element deformations of asymmetric- and symmetric-plan systems, u_{max}/u_o, for elastic systems and inelastic systems (e_p=0 and e_s; c = 0.25 and 0.5); T/t_1 = 1.5 for simple input and T = 1 for El Centro input; e_s/r = 0.5 and ξ = 5%.

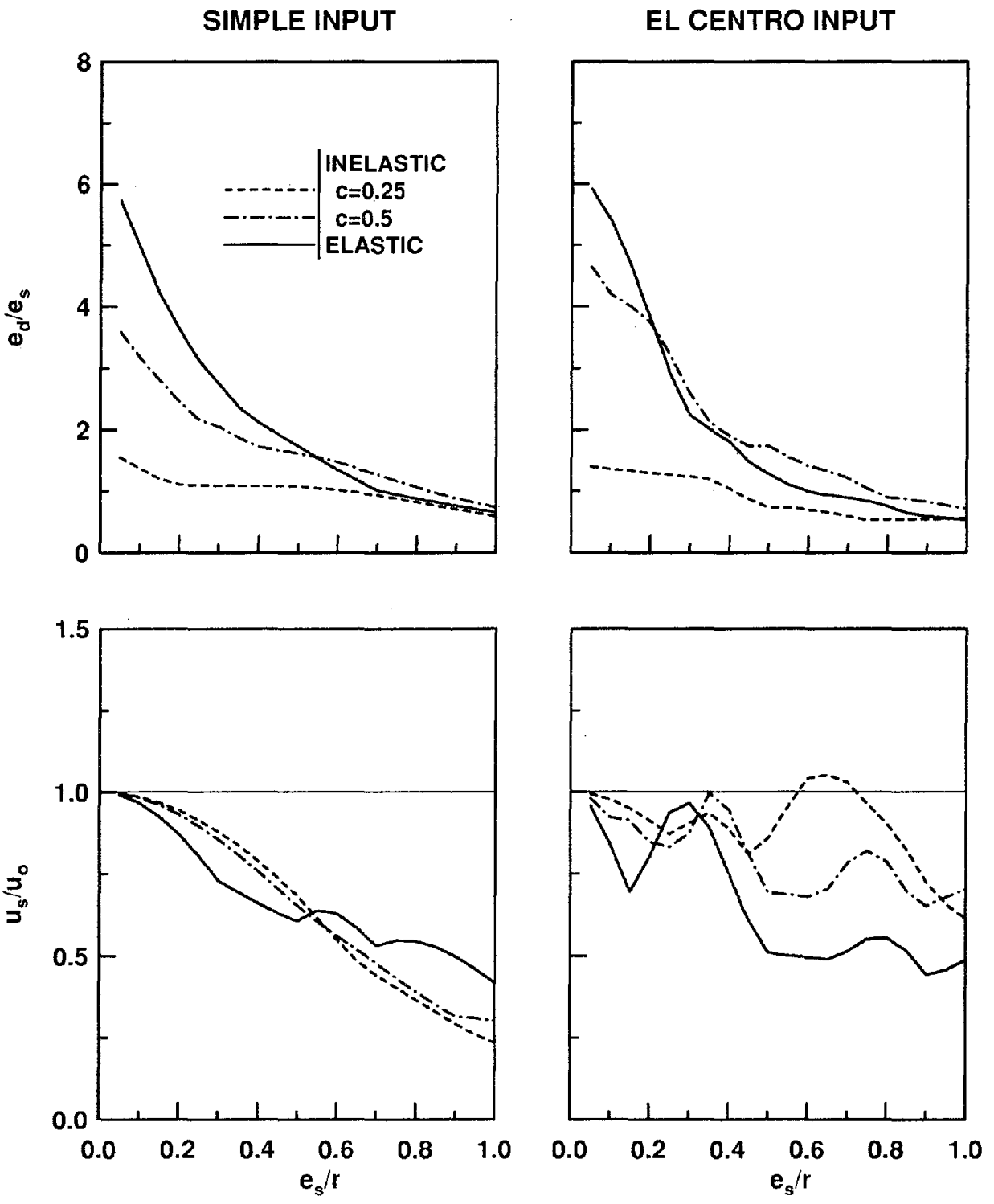

Figure 6.18 Ratio of peak lateral deformations of asymmetric- and symmetric-plan systems, u_s/u_o, and ratio of dynamic and static eccentricities, e_d/e_s, for elastic systems and inelastic systems (e_p=e_s; c = 0.25 and 0.5); T/t_1 = 1.5 for simple input and T = 1 for El Centro input; Ω_θ = 1 and ξ = 5%.

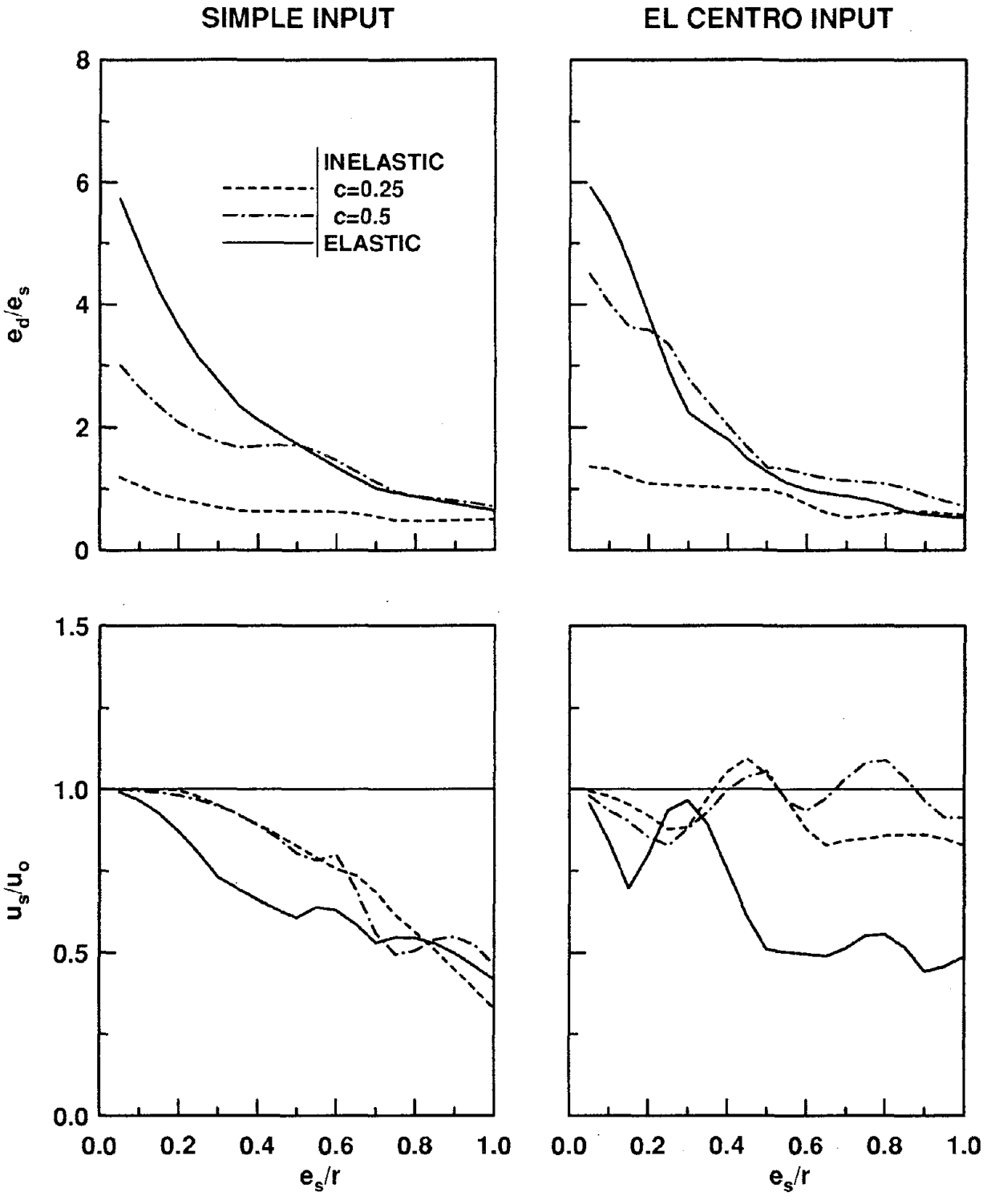

Figure 6.19 Ratio of peak lateral deformations of asymmetric- and symmetric-plan systems, u_s/u_o, and ratio of dynamic and static eccentricities, e_d/e_s, for elastic systems and inelastic systems (e_p=0; c = 0.25 and 0.5); T/t_1 = 1.5 for simple input and T = 1 for El Centro input; Ω_θ = 1 and ξ = 5%.

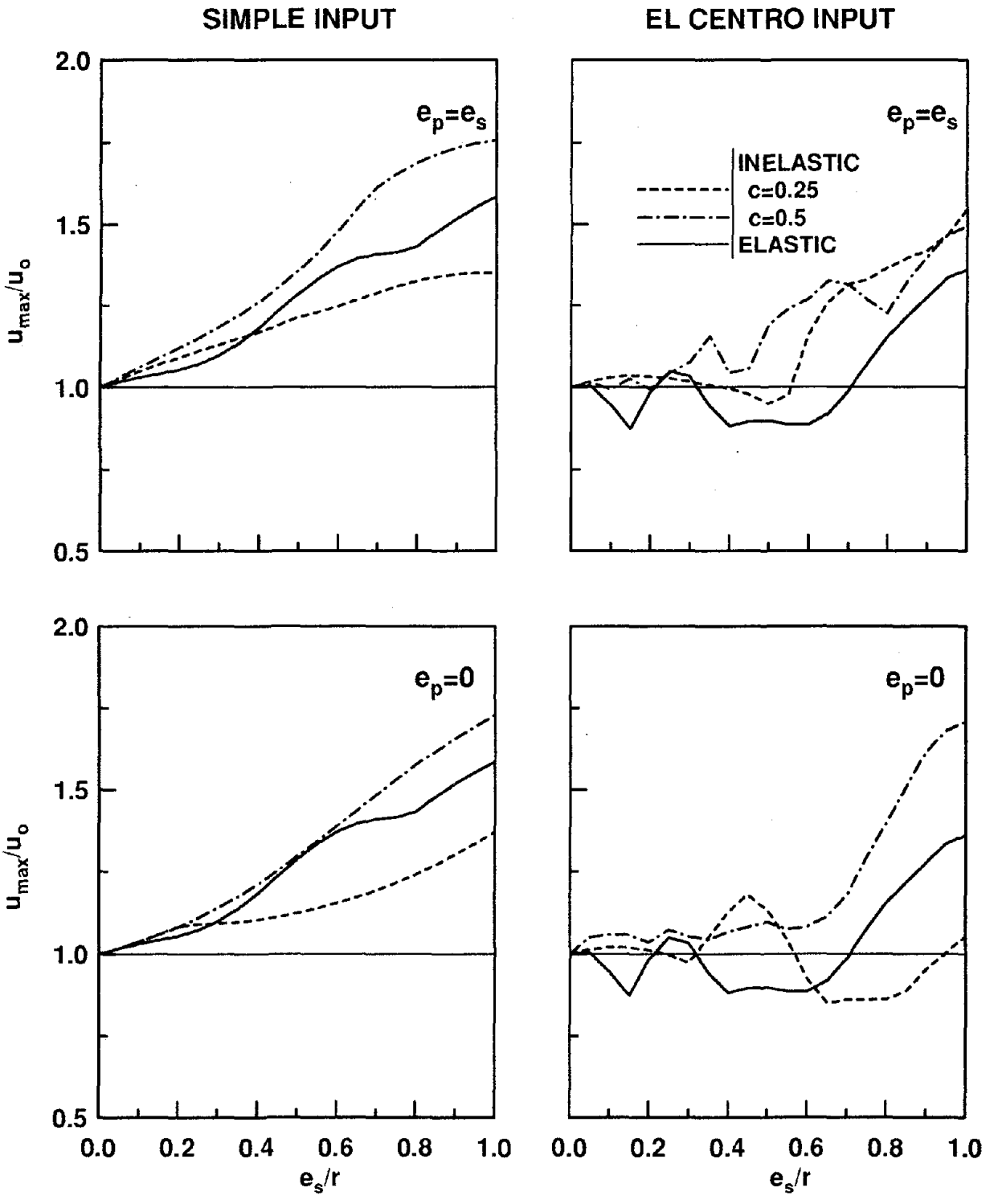

Figure 6.20 Ratio of peak element deformations of asymmetric- and symmetric-plan systems, u_{max}/u_o, for elastic systems and inelastic systems (e_p= 0 and e_s; c = 0.25 and 0.5); T/t_1 = 1.5 for simple input and T = 1 for El Centro input; Ω_θ = 1 and ξ = 5%.

of parameters, e_d/e_s exceeds one indicating dynamic amplification of torsional deformation (Figures 6.8 and 6.11). These effects of plan-asymmetry tend to increase as e_s/r increases, i.e., the system-plan becomes increasingly asymmetric. Thus, u_s is increasingly reduced below u_o as e_s/r increases; and the torsional deformation, as indicated by e_d, increases as e_s/r becomes larger although the ratio e_d/e_s is largest for the smallest e_s/r.

The effects of plan-asymmetry on the response of elastic systems depend in an important way on Ω_θ, the ratio of uncoupled torsional and lateral frequencies (Figures 6.8 and 6.11). For slightly asymmetric systems (small e_s/r) these effects are most pronounced in systems with equal torsional and lateral frequencies (Ω_θ=1) compared to any other value of Ω_θ. As e_s/r increases, the asymmetry effects are not necessarily most pronounced at Ω_θ=1; in case of the simple input, u_s/u_o reaches its minimum value at Ω_θ values below unity while e_d/e_s reaches its maximum at Ω_θ larger than unity; the trends are not as systematic in case of the El Centro excitation. In both cases, the sharp peak at Ω_θ around one for systems with small e_s/r becomes flatter as e_s/r increases, resulting in less dependence of response on Ω_θ in the range 0.8 to 1.25, which covers many buildings [10].

The response of inelastic systems to the simple input is affected by Ω_θ and e_s/r in a manner similar to elastic systems but generally to a lesser degree (Figures 6.9-6.10, 6.12-6.13, 6.14-6.15, and 6.18-6.19). With decreasing yield factor c, which implies increased inelastic action, the peak of e_d/e_s, which still occurs for systems with Ω_θ around one, becomes smaller and flatter, implying less dynamic amplification of torsional deformation and its decreasing dependence on Ω_θ (Figures 6.9-6.10 and 6.14-6.15). Yielding of the system decreases the dynamic amplification of torsional deformation and its dependence on Ω_θ for two reasons: the uncoupled torsional and lateral vibration frequencies which are close to each other in a system with initial elastic value of $\Omega_\theta \approx 1$ are temporarily separated because of inelastic action; and the system behaves as rigid in torsion for extended time durations as the yield strength decreases (Chapter 4). Secondly, as the yield factor c decreases, implying

greater yielding, e_d/e_s becomes increasingly independent of e_s/r (Figures 6.12-6.13 and 6.18-6.19) because in a yielding system, the instantaneous CS may move farther from its initial elastic location or shift to the opposite side leading to cancellation of effects of eccentricity. It is apparent from Figures 6.18 and 6.19 that inelastic action causes the greatest reduction in e_d/e_s for systems with the smallest eccentricity ratio, in which case the elastic response is magnified most; the response of systems with large e_s/r is reduced to a lesser degree by yielding. For a wide range of e_s/r and Ω_θ values, e_d/e_s is less than one for system with small yield strength, especially for 'strength-symmetric' systems (Figures 6.14-6.15 and 6.18-6.19).

The lateral deformation u_s of inelastic systems with $e_p=e_s$ due to the simple input decreases below u_o because of plan-asymmetry (Figures 6.9, 6.12, and 6.14) as in the case of elastic systems (Figures 6.8 and 6.11). The reduction tends to be the largest for the Ω_θ value where the e_d/e_s is the largest. As the yield factor decreases, implying increased inelastic action, the reduction in the lateral deformation due to plan-asymmetry becomes smaller in systems with smaller e_s/r; however, the greater reduction occurs for the larger stiffness eccentricities (Figure 6.18). In case of 'strength-symmetric' ($e_p=0$) inelastic systems, yielding affects the variation of u_s/u_o with Ω_θ in a much different way compared to inelastic systems with $e_p=e_s$, resulting in increased lateral deformation for asymmetric-plan systems with larger Ω_θ and e_s/r or very small Ω_θ (Figures 6.10, 6.13, and 6.15).

As Ω_θ increases above one, i.e., the system becomes increasingly stiff in torsion, the normalized responses of the elastic system are less sensitive to e_s/r, u_s/u_o approaches one indicating that the lateral deformation is affected very little by plan-asymmetry, and e_d/e_s also tends to one implying that the dynamic torsional deformation is the same as the static torsional deformation defined above (Figure 6.8). These limiting values are analytically demonstrated in Appendix D. In particular, for systems with $\Omega_\theta>2$, the normalized responses are not sensitive to e_s/r, and the effects of plan-asymmetry on lateral deformation may be

ignored and the dynamic amplification of torsional deformation neglected. Even for yielding systems, the effects of plan-asymmetry on lateral deformation may be ignored (Figures 6.14 and 6.15). However, the dynamic amplification of torsional deformation may be significant for some values of the yield factor, c.

As Ω_θ becomes small, i.e., the elastic system becomes increasingly flexible in torsion, e_d approaches zero, implying no torsional deformation, regardless of the stiffness eccentricity. However, the lateral deformation u_s is sensitive to the stiffness eccentricity, with a limiting value of u_s/u_o approximately equal to $1/[1+(e_s/r)^2]$, which approaches one as e_s/r becomes small (Figure 6.8). This approximation deteriorates as the stiffness eccentricity increases. These limiting values are analytically demonstrated in Appendix D. Inelastic action has little influence on e_d/e_s which tends to zero as Ω_θ becomes small for all values of c (Figure 6.14 and 6.15). However, the limiting value of u_s/u_o seems to be different for the two types of inelastic systems and depends on c with no apparently systematic trends.

The reduction in the lateral deformation u_s of the asymmetric-plan system below the deformation u_o of the corresponding symmetric-plan system due to plan-asymmetry, observed in this section, for systems with fixed value of the vibration period T may not occur for other values of T; on the contrary, as indicated in the preceding section, plan-asymmetry may increase u_s over u_o for systems with other T values. However, the effects of plan-asymmetry on the lateral deformation, which make u_s different -- larger or smaller -- than u_o is likely to decrease, i.e., u_s is likely to become close to u_o, with all the factors identified in this section.

The effects of plan-asymmetry on the response of inelastic systems are similar in a rough overall sense for the simple input and the El Centro excitation but differ considerably in detail and for certain values of Ω_θ and e_s/r. Furthermore, the variation of u_s/u_o with Ω_θ or e_s/r is much more complicated and irregular for the El Centro excitation. In particular, these complications result in increased lateral deformations in highly asymmetric-plan

systems (large e_s/r) for some values of Ω_θ; the increases are relatively small, however. These differences are in part because of the irregular shape of the response spectrum for a single ground motion. They are likely to decrease if the results were averaged over several ground motions. The values of e_d/e_s for elastic systems are about the same for both excitations, but in case of inelastic systems, they tend to be larger for the El Centro input.

Over a wide range of Ω_θ and e_s/r values, the maximum element deformation, $u_{\max}$, in an asymmetric-plan system due to the simple input is generally, but not always, larger than the element deformation, u_o, in the corresponding symmetric-plan system (Figures 6.16, 6.17, and 6.20). This increase in $u_{\max}$ tends to increase with the stiffness eccentricity e_s/r (Figure 6.20), but its dependence on Ω_θ is not strong or systematic (Figures 6.16 and 6.17). The increase in $u_{\max}$ due to plan-asymmetry may be larger or smaller in inelastic systems. For the smaller values of c, implying much yielding, $u_{\max}/u_o$ is close to one (Figures 6.16 and 6.17), especially for 'strength-symmetric' (e_p=0) systems. However, for some values of c, $u_{\max}/u_o$ for inelastic systems may be larger than that for elastic systems (Figures 6.16 and 6.17). As an exception to the general trend, the element deformation decreases because of plan-asymmetry for very small values of Ω_θ in case of simple input. Furthermore, as the yield factor decreases, implying increased inelastic action, $u_{\max}/u_o$ becomes increasingly insensitive to Ω_θ (Figures 6.16 and 6.17). While the variation of $u_{\max}/u_o$ with Ω_θ or e_s/r is gradual in case of the simple input, it is irregular for the El Centro excitation. In particular, the $u_{\max}$ increases over u_o, as in the case of simple input, for some values of e_s/r, but decreases relative to u_o for other values of e_s/r (Figure 6.20). Similarly $u_{\max}$ decreases below u_o because of plan-asymmetry for sporadic values of Ω_θ (Figures 6.16 and 6.17). If the results were averaged over several ground motions, the variations would tend to be smoother.

7. EVALUATION OF TORSIONAL PROVISIONS IN SEISMIC CODES

7.1 Introduction

In order to develop a basic understanding of the effects of plan-asymmetry on structural response, systems with simple plan-wise distribution of strength -- strength eccentricity e_p=0 or e_s, and overstrength factor O_s=1 -- have been investigated in Chapter 6. However, the resulting conclusions may not be directly applicable to code-designed buildings because the plan-wise distribution of structural strength is not representative of code-designed buildings, and the strength distribution can significantly influence inelastic structural response (Chapter 4). Therefore, the main objective of this chapter is to investigate the effects of plan-asymmetry on the earthquake response of code-designed systems and to determine how well these effects are represented by torsional provisions in building codes. For this purpose, we first determine how the design provisions in various codes influence the element design forces, strength eccentricity, and overstrength factor. Subsequently, the deformation and ductility demands on resisting elements of asymmetric-plan systems are compared with their values if the system plan were symmetric. Based on these results, deficiencies in code provisions are identified and improvements suggested.

7.2 Response Quantities

From a design point of view, it is useful to know how the deformations and ductility demands of resisting elements in an asymmetric-plan system differ from those in the corresponding symmetric-plan system. For this purpose, presented in this investigation are the deformations u_i and ductility demands μ_i of resisting elements in the asymmetric-plan system, normalized by the respective response quantities of the corresponding symmetric-plan system -- a system with e_s=0 but m, K_y, $K_{\theta s}$, and element stiffnesses k_{jy} same as in the asymmetric-plan system (Chapter 3). As will be demonstrated later, if the accidental eccentricity is included in the design of the corresponding symmetric-plan system, it experiences coupled lateral-torsional motions when excited into the inelastic range; consequently, the deformations and ductility demands, u_{io} and μ_{io}, for all the resisting elements of such system

are not identical. However, if the accidental eccentricity is ignored, this system responds only in lateral vibration as a SDF system and $u_{io}=u_o$ and $\mu_{io}=\mu_o$, where u_o and μ_o are the deformation and ductility demand of the SDF system. Thus, the response quantities considered in this investigation are u_i/u_{io} and μ_i/μ_{io} when the accidental eccentricity is included in the system design, and u_i/u_o and μ_i/μ_o when it is ignored. The differences between the response of asymmetric-plan and the corresponding symmetric-plan system are measured by the deviations of normalized response quantities, u_i/u_{io} and μ_i/μ_{io}, or u_i/u_o and μ_i/μ_o, from one.

7.3 Torsional Provisions in Seismic Codes

7.3.1 Method for Computing Design Forces

The design force V specified in building codes is usually much smaller than the strength V_o required for the system to remain elastic during intense ground shaking. Instead of computing the base shear from code formulas which would result in different values according to different codes, the base shear is defined as

$$V = \frac{1}{R}V_o \tag{7.1}$$

where R is a reduction factor depending on the capacity of the system to safely undergo inelastic deformation during intense ground shaking [27]. Thus, the element design forces according to various codes would differ only because of differences in the torsional provisions in various codes.

In a one-story, symmetric-plan system, the design force V is applied at the CS. If the floor diaphragm is rigid, all resisting elements along the direction of ground motion undergo the same lateral displacement u, the lateral resisting force in the element is $k_{jy}u$, and the total resisting force is $V=K_yu$. Thus, the design force in the j^{th} resisting elements is $(k_{jy}/K_y)V$ and the forces are distributed to the elements in proportion to their lateral stiffnesses or rigidities.

In asymmetric-plan systems, the design force V is applied eccentric from the CS at a distance equal to design eccentricity, e_d, which is defined in the next section. Under the action of the resulting torque, $e_d V$, the rigid roof deck will undergo rotation of $e_d V/K_{\theta s}$ about the CS where $K_{\theta s} = \sum k_{jy}(x'_j)^2 + \sum k_{ix} y_i^2$ is the torsional stiffness about the CS, in which $x'_j = x_j - e_s$ is the distance of the j^{th} element oriented in the Y-direction from the CS, and y_i defines the location of the i^{th} element oriented in the X-direction. Thus the design force in the j^{th} element along the direction of ground motion is

$$V_j = \frac{k_{jy}}{K_y} V + \frac{e_d V}{K_{\theta s}}(-x'_j) k_{jy} \tag{7.2}$$

The second term represents the element force associated with its deformation resulting from deck rotation and thus the change in element force due to plan-asymmetry. Obviously, the torsion induced forces are distributed to the various resisting elements in proportion to their torsional stiffnesses or rigidities.

7.3.2 Design Eccentricity

Most building codes require that the lateral earthquake force at each floor level of an asymmetric-plan building be applied eccentrically relative to the center of stiffness. The design eccentricity e_d specified in most seismic codes is of the form [15]

$$e_d = \alpha e_s + \beta b \tag{7.3a}$$

$$e_d = \delta e_s - \beta b \tag{7.3b}$$

where e_s is the stiffness eccentricity; b is the plan dimension of the building perpendicular to the direction of ground motion; and α, β, and δ are specified coefficients. For each element the e_d value leading to the larger design force is to be used. Consequently, equation (7.3a) is the design eccentricity for elements located within the flexible-side of the building and equation (7.3b) for the stiff-side elements [25].

The coefficients, α, β, and δ vary among building codes. For example, the Uniform Building Code (UBC-88) [16] and Applied Technology Council (ATC-3) provisions [32] specify β=0.05 and α=δ=1, the latter implying no dynamic amplification of torsional response; the Mexico Federal District Code (MFDC-77) [5,28] specifies β=0.1, δ=1, and α=1.5, the latter implies dynamic amplification; the National Building Code of Canada (NBCC-85) [22] specifies β=0.1, α=1.5, and δ=0.5; and the New Zealand Code (NZC-84) [23] specifies β=0.1 and α=δ=1.

The first term in equation (7.3) involving e_s is intended to account for the coupled lateral-torsional response of the building arising from lack of symmetry in plan, whereas the second term is included to consider torsional effects due to other factors such as the rotational component of ground motion about a vertical axis; differences between computed and actual values of stiffnesses, yield strengths, and dead-load masses; and unforeseeable unfavorable distribution of live-load masses. This accidental eccentricity, βb, which is a fraction of the plan dimension, b, is obviously considered in design to be on either side of the CS. It is considered even for the design of symmetric-plan systems, in which case it becomes the total design eccentricity because e_s=0.

7.3.3 Element Design Forces

The element design forces for an asymmetric-plan system are given by equation (7.2) with the design eccentricity, e_d, defined by equation (7.3a) or (7.3b). The first value of e_d will lead to the larger design force in an element located in the flexible-side of the building:

$$V_j = \left[\frac{k_{jy}}{K_y}V + \frac{\beta b V}{K_{\theta s}}(-x'_j)k_{jy}\right] + \left[\frac{\alpha e_s V}{K_{\theta s}}(-x'_j)k_{jy}\right] \tag{7.4}$$

and the second value of e_d results in the larger design force in stiff-side elements:

$$V_j = \left[\frac{k_{jy}}{K_y}V + \frac{-\beta b V}{K_{\theta s}}(-x'_j)k_{jy}\right] + \left[\frac{\delta e_s V}{K_{\theta s}}(-x'_j)k_{jy}\right] \tag{7.5}$$

The first term in equations (7.4) and (7.5) is the element force if the system plan were

symmetric (e_s=0), and the second term arises from plan-asymmetry.

Thus, the element design forces for buildings with symmetrical plan are

$$V_{jo} = \frac{k_{jy}}{K_y} V + \frac{\beta b V}{K_{\theta s}} k_{jy} \mid x'_j \mid \tag{7.6}$$

wherein the first terms of equations (7.4) and (7.5) have been rewritten to emphasize that the accidental eccentricity always leads to an increased force in all resisting elements, with this increase being larger from codes with larger values of β.

The design force, V_j, in a resisting element of the asymmetric-plan system of Figure 5.1, normalized by the design force, V_{jo}, in the element if the system plan were symmetric is presented in Figure 7.1 for several codes. The ratio V_j/V_{jo} is also equal to the ratio of the yield deformation of the element in asymmetric-plan and symmetric-plan systems. In calculating V_j and V_{jo}, the accidental eccentricity βb is considered in one case but ignored in the other. The second term, arising from plan-asymmetry is alway additive for flexible-side resisting elements (equation (7.4)) leading to larger design forces; this term is subtractive for stiff-side elements (equation (7.5)) resulting in smaller design forces because δ>0 in all codes.

The increase in design force for a flexible-side element grows with e_s and the coefficient α in the design code (Figure 7.1). Thus, among the building codes considered, NBCC-85 and MFDC-77 which specify α=1.5 lead to the largest increase in the design force, and UBC-88, ATC-3, and NZC-84 which specify α=1 result in the smallest increase; NZC-84 leads to a smaller increase compared to UBC-88 although α=1 is the same in both codes because the force V_{jo} is larger in a symmetric-plan system designed by the NZC-84, which specifies a larger accidental eccentricity (β=0.1), compared to UBC-88 with smaller accidental eccentricity (β=0.05). Obviously, if the accidental eccentricity is ignored, all codes which specify α=1 -- UBC-88, ATC-3, and NZC-84 -- lead to the same design force in the flexible-side element.

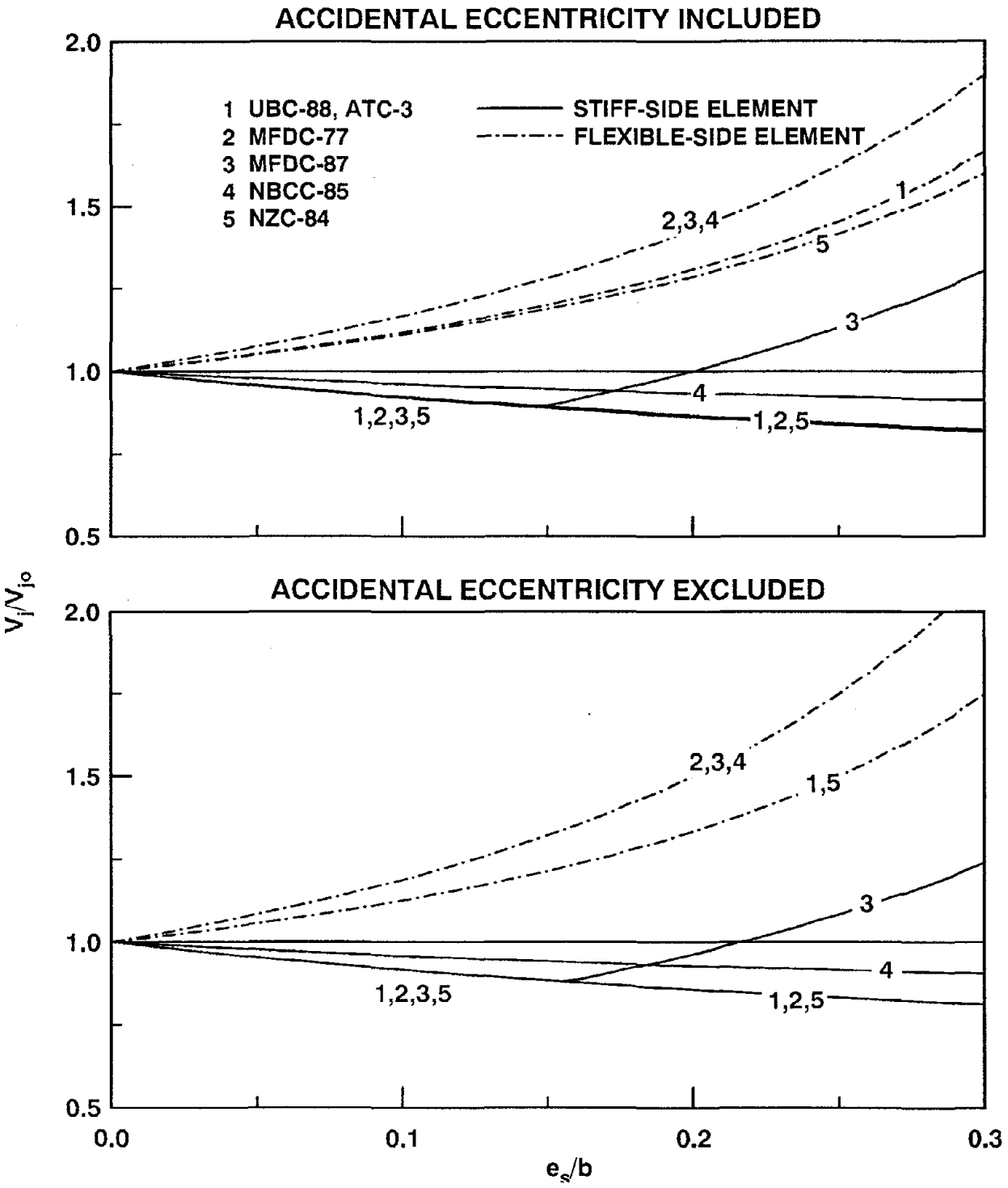

Figure 7.1 Element design force, V_j, in asymmetric-plan system computed for several design codes normalized by its value, V_{jo}, if the system plan were symmetric. In calculating V_j and V_{jo}, the accidental eccentricity is included in one case but excluded in the other.

The decrease in design force for a resisting element within the stiff-side of the building grows with e_s and the coefficient δ in the design code (Figure 7.1). Thus, among the codes considered, UBC-88, ATC-3, MFDC-77, and NZC-84 all of which specify $\delta=1$ lead to a decrease in the design force which is more than from NBCC-85 which specifies $\delta=0.5$; MFDC-77 and NZC-84 lead to a further reduction compared to UBC-88 although $\delta=1$ in all these codes because the force V_{jo} is smaller in the latter case due to smaller β. Obviously, if the accidental eccentricity is ignored, all the codes which specify $\delta=1$ -- UBC-88, ATC-3, NZC-84, and MFDC-77 -- lead to the same design force in the stiff-side element.

Such reduction in design forces for stiff-side elements is not permitted by several building codes, e.g., UBC-88, Peru, and India [15]. According to these codes, the element design forces should be increased due to plan-asymmetry but not reduced below their values for a symmetric-plan system, implying that the second term in equation (7.5) must be ignored. However, other codes and recommendations, e.g., ATC-3, MFDC-77, NBCC-85, and NZC-84, apparently do not explicitly preclude such reduction in element design forces, thus leaving open this possibility in the design process.

The 1977 Mexico Federal District Code (MFDC-77) specified the design eccentricity by equation (7.3) with $\alpha=1.5$, $\delta=1$, and $\beta=0.1$ [5,28]. The most recent edition of the Code, MFDC-87, imposes the additional requirement that element strengths shall be such that: e_p and e_s have the same sign, $e_p \geq e_s - 0.2b$ when $Q \leq 3$, and $e_p \geq e_s - 0.1b$ when $Q > 3$ [9], where Q is related to the reduction factor R; for medium-period and long-period systems, $Q=R$. The additional requirements of MFDC-87, if not satisfied by the element forces from MFDC-77, may be met by increasing the strengths of stiff-side elements as shown in Figure 7.1, or by the undesirable alternative of decreasing the strengths of flexible-side elements.

7.3.4 Overstrength Factor

The total lateral design force is generally increased due to plan-asymmetry because for each resisting element the more unfavorable of the two values of e_d (equation (7.3)) is used

to compute the design force and because some codes specify that the design force for any resisting element should not be smaller than its value if the system plan were symmetric. The ratio of the total design force for a one-story asymmetric-plan building to the corresponding value for the symmetric-plan system is:

$$O_s = \frac{\sum V_j}{\sum V_{jo}} \tag{7.7}$$

where the element design forces V_j are given by equations (7.4) and (7.5) and V_{jo} by equation (7.6). The overstrength factor, O_s, depends on the coefficients α, β, and δ in the governing code, and whether the reduction in design forces of the stiff-side elements below their symmetric-plan values is permitted. Figures 7.2 and 7.3 show that buildings designed according to UBC-88 or ATC-3 would possess the lowest overstrength, whereas those designed by NBCC-85 generally posses the largest overstrength; however, for large values of the stiffness eccentricity, systems designed by MFDC-87 have the largest overstrength because of the increased design force for stiff-side elements (Figure 7.1). The overstrength factor increases with e_s and is larger if reduction in design forces of stiff-side elements is precluded. If design forces computed from equation (7.5) were permitted to be less than symmetric-plan values and a single e_d value was used instead of the more unfavorable of the two values of equation (7.3), the total design force would be unaffected by asymmetry of building plan and $O_s = 1$.

7.3.5 Strength Eccentricity

The strength eccentricity, e_p, of a code-designed, one-story system with asymmetric plan is generally smaller than its stiffness eccentricity, e_s. This is demonstrated in Figures 7.4 and 7.5 where e_p is plotted against e_s, and the differences between the two are seen to depend on the particular code; e_p is the largest and hence closest to e_s for systems designed according to the UBC-88 and ATC-3 and is the smallest and hence farthest from e_s in case of MFDC-77. However, MFDC-87 specifies a minimum value of e_p which for systems with

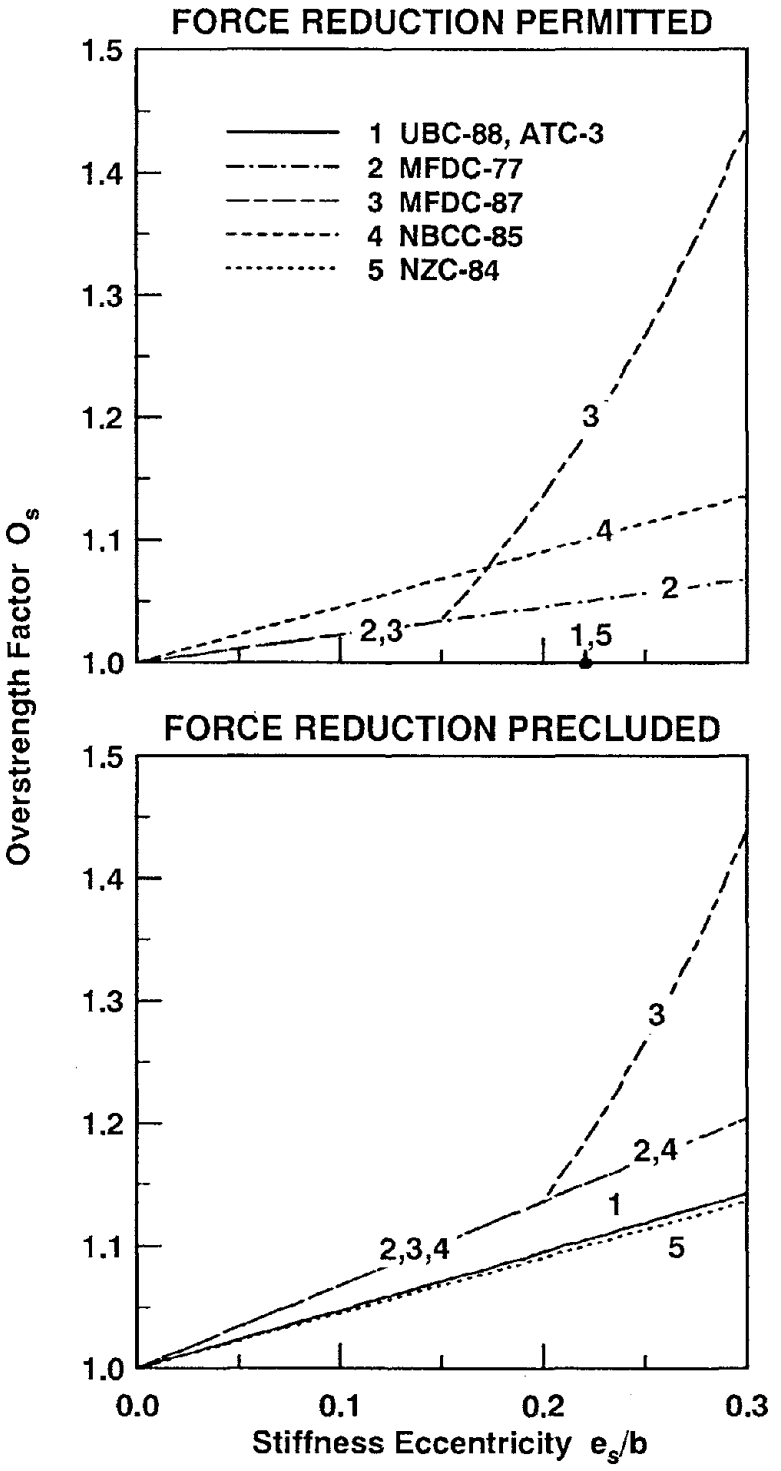

Figure 7.2 Variation in overstrength factor, O_s, with stiffness eccentricity, e_s, for systems designed by several codes, including accidental eccentricity. Reduction in design force of stiff-side element is permitted in one case but precluded in the other.

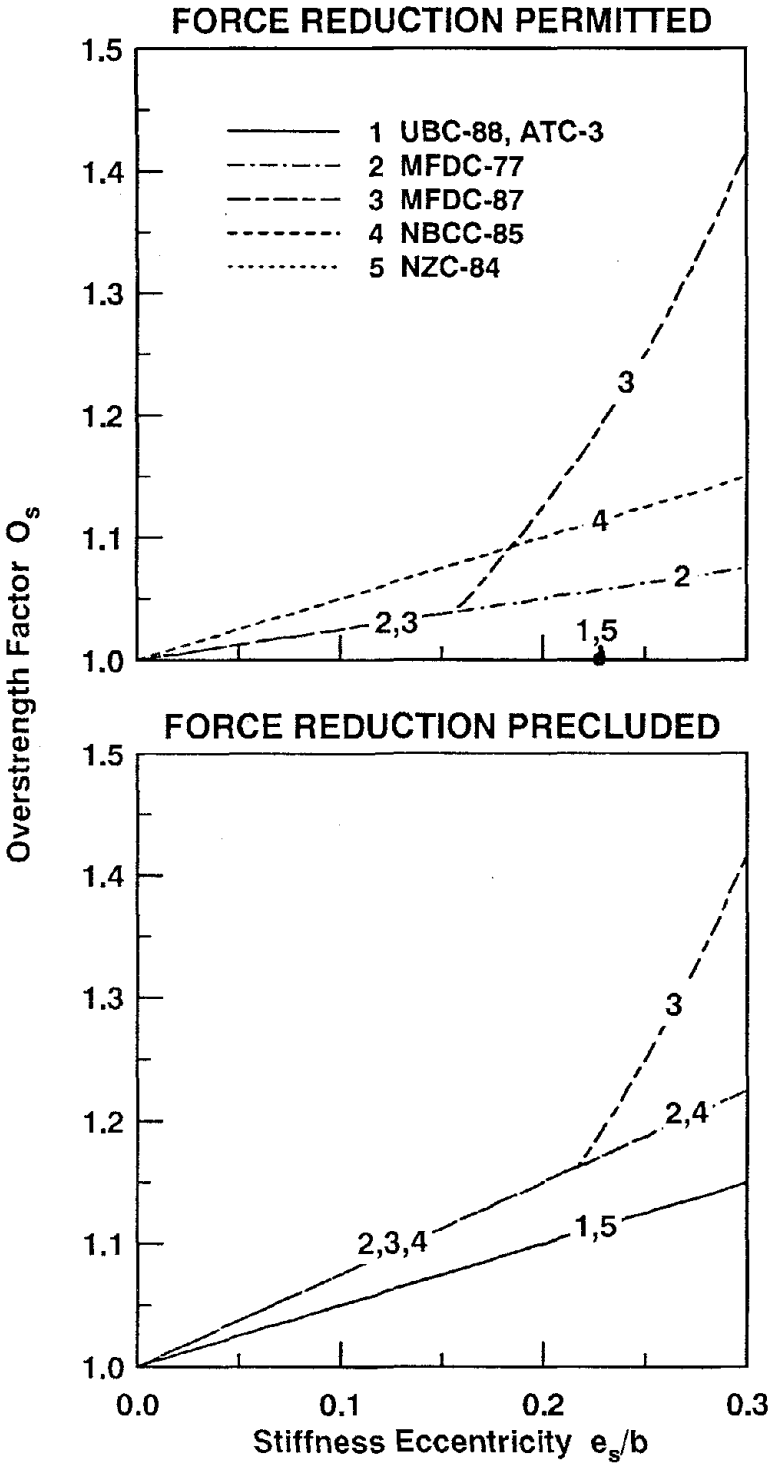

Figure 7.3 Variation in overstrength factor, O_s, with stiffness eccentricity, e_s, for systems designed by several codes, excluding accidental eccentricity. Reduction in design force of stiff-side element is permitted in one case but precluded in the other.

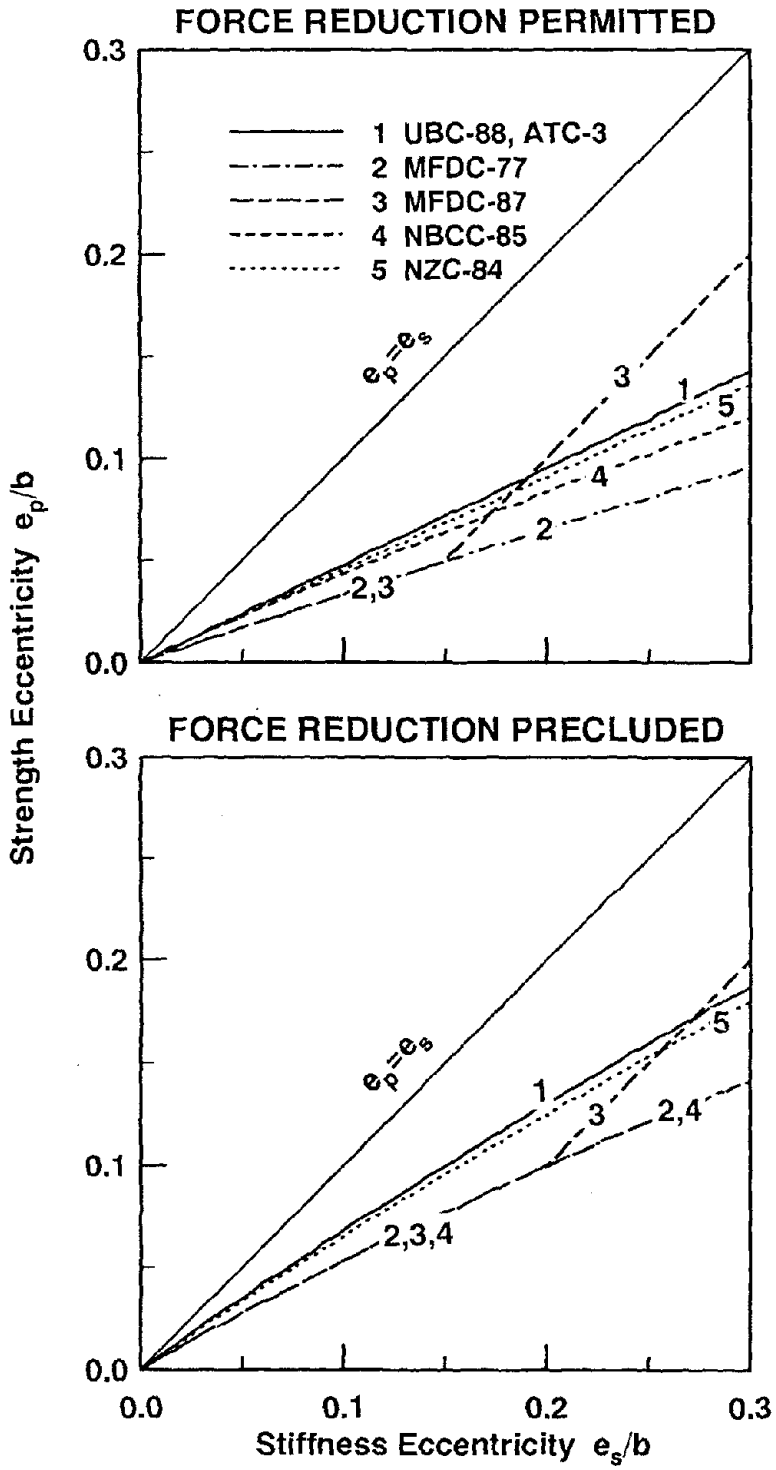

Figure 7.4 Variation in strength eccentricity, e_p, with stiffness eccentricity, e_s, for systems designed by several codes, including accidental eccentricity. Reduction in design force of stiff-side element is permitted in one case but precluded in the other.

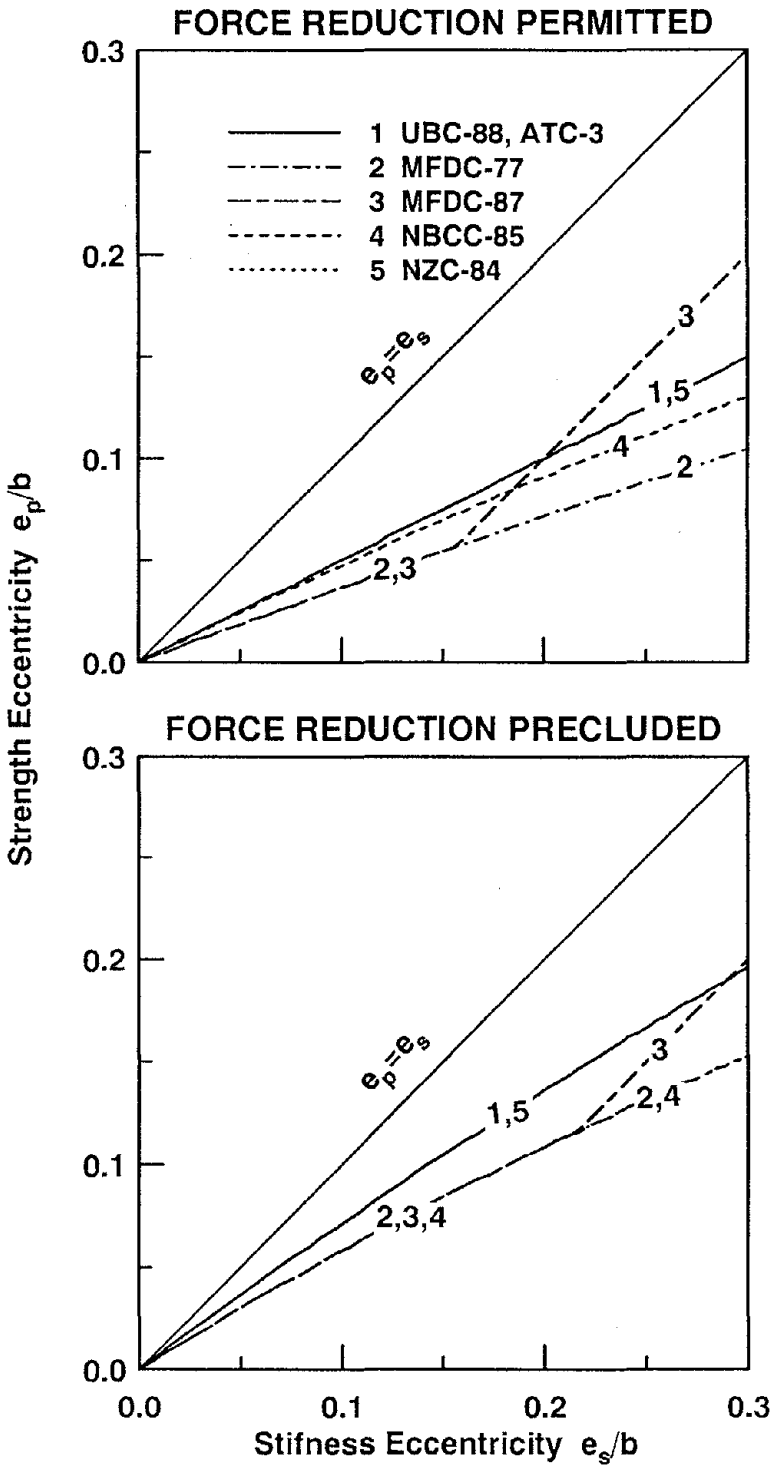

Figure 7.5 Variation in strength eccentricity, e_p, with stiffness eccentricity, e_s, for systems designed by several codes, excluding accidental eccentricity. Reduction in design force of stiff-side element is permitted in one case but precluded in the other.

large e_s turns out to be the largest among all codes considered. The e_p is larger if the code restricts the element design forces to be no smaller than in the symmetric-plan system, and is slightly different if the accidental eccentricity is ignored (Figure 7.5) compared to when it is included (Figure 7.4).

In contrast to the strength eccentricity, e_p, values presented in Figures 7.4 and 7.5 for the four-element systems, it was recently reported that the e_p is approximately equal to zero for code-designed, asymmetric-plan systems [36]. In order to identify the reasons for this apparent contradiction, the strength eccentricity is presented in Figure 7.6 for the system of Reference [36], with all three resisting elements oriented along the direction of ground motion. It is seen that e_p is close to zero provided that the reduction in design forces of stiff-side elements below their symmetric-plan values is permitted, but not if such a reduction is precluded. Thus, the conclusion of Reference [36] that $e_p \approx 0$ is not applicable to most buildings which invariably include resisting elements in both lateral directions to provide resistance to the two horizontal components of ground motion, and because design forces for stiff-side elements are usually not reduced below their symmetric-plan values.

The strength eccentricity of a code-designed system with symmetric plan ($e_s=0$) is given by equation (2.5) with element yield forces replaced by V_{jo}, obtained from equation (7.6), which reduces to (Appendix E)

$$e_p = \frac{1}{\sum_j V_{jo}} \frac{\beta b V}{K_{\theta s}} \left[\sum_j k_{jy} x_j \mid x_j \mid \right] \tag{7.8}$$

Thus the strength eccentricity, e_p, would be zero only if the term in square brackets of equation (7.8) vanishes. Such is the case for the system of Figure 5.1 with $e_s=0$ or its generalized version with resisting elements appearing in pairs, each pair having equal stiffness and located symmetrically about the CM. In general, the strength eccentricity, e_p, would not be zero for a system designed to include the effects of accidental eccentricity, even if its stiffness eccentricity $e_s=0$. Such a system, although displaying only lateral motion in the

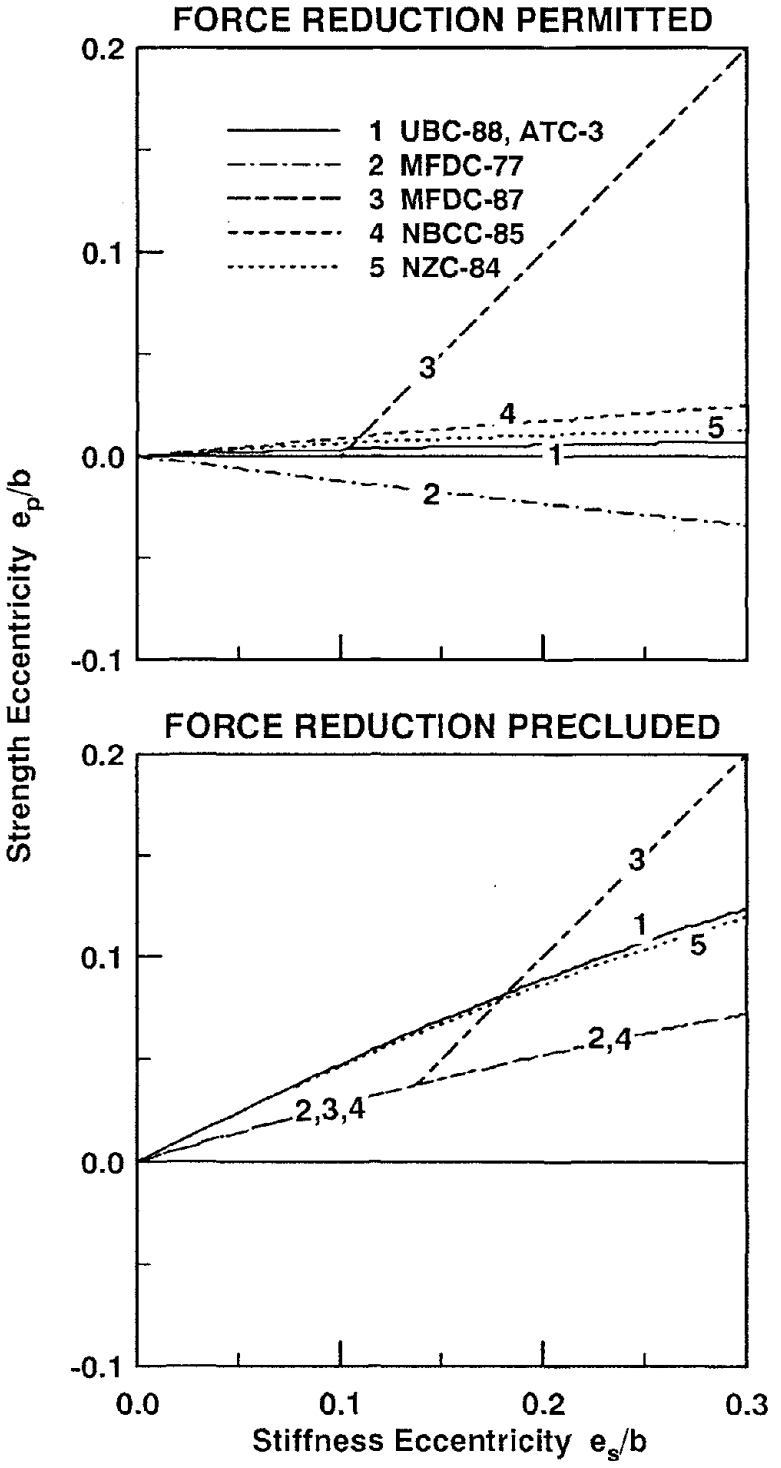

Figure 7.6 Variation in strength eccentricity, e_p, with stiffness eccentricity, e_s, for a three-element system designed by several codes, including accidental eccentricity. Reduction in design force of stiff-side element is permitted in one case but precluded in the other.

elastic range would undergo coupled lateral-torsional motions in the inelastic range.

7.4 Preliminaries

Before investigating how the earthquake response of asymmetric-plan systems differ from that of symmetric-plan systems, two preliminary issues are investigated.

7.4.1 Yielding of Perpendicular Elements

The need to consider the yielding of resisting elements oriented perpendicular to the ground motion in the inelastic response of asymmetric-plan systems is examined first. These elements do not yield in symmetric-plan systems, but they yield over short time durations in asymmetric-plan systems for some values of the system period (Figures 7.7 and 7.8). These results are for systems of Figure 5.1 with $e_s/r = 0.5$, $R=4$ in equation (7.1), and elements along the direction of ground motion designed according to UBC-88. The normalized response quantities, u_i/u_o and μ_i/μ_o, defined earlier, are compared in Figures 7.9 and 7.10 for two systems: in the first system, the perpendicular elements have a yield deformation of u_y, the yield deformation of the symmetric-plan system defined earlier, whereas these elements are assumed to remain elastic in the second. It is apparent that the perpendicular elements yield only for short time durations and their yielding has essentially no influence on the system response. Thus, for simplicity, the strengths of these perpendicular elements are defined to be large enough in the rest of this investigation so that they remain elastic during the response.

7.4.2 Effects of Accidental Eccentricity

As mentioned earlier, and shown in Appendix E, because of accidental eccentricity the strength eccentricity of code-designed symmetric-plan systems may not be zero. Such is the case for the symmetric-plan systems, defined earlier, corresponding to the code-designed asymmetric-plan systems. Therefore, these systems would experience coupled lateral-torsional motions if excited into the inelastic range and the deformations and ductility demands, u_{io} and μ_{io}, for all the resisting elements oriented along the direction of ground

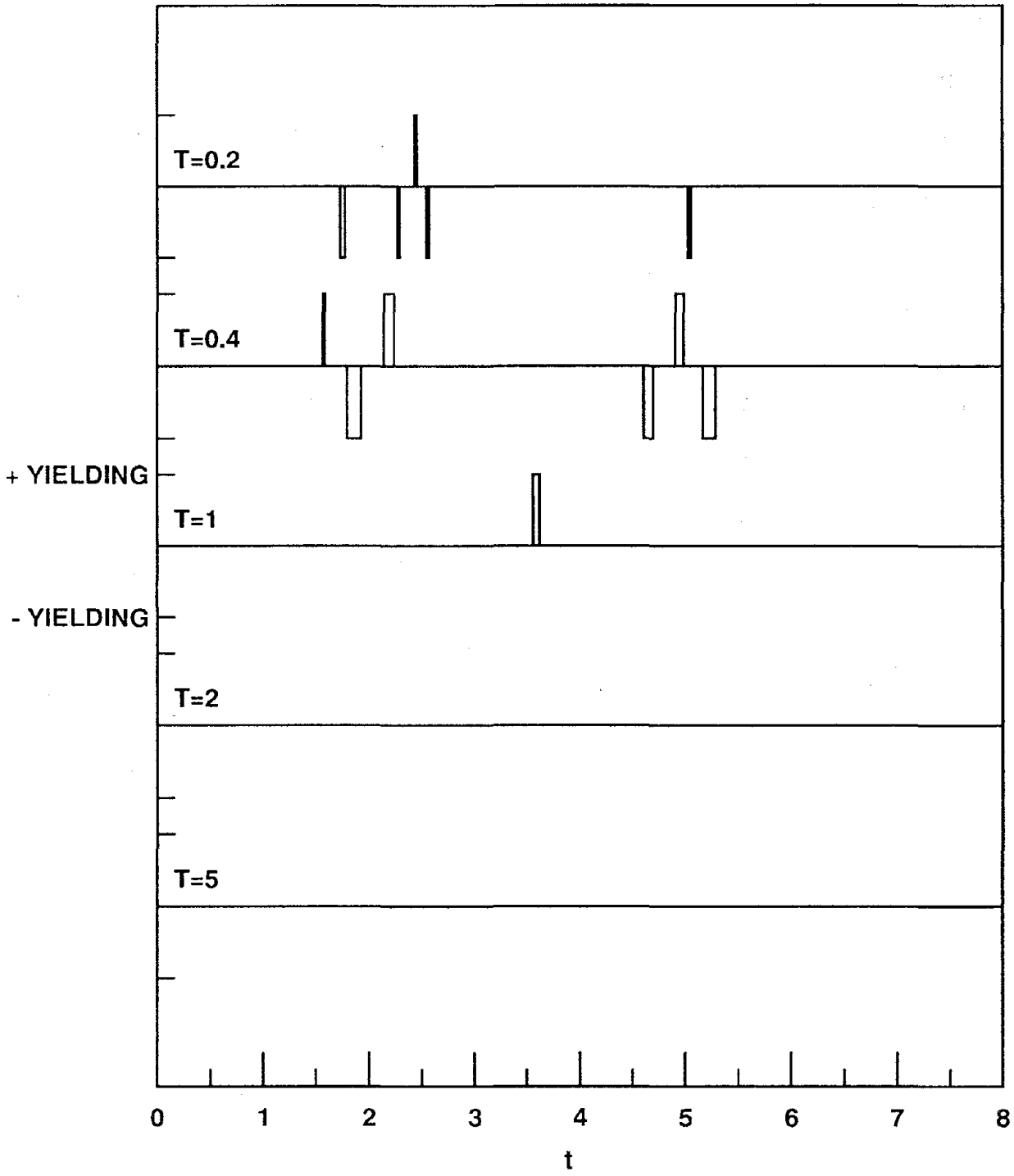

Figure 7.7 Yielding histories of resisting elements oriented perpendicular to the direction of ground motion due to El Centro excitation. Resisting elements oriented along the direction of ground motion are designed according to UBC-88 excluding accidental eccentricity; $e_s/r=0.5$, $\Omega_\theta=1$, $R=4$, and $\xi=5\%$.

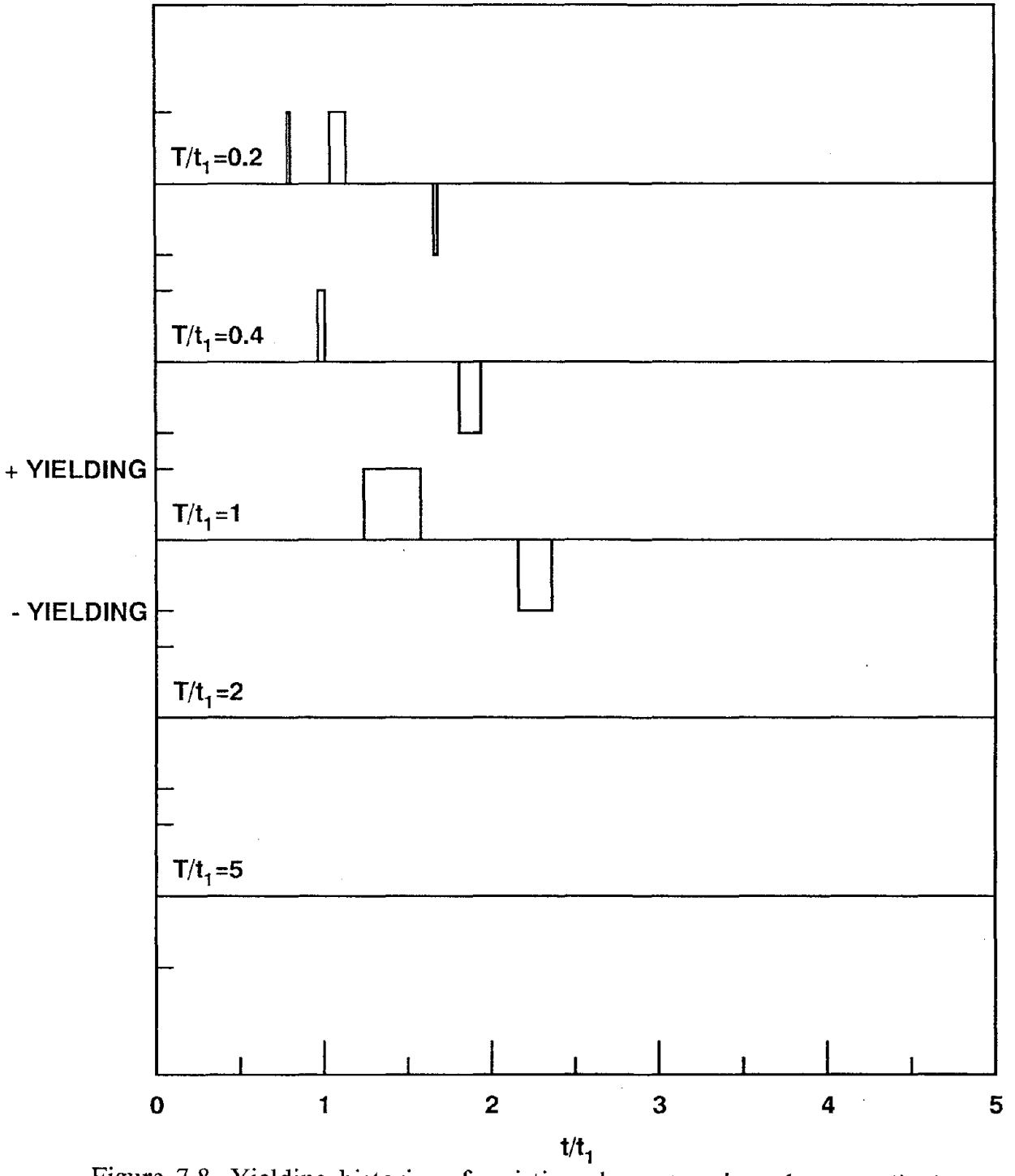

Figure 7.8 Yielding histories of resisting elements oriented perpendicular to the direction of ground motion due to simple input. Resisting elements oriented along the direction of ground motion are designed according to UBC-88 excluding accidental eccentricity; $e_s/r=0.5$, $\Omega_\theta=1$, $R=4$, and $\xi=5\%$.

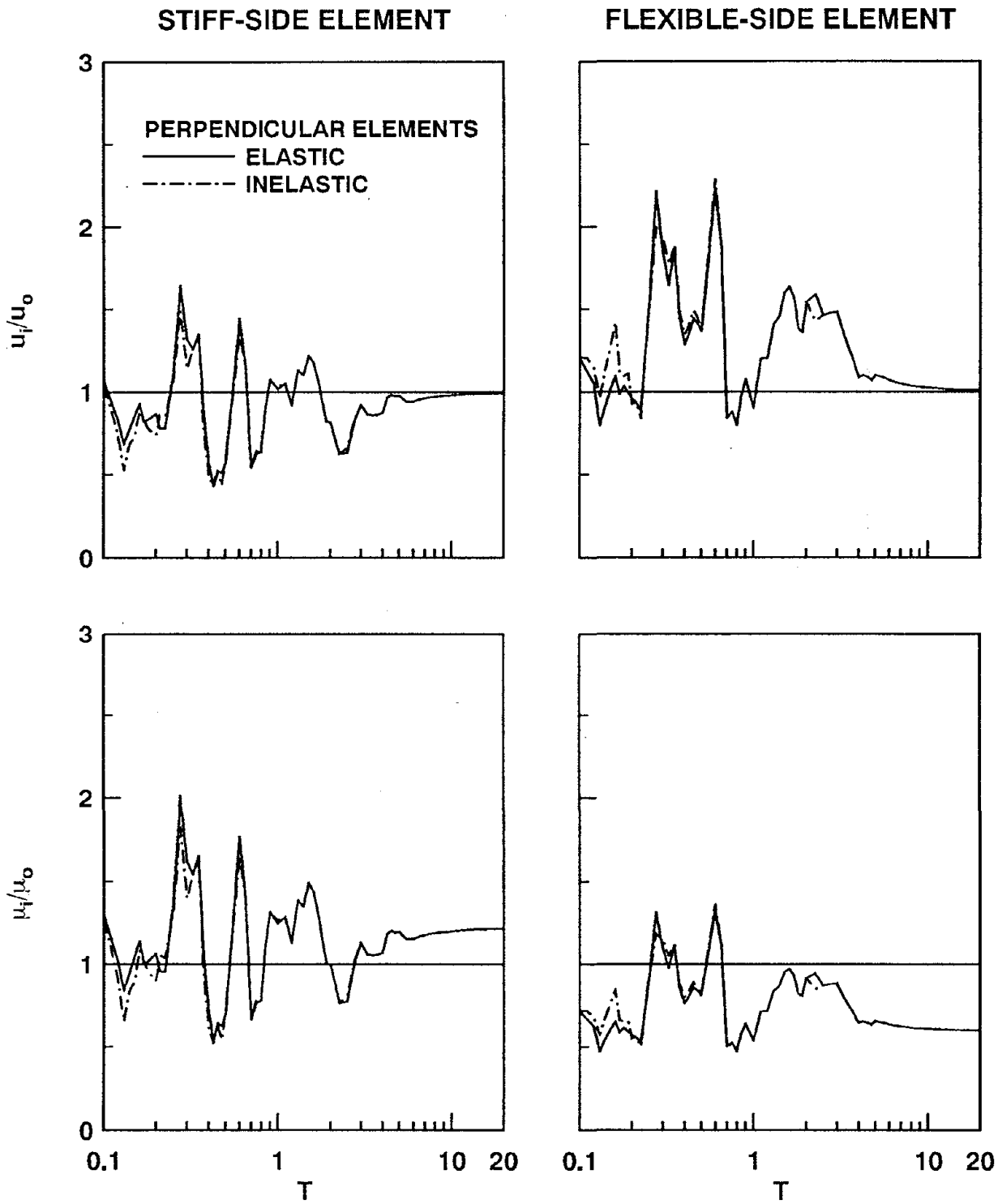

Figure 7.9 Ratio of element deformations, u_i/u_o, and ductility demands, μ_i/μ_o, of asymmetric- and symmetric-plan systems due to El Centro excitation computed for two cases: perpendicular elements are elastic or inelastic. Results are presented for systems designed by UBC-88 excluding accidental eccentricity; $e_s/r=0.5$, $\Omega_\theta=1$, $R=4$, and $\xi=5\%$.

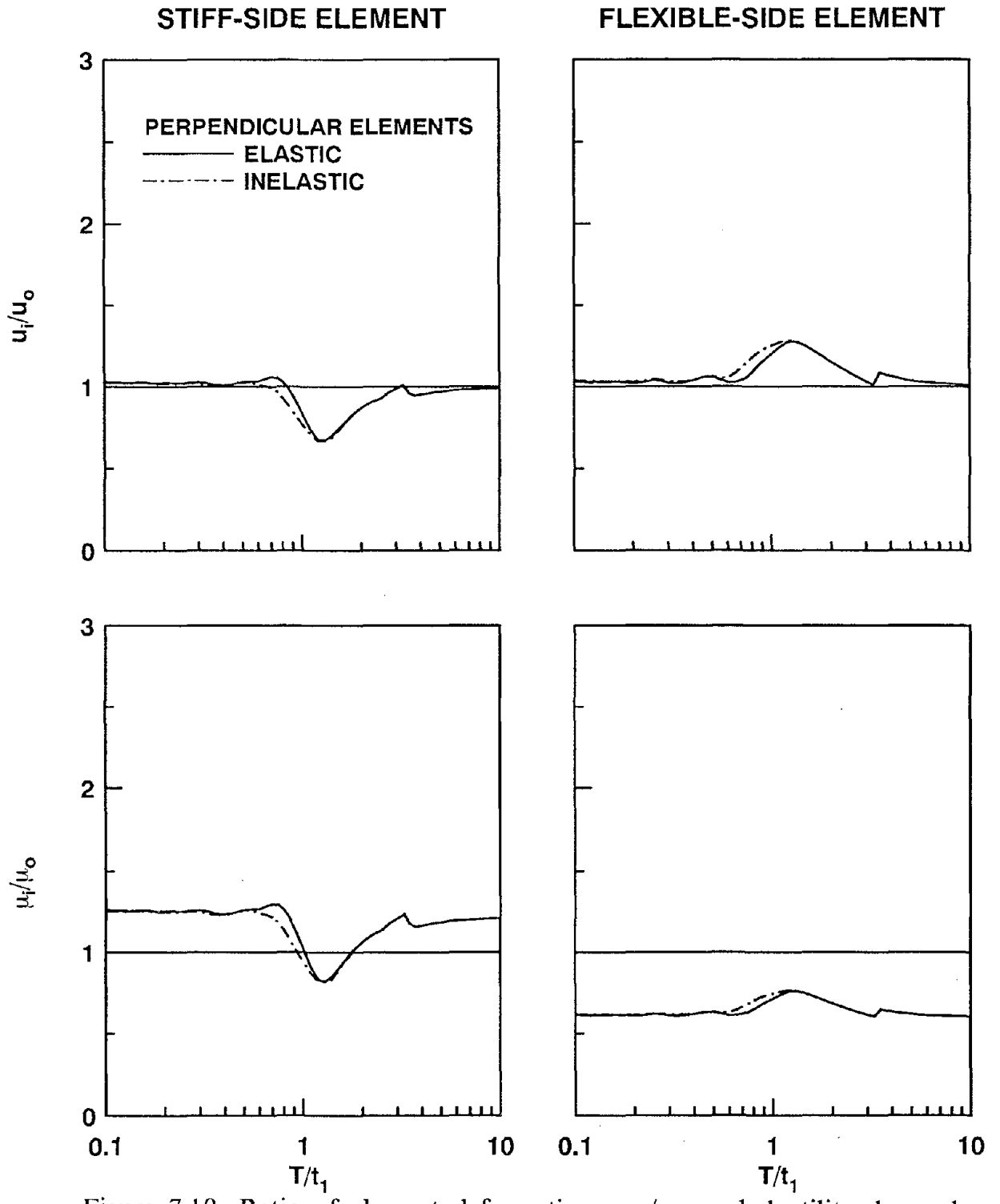

Figure 7.10 Ratio of element deformations, u_i/u_o, and ductility demands, μ_i/μ_o, of asymmetric- and symmetric-plan systems due to simple input computed for two cases: perpendicular elements are elastic or inelastic. Results are presented for systems designed by UBC-88 excluding accidental eccentricity; $e_s/r=0.5$, $\Omega_\theta=1$, $R=4$, and $\xi=5\%$.

motion would not be identical. This is demonstrated in Figures 7.11 and 7.12 for the symmetric-plan system corresponding to the asymmetric-plan system of Figure 5.1 where the responses of elements 1 and 2 are slightly different indicating that the contribution of torsional motion to element response is small. Obviously, if the accidental eccentricity is ignored in equation (7.6) in computing the element yield forces, the system would respond as a SDF system and the deformations and ductility demands for all elements would be identical.

Next, the response quantities, u_i/u_{io} and μ_i/μ_{io}, defined earlier, are compared in Figures 7.13 to 7.16 for two types of systems: (1) the accidental eccentricity is included in computing the design forces for both the asymmetric-plan (equations (7.4) and (7.5)) and corresponding symmetric-plan (equation (7.6)) systems, and (2) excluded from both. Figures 7.13 to 7.16 show that the response ratios u_i/u_{io} and μ_i/μ_{io} are essentially identical for the two system types, indicating that the effects of plan-asymmetry in code-designed systems are essentially independent of the accidental eccentricity. Thus, the accidental eccentricity is not considered in the design of systems for which response results are presented subsequently.

7.5 Inelastic Response

Code-designed buildings typically possess a yield force much smaller than that required for this system to remain elastic during intense ground shaking. Thus, the yield force for the system is defined by equation (7.1) and the element yield forces are determined in accordance with the torsional provision of various codes. The inelastic response of systems designed according to UBC-88 is investigated first which is subsequently compared with systems designed according to several codes.

The normalized response quantities, u_i/u_o and μ_i/μ_o, defined earlier, for the system of Figure 5.1 are presented in the form of response spectra for the El Centro ground motion and simple input introduced before; values for other parameters are fixed: $e_s/r=0.5$, $R=4$, and $\xi=5$ percent. Because, as shown earlier, these responses are affected very little by the accidental eccentricity, it is not included in computing the design forces for the resisting

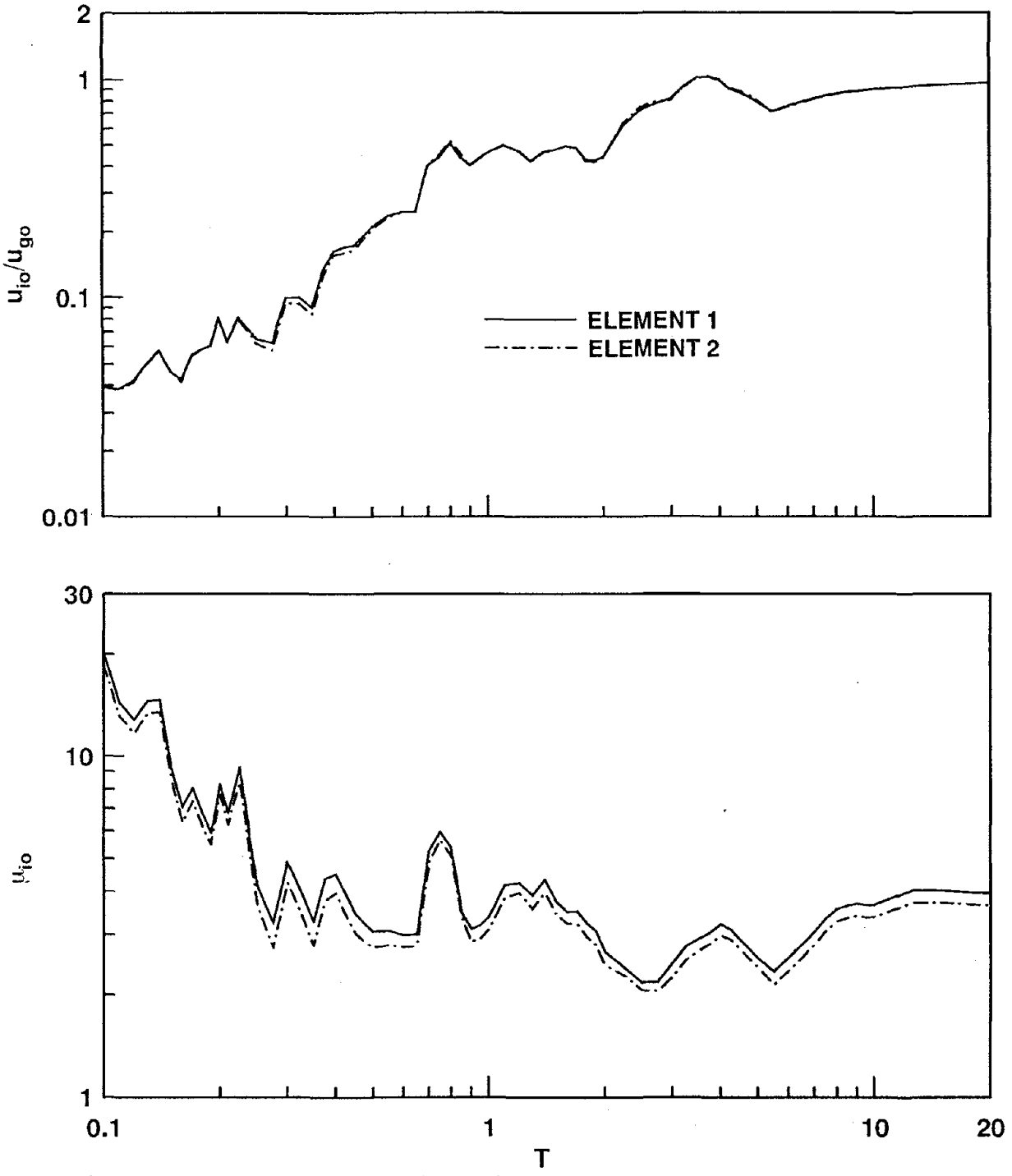

Figure 7.11 Peak element deformations and ductility demands in symmetric-plan systems corresponding to asymmetric-plan systems ($R=4$, $e_s/r=0.5$, $\Omega_\theta=1$, and $\xi=5\%$) due to El Centro excitation. Results are presented for systems designed by UBC-88 including accidental eccentricity.

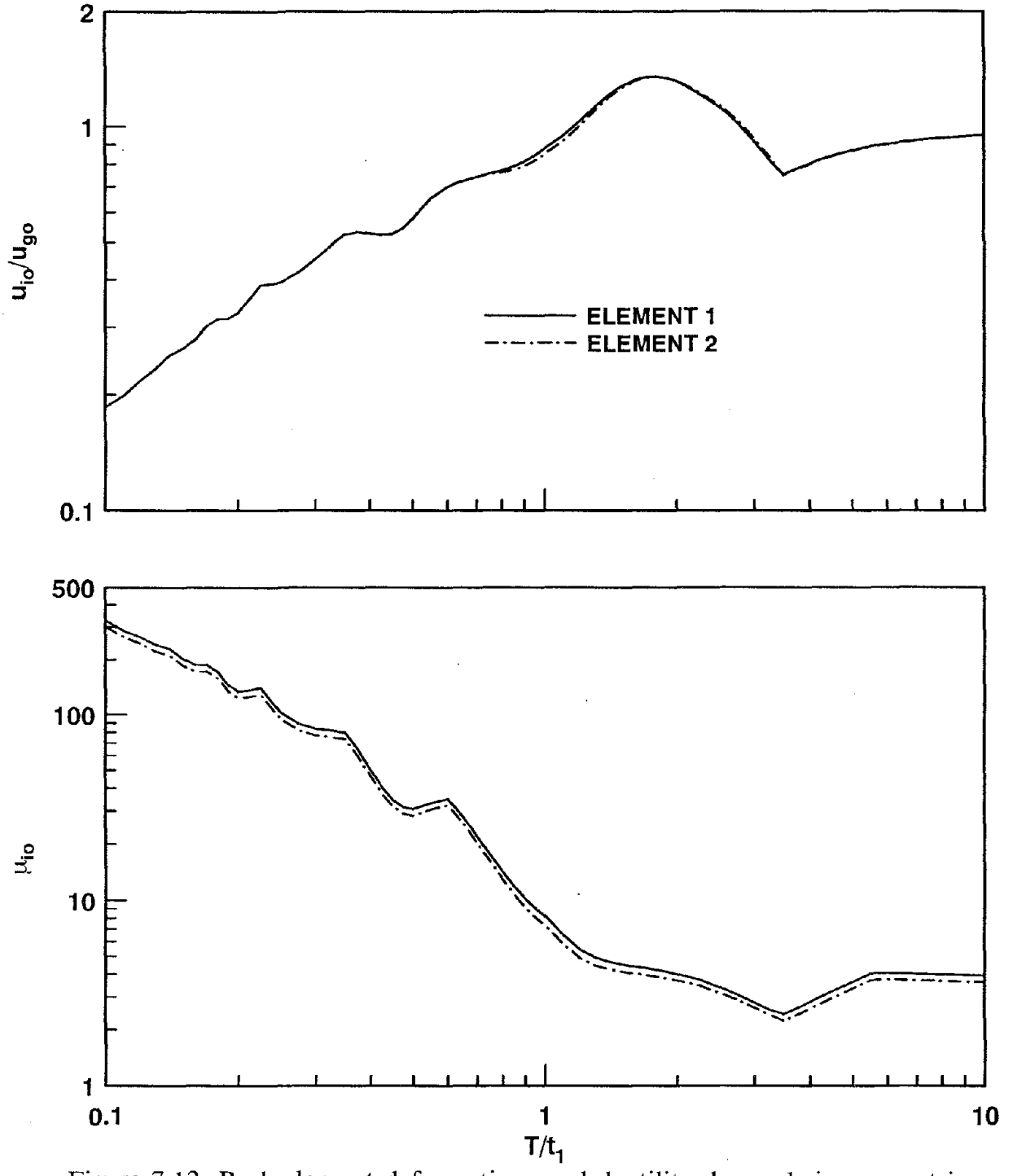

Figure 7.12 Peak element deformations and ductility demands in symmetric-plan systems corresponding to asymmetric-plan systems ($R=4$, $e_s/r=0.5$, $\Omega_\theta=1$, and $\xi=5\%$) due to simple input. Results are presented for systems designed by UBC-88 including accidental eccentricity.

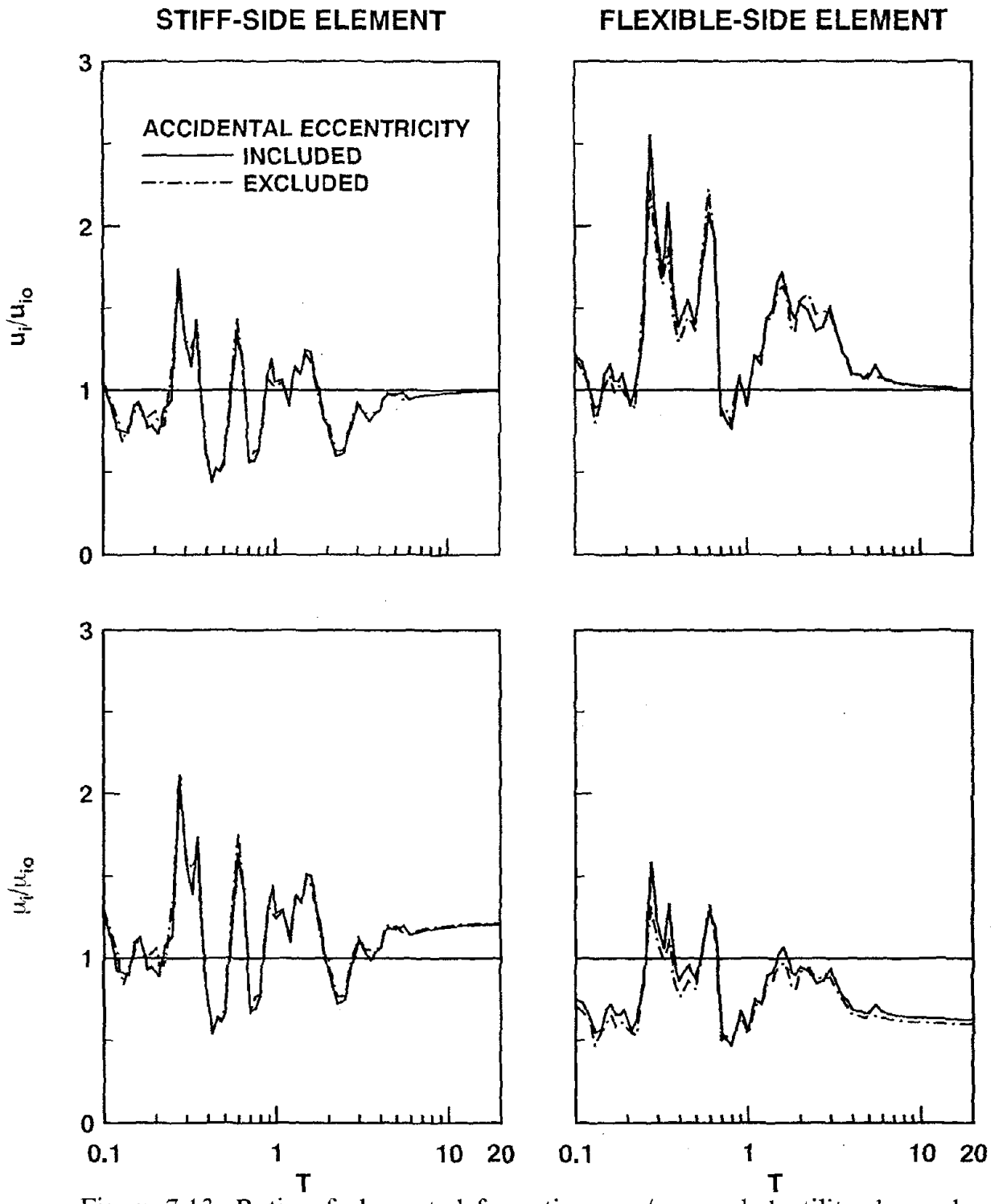

Figure 7.13 Ratio of element deformations, u_i/u_{io}, and ductility demands, μ_i/μ_{io}, for asymmetric-plan ($R=4$, $e_s/r=0.5$, $\Omega_\theta=1$, and $\xi=5\%$) and corresponding symmetric-plan systems designed by UBC-88 due to El Centro excitation. Results are presented for two cases: accidental eccentricity is included or excluded; reduction of element design forces below their symmetric-plan values is permitted.

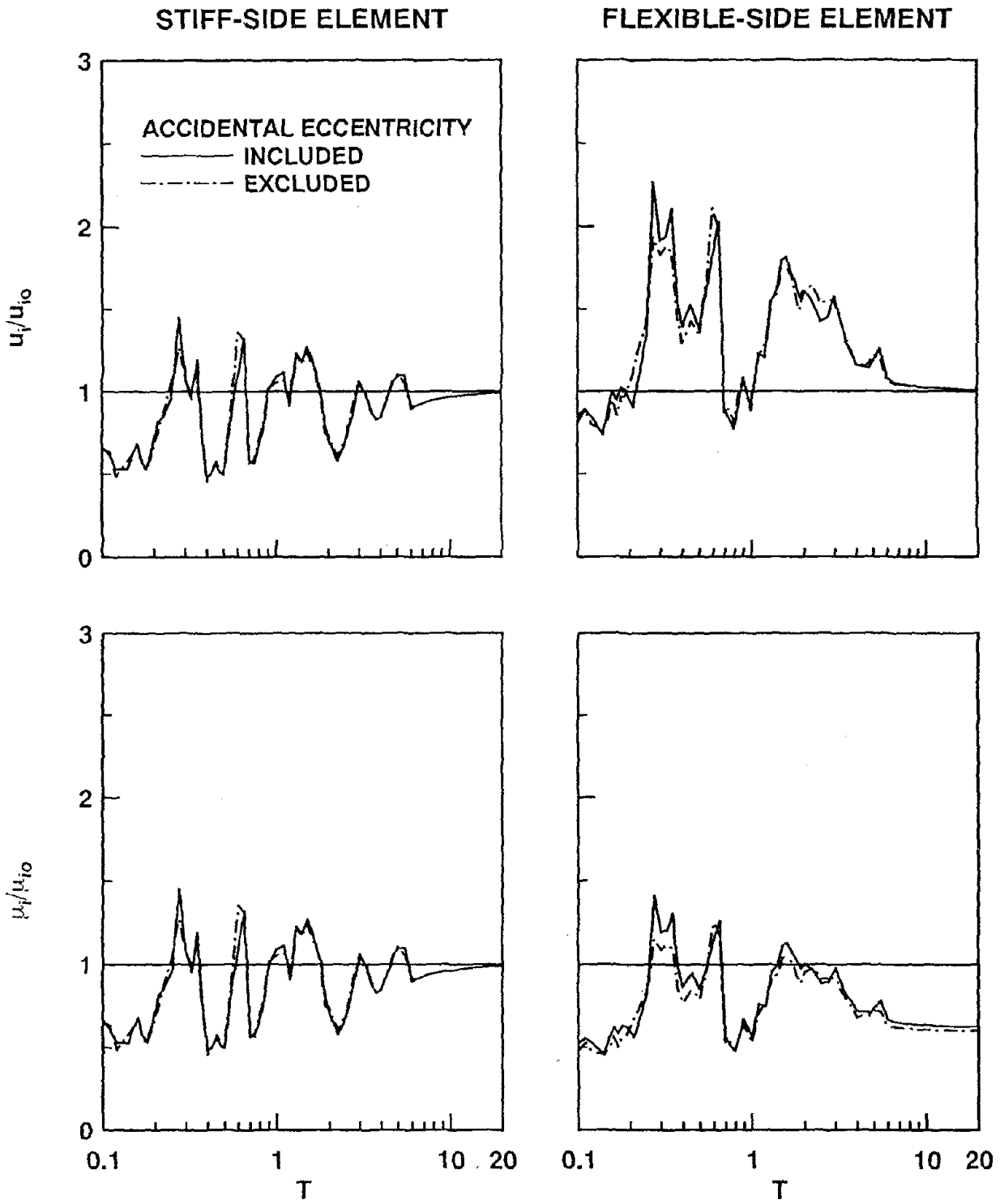

Figure 7.14 Ratio of element deformations, u_i/u_{io}, and ductility demands, μ_i/μ_{io}, for asymmetric-plan ($R=4$, $e_s/r=0.5$, $\Omega_\theta=1$, and $\xi=5\%$) and corresponding symmetric-plan systems designed by UBC-88 due to El Centro excitation. Results are presented for two cases: accidental eccentricity is included or excluded; reduction of element design forces below their symmetric-plan values is precluded.

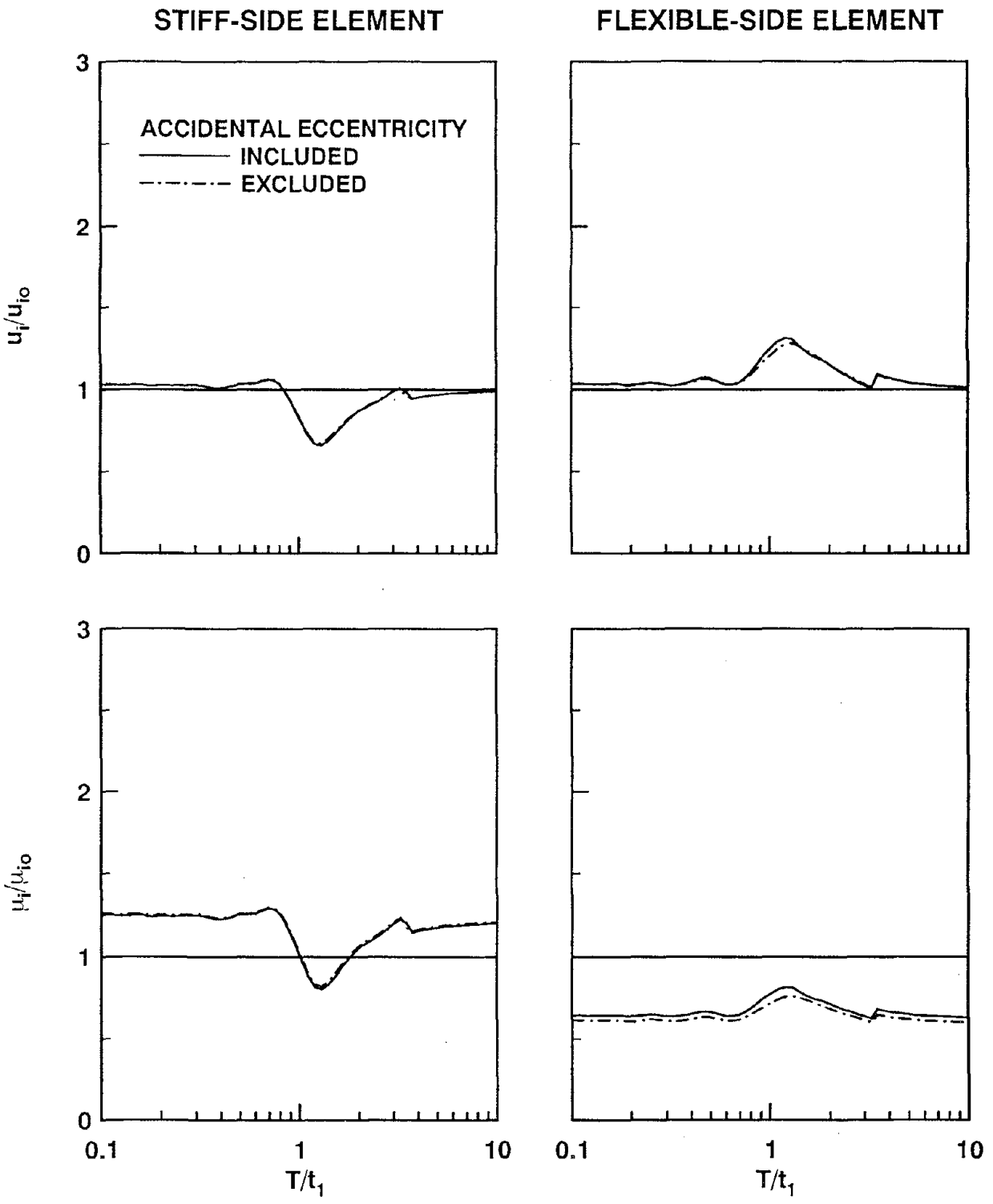

Figure 7.15 Ratio of element deformations, u_i/u_{io}, and ductility demands, μ_i/μ_{io}, for asymmetric-plan ($R=4$, $e_s/r=0.5$, $\Omega_\theta=1$, and $\xi=5\%$) and corresponding symmetric-plan systems designed by UBC-88 due to simple input. Results are presented for two cases: accidental eccentricity is included or excluded; reduction of element design forces below their symmetric-plan values is permitted.

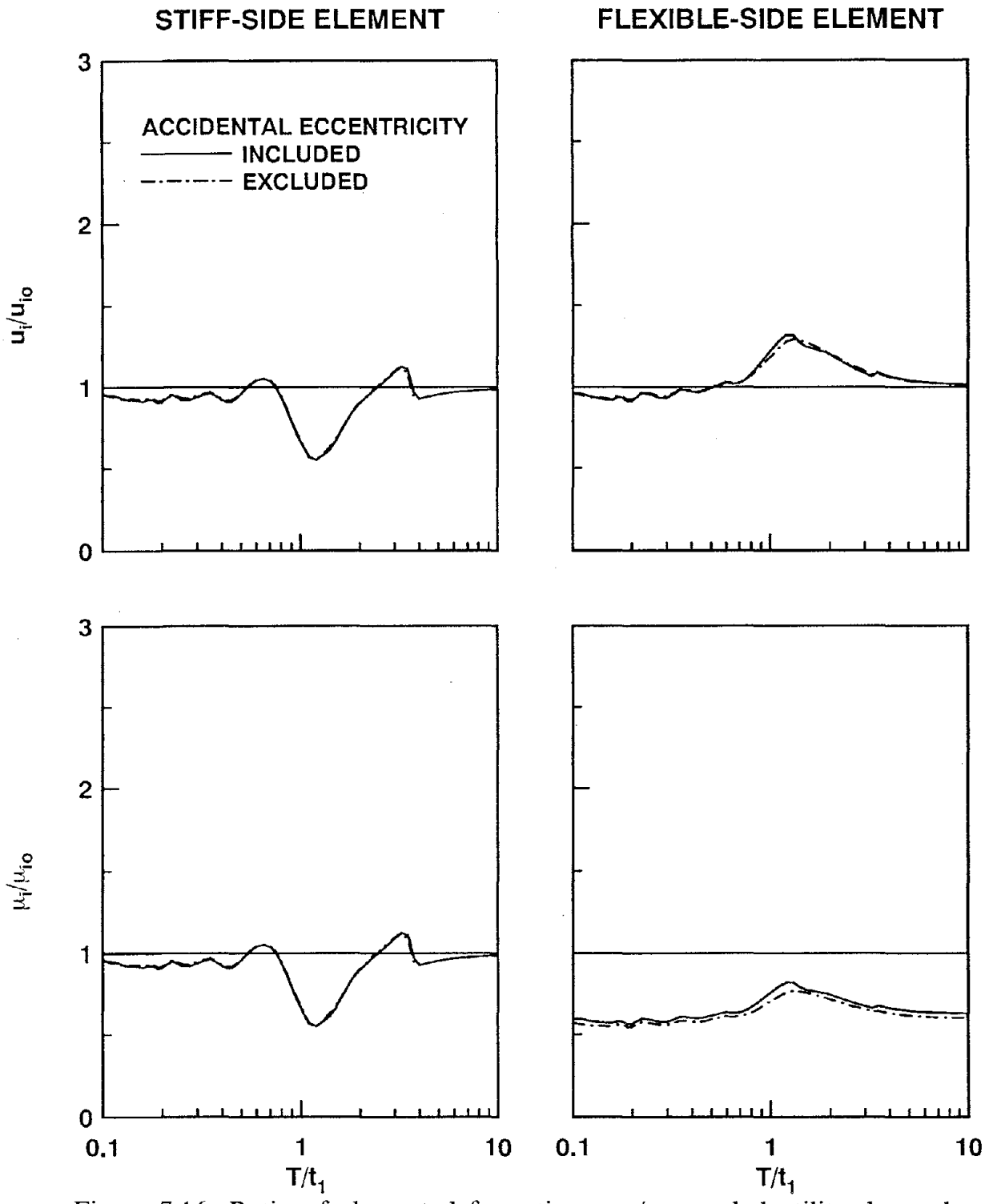

Figure 7.16 Ratio of element deformations, u_i/u_{io}, and ductility demands, μ_i/μ_{io}, for asymmetric-plan ($R=4$, $e_s/r=0.5$, $\Omega_\theta=1$, and $\xi=5\%$) and corresponding symmetric-plan systems designed by UBC-88 due to simple input. Results are presented for two cases: accidental eccentricity is included or excluded; reduction of element design forces below their symmetric-plan values is precluded.

elements of the asymmetric-plan system and its corresponding symmetric-plan system. Two types of asymmetric-plan systems are considered: in the first system, the code design force for the stiff-side element can be smaller than the design force of the same element in the corresponding symmetric-plan system; and in the second type, such a reduction is precluded.

7.5.1 Systems Designed by UBC-88

The deformations of resisting elements in the system designed according to UBC-88 may be significantly affected by plan-asymmetry. In the medium-period, velocity-sensitive and its transition regions (Figures 2.3 and 2.5), where the effects of plan-asymmetry are known to be most pronounced (Chapter 6), the ratio u_i/u_o for element 1, the stiff-side element, tends to be smaller than one, with exceptions at some period values, whereas for the flexible-side element this ratio tends to be larger than one (Figures 7.17 and 7.18). Thus plan-asymmetry tends to reduce the deformation of the stiff-side element and increase the deformation of the flexible-side element compared to their respective deformations in the corresponding symmetric-plan system. The ratio u_i/u_o for both resisting elements is close to one for systems in the long-period, displacement-sensitive region, implying that the element deformations are essentially unaffected by plan-asymmetry in this period region (Figures 7.17 and 7.18). Similarly, the effects of plan-asymmetry on element deformations are small for short-period, acceleration-sensitive systems. These effects of plan-asymmetry on element deformations of code-designed systems are similar to the ones observed earlier for 'strength-symmetric' (e_p=0) systems (Chapter 6).

The increased strength of the system resulting from the restriction that the stiff-side element design force must not fall below its symmetric-plan value leads to smaller response ratio, u_i/u_o, in the short-period, acceleration-sensitive region and portions of the medium-period, velocity-sensitive region. However, this response ratio may increase for some period values in the latter region; and is essentially unaffected for long-period, displacement-sensitive systems (Figures 7.17 and 7.18). This response behavior is consistent with the effects of strength increase on the response of SDF systems [38]. In comparing Figures 7.17

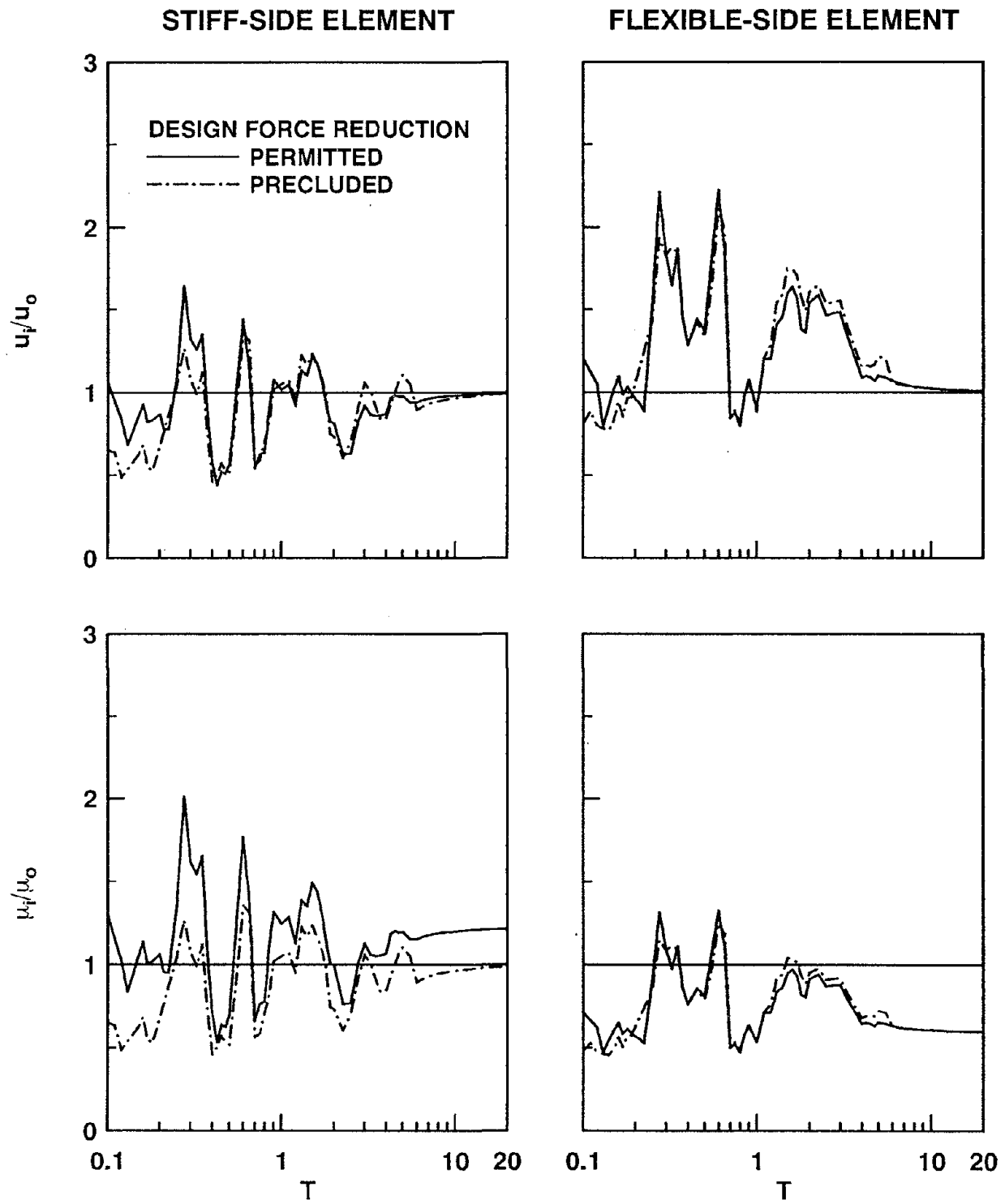

Figure 7.17 Ratio of element deformations, u_i/u_o, and ductility demands, μ_i/μ_o, for asymmetric-plan ($R=4$, $e_s/r=0.5$, $\Omega_\theta=1$, and $\xi=5\%$) and corresponding symmetric-plan systems designed by UBC-88, excluding accidental eccentricity, due to El Centro excitation. Results are presented for two cases: reduction in stiff-side element design force below its symmetric-plan value is permitted or precluded.

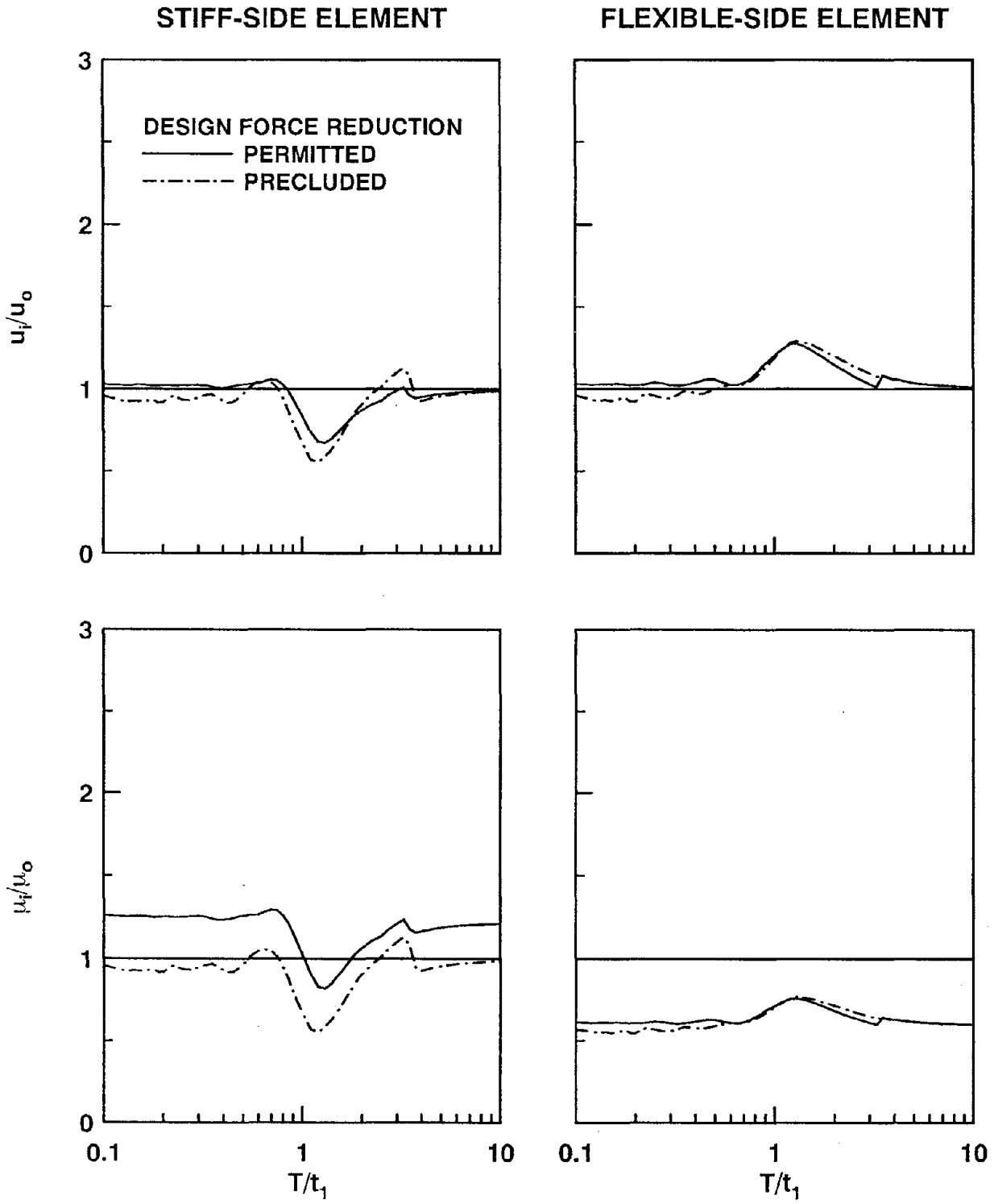

Figure 7.18 Ratio of element deformations, u_i/u_o, and ductility demands, μ_i/μ_o, for asymmetric-plan ($R=4$, $e_s/r=0.5$, $\Omega_\theta=1$, and $\xi=5\%$) and corresponding symmetric-plan systems designed by UBC-88, excluding accidental eccentricity, due to simple input. Results are presented for two cases: reduction in stiff-side element design force below its symmetric-plan value is permitted or precluded.

and 7.18 for the El Centro and simple inputs, it should be noted that the response spectra for the former input (Figure 7.17) do not extend to period values as extremely-short as in the case of the latter input (Figure 7.18).

The ratio μ_i/μ_o of the element ductility demands in an asymmetric-plan system and the corresponding symmetric-plan system are also presented in Figures 7.17 and 7.18. If the design force for the stiff-side element is permitted to be smaller than its value in the corresponding symmetric-plan system, over a wide range of periods the ductility demand μ_i on this element in the asymmetric-plan system is significantly larger than the value μ_o for this element in the corresponding symmetric-plan system. The ductility ratio μ_i/μ_o for the stiff-side element exceeds one, although the deformation ratio u_i/u_o is either close to or smaller than one, primarily because the yield deformation of the element is smaller because of plan-asymmetry if reduction in its design force is permitted (Figure 7.1). However, if reduction in the element design force is precluded, $\mu_i/\mu_o=u_i/u_o$ because the yield deformations of this element are identical in the symmetric-plan and asymmetric-plan systems. Thus, as observed earlier for u_i/u_o, μ_i/μ_o for the stiff-side element either remains close to one over a wide range of period values, exceeds one at some period values and stays lower at other periods (Figure 7.17), implying that the ductility demand μ_i on this element in the asymmetric-plan system is roughly similar to the ductility demand of the corresponding symmetric-plan system (Figures 7.17 and 7.18).

The ductility demand on the flexible-side element is significantly smaller than that on the corresponding symmetric-plan system, with exceptions at few periods, (Figures 7.17 and 7.18) because the yield deformation of this element in the code-designed asymmetric-plan system is significantly larger than in the symmetric-plan system (Figure 7.1). These trends are unaffected by whether the design force reduction for the stiff-side elements is permitted or not (Figures 7.17 and 7.18), primarily because the yield deformation of the flexible-side element is unaffected by such reduction.

It is apparent from the preceding results that the response of systems with or without reduction in the stiff-side element design force, arising from plan-asymmetry, may differ significantly. In particular, the ductility demand on the stiff-side element in the former system may become significantly larger compared to the symmetric-plan system. Since it is desirable that the element ductility demand not increase because of plan-asymmetry, it seems that seismic codes should preclude reduction in the design forces of the stiff-side elements below their values for symmetric-plan systems.

Several earlier investigations [1,35,36] of the earthquake response of asymmetric-plan systems with $e_p=e_s$ indicate that the largest deformation as well as the largest ductility demand generally occurs in the flexible-side elements, which were therefore interpreted as the most critical elements for design purposes. However, the preceding results for the system of Figure 5.1 indicate that, although the largest deformation among all the resisting elements of the code-designed asymmetric-plan systems, for which $e_p<<e_s$, occurs in the flexible-side element, the largest ductility demand may occur in the stiff-side element. Thus, additional care is required not only in the design of flexible-side elements for deformation demand, but also in the design of stiff-side elements for ductility demand; this observation also appears in Reference [30].

7.5.2 Systems Designed by Various Codes

The inelastic response of the asymmetric-plan system of Figure 5.1 with the element design forces determined according to various codes is compared next. The differences in the element design forces arise only from the torsional provisions in various codes because the base shear defined by equation (7.1) is identical in each case. In particular, the corresponding symmetric-plan systems are identical for all the codes with the same design base shear because the accidental eccentricity is not considered in their design. Thus, the deformation ratio u_i/u_o and ductility ratio μ_i/μ_o presented in Figures 7.19 to 7.22 differ among various codes because of differences in u_i and μ_i, whereas the responses u_o and μ_o for the corresponding symmetric-plan system apply to all codes. Consequently, in discussing

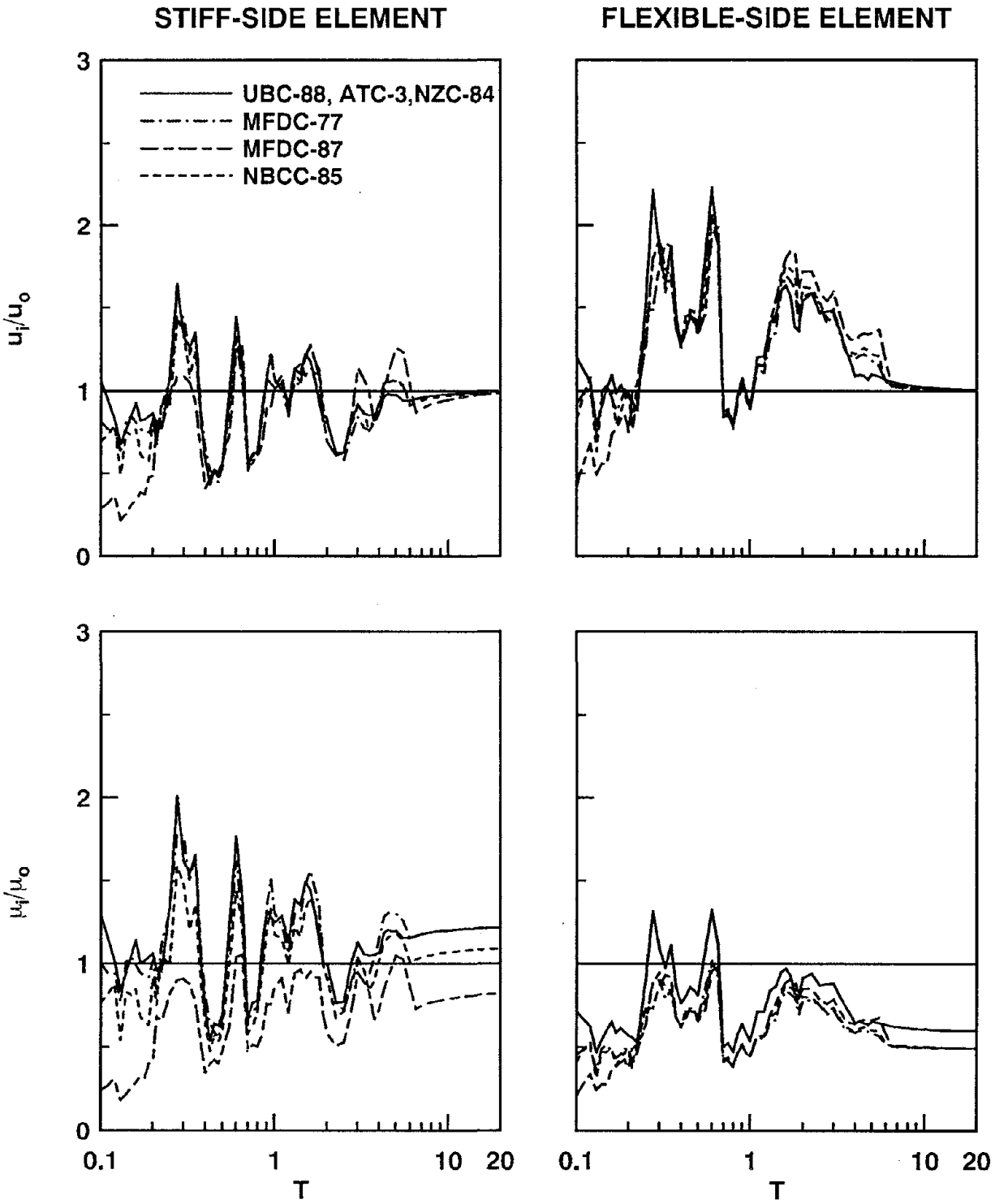

Figure 7.19 Ratio of element deformations, u_i/u_o, and ductility demands, μ_i/μ_o, for asymmetric-plan ($R=4$, $e_s/r=0.5$, $\Omega_\theta=1$, and $\xi=5\%$) and corresponding symmetric-plan systems designed by various codes, excluding accidental eccentricity, due to El Centro excitation; reduction in stiff-side element design force below its symmetric-plan value is permitted.

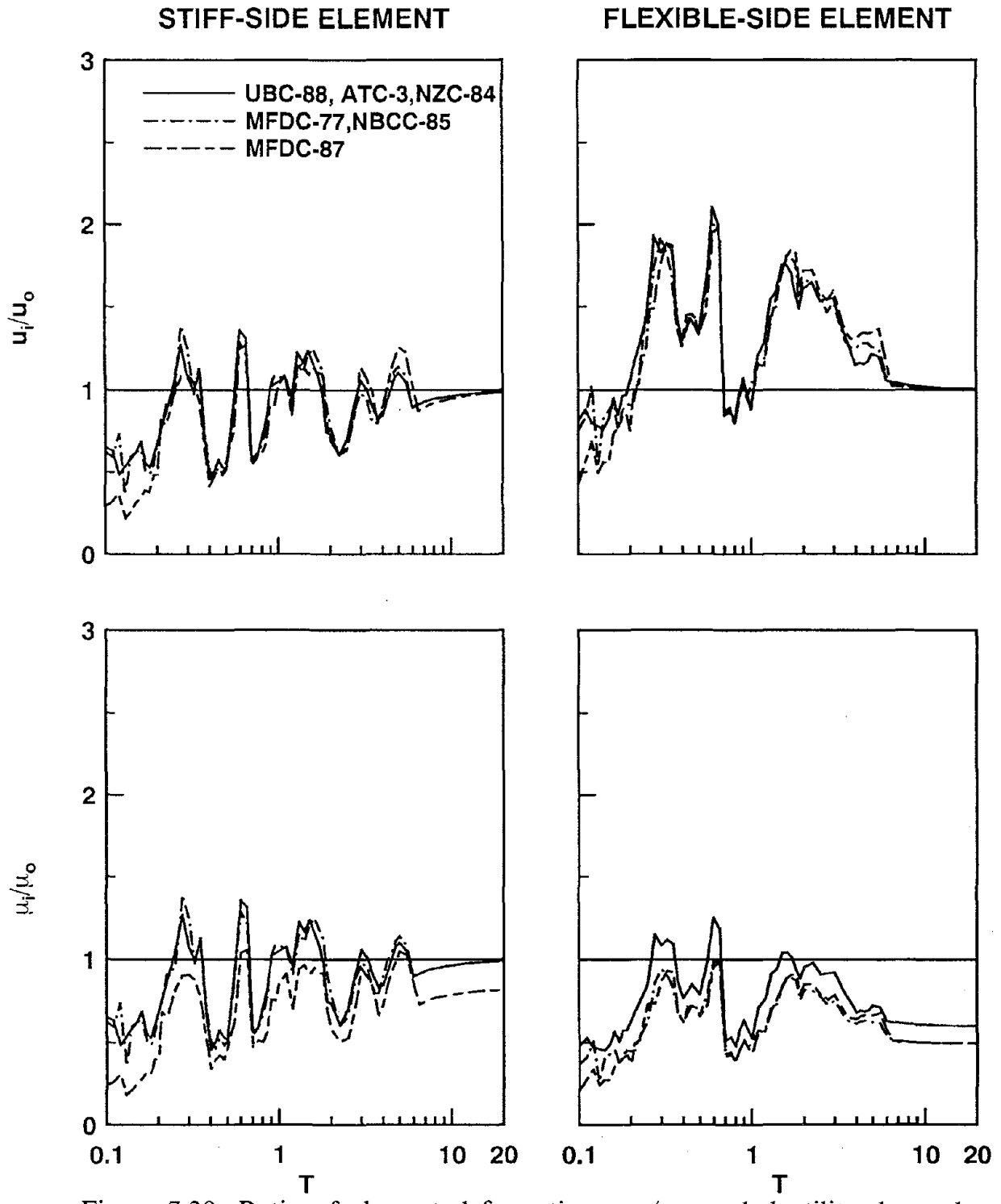

Figure 7.20 Ratio of element deformations, u_i/u_o, and ductility demands, μ_i/μ_o, for asymmetric-plan ($R=4$, $e_s/r=0.5$, $\Omega_\theta=1$, and $\xi=5\%$) and corresponding symmetric-plan systems designed by various codes, excluding accidental eccentricity, due to El Centro excitation; reduction in stiff-side element design force below its symmetric-plan value is precluded.

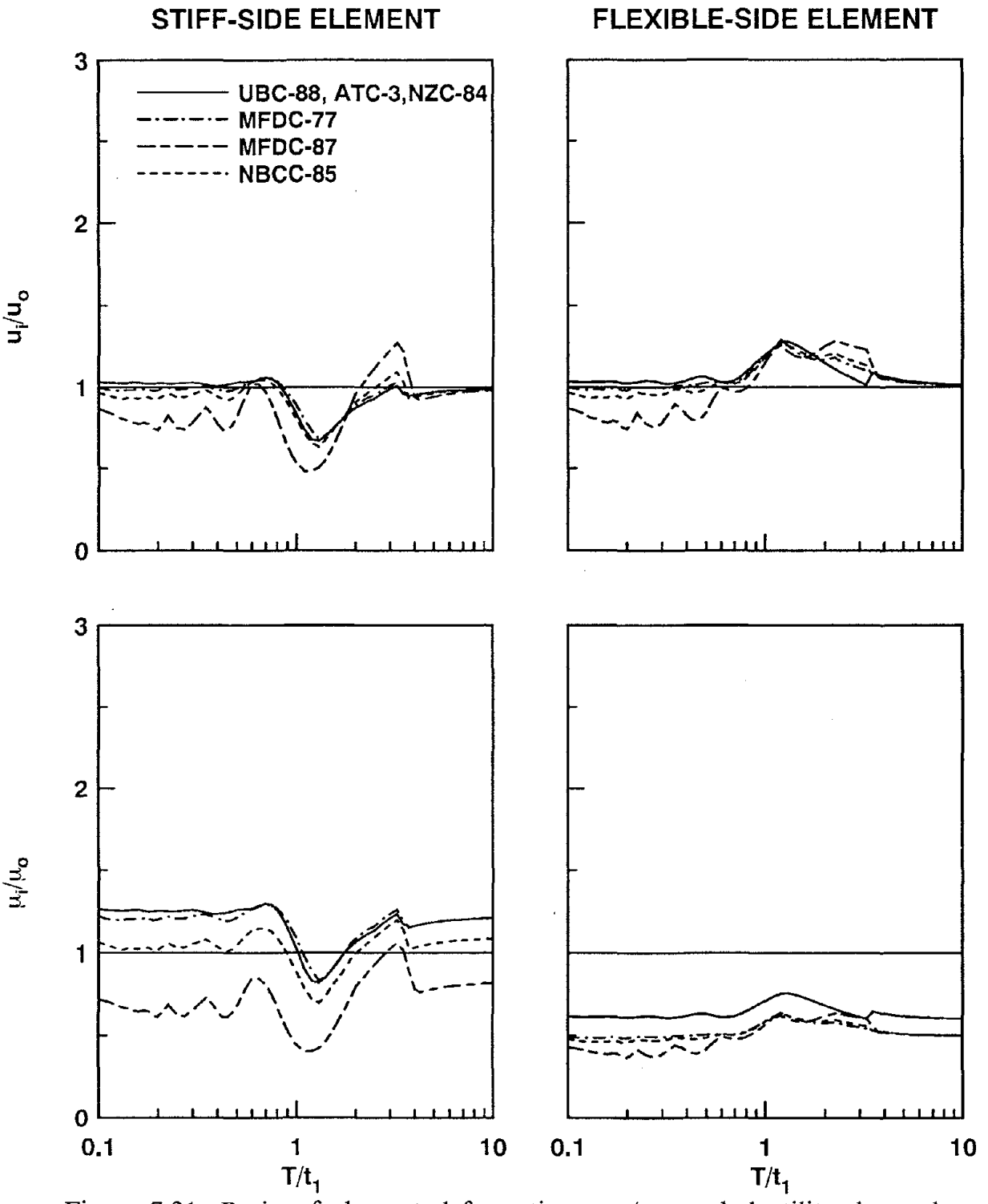

Figure 7.21 Ratio of element deformations, u_i/u_o, and ductility demands, μ_i/μ_o, for asymmetric-plan ($R=4$, $e_s/r=0.5$, $\Omega_\theta=1$, and $\xi=5\%$) and corresponding symmetric-plan systems designed by various codes, excluding accidental eccentricity, due to simple input; reduction in stiff-side element design force below its symmetric-plan value is permitted.

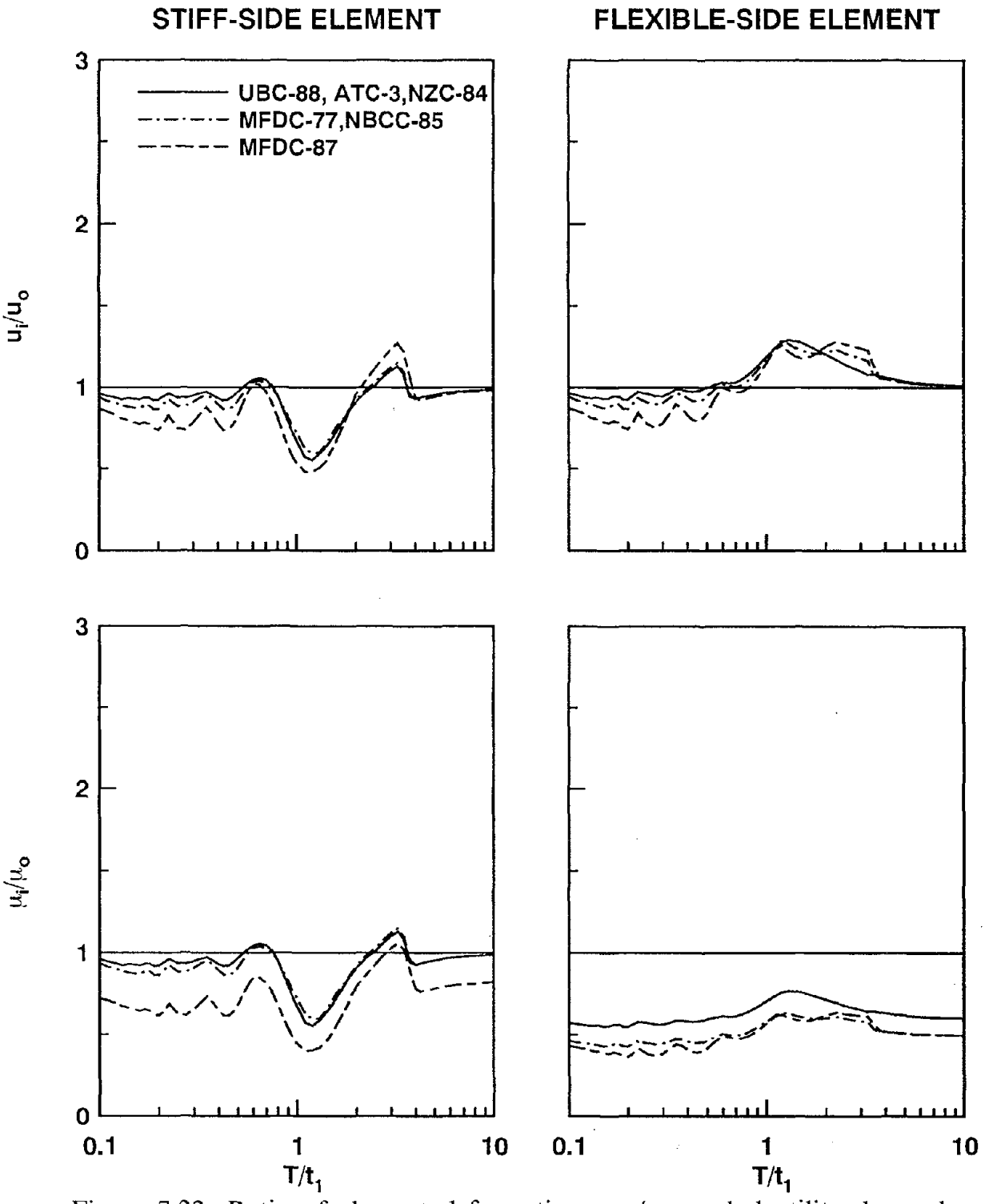

Figure 7.22 Ratio of element deformations, u_i/u_o, and ductility demands, μ_i/μ_o, for asymmetric-plan ($R=4$, $e_s/r=0.5$, $\Omega_\theta=1$, and $\xi=5\%$) and corresponding symmetric-plan systems designed by various codes, excluding accidental eccentricity, due to simple input; reduction in stiff-side element design force below its symmetric-plan value is precluded.

differences in system response designed by various codes, the response ratios and the response quantities have been used interchangeably.

The element deformation ratio, u_i/u_o, depends on the design code in the short-period, acceleration-sensitive and medium-period, velocity-sensitive regions of the spectrum; however, the response of long-period, displacement-sensitive systems is essentially independent of the design code. In the short-period spectral region, the deformation varies inversely with the strength provided by the various codes, a result that is consistent with earlier observations for SDF systems [38]. Thus the system designed by UBC-88, which possesses the smallest strength (Figure 7.3), experiences the largest deformation, whereas the MFDC-87 designed system with the largest strength undergoes the smallest deformation, and the deformation of systems designed according to other codes falls between the two extremes (Figures 7.19 to 7.22). In the medium-period spectral region, the deformation also decreases with increasing strength for some period values but it may increase with strength for other period values, which again is consistent with earlier results for SDF systems [38]. Furthermore, because the structural deformation is known to be insensitive to the strength of the system in the long-period region [38], the element deformations in systems designed by all the codes are essentially the same in this period region.

The trends identified above are generally applicable to systems with strength of stiff-side element permitted to be below that of the symmetric-plan system (Figures 7.19 and 7.21) as well as to systems where such design force reduction is precluded (Figures 7.20 and 7.22), except that the deformation tends to be smaller in the latter case because of increased strength, especially for short-period systems. It may be noted that element deformations in systems designed according to MFDC-77 and NBCC-85 are the same in the latter case (Figures 7.20 and 7.22) because the strengths of the two systems are identical (Figure 7.3).

It is also apparent from the results of Figures 7.19 to 7.22 that, although the deformations of resisting elements in the asymmetric-plan system depend on the design code, the differences are usually small except for MFDC-87. Such is the case because the strengths of

various code-designed systems are not too different except that systems designed according to MFDC-87 possess significantly larger strength in order to satisfy the strength eccentricity requirement, i.e., $e_p \geq e_s - 0.1b$ (Figure 7.3). For reasons that are not apparent, the differences among the deformations of systems designed by various codes are less pronounced for the El Centro excitation (Figures 7.19 and 7.20) compared to the simple input (Figures 7.21 and 7.22).

The building code by which the system is designed influences the ductility demand ratio, μ_i/μ_o, and hence the ductility demand, μ_i, for the resisting elements; recall that μ_o is independent of the design code. The ductility demand on a resisting element varies inversely with its yield deformation and increases proportional to the element deformation. Thus, systems designed by UBC-88, which possess the smallest element yield deformation (Figure 7.1) and undergo the largest element deformation, especially in the short-period region, experience the largest ductility demand. In contrast, systems designed by MFDC-87 with the smallest element deformation and largest element yield deformation (Figure 7.1) undergo the smallest ductility demand. Responses for systems designed by other codes fall in between the two extremes (Figures 7.19 to 7.22).

If the yield force for the stiff-side element in an asymmetric-plan system is permitted to be smaller than its symmetric-plan value, the resulting force reduction (Figure 7.1) causes the ductility demand μ_i to be larger than its symmetric-plan value, μ_o (Figures 7.19 to 7.22). Among the codes considered, this increase in ductility demand is the greatest in systems designed by UBC-88 and MFDC-77 with $\delta=1$ which leads to the largest increase of μ_i over μ_o (Figures 7.19 and 7.21). If the yield force for the stiff-side element in an asymmetric-plan system can not fall below its symmetric-plan value, i.e., $\delta=0$ in equation (7.5), the ductility demand μ_i on this element in asymmetric-plan systems designed by any of the codes become similar to its symmetric-plan value μ_o over a wide range of periods, indicating that the ductility demand is influenced little by plan-asymmetry (Figures 7.20 and 7.22).

The ductility demand on the flexible-side element tends to be smaller than on the stiff-side element or on the corresponding symmetric-plan system (Figures 7.19 to 7.22). This difference in ductility demands results primarily from the differences in element yield deformation which is larger for the flexible-side element compared to the stiff-side element or to the symmetric-plan system (Figure 7.1). Codes such as NBCC-85, MFDC-77, and MFDC-87, which specify $\alpha>1$, lead to a larger increase in the yield deformation of the flexible-side element (Figure 7.1). As a result, the flexible-side element in systems designed according to these codes experiences smaller ductility demand compared to other codes; short-period systems designed according to MFDC-87 tend to experience the smallest ductility demand because the element deformation is smaller than in systems designed by other codes. The above-mentioned trends are similar in systems with design force reduction in stiff-side element (Figures 7.19 and 7.21) and without such force reduction (Figures 7.20 and 7.22) primarily because the yield deformation of the flexible-side element is identical in the two types of systems (Figure 7.1).

It is apparent from the preceding results that element deformations of systems designed according to most building codes, except MFDC-87, are not very different; however, the ductility demands may differ significantly among these systems. If reduction in design force of the stiff-side element below its symmetric-plan value is permitted, the NBCC-85 designed system has the desirable property that the ductility demand on the stiff-side element is closest, among all codes considered, to its symmetric-plan value (Figures 7.19 and 7.21). If such design force reduction is not permitted, the ductility demand on the stiff-side element of systems designed according to all codes considered, except MFDC-87, are similar and close to or slightly below the symmetric-plan value. In particular, the ductility demand on the stiff-side element in the MFDC-87 designed system tends to be significantly reduced because of plan-asymmetry, suggesting that the additional requirement imposed in this code to restrict the strength eccentricity may be unnecessary.

7.6 'Elastic' Response

It is the intent of most seismic codes that buildings suffer no damage during some, usually unspecified, level of moderate ground shaking: Thus, the elastic response of asymmetric-plan systems designed according to several building codes is examined next.

The response quantities, u_i/u_o and $\mu_i = u_i/u_{y_i}$, where u_{y_i} is the yield deformation of the i^{th} resisting element, are presented in the form of response spectra for the El Centro ground motion and simple input; values for other parameters are fixed: $e_s/r = 0.5$, $R = 1$, and $\xi = 5$ percent. $R = 1$ implies that the design strength V of the corresponding symmetric-plan system is just sufficient for it to remain elastic during the selected excitation. However, as will be shown in subsequent sections, the code-designed asymmetric-plan system may not remain elastic.

7.6.1 Systems Designed by UBC-88

The deformation of resisting elements in systems designed by UBC-88 may be significantly affected by plan-asymmetry. The deformation ratio u_i/u_o for the stiff-side element remains smaller than one for most short-period, acceleration-sensitive and medium-period, velocity-sensitive systems whereas for the flexible-side element u_i/u_o is much larger than one (Figures 7.23 and 7.24). This indicates that the deformation of the stiff-side element is generally reduced because of plan-asymmetry whereas that of the flexible-side element is considerably increased. The ratio u_i/u_o for both the resisting elements is essentially equal to one for long-period, displacement-sensitive systems implying that the effects of plan-asymmetry are negligible (Figures 7.23 and 7.24).

The ductility demand for stiff-side and flexible-side elements in the asymmetric-plan system exceeds one in some period ranges (Figures 7.23 and 7.24) indicating yielding in these elements, which were designed to remain elastic if the building plan were symmetric. The stiff-side element yields more if its design force is permitted to fall below its symmetric-plan value because this results in smaller yield deformation (Figure 7.1). As a

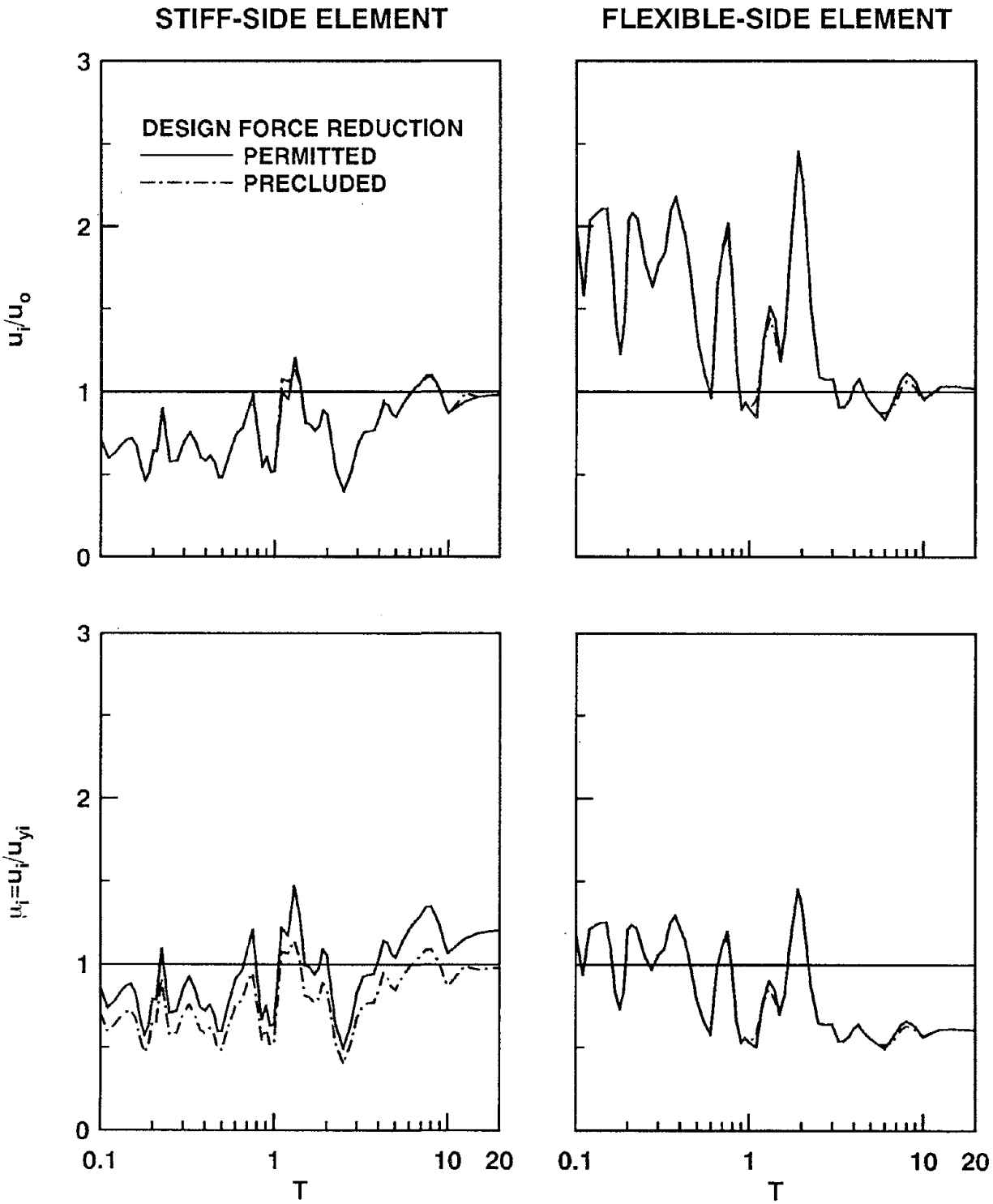

Figure 7.23 Ratio of element deformations, u_i/u_o, for asymmetric-plan ($R=1$, $e_s/r=0.5$, $\Omega_\theta=1$, and $\xi=5\%$) and corresponding symmetric-plan systems, and element ductility demands, μ_i, for asymmetric-plan systems due to El Centro Excitation; systems are designed by UBC-88 excluding accidental eccentricity. Results are presented for two cases: reduction in stiff-side element design force below its symmetric-plan value is permitted or precluded.

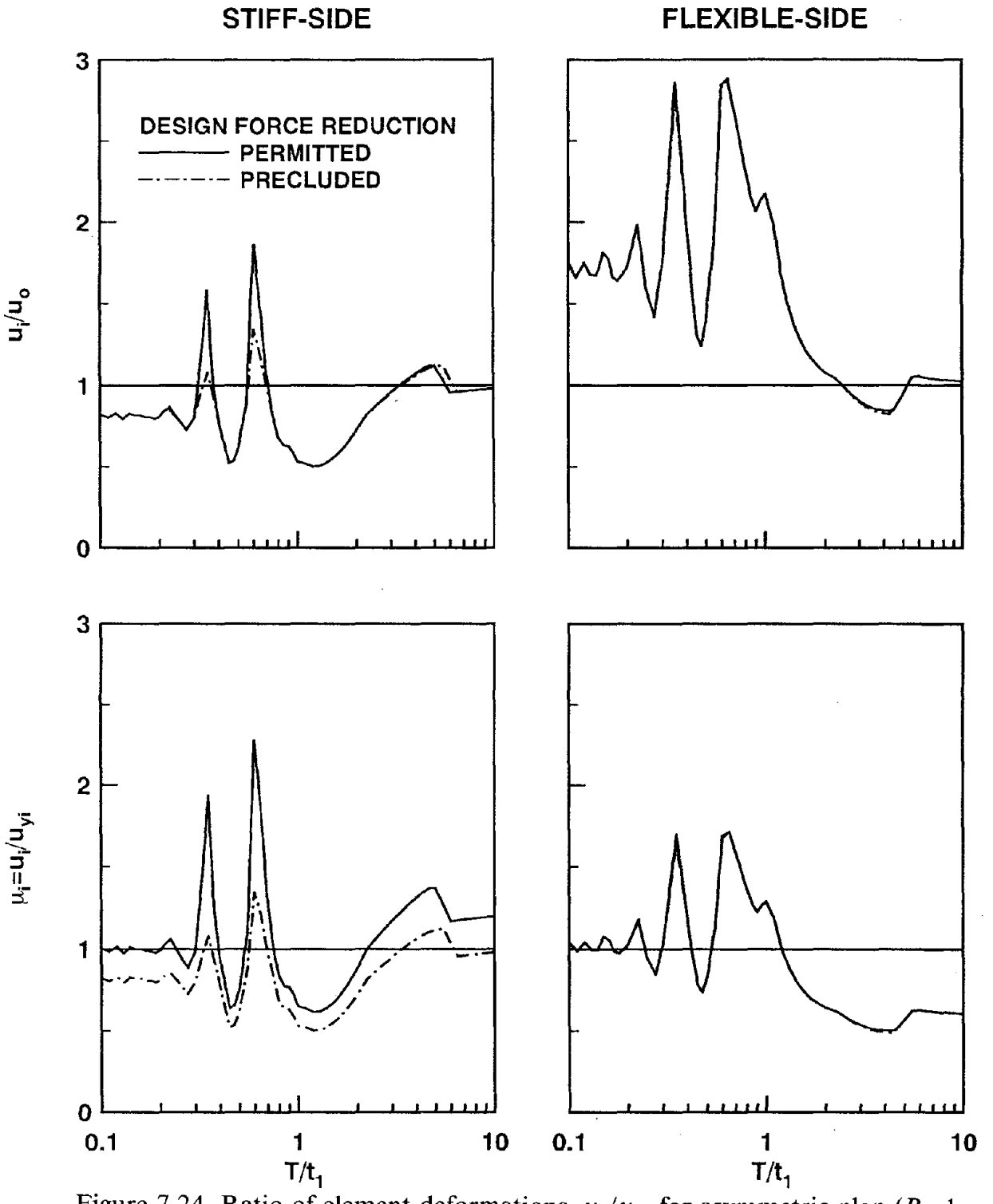

Figure 7.24 Ratio of element deformations, u_i/u_o, for asymmetric-plan ($R=1$, $e_s/r=0.5$, $\Omega_\theta=1$, and $\xi=5\%$) and corresponding symmetric-plan systems, and element ductility demands, μ_i, for asymmetric-plan systems due to simple input; systems are designed by UBC-88 excluding accidental eccentricity. Results are presented for two cases: reduction in stiff-side element design force below its symmetric-plan value is permitted or precluded.

corollary, this element yields less if reduction in its strength is not permitted. The flexible-side element yields primarily because of its significantly larger deformation (Figure 7.23 and 7.24) compared to the symmetric-plan system, although its yield deformation is also larger (Figure 7.1). However, its ductility demand is unaffected whether reduction in the stiff-side element design force is permitted or not because the peak deformation as well as the yield deformation of the flexible-side element is unaffected by such reduction.

7.6.2 Systems Designed by Various Codes

The results of Figures 7.25 to 7.28 indicate that the deformation ratio, u_i/u_o, of resisting elements in systems designed according to various codes is essentially identical over a wide range of period values; and, as mentioned earlier, at each period value u_o does not vary with the code because u_o is identical. Therefore, the element deformations are essentially independent of the design code. This similarity results from the fact that asymmetric-plan systems designed with $R = 1$ (equation (7.1)) respond only slightly beyond the elastic range, in which case the differences in the strengths of systems designed by various codes (Figure 7.3) have very little influence on the response.

Although the element deformation u_i in systems designed by various codes is essentially identical, the ductility demand μ_i may differ significantly because the ductility demand of a resisting element varies inversely with its yield deformation; note that inelastic behavior is implied when μ_i exceeds one which does not happen for most period values (Figures 7.25 to 7.28). Thus, systems designed by UBC-88, which possess the smallest element yield deformation (Figure 7.1), experience the largest element ductility demands, whereas systems designed by MFDC-87 with the largest element yield forces undergo the smallest element ductility demands; responses of systems designed by other codes fall in between these two extremes. The ductility demand on the flexible-side element is essentially the same in systems designed by MFDC-77, NBCC-85, and MFDC-87 because the element yield deformation is identical (Figure 7.1). Similarly, if the yield force of the stiff-side element is not permitted to be below its symmetric-plan value, the ductility demand on this element is the

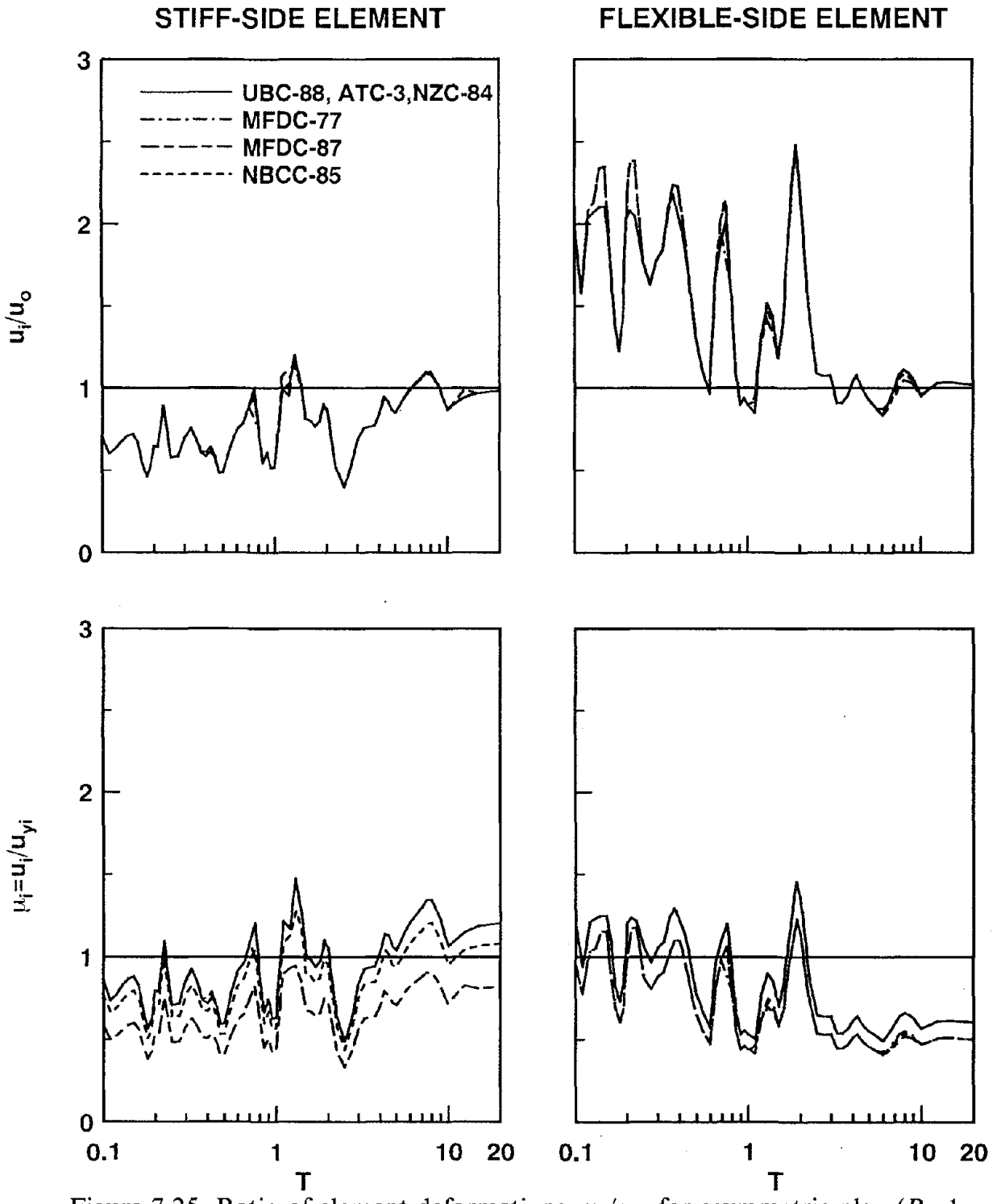

Figure 7.25 Ratio of element deformations, u_i/u_o, for asymmetric-plan ($R=1$, $e_s/r=0.5$, $\Omega_\theta=1$, and $\xi=5\%$) and corresponding symmetric-plan systems, and element ductility demands, μ_i, for asymmetric-plan systems due to El Centro excitation; systems are designed by various codes excluding accidental eccentricity, and reduction in stiff-side element design force below its symmetric-plan value is permitted.

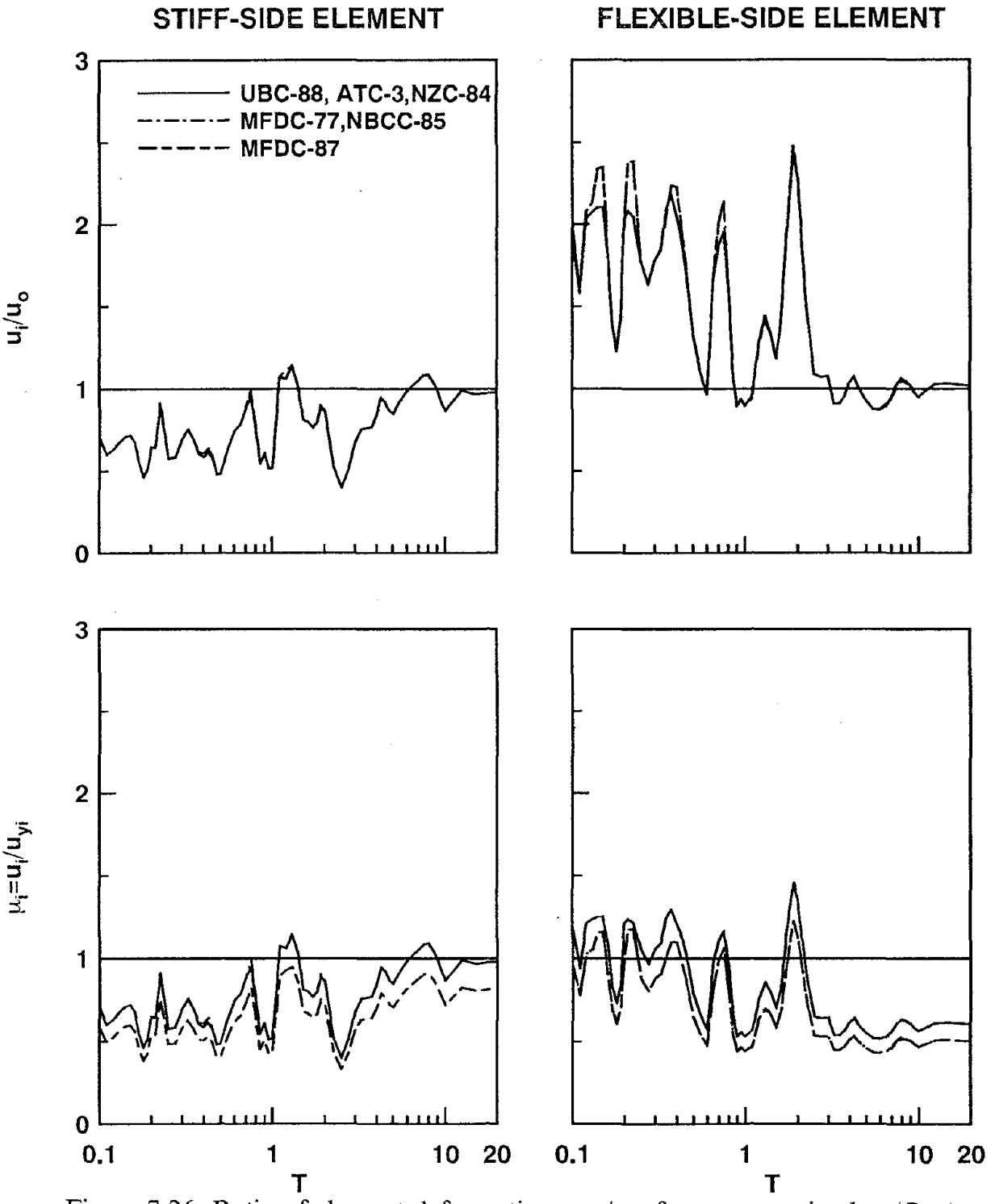

Figure 7.26 Ratio of element deformations, u_i/u_o, for asymmetric-plan ($R=1$, $e_s/r=0.5$, $\Omega_\theta=1$, and $\xi=5\%$) and corresponding symmetric-plan systems, and element ductility demands, μ_i, for asymmetric-plan systems due to El Centro excitation; systems are designed by various codes excluding accidental eccentricity, and reduction in stiff-side element design force below its symmetric-plan value is precluded.

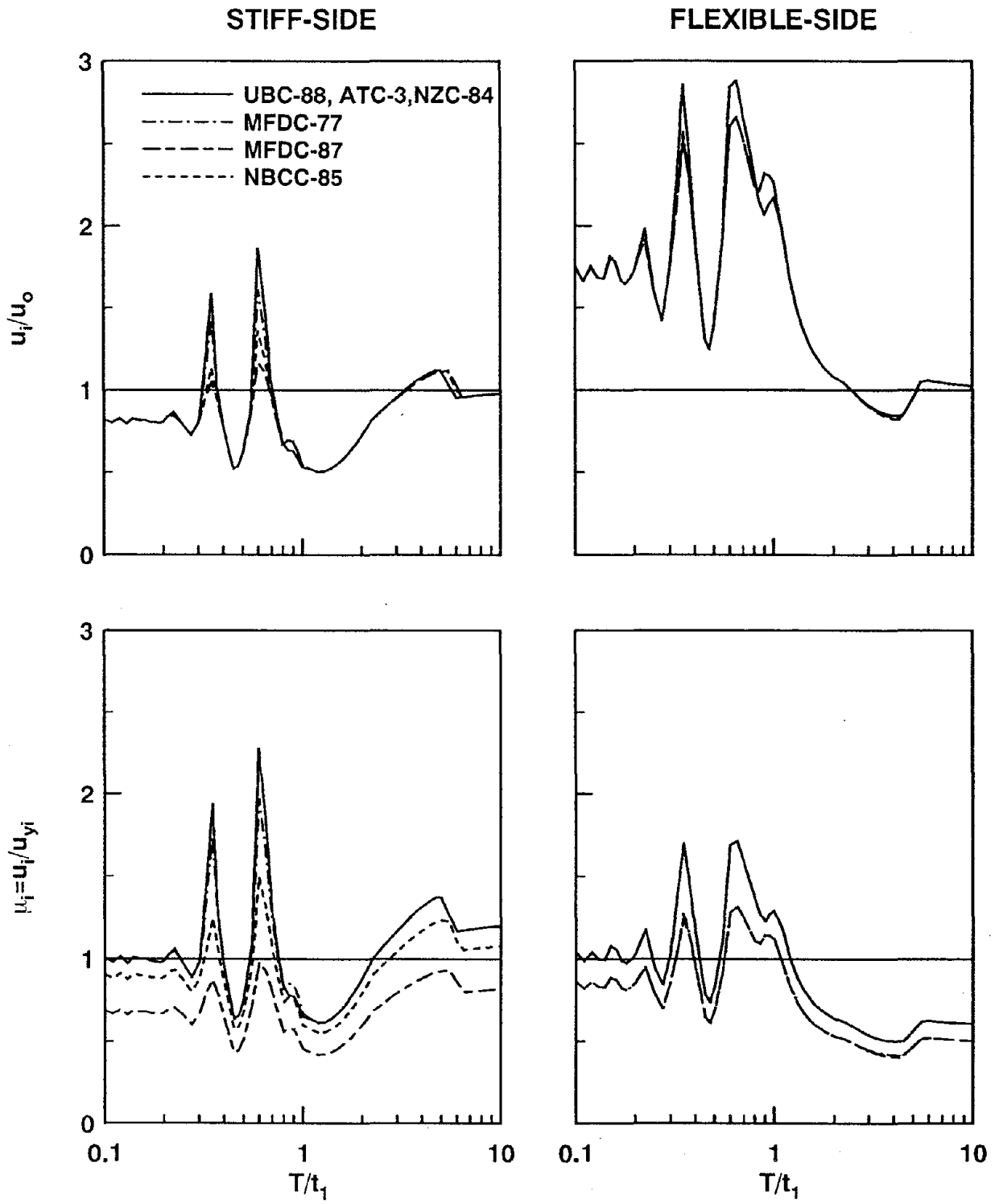

Figure 7.27 Ratio of element deformations, u_i/u_o, for asymmetric-plan ($R=1$, $e_s/r=0.5$, $\Omega_\theta=1$, and $\xi=5\%$) and corresponding symmetric-plan systems, and element ductility demands, μ_i, for asymmetric-plan systems due to simple input; systems are designed by various codes excluding accidental eccentricity, and reduction in stiff-side element design force below its symmetric-plan value is permitted.

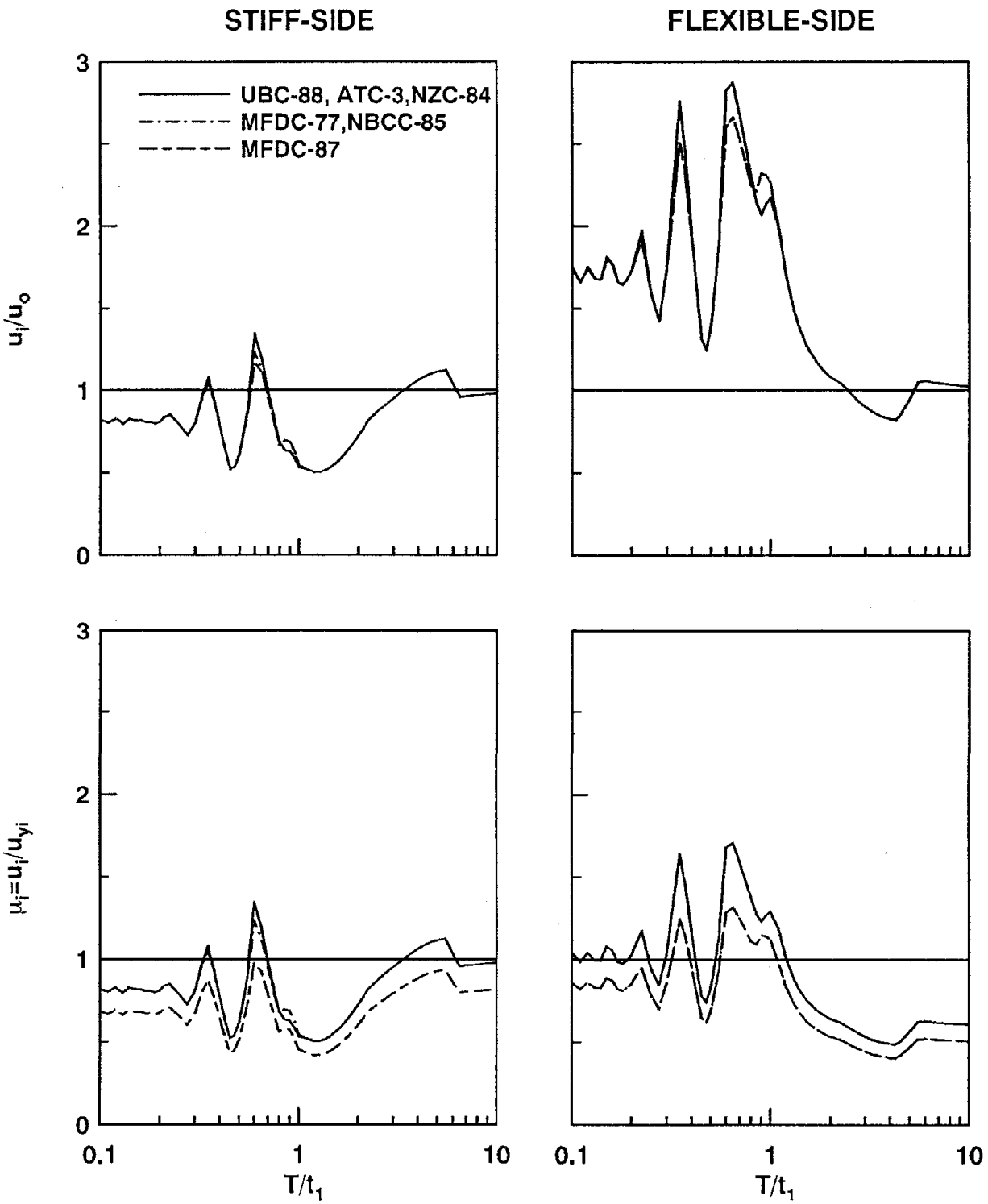

Figure 7.28 Ratio of element deformations, u_i/u_o, for asymmetric-plan ($R=1$, $e_s/r=0.5$, $\Omega_\theta=1$, and $\xi=5\%$) and corresponding symmetric-plan systems, and element ductility demands, μ_i, for asymmetric-plan systems due to simple input; systems are designed by various codes excluding accidental eccentricity, and reduction in stiff-side element design force below its symmetric-plan value is precluded.

same in systems designed by UBC-88, MFDC-77, and NBCC-85 (Figures 7.25 to 7.28) because the element yield deformation is identical (Figure 7.1).

It is apparent from the preceding results that, although symmetric-plan systems with lateral yield force given by equation (7.1) with $R=1$ would remain elastic during the selected ground motion, similarly designed asymmetric-plan systems may deform into the inelastic range. Also, because of torsional motions, the element deformations may significantly exceed the deformation of the corresponding symmetric-plan system. Thus, the asymmetric-plan system may experience structural damage due to yielding and nonstructural damage resulting from increased deformation.

7.7 Modifications in Design Eccentricity

The results of preceding sections indicate that deformations and ductility demands on resisting elements in a code-designed asymmetric-plan system differ from those for the corresponding symmetric-plan system. However, it would be desirable that the responses of the two systems be similar so that the earthquake performance of the asymmetric-plan system would be similar to, and specifically no worse than, that of the symmetric-plan system. Earlier results demonstrated that if the yield force of the stiff-side element is permitted to be below its symmetric-plan value, the earthquake induced ductility demand in this element may be larger because of plan-asymmetry (Figures 7.17 to 7.28). This would suggest that building codes should preclude reduction in the design forces of the stiff-side elements below their symmetric-plan values; $\delta=0$ in equation (7.3b) is equivalent to this restriction.

In order to investigate this issue further, Figures 7.29 and 7.30 present the response of asymmetric-plan systems with their element yield forces computed from equations (7.4) and (7.5) with three different values of $\delta=1$, 0.5, and 0. The first value, $\delta=1$, is typical of several codes: UBC-88, MFDC-77, and NZC-84; $\delta=0.5$ is specified in NBCC-85; and $\delta=0$ implies no reduction in the stiff-side element design force. In all cases, $\alpha=1$ and four different values of R -- 1, 2, 4, and 8 -- were considered in equation (7.1). The ductility demand of the stiff-side element is the only response presented because other response quantities are affected

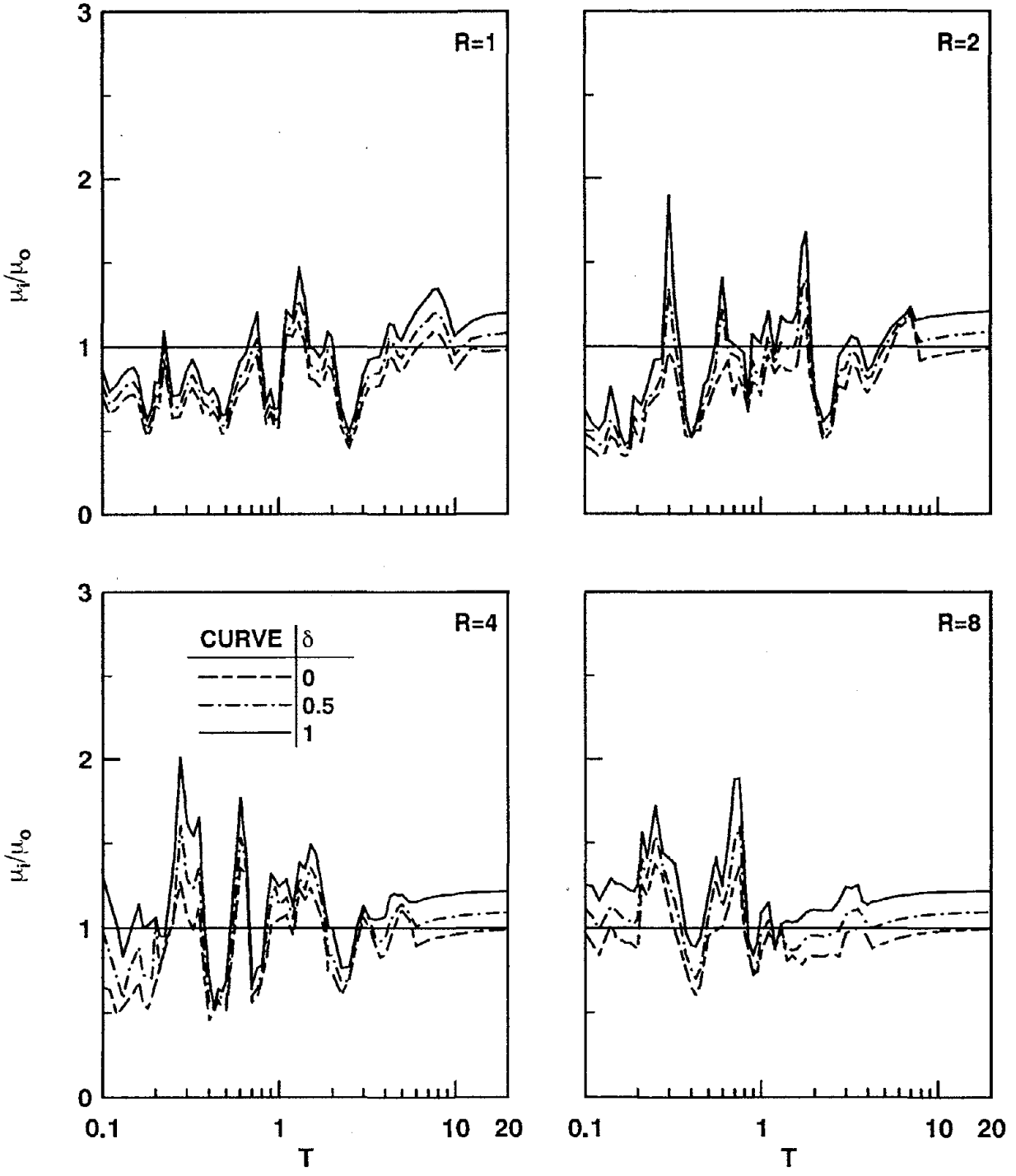

Figure 7.29 Ratio of stiff-side element ductility demands, μ_i/μ_o, for asymmetric-plan ($e_s/r=0.5$, $\Omega_\theta=1$, and $\xi=5\%$) and corresponding symmetric-plan systems due to El Centro excitation. Results are presented for three value of δ, fixed $\alpha=1$ and $\beta=0$, and $R=1$, 2, 4, or 8.

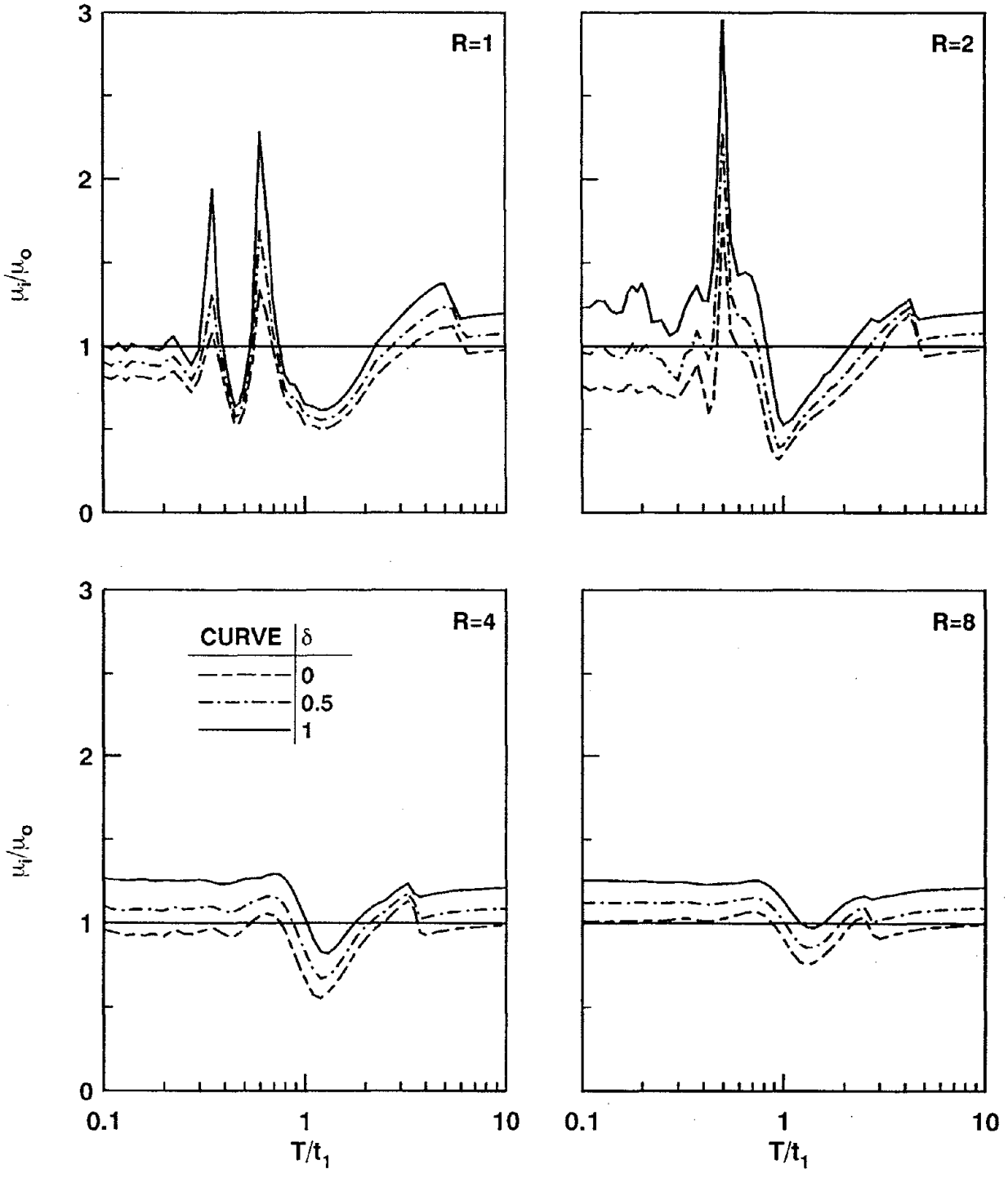

Figure 7.30 Ratio of stiff-side element ductility demands, μ_i/μ_o, for asymmetric-plan ($e_s/r=0.5$, $\Omega_\theta=1$, and $\xi=5\%$) and corresponding symmetric-plan systems due to simple input. Results are presented for three value of δ, fixed $\alpha=1$ and $\beta=0$, and $R=1$, 2, 4, or 8.

very little by δ. It is apparent that the ductility demand μ_i on the stiff-side element in the asymmetric-plan systems designed with δ=0 is generally below the element ductility demand, μ_o, if the system plan were symmetric. However, for some period values, precluding reduction of stiff-side element design force (δ=0) is not sufficient to keep μ_i below μ_o. In order to achieve this objective, perhaps this design force should be increased relative to its symmetric-plan value, which implies a negative value of δ in equation (7.3b); such a suggestion appeared in an earlier work on elastic systems [25].

Even if such a reduction in the stiff-side element design force is precluded, earlier inelastic response results for systems designed with R=4 have demonstrated that the ductility demand on the flexible-side element may be reduced because of plan-asymmetry (Figures 7.17 to 7.22). Thus, the ductility capacity of the flexible-side element is underutilized in an asymmetric-plan system if it is designed for the ductility demand in a symmetric-plan system. In order to better utilize the element ductility capacity, the design eccentricity, e_d, in equation (7.3a) should be modified by decreasing α to reduce the strength of this element. On the other hand for systems with R=1, i.e., systems designed to remain elastic if their plan were symmetric, the ductility demand on the flexible-side element in an asymmetric-plan system may exceed one indicating yielding of the element because of torsional motions. Thus the strength of this element should be increased by increasing α in equation (7.3a) to compute the design eccentricity, e_d.

In order to further investigate these concepts, Figures 7.31 and 7.32 present the response of asymmetric-plan systems with their element yield forces computed from equations (7.4) and (7.5) with three different value of α. In addition to α=1, two larger values are considered for systems designed with R=1 or 2; two smaller values are considered when R=8; and one smaller and another larger value is selected when R=4. The ductility demand of the flexible-side element is the only response quantity presented because other response quantities are affected very little by α. These results demonstrate that, in order to keep the ductility demand on the flexible-side element in the asymmetric-plan system below its

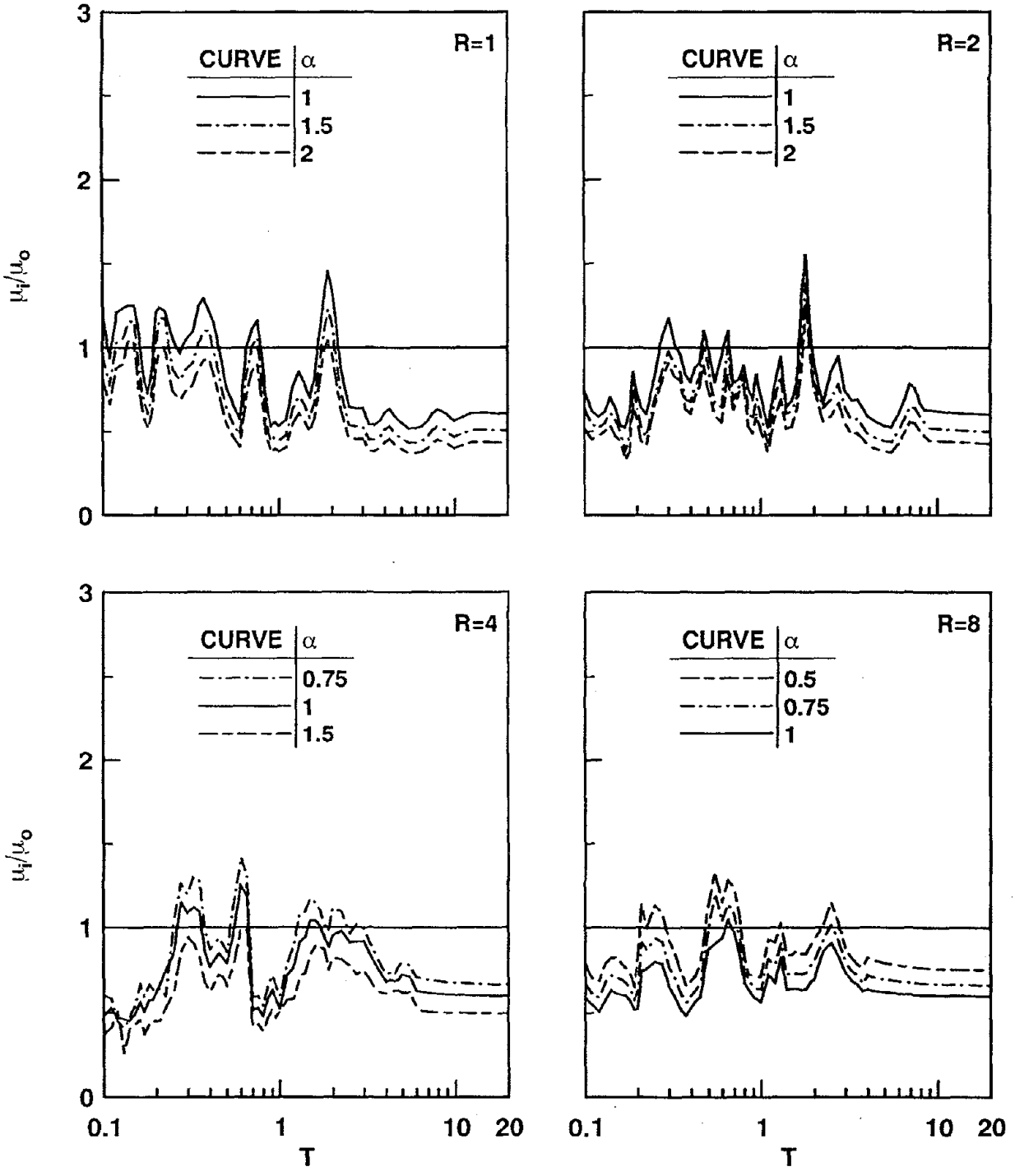

Figure 7.31 Ratio of flexible-side element ductility demands, μ_i/μ_o, for asymmetric-plan ($e_s/r=0.5$, $\Omega_\theta=1$, and $\xi=5\%$) and corresponding symmetric-plan systems due to El Centro excitation. Results are presented for three value of α, fixed $\delta=0$ and $\beta=0$, and $R=1$, 2, 4, or 8.

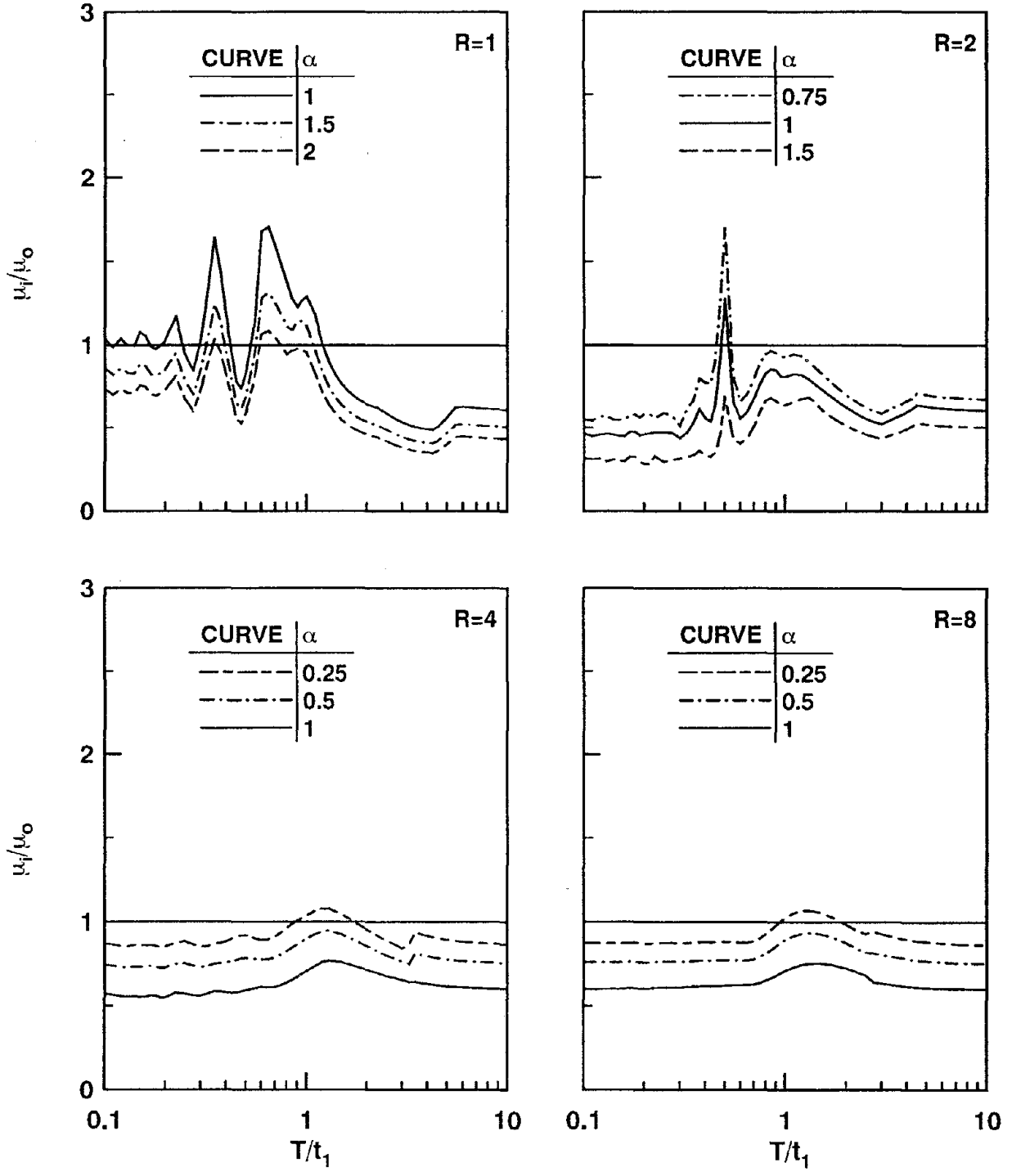

Figure 7.32 Ratio of flexible-side element ductility demands, μ_i/μ_o, for asymmetric-plan (e_s/r=0.5, Ω_θ=1, and ξ=5%) and corresponding symmetric-plan systems due to simple input. Results are presented for three value of α, fixed δ=0 and β=0, and R=1, 2, 4, or 8.

symmetric-plan value, α should be selected as follows: $\alpha=1$ if $R=8$; $\alpha=1.5$ if $R=2$ and 4; and $\alpha=2$ if $R=1$. Obviously, as indicated by comparing Figures 7.31 and 7.32, the optimal α values may differ with the ground motion. Thus, response results should be generated for several ground motions to determine for code use the coefficient α which should depend on the design value of the reduction factor R.

Even if the asymmetric-plan system can be designed for significant yielding in such a way that the ductility demand on the flexible-side element does not exceed the symmetric-plan value, the element deformation may still be larger because of plan-asymmetry. It may not be possible to reduce this deformation by increasing the strength of the system because, as shown by the responses of SDF systems [38], the deformation is not strongly affected by the strength in the medium-period, velocity-sensitive region of the spectrum and it is in this period region that the additional deformation due to plan-asymmetry is most significant (Figures 7.18 to 7.22). Because increasing the strength of a system beyond that required for it to remain elastic would not influence its response if it is within the elastic range, the additional deformations of elastic systems resulting from plan-asymmetry also can not be reduced. Thus, these larger deformations in asymmetric-plan systems should be provided for in the design of structures.

7.8 Dual Design Philosophy

It is widely accepted that most buildings should be designed to: (1) safely dissipate vibrational energy through inelastic action during intense ground shaking, and (2) remain structurally undamaged during moderate ground shaking. The first design requirement leads to the yield forces for which the structural elements should be designed to ensure that their ductility capacity is not exceeded during intense ground shaking. The second design requirement defines the strength required for the structural elements to remain elastic during moderate ground motion. Obviously, the larger of the two forces for each element is the critical design force.

The element design force in an asymmetric-plan system depends on the base shear V and the design eccentricity e_d (equation (7.2)). The base shear depends on the elastic spectrum and the selected reduction factor R (equation (7.1)). As indicated by the preceding section, the design eccentricity (equation (7.3)) should be defined differently for elastic and inelastic systems; in particular, the coefficient α and hence e_d should increase as the reduction factor R decreases. Thus, two values of the design force corresponding to the two levels of shaking should be computed for each structural element from equations (7.4) and (7.5) using the appropriate values of R and α, and the critical design force taken as the larger of the two forces.

8. CONCLUSIONS

The inelastic earthquake response of one-story, asymmetric-plan systems is affected by the location, stiffness, and yield deformation of each of the resisting elements as well as their number, indicating that a large number of parameters would be needed to fully characterize the inelastic response; whereas the elastic response of such systems depends only on the following system parameters: uncoupled vibration period, T; normalized stiffness eccentricity, e_s/r; ratio of the uncoupled torsional and lateral vibration frequencies, $\Omega_\theta=\omega_\theta/\omega$; and the damping ratio ξ. Because it would be unmanageable to conduct a parametric study with such a large number of parameters and impossible to identify in a meaningful manner the influence of each parameter on the inelastic response, only five additional parameters believed to be the most important in characterizing the inelastic response of asymmetric-plan systems are introduced: ratio of the uncoupled vibration frequencies in X- and Y-translation, ω_x/ω; the ratio γ_x of the torsional stiffness due to the resisting elements oriented perpendicular to the direction of ground motion to the total torsional stiffness at the center of stiffness (CS) of the system; yield coefficient, c, which is the ratio of the yield deformation, u_y, of the corresponding symmetric-plan system to the peak earthquake-induced deformation of the associated elastic system; the value of the strength eccentricity e_p relative to the stiffness eccentricity e_s; and the overstrength factor, O_s, by which the strength of the system exceeds the value if it had no asymmetry in plan.

The inelastic response of several asymmetric-plan systems is investigated in Chapter 4 with the objective of identifying how the plan-wise distribution of stiffness and strength affects the inelastic response, leading to the following conclusions:

1. The inelastic response of systems is influenced significantly by the contribution to the torsional stiffness from the resisting elements perpendicular to the direction of ground motion. The effects of plan-asymmetry are larger in systems without such elements compared to systems with these perpendicular elements. More specifically, plan-asymmetry decreases the lateral deformation to a greater degree, and increases the

torsional deformation, the element deformations, and the maximum ductility demand to a greater degree in systems without perpendicular elements.

2. Because these effects of perpendicular elements tend to increase with larger inelastic deformations of the system, the perpendicular elements significantly affect the response of short-period, acceleration-sensitive systems but their influence is small for medium-period, velocity-sensitive and long-period, displacement-sensitive systems. Thus, the conclusions from earlier studies of systems without perpendicular elements are generally not applicable to most actual buildings which invariably include resisting elements in the two lateral directions to provide resistance to both horizontal components of ground motion. In particular, the large increases in ductility demand and edge displacements observed in such studies are overly excessive for the design of most buildings.

3. The parameters γ_x and ω_x/ω -- characterizing the relative contribution of perpendicular elements to the torsional stiffness and the relative translational stiffness in the two principal directions, respectively -- affect the inelastic response of short-period, acceleration-sensitive systems with $e_p=e_s$ to a significant degree but the response of medium-period, velocity-sensitive and long-period, displacement-sensitive systems is affected very little. However, the response of 'strength-symmetric' ($e_p=0$) systems is essentially unaffected by these parameters in the parameter range considered over the entire range of values of the vibration period, T.

4. The number of resisting elements oriented along the direction of ground motion has little influence on the response of a system with similar strength and stiffness eccentricities. Thus a system with only two resisting elements should provide a satisfactory estimate of the response of a system with larger number of resisting elements provided the parameters T, e_s/r, Ω_θ, γ_x, ω_x/ω, c, e_p, O_s, and ξ are the same for the two systems.

5. In systems with strength eccentricity much smaller than stiffness eccentricity, the number of resisting elements also has very little influence on the lateral and torsional

displacements at the center of stiffness and element deformations. However, the maximum ductility demand can be significantly influenced. Therefore for such structures, the actual number of elements should be considered in predicting the ductility demand from the other response quantities; the latter may be determined from the dynamic analysis of a system with two elements.

6. While the elastic response of mass-eccentric and stiffness-eccentric systems is identical provided that the elastic parameters, T, Ω_θ, e_s/r, and ξ are the same for both systems, the inelastic response of the two systems may differ even if the inelastic parameters c, O_s, and e_p are identical. For a system with equal strength and stiffness eccentricities, mass-eccentric and stiffness-eccentric systems may be used interchangeably to estimate the deformations at the CS but not for predicting the maximum ductility demand. For 'strength-symmetric' (e_p=0) systems and systems with strength eccentricity much smaller than stiffness eccentricity, the two systems respond very differently. Since the plan-asymmetry in most buildings arises from distribution of stiffness and not of mass, the mass-eccentric system should not be used in estimating the inelastic response of such buildings.

7. The overstrength in short-period, acceleration-sensitive systems significantly reduces the lateral deformation at the CS, the element deformations, and the maximum ductility demand. Because code-designed, asymmetric-plan buildings are generally stronger than the corresponding symmetric-plan buildings, such reduction in the response may merit consideration in the design process. Furthermore, because most earlier investigations assumed the combined strength of all resisting elements in an asymmetric-plan building to be equal to that of the symmetric-plan building, their conclusions are not directly applicable to code-designed buildings.

8. The inelastic response of short-period, acceleration-sensitive systems is influenced significantly by the relative values of its strength eccentricity and stiffness eccentricity. In particular, the torsional deformation decreases, and the lateral deformation increases

as the e_p value decreases relative to the e_s value. The results of many investigations using systems with $e_p=e_s$ are therefore not directly applicable to code-designed buildings for which the strength eccentricity tends to be much smaller than the stiffness eccentricity.

9. The overall inelastic response of one-story, asymmetric-plan systems with mass, stiffness, and strength properties symmetric about the X-axis but not about the Y-axis may be characterized to a useful degree of accuracy by nine parameters: T, Ω_θ, e_s/r, γ_x, ω_x/ω, e_p, O_s, c, and ξ. Thus, the overall inelastic response of an actual asymmetric-plan system may be estimated by analyzing a simpler system with fewer resisting elements but having the same values of the above-mentioned system parameters as in the actual system. However, a mass-eccentric system should not be used to estimate the response of a stiffness-eccentric system and vice-versa, especially if the strength eccentricity of the system is much smaller than the stiffness eccentricity.

The response of an asymmetric-plan system, chosen -- based on the conclusions of Chapter 4 -- to ensure wide applicability of results, has been presented in Chapter 5 with the objective of identifying the influence of system parameters. These response results lead to the following conclusions:

1. The torsional deformation of elastic as well as inelastic systems tends to increase with increasing stiffness eccentricity, e_s/r, and decreasing frequency ratio, Ω_θ, over a wide range of structural vibration periods. For very-short-period, acceleration-sensitive, elastic systems, the torsional deformation increases linearly with increasing e_s/r and decreases by a factor of $1/\Omega_\theta^2$ with increasing Ω_θ; however, inelastic systems in the same period range may experience significantly larger increase in deformation. For very-long-period, displacement-sensitive, elastic systems, the torsional deformation tends to zero regardless of e_s/r and Ω_θ values; however, such may not be the case for inelastic systems. The largest increase in the torsional deformation of systems with small e_s/r

due to increasing e_s/r occurs in the medium-period, velocity-sensitive region of the spectrum. However, as the stiffness eccentricity becomes large, short-period, acceleration-sensitive systems may experience larger increase in the torsional deformation with increasing e_s/r compared to systems in other spectral regions.

2. The lateral deformation of elastic as well as inelastic systems is affected by the stiffness eccentricity, e_s/r, and the frequency ratio, Ω_θ, primarily in the medium-period, velocity-sensitive region of the spectrum, where it generally decreases with increasing e_s/r and decreasing Ω_θ. In the short-period, acceleration-sensitive and long-period, displacement-sensitive regions, the lateral deformation is essentially unaffected by e_s/r and Ω_θ. In the transition regions, the lateral deformation depends on e_s/r and Ω_θ in a complex manner, increasing for some period values and decreasing for others; however, the dependence is small.

3. The largest of peak deformations among all resisting elements in the short-period, acceleration-sensitive region increases as the stiffness eccentricity, e_s/r increases and the frequency ratio, Ω_θ decreases. In the medium-period, velocity-sensitive region, while the element deformation increases with increasing e_s/r, it may decrease as Ω_θ decreases. The peak element deformation is essentially unaffected by e_s/r and Ω_θ in the long-period, displacement-sensitive region, where it becomes the same as the peak ground displacement. The element deformation of elastic systems is affected more by e_s/r and Ω_θ compared to inelastic systems.

4. The response of 'strength-symmetric' (e_p=0) systems is influenced to a lesser degree by e_s/r and Ω_θ compared to systems with equal strength and stiffness eccentricities (e_p=e_s).

5. Inelastic behavior (or yielding) influences the lateral deformation of asymmetric-plan systems in a manner similar to symmetric-plan systems. In particular, as the yield strength (or yield factor) decreases, the lateral deformation increases significantly in the short-period, acceleration-sensitive region; increases or decreases, depending on the

lateral vibration period T, in the medium-period, velocity-sensitive and neighboring transition regions; and remains unaffected in the long-period, displacement-sensitive region.

6. The effects of yielding on the torsional deformation depend on the lateral vibration period, yield strength and on the stiffness and strength eccentricities of the asymmetric-plan system. For short-period, acceleration-sensitive systems with yield strength about one-half of that required for the system to remain elastic ($c = ½$), yielding has the effect of slightly increasing the deformation. However, if the yield strength is much smaller, torsional deformation of short-period, inelastic systems with equal strength and stiffness eccentricities ($e_p = e_s$) and large stiffness eccentricity is larger compared to elastic systems; in case of systems with small stiffness eccentricity, yielding results in reduced torsional deformation; torsional deformation of 'strength-symmetric' ($e_p = 0$) systems becomes smaller as result of yielding regardless of e_s/r value. Yielding leads to reduced torsional deformation of medium-period, velocity-sensitive and long-period, displacement-sensitive systems, regardless of their stiffness eccentricity. Thus, if the system is well into the inelastic range, the effects of plan-asymmetry on system response are small.

7. Inelastic action influences the largest of peak deformations among all resisting elements of systems in various spectral regions in generally a similar manner as it influences the lateral deformation.

8. The ratio of lateral deformations at the CS of inelastic and elastic asymmetric-plan systems is significantly different than for SDF (symmetric-plan) systems when the effects of plan-asymmetry are significant in structural response. Such may be the case for systems with lateral vibration period in the velocity-sensitive spectral region, large stiffness eccentricity, or yield factor close to one; for such systems this ratio for asymmetric-plan systems may be slightly higher or lower compared to symmetric-plan systems.

9. The ratio of element deformations for inelastic and elastic systems is affected by plan-asymmetry to a greater degree compared to the ratio for deformations at the CS, and is smaller for asymmetric-plan systems.

The effects of plan-asymmetry in the earthquake response of one-story systems are identified in Chapter 6, by comparing the dynamic responses of an asymmetric-plan system and of the corresponding symmetric-plan system for a wide range of system parameters. This comparison leads to the following conclusions:

1. Plan-asymmetry causes torsional deformation, which does not occur in the corresponding symmetric-plan system; modifies the lateral deformation experienced by the corresponding symmetric-plan system, resulting in a smaller or larger deformation; and generally increases the largest of peak deformations among all resisting elements compared to the deformation of the same element in the corresponding symmetric-plan system.

2. The effects of plan-asymmetry on the lateral and torsional deformations of elastic systems depend significantly on the uncoupled lateral vibration period of the system, especially for realistic excitations, such as the El Centro ground motion, being most pronounced in the medium-period, velocity-sensitive and its transition regions of the spectrum. However, the period dependence of the effects of plan-asymmetry is less pronounced for inelastic systems and decreases with increased yielding resulting from decreasing yield strength.

3. The lateral deformation of short-period, acceleration-sensitive and of long-period, displacement-sensitive systems is affected very little by plan-asymmetry or by inelastic behavior. The dynamic amplification of torsional deformation is quite different between elastic and inelastic systems. The dynamic torsional deformation of elastic systems becomes equal to its static value -- the deformation due to V_o applied at a distance e_s -- for very short-period systems, and zero for very long-period systems. However, very long-period as well as very short-period inelastic systems generally experience

very little torsional deformation.

4. The effects of plan-asymmetry on the response of elastic systems depend in an important way on the ratio Ω_θ of uncoupled torsional and lateral frequencies, and are most pronounced in systems with close frequencies. In particular, considerable dynamic amplification of the torsional deformation occurs for systems with Ω_θ around unity, and this amplification is greater for slightly asymmetric (small values of normalized stiffness eccentricity, e_s/r) systems. The modification of lateral deformation is largest for highly asymmetric (large e_s/r) systems. Because of yielding of the system, the peak of e_d/e_s, which still occurs for systems with Ω_θ around one, becomes smaller and flatter implying less dynamic amplification of torsional deformation and its decreasing dependence on Ω_θ. As the yield strength of the system decreases, implying increased yielding, the torsional deformation decreases and it becomes increasingly insensitive to e_s/r.

5. The lateral deformation of torsionally-very-stiff (large Ω_θ) systems is affected very little by plan-asymmetry, and their dynamic torsional deformation is essentially the same as its static value. In particular, for systems with $\Omega_\theta>2$ the normalized responses are not sensitive to e_s/r, and the effects of plan-asymmetry on lateral deformation may be ignored and the dynamic amplification of torsional deformation neglected. This conclusion is valid for elastic systems and generally also for inelastic systems except that in the latter case the dynamic amplification of torsional deformation may be significant for some values of yield strength.

6. The largest of peak deformations among all resisting elements is generally increased by plan-asymmetry for systems in the acceleration- and velocity-sensitive regions of the spectrum; however, the element deformation is affected little by plan-asymmetry in the displacement-sensitive region. For elastic systems, this increase in element deformation becomes larger as the stiffness eccentricity increases and is relatively insensitive to the frequency ratio. The increase in element deformation due to plan-asymmetry is generally smaller for inelastic systems, especially for 'strength-symmetric' ($e_p=0$) systems,

compared to elastic systems. With increasing inelastic action, the element deformation in an asymmetric-plan system becomes closer to that of the symmetric-plan system.

7. As mentioned earlier, the response of inelastic systems is affected less by plan-asymmetry compared to elastic systems. Between the two types of inelastic systems considered, the response of 'strength-symmetric' (e_p=0) systems is affected by plan-asymmetry generally to a smaller degree compared to systems with equal stiffness and strength eccentricities. In particular, the dynamic amplification of torsional deformation is smaller, and the increase in element deformation due to plan-asymmetry is less in 'strength-symmetric' (e_p=0) systems.

The effects of plan-asymmetry on the earthquake response of code-designed systems are investigated in Chapter 7 in order to determine how well these effects are represented by torsional provisions in building codes. The following conclusions may be drawn from these response results:

1. The strength eccentricity of a code-designed symmetric-plan system, which by definition has zero stiffness eccentricity, is generally nonzero because of the accidental eccentricity provision in codes. Such a system, although displaying only lateral motions in the elastic range, would undergo coupled lateral-torsional motions in the inelastic range; however, the torsional motions are found to be small.

2. Buildings designed according to codes are expected to undergo considerable yielding during intense ground shaking. The inelastic response of code-designed asymmetric-plan systems generally differs from that of the corresponding symmetric-plan system. Plan-asymmetry tends to increase the deformation of the flexible-side element and reduce the deformation of the stiff-side element in medium-period, velocity-sensitive systems; however, the element deformations are affected very little for short-period, acceleration-sensitive systems and long-period, displacement-sensitive systems.

3. Application of code procedures leads to decrease in the design force for elements within the stiff-side of the building because of plan-asymmetry; however such reduction in

element design forces is not permitted by several codes. According to these codes, the element design forces should be increased due to plan-asymmetry but not reduced below their values for a symmetric-plan system. If such force reduction is permitted, the ductility demand on the stiff-side element is larger than its symmetric-plan value; however, if the force reduction is precluded, the ductility demand on this element is roughly unaffected by plan-asymmetry. The ductility demand on the flexible-side element is significantly smaller than in the symmetric-plan system, with exceptions at few periods, regardless of whether the design force reduction for the stiff-side element is permitted or not.

4. The element deformations of systems designed according to most building codes, except MFDC-87, are not very different; however, the ductility demands may differ significantly among these systems. If the reduction in design force of the stiff-side element below its symmetric-plan value is permitted, the NBCC-85 designed system has the desirable property that the ductility demand on the stiff-side element is closest, among all codes considered, to the ductility demand of the symmetric-plan system. If such design force reduction is not permitted, the ductility demand on the stiff-side element of systems designed according to all codes considered, except MFDC-87, is close to the symmetric-plan value. In particular, the ductility demand on the stiff-side element in the MFDC-87 designed system tends to be significantly reduced because of plan-asymmetry, suggesting that the additional requirement imposed in this code to restrict the strength eccentricity may be unnecessary.

5. It is the intent of most seismic codes that buildings suffer no damage during some, usually unspecified, level of moderate ground shaking. Although, symmetric-plan systems designed with $R=1$ would be expected to remain elastic during the design ground motion, similarly designed asymmetric-plan systems may deform into the inelastic range. Also because of torsional motions, the element deformation may significantly exceed the deformation of the corresponding symmetric-plan system. Thus,

asymmetric-plan systems designed with $R=1$ may experience structural damage due to yielding and nonstructural damage resulting from increased deformations.

6. Although the element deformation in systems designed by various codes is similar, the ductility demand may differ significantly. Among the codes considered, systems designed by UBC-88 experience the largest ductility demand, whereas systems designed by MFDC-87 undergo the smallest ductility demand; response of systems designed by other codes fall in between these two extremes.

7. It would be desirable that the expected earthquake performance of a code-designed asymmetric-plan system be similar to that for the similarly designed corresponding symmetric-plan system. Thus, the deformations and ductility demands on resisting elements of the two systems should be similar. This requirement is not satisfied by the torsional provisions in most building codes, which suggests that the design eccentricity should be modified. The presented results have demonstrated that this goal can usually be achieved for stiff-side elements by precluding any reduction in their design forces below their symmetric-plan values; $\delta=0$ in the design eccentricity, e_d, is equivalent to this requirement. However, for some period values, precluding reduction of stiff-side element design forces ($\delta=0$) is not sufficient to prevent the ductility demand on this element in the asymmetric-plan system from exceeding the value for the symmetric-plan system. In order to achieve this objective, perhaps the design force for this element should be increased relative to its symmetric-plan value, which implies a negative value of δ.

8. Similarly, the ductility demand on the flexible-side element can be kept below and close to its symmetric-plan value by modifying the coefficient α in the design eccentricity, e_d. The optimal value of α in equation (7.3) has been shown to depend on the design value of the reduction factor R and may differ with the ground motion. Thus, response results should be generated for several ground motions to determine the coefficient α appropriate for use in building codes.

9. However, it does not appear possible to reduce the additional deformations of code-designed systems due to plan-asymmetry by modifying the design eccentricity. Thus, these larger deformations in asymmetric-plan systems should be provided for in building design.

10. Although the largest deformation among all the resisting elements of code-designed asymmetric-plan systems occurs in the flexible-side element, the largest ductility demand may occur in the stiff-side element. Thus, additional care is required not only in the design of flexible-side elements for deformation demand, but also in the design of stiff-side elements for ductility demand.

11. It is widely accepted that most buildings should be designed to: (1) safely dissipate vibrational energy though inelastic action during intense ground shaking, and (2) remain structurally undamaged during moderate ground shaking. Explicit implementation of this dual design philosophy is especially important for asymmetric-plan buildings because the design eccentricity should be defined differently for elastic and inelastic systems, and should vary with the reduction factor R in the latter case. Thus, two values of the design force corresponding to two levels of shaking should be computed for each resisting element, using appropriate values of R and e_d, and the critical design force taken as the larger of the two forces.

The response behavior of asymmetric-plan systems investigated in Chapters 5, 6, and 7 is similar in an overall sense for the corresponding spectral regions of the simple input and the El Centro excitation, but may differ considerably in detail; furthermore, the variation of plan-asymmetry effects with systems parameters is more complicated in case of the latter excitation. These complications are in part due to the irregular shape of the response spectrum for a single ground motion; they would depend on ground motion properties and details; and are likely to decrease if the results are averaged over several ground motions. Because the response behavior is investigated using a broad-frequency-band earthquake motion, the conclusions may not be valid for narrow-frequency-band excitations.

REFERENCES

1. Bozorgnia, Y. and Tso, W.K., " Inelastic earthquake response of asymmetric structures," *Journal of Structural Engineering*, ASCE, Vol. 112, No. 2, Feb. 1986, pp. 383-399.
2. Chandler, A.M., and Hutchinson, G.L., "Evaluation of code torsional provisions by a time history approach," *Journal of Earthquake Engineering and Structural Dynamics*, Vol. 15, 1987, pp. 491-516.
3. Cheung, V.W.-T., and Tso, W.K., "Eccentricity in irregular multistory buildings," *Canadian Journal of Civil Engineering*, Vol. 13, 1986, pp. 46-52.
4. Dempsey, K.M., and Tso, W.K., "An alternative path to seismic torsional provisions," *Soil Dynamics and Earthquake Engineering*, Vol. 1, No. 1, 1982, pp. 3-10.
5. *Design Manual for Earthquake Construction Regulation for the Federal District of Mexico*, National University of Mexico, No. 406, July 1977.
6. Elms, D.G., "Seismic torsional effects on buildings," *Bulletin of New Zealand National Society for Earthquake Engineering*, Vol. 9, No. 1, March 1976, pp. 79-83.
7. Erdik, M.O., *Torsional effects in dynamically excited structures*, Ph.D. Thesis, Rice University, Houston, Texas, May 1975.
8. Esteva, L., "Earthquake engineering research and practice in Mexico after the 1985 earthquakes," *Bulletin of the New Zealand National Society for Earthquake Engineering*, Vol. 20, No. 3, Sept. 1987, pp. 159-200.
9. Gomez, R. and Garcia-Ranz, F., "The Mexico earthquake of September 19, 1985 - complementary technical norms for earthquake resistant design," *Earthquake Spectra*, Vol. 4, No. 3, Aug. 1988, pp. 441-460.
10. Hart, G.C., DiJulio, R.M., and Lew, M., "Torsional response of high-rise buildings," *Journal of Structural Division*, ASCE, Vol. 101, No. ST2, Proc. Paper 11126, Feb. 1975, pp. 397-416.
11. Hejal, R., and Chopra, A.K., *Earthquake response of torsionally-coupled buildings*, Report No. UCB/EERC-87/20, Earthquake Engineering Research Center, University of California, Berkeley, California, Dec. 1987.
12. Hejal, R. and Chopra, A.K., "Lateral-torsional coupling in earthquake response of frame buildings," *Journal of Structural Engineering*, ASCE, Vol. 115, April 1989, pp. 852-867.
13. Humar, J.L., "Design for seismic torsional forces," *Canadian Journal of Civil Engineering*, Vol. 11, 1984, pp. 150-163.
14. Humar, J.L., and Awad, A.M., "Design for seismic torsional forces," *Proceedings of the 4th Canadian Conference on Earthquake Engineering*, Vancouver, June 1983, pp. 251-260.
15. International Association for Earthquake Engineering, *Earthquake Resistant Regulations, A World List, 1988*, Tokyo, August 1988.
16. International Conference of Building Officials, *Uniform Building Code*, 1988.

17. Irvine, H.M. and Kountouris, G.E., "Peak ductility demands in simple torsionally unbalanced building models subjected to earthquake ground excitation," *Proceedings of the 7th World Conference on Earthquake Engineering*, Istanbul, Turkey, Vol. 4, 1980, pp. 117-120.

18. Kan, C.L. and Chopra, A.K., "Effects of torsional coupling on earthquake forces in buildings," *Journal of Structural Division*, ASCE, Vol. 103, No. ST4, 1977, pp. 805-820.

19. Kan, C.L. and Chopra, A.K., *Linear and nonlinear earthquake response of simple torsionally coupled systems,* Report No. UCB/EERC-79/03, Earthquake Engineering Research Center, University of California, Berkeley, California, Feb. 1979.

20. Kan, C.L. and Chopra, A.K., "Torsional coupling and earthquake response of simple elastic and inelastic systems," *Journal of Structural Division*, ASCE, Vol. 107, No. ST8, Aug. 1981, pp.1569-1588.

21. Mondkar, D.P. and Powell, G.H., *ANSR 1 - Static and dynamic analysis of nonlinear structures,* Report No. UCB/EERC-75/10, Earthquake Engineering Research Center, University of California, Berkeley, California, Dec. 1975.

22. *National Building Code of Canada*, 1985, Associate Committee on the National Building Code, National Research Council of Canada, Ottawa, Ontario.

23. New Zealand Standard NZS 4203:1984, "Code of practice for general structural design loadings for buildings," *Standards Association of New Zealand*, Willington, New Zealand, 1984.

24. Palazzo, B., and Fraternali, F., "Seismic ductility demand in buildings irregular in plan: A new single story nonlinear model," *Proceedings of 9th World Conference on Earthquake Engineering,* Tokyo-Kyoto, Japan, Vol. V, Aug. 1988, pp. V-43 to V-48.

25. Pekau, O.A., and Rutenberg, A., "Evaluation of the torsional provisions in the 1985 NBCC," *Proceedings of the 5th Canadian Conference on Earthquake Engineering*, Ottawa, 1987, pp. 739-746.

26. Poole, R.A., "Analysis for torsion employing provisions of NZRS 4203:1974," *Bulletin of New Zealand National Society for Earthquake Engineering*, Vol. 10, No. 4, 1977, pp. 219-225.

27. *Recommended Lateral Force Requirements and Tentative Commentary*, Seismology Committee, Structural Engineers Association of California, 1988.

28. Rosenblueth, R., "Seismic design requirements in a Mexican 1976 code," *Journal of Earthquake Engineering and Structural Dynamics*, Vol. 7, 1979, pp. 49-61.

29. Rutenberg, A. and Pekau, O.A., "Earthquake response of asymmetric buildings: a parametric study," *Proceedings of the 4th Canadian Conference on Earthquake Engineering*, Vancouver, June 1983, pp. 271-281.

30. Rutenberg, A., Shohet, G., and Eisenberger, M., *Inelastic seismic response of code designed asymmetric structures*, Faculty Publication No. 303, Technion - Israel Institute of Technology, Haifa, December 1989.

31. Sadek, A.W. and Tso, W.K., "Strength eccentricity concept for inelastic analysis of asymmetric structures," *Proceedings of 9th World Conference on Earthquake Engineering*, Tokyo-Kyoto, Japan, Vol. V, Aug. 1988, pp. V-91 to V-96.

32. *Tentative Provisions for the Development of Seismic Regulations for Buildings*, ATC3-06, Applied Technological Council, Palo Alto, CA, 1978.

33. Tso, W.K., and Meng, V., "Torsional provisions in building codes," *Canadian Journal of Civil Engineering*, Vol. 9, 1982, pp. 38-46.

34. Tso, W.K., "A proposal to improve the static torsional provisions for the National Building Code of Canada," *Canadian Journal of Civil Engineering*, Vol. 10, 1983, pp. 561-565.

35. Tso, W.K. and Sadek, A.W., "Inelastic seismic response of simple eccentric structures," *Journal of Earthquake Engineering and Structural Dynamics*, Vol. 13, 1985, pp. 255-269.

36. Tso, W.K., and Hongshan, Y., "Additional seismic inelastic deformation caused by structural asymmetry", *Journal of Earthquake Engineering and Structural Dynamics*, Vol. 19, No. 2, 1990, pp. 243-258.

37. Veletsos, A.S., Newmark, N.M., and Chelapati, C.V., "Deformation spectra for elastic and elastoplastic systems subjected to ground shock and earthquake motions," *Proceeding of the 3rd World Conference on Earthquake Engineering*, Vol. II, 1965, pp. 1-17.

38. Veletsos, A.S. and Vann, W.P., "Response of ground-excited elastoplastic systems," *Journal of Structural Division*, ASCE, Vol. 97, No. ST4, Apr. 1971, pp. 1257-1281.

NOTATION

a	location coordinate of resisting elements measured along X-direction
a_{go}	maximum ground acceleration
$a_g(t)$	time-history of ground acceleration due to earthquake ground motion
b	plan dimension of the building along X-direction
c	dimensionless yield factor
d	location coordinate of resisting element measured along Y-direction
e_d	design eccentricity specified in building codes
e_p	strength eccentricity, i.e., the distance from the center of mass to the center of strength
e_{px}, e_{py}	X and Y components of e_p
e_s	stiffness eccentricity, i.e., the distance from the center of mass to the center of stiffness
e_{sx}, e_{sy}	X and Y components of e_s
$\mathbf{F}(t)$	vector of restoring forces
f	lateral vibration frequency of symmetric-plan (or SDF) system (Hz)
K_x, K_y	translational stiffness of structure in X- and Y-directions
K_θ	torsional stiffness of structure defined at the center of mass
$K_{\theta s}$	torsional stiffness of structure defined at the center of stiffness
k_{ix}, k_{jy}	lateral stiffness of i^{th} element in X-direction and j^{th} elements in Y-direction
n_x, n_y	number of resisting elements along X- and Y-directions
m	mass of the deck

O_s	overstrength factor
r	radius of gyration
R	reduction factor = 1/c
S_d, S_v, S_a	spectral values of displacement, pseudo-velocity, and pseudo-acceleration response of a SDF system
S_{an}	pseudo-acceleration response spectrum coordinate corresponding to ω_n (n=1,2), and ξ
T	lateral vibration period of symmetric-plan (or SDF) system
T_n	n^{th} natural vibration period of asymmetric-plan system
T_s	base torque of the asymmetric-plan system at the CS
T_{sn}	base torque of the asymmetric-plan system at the CS due to the n^{th} mode of vibration
t_1	half duration of the half-cycle displacement ground motion
u	lateral displacement at center of mass of the deck
u_{go}	maximum ground displacement
u_i	deformation of the i^{th} element in the asymmetric-plan system
u_{io}	deformation of the i^{th} element in the symmetric-plan system
$u_{\max}$	largest of peak deformations among all resisting elements
$\mathbf{u}_n$	$\mathbf{u}_n{}^T = \langle u_n \; r u_{\theta n} \rangle$
u_n, $u_{\theta n}$	lateral and torsional displacements in the n^{th} mode of vibration
u_o	maximum deformation of the symmetric-plan (SDF) system
u_s	lateral displacement at center of stiffness

u_{sn}	lateral displacement at the CS in the n^{th} mode of vibration
u_θ	torsional displacement of the deck
u_y	yield deformation of the corresponding symmetric-plan (SDF) system
u_{yi}, u_{yj}	yield deformations of i^{th} and j^{th} elements
V	design force $=V_o/R$
V_{ixp}, V_{jyp}	yield force of i^{th} element oriented along the X-direction and j^{th} element oriented along the Y-direction
V_j, V_{jo}	design in the j^{th} resisting element of the asymmetric- and symmetric-plan system, respectively
V_o	base shear of the elastic symmetric-plan (SDF) system
V_s	base shear of the elastic asymmetric-plan system
V_{xp}, V_{yp}	total yield force of the system in X- and Y-directions
v_{go}	maximum ground velocity
x_j, y_i	measured from the CM, they define locations of the j^{th} element oriented along the Y-direction and i^{th} element located along the X-direction
x'_j	$=x_j-e_s$, the distance of the j^{th} element oriented along the Y-direction from the CS
α, β, δ	coefficients used to define the design eccentricity in seismic codes
$\boldsymbol{\alpha}_n$	$\boldsymbol{\alpha}_n{}^T=<\alpha_{yn}\alpha_{\theta n}>$, (n=1,2)
α_{yn}, $\alpha_{\theta n}$	lateral and torsional components of the n^{th} natural coupled mode shape
ω	lateral circular frequency of the symmetric-plan (or uncoupled) system in Y-translation
ω_n	n^{th} circular vibration frequency of the asymmetric-plan system

$\bar{\omega}_n$	$=\omega_n/\omega$
ω_x	lateral circular frequency of the symmetric-plan system in X-translation
ω_θ	torsional circular frequency of the symmetric-plan (or uncoupled) system
Ω_θ	$=\omega_\theta/\omega$, ratio of the uncoupled torsional and translational frequencies
γ_x	relative torsional stiffness parameter, i.e., torsional stiffness of the system arising from the resisting elements oriented along the X-direction divided by the total torsional stiffness of the system
ξ	damping ratio
$\mu_{\max}$	largest of ductility demands among all resisting elements
μ_i	maximum ductility demand on i^{th} resisting element in the asymmetric-plan system
μ_{io}	maximum ductility demand on i^{th} resisting element in the symmetric-plan system
μ_o	maximum ductility demand on the symmetric-plan (SDF) system

APPENDIX A

INDEPENDENCE OF PARAMETERS γ_x AND ω_x/ω

In a system with fixed values of ω, Ω_θ, and e_s/r, the parameters γ_x and ω_x/ω may not be independent under certain restrictions on locations of resisting elements. The condition under which the independence of γ_x and ω_x/ω ceases is identified in this Appendix. Although this condition is identified for an asymmetric-plan system of Figure 4.1b having two resisting elements along each of the two principal directions, similar conditions would also apply to systems with larger number of resisting elements (Figures 4.3b and 4.3c). Since the parameters γ_x and ω_x/ω are related to the stiffnesses and locations of the perpendicular elements, the question about the independence of γ_x and ω_x/ω is valid only for systems with perpendicular elements; the parameters γ_x and ω_x/ω may be ignored for systems without perpendicular elements.

Consider a system in which the resisting elements are located at the edges of the deck. For such a system, the equations governing the parameters ω, Ω_θ, and e_s/r are:

$$\frac{k_{1y}}{m}+\frac{k_{2y}}{m} = \omega^2 \tag{A.1}$$

$$\frac{\dfrac{k_{1y}}{m}\dfrac{a}{r}-\dfrac{k_{2y}}{m}\dfrac{a}{r}}{\dfrac{k_{1y}}{m}+\dfrac{k_{2y}}{m}} = \frac{e_s}{r} \tag{A.2}$$

$$\frac{k_{1y}}{m}\left[\frac{a}{r}-\frac{e_s}{r}\right]^2+\frac{k_{2y}}{m}\left[\frac{a}{r}+\frac{e_s}{r}\right]^2+2\frac{k_x}{m}\left[\frac{d}{r}\right]^2 = \Omega_\theta^2\omega^2 \tag{A.3}$$

Since the resisting elements are located at the edges of the deck

$$\sqrt{\frac{\left[(2a/r)^2+(2d/r)^2\right]}{12}} = 1 \tag{A.4}$$

to satisfy the radius of gyration requirement.

Thus, to determine the variables k_{1y}/m, k_{2y}/m, k_x/m, a/r, and d/r, only one additional restriction is required. This additional restriction may be obtained either by fixing one of the two parameters, γ_x and ω_x/ω, which are related to the other system properties as:

$$2\frac{k_x}{m}\left[\frac{d}{r}\right]^2 = \gamma_x \Omega_\theta^2 \omega^2 \tag{A.5}$$

$$2\frac{k_x}{m} = \left[\frac{\omega_x}{\omega}\right]^2 \omega^2 \tag{A.6}$$

or by fixing the aspect ratio of the deck, which is defined as the ratio of the plan dimensions along the two direction -- perpendicular to and along the direction of ground motion. Clearly, if one of the two parameters, γ_x and ω_x/ω, or the aspect ratio is specified, values of the others will automatically be fixed. This indicates that these parameters and the aspect ratio may not be varied independently in a system with fixed values of ω, Ω_θ, and e_s/r if the resisting elements are located at the edges of the deck.

However, for want of open space on the periphery of the building, the major lateral load resistance in many buildings is provided by resisting elements that are located away from the edges. To characterize such buildings, it is useful to consider a system of Figure 4.1b in which resisting elements are located away from the edges. For such a system, the equality of equation (A.4) becomes the inequality given as:

$$\sqrt{\frac{\left[(2a/r)^2+(2d/r)^2\right]}{12}} < 1 \tag{A.7}$$

Clearly equation (A.7) is no longer useful for the purpose of determining the locations and stiffnesses of resisting elements. Thus, both the equations (A.5) and (A.6) are required, in addition to the equations (A.1) to (A.3), to compute the variables k_{1y}/m, k_{2y}/m, k_x/m, a/r, and d/r. This indicates that both the parameters γ_x and ω_x/ω may be varied independently. However, the variables a/r and d/r must satisfy the restriction of equation (A.7); the limiting values of a/r and d/r is reached when the left hand side in equation (A.7) just becomes

equal to one, i.e., the resisting elements are located at the edges of the deck. For this limiting situation, it has already been demonstrated that only one of the two parameters, γ_x and ω_x/ω, may be varied independently. Thus, both these parameters may be varied independently at the same instant as long as the inequality in equation (A.7) is true, i.e., as long as the resisting elements are confined within the deck plan.

It may be noted that the aspect ratio, unlike γ_x and ω_x/ω, plays no role in determining the locations of resisting elements because they are no longer located at the edges of the deck; consequently, it would not influence the inelastic response and thus is not considered as a system parameter.

APPENDIX B

LOCATIONS AND STIFFNESSES OF RESISTING ELEMENTS

The inelastic response of asymmetric-plan systems depends on locations, stiffnesses, and yield deformations of each of the resisting elements as well as their number in addition to all the parameters -- ω, Ω_θ, e_s/r, and ξ -- characterizing the elastic response. Thus, a large number of parameters would be required to fully characterize the inelastic response of asymmetric-plan systems. However, only a few parameters -- ω, Ω_θ, e_s/r, γ_x, ω_x/ω, e_p, O_s, and c (or u_y) -- have been used in this investigation to define the locations, stiffnesses, and yield deformations of all the resisting elements in the asymmetric-plan systems of Figures 4.1 to 4.3. Clearly, these parameters are not sufficient to uniquely determine the locations, stiffnesses, and yield deformations of all the resisting elements in these systems. This Appendix describes how the locations and stiffnesses of resisting elements in systems of Figure 4.1 to 4.3 are related to the parameters ω, Ω_θ, e_s/r, γ_x, and ω_x/ω; and what additional restrictions are needed to define the locations and stiffnesses of resisting elements. How the yield deformations of resisting elements are related to the parameters e_p, O_s, and u_y is described in Appendix C.

The systems considered in this investigation are symmetric about the X-axis. Thus, the two resisting elements oriented along the X-axis in Figures 4.1b, 4.2a, 4.2b, 4.2c, 4.3a, and 4.3b are located symmetrically along the X-direction at a distance d from the CM and possess equal values of linear elastic stiffnesses.

The equations governing the uncoupled vibration frequency along the Y-direction, ω, the normalized eccentricity, e_s/r, the uncoupled torsional to lateral frequency ratio, Ω_θ, the torsional stiffness parameter, γ_x, and the lateral vibration frequency ratio, ω_x/ω, are:

$$\sum_j \frac{k_{jy}}{m} = \omega^2 \tag{B.1}$$

$$\frac{\sum_j \frac{k_{jy}}{m}\frac{x_j}{r}}{\sum_j \frac{k_{jy}}{m}} = \frac{e_s}{r} \tag{B.2}$$

$$\sum_j \frac{k_{jy}}{m}\left[\frac{x_j}{r} - \frac{e_s}{r}\right]^2 + \sum_i \frac{k_{ix}}{m}\left[\frac{d}{r}\right]^2 = \Omega_\theta^2 \omega^2 \tag{B.3}$$

$$\sum_i \frac{k_{ix}}{m}\left[\frac{d}{r}\right]^2 = \gamma_x \Omega_\theta^2 \omega^2 \tag{B.4}$$

$$\sum_i \frac{k_{ix}}{m} = \left[\frac{\omega_x}{\omega}\right]^2 \omega^2 \tag{B.5}$$

In the following sections, it is shown how the locations and stiffness of the resisting elements in the systems of Figures 4.1 to 4.3 are determined from these equations.

B.1 Systems with Two Resisting Elements Along Y-Direction

In the system with two resisting elements along each of the two principal directions (Figures 4.1b, 4.2a, 4.3a, and 4.3b), the variables to be determined are: the stiffnesses, k_{1y}/m and k_{2y}/m, and the locations, x_1/r and x_2/r, of the resisting elements along the direction of ground motion; and the stiffness k_x/m and location d/r of the resisting elements along the X-direction. Clearly, the five equations (equations (B.1) to (B.5)) are not sufficient to uniquely determine these six variables -- k_{1y}/m, k_{2y}/m, x_1/r, x_2/r, k_x/m, and d/r. Thus, it is necessary to specify additional restrictions on the system. The two possible types of restriction are: (1) $|x_1/r| = |x_2/r| = a/r$, and (2) $k_{1y}/m = k_{2y}/m = k_y/m$; it will be shown in the following sections that the first type of restriction is equivalent to specifying that the system is stiffness-eccentric, whereas the second type is equivalent to specifying that the system is mass-eccentric.

B.1.1 Stiffness-Eccentric System

As mentioned previously, one of the two types of restrictions is $|x_1/r| = |x_2/r| = a/r$, i.e., the two resisting elements along the direction of ground motion are located

symmetrically about the CM. For systems with this type of restriction, values of the five variables -- k_{1y}/m, k_{2y}/m, a/r, k_x/m, and d/r --, determined from equations (B.1) to (B.5), are given as:

$$\frac{d}{r} = \sqrt{\gamma_x}\,\Omega_\theta/(\omega_x/\omega) \tag{B.6}$$

$$\frac{a}{r} = \sqrt{(1-\gamma_x)\Omega_\theta^2+(e_s/r)^2} \tag{B.7}$$

$$\frac{k_{1y}}{m} = \frac{\omega^2}{2}\,\frac{\frac{a}{r}+\frac{e_s}{r}}{\frac{a}{r}} \tag{B.8}$$

$$\frac{k_{2y}}{m} = \frac{\omega^2}{2}\,\frac{\frac{a}{r}-\frac{e_s}{r}}{\frac{a}{r}} \tag{B.9}$$

$$\frac{k_x}{m} = \frac{1}{2}\left[\frac{\omega_x}{\omega}\right]^2\omega^2 \tag{B.10}$$

The equations (B.8) and (B.9) indicate that $k_{1y}/m > k_{2y}/m$, i.e., element 1 has higher stiffness than element 2. Thus the restriction $|x_1/r| = |x_2/r| = a/r$ is equivalent to specifying that the system is stiffness-eccentric.

The locations and stiffnesses of all the resisting elements of the system of Figures 4.1b, 4.2a, and 4.3a are given by equations (B.6) to (B.10). Since a system with perpendicular elements degenerates into a system without perpendicular elements for $\gamma_x=0$, locations and stiffnesses of resisting elements in the system of Figure 4.1a may also be computed from these equations.

B.1.2 Mass-Eccentric System

Another type of restriction that may be imposed on the system is $k_{1y}/m = k_{2y}/m = k_y/m$, i.e., the two resisting elements along the direction of ground motion possess identical stiffness. Under this restriction, values of the variables k_y/m, x_1/r, x_2/r, k_x/m, and d/r,

determined from equations (B.1) to (B.5), are given as:

$$\frac{d}{r} = \sqrt{\gamma_x}\,\Omega_\theta/(\omega_x/\omega) \tag{B.11}$$

$$\frac{x_1}{r} = \sqrt{(1-\gamma_x)}\,\Omega_\theta + \frac{e_s}{r} \tag{B.12}$$

$$\frac{x_2}{r} = \sqrt{(1-\gamma_x)}\,\Omega_\theta - \frac{e_s}{r} \tag{B.13}$$

$$\frac{k_y}{m} = \frac{\omega^2}{2} \tag{B.14}$$

$$\frac{k_x}{m} = \frac{1}{2}\left[\frac{\omega_x}{\omega}\right]^2 \omega^2 \tag{B.15}$$

Equations (B.12) and (B.13) indicate that the resisting elements 1 and 2 are located symmetrically about the CS. Furthermore, the stiffness of the two elements are identical (equation (B.14)). Thus, the restriction $k_{1y}/m = k_{2y}/m = k_y/m$ is equivalent to specifying that the system is mass-eccentric.

B.2 System with Three Resisting Elements Along Y-Direction

In the system of Figure 4.2b, the variables to be determined are: k_{1y}/m, k_{2y}/m, k_{3y}/m, k_x/m, x_1/r, x_2/r, x_3/r, and d/r. Thus it is necessary to specify three additional restriction if these variables are to be determined from equations (B.1) to (B.5). The three restriction imposed in this investigation on the system of Figure 4.2b are: (1) $|x_1/r| = |x_3/r| = a/r$ i.e., elements 1 and 3 are located symmetrically about the CM; (2) $x_2/r = 0$, i.e., element 2 is located at the CM; and (3) $k_{2y}/m = k_{3y}/m$, i.e., elements 2 and 3 have identical stiffness. Under these restrictions, the locations and stiffnesses of all the resisting elements, determined from equations (B.1) to (B.5), are given as:

$$\frac{d}{r} = \sqrt{\gamma_x}\,\Omega_\theta/(\omega_x/\omega) \tag{B.16}$$

$$\frac{a}{r} = \frac{1}{4}\left[-\frac{e_s}{r}+\sqrt{24(1-\gamma_x)\Omega_\theta^2+25(e_s/r)^2}\right] \tag{B.17}$$

$$\frac{k_{1y}}{m} = \frac{\omega^2}{3}\,\frac{\frac{a}{r}+2\frac{e_s}{r}}{\frac{a}{r}} \tag{B.18}$$

$$\frac{k_{2y}}{m} = \frac{k_{3y}}{m} = \frac{\omega^2}{3}\,\frac{\frac{a}{r}-\frac{e_s}{r}}{\frac{a}{r}} \tag{B.19}$$

$$\frac{k_x}{m} = \frac{1}{2}\left[\frac{\omega_x}{\omega}\right]^2\omega^2 \tag{B.20}$$

B.3 System with Four Resisting Elements Along Y-Direction

In the system of Figure 4.2c, the variables to be determined are: k_{1y}/m, k_{2y}/m, k_{3y}/m, k_{4y}/m, k_x/m, x_1/r, x_2/r, x_3/r, x_4/r, and d/r. Thus, it is necessary to specify five additional restriction if these variables are to be determined from equations (B.1) to (B.5). The five restriction imposed in this investigation on the system of Figure 4.2c are: (1) $|x_1/r| = |x_4/r| = a_1/r$, i.e., elements 1 and 4 are located symmetrically about the CM; (2) $|x_2/r| = |x_3/r| = a_2/r$, i.e., elements 2 and 3 are located symmetrically about the CM; (3) $a_1/r = 3a_2/r = (3/2)a/r$, i.e., elements are located at a spacing of a/r; (4) $k_{1y}/m = k_{2y}/m$, i.e., elements 1 and 2 have identical stiffness; and (5) $k_{3y}/m = k_{4y}/m$, i.e., elements 3 and 4 have identical stiffness. Under these restrictions, the locations and stiffnesses of all the resisting elements, determined from equations (B.1) to (B.5), are given as:

$$\frac{d}{r} = \sqrt{\gamma_x}\,\Omega_\theta/(\omega_x/\omega) \tag{B.21}$$

$$\frac{a}{r} = \sqrt{\frac{4}{5}(1-\gamma_x)\Omega_\theta^2+(e_s/r)^2} \tag{B.22}$$

$$\frac{k_{1y}}{m} = \frac{k_{2y}}{m} = \frac{\omega^2}{4} \frac{\frac{a}{r} + \frac{e_s}{r}}{\frac{a}{r}} \tag{B.23}$$

$$\frac{k_{3y}}{m} = \frac{k_{4y}}{m} = \frac{\omega^2}{4} \frac{\frac{a}{r} - \frac{e_s}{r}}{\frac{a}{r}} \tag{B.24}$$

$$\frac{k_x}{m} = \frac{1}{2} \left[\frac{\omega_x}{\omega} \right]^2 \omega^2 \tag{B.25}$$

APPENDIX C

YIELD DEFORMATIONS OF RESISTING ELEMENTS

The inelastic response of asymmetric-plan system with a particular number, location, and orientation of resisting elements depends on the yield deformation of each resisting element in addition to the parameters ω, Ω_θ, e_s/r, and ξ influencing the elastic response. In most of the earlier investigations, the yield deformations of all the resisting elements have been assumed to be identical and equal to the yield deformation u_y of the corresponding symmetric-plan system. As shown in Chapter 2, this assumption implies that the strength eccentricity of the system equals its stiffness eccentricity, i.e., $e_p=e_s$. However, the yield deformations of resisting elements in code-designed buildings are generally not equal to u_y, but are such that the combined strength of all resisting elements is greater than that of the corresponding symmetric-plan system and the strength eccentricity is significantly smaller than the stiffness eccentricity. Therefore, the system is characterized by the overstrength factor O_s and the strength eccentricity e_p, in addition to u_y. The yield deformations of the various resisting elements are then determined in terms of O_s and e_p.

The equations governing the total strength along Y-direction and the strength eccentricity along X-direction are:

$$\sum_j V_{jyp} = O_s V_{yp} = O_s K_y u_y \tag{C.1}$$

$$e_{px} = e_p = \frac{1}{O_s V_{yp}} \sum_j x_j V_{jyp} \tag{C.2}$$

Yield forces, V_{jyp}, of resisting elements can be obtained in terms of the other known quantities by solving equations (C.1) and (C.2). However, if the system has more than two resisting elements, the yield forces of all the elements can not be determined uniquely from these equations. One additional equation is therefore needed for each element. For this purpose, the following equation is introduced:

$$V_{jyp} - k_{jy}u_y = \frac{K_y u_y e_s}{K_{\theta s}} x_j k_{jy} \tag{C.3}$$

in which $k_{jy}u_y$ is the yield force of the same element if the system had symmetric plan. Equation (C.3) gives the additional forces on the elements arising from torsion, determined by applying the yield force $K_y u_y$ of the corresponding symmetric-plan system at a distance e_s from the CS, and distributing the resulting torque to the elements in proportional to their torsional stiffnesses. This is consistent with the procedures in many seismic codes to compute the additional forces in the resisting elements arising from torsion of the system.

This investigation is restricted to asymmetric-plan systems which are symmetric in stiffness and strength about the X-axis. Thus, the two resisting elements oriented perpendicular to the direction of ground motion in Figures 4.1b, 4.2a, 4.2b, 4.2c, 4.3a, and 4.3b are located symmetrically along the X-direction at a distance d from the CM, and their stiffnesses are the same and equal to $k_x/2$. Furthermore, the yield deformations of these elements are chosen to be identical, and for simplicity are selected as u_y.

C.1 System With Two Resisting Elements Along Y-Direction

C.1.1 Stiffness-Eccentric System

The two resisting elements along the Y-direction (denoted as element 1 and 2 in Figures 4.1b, 4.2a, and 4.3a) are located symmetrically at a distance a from the CM. The elastic stiffnesses of these elements are given by (Appendix B):

$$k_{1y} = \frac{K_y}{2}\left[\frac{a+e_s}{a}\right] \quad \text{and} \quad k_{2y} = \frac{K_y}{2}\left[\frac{a-e_s}{a}\right] \tag{C.4}$$

If u_{y1} and u_{y2} are the yield deformations of elements 1 and 2, respectively, the yield forces of these elements are

$$V_{1yp} = u_{y1}k_{1y} = u_{y1}\frac{K_y}{2}\left[\frac{a+e_s}{a}\right] \quad \text{and} \quad V_{2yp} = u_{y2}k_{2y} = u_{y2}\frac{K_y}{2}\left[\frac{a-e_s}{a}\right] \tag{C.5}$$

Substituting equation (C.5) into equations (C.1) and (C.2) and solving for the yield

deformations of resisting elements 1 and 2 gives:

$$\frac{u_{y1}}{u_y} = O_s\left[\frac{a+e_p}{a+e_s}\right] \quad \text{and} \quad \frac{u_{y2}}{u_y} = O_s\left[\frac{a-e_p}{a-e_s}\right] \tag{C.6}$$

C.1.2 Mass-Eccentric System

In the mass-eccentric system of Figure 4.3b, elements 1 and 2 are located symmetrically at a distance a from the CS. The elastic stiffnesses of these elements are identical and are given as (Appendix B):

$$k_{1y} = k_{2y} = \frac{K_y}{2} \tag{C.7}$$

The yield force of these elements in this case are

$$V_{1yp} = u_{y1}k_{1y} = u_{y1}\frac{K_y}{2} \quad \text{and} \quad V_{2yp} = u_{y2}k_{2y} = u_{y2}\frac{K_y}{2} \tag{C.8}$$

Substituting equation (C.8) in equations (C.1) and (C.2) and solving for yield displacements of elements 1 and 2 gives:

$$\frac{u_{y1}}{u_y} = O_s\left[\frac{a+e_p-e_s}{a}\right] \quad \text{and} \quad \frac{u_{y2}}{u_y} = O_s\left[\frac{a-e_p+e_s}{a}\right] \tag{C.9}$$

C.2 System With Three Resisting Elements Along Y-direction

In the system of Figure 4.2b, resisting elements 1 and 3 are located symmetrically at a distance a from the CM and the element 2 is located at the location of the CM. The elastic stiffnesses of these elements are given as (Appendix B):

$$k_{1y} = \frac{K_y}{3}\left[\frac{a+2e_s}{a}\right] \quad \text{and} \quad k_{2y} = k_{3y} = \frac{K_y}{3}\left[\frac{a-e_s}{a}\right] \tag{C.10}$$

If u_{y1}, u_{y2}, and u_{y3} are the yield deformations of elements 1, 2 , and 3, respectively, the yield forces in these elements become:

$$V_{1yp} = u_{y1}\frac{K_y}{3}\left[\frac{a+2e_s}{a}\right], \quad V_{2yp} = u_{y2}\frac{K_y}{3}\left[\frac{a-e_s}{a}\right], \quad \text{and} \quad V_{3yp} = u_{y3}\frac{K_y}{3}\left[\frac{a-e_s}{a}\right] \tag{C.11}$$

Utilizing additional assumption of equation (C.3) for elements 2 and 3 gives

$$\frac{V_{2yp} - k_{2y}u_y}{V_{3yp} - k_{3y}u_y} = \frac{e_s}{e_s+a} \tag{C.12}$$

Replacing equation (C.11) in equations (C.1) and (C.2) and then solving these equations, along with equation (C.12), for yield deformations of elements 1, 2, and 3 gives:

$$\frac{u_{y1}}{u_y} = 3\left[\frac{a}{a+2e_s}\right]\left[O_s\frac{e_p}{a} + \left[\frac{a+e_s}{2a+3e_s}\right]\left\{O_s\left[\frac{a-e_p}{a}\right] - \frac{1}{3}\left[\frac{a-e_s}{a+e_s}\right]\right\}\right] \tag{C.13a}$$

$$\frac{u_{y2}}{u_y} = 3\left[\frac{a}{a-e_s}\right]\left[\left[\frac{a+e_s}{2a+3e_s}\right]\left\{O_s\left[\frac{a-e_p}{a}\right] - \frac{1}{3}\left[\frac{a-e_s}{a+e_s}\right]\right\}\left[\frac{e_s}{a+e_s}\right] + \frac{1}{3}\left[\frac{a}{a+e_s}\right]\right] \tag{C.13b}$$

$$u_{y3} = 3\left[\frac{a}{a-e_s}\right]\left[\frac{a+e_s}{2a+3e_s}\right]\left[O_s\left[\frac{a-e_p}{a}\right] - \frac{1}{3}\left[\frac{a-e_s}{a+e_s}\right]\right] \tag{C.13c}$$

C.3 System With Four Resisting Elements Along Y-Direction

In the system of Figure 4.2c, resisting elements 1 and 4 are located symmetrically at a distance $3a/2$ from the CM and elements 2 and 3 are located symmetrically at a distance of $a/2$ from the CM. The elastic stiffnesses of these elements are given as (Appendix B):

$$k_{1y} = k_{2y} = \frac{K_y}{4}\left[\frac{a+e_s}{a}\right] \quad \text{and} \quad k_{3y} = k_{4y} = \frac{K_y}{4}\left[\frac{a-e_s}{a}\right] \tag{C.14}$$

If u_{y1}, u_{y2}, u_{y3}, and u_{y4} are yield deformations of elements 1, 2 , 3, and 4, respectively, the yield forces in these elements become:

$$V_{1yp} = u_{y1}\frac{K_y}{4}\left[\frac{a+e_s}{a}\right], \quad V_{2yp} = u_{y2}\frac{K_y}{4}\left[\frac{a+e_s}{a}\right], \quad V_{3yp} = u_{y3}\frac{K_y}{4}\left[\frac{a-e_s}{a}\right], \quad \text{and}$$

$$V_{4yp} = u_{y4}\frac{K_y}{4}\left[\frac{a-e_s}{a}\right] \tag{C.15}$$

Utilizing additional assumption of equation (C.3) for elements 1 and 2 gives

$$\frac{V_{1yp} - k_{1y}u_y}{V_{2yp} - k_{2y}u_y} = \frac{3a/2-e_s}{a/2-e_s} \tag{C.16}$$

and for elements 3 and 4 gives

$$\frac{V_{4yp} - k_{4y}u_y}{V_{3yp} - k_{3y}u_y} = \frac{3a/2+e_s}{a/2+e_s} \tag{C.17}$$

Replacing equation (C.15) in equations (C.1) and (C.2) and then solving these equations, along with equations (C.16) and (C.17), for yield deformations of elements 1, 2, 3 and 4 gives:

$$\frac{u_{y1}}{u_y} = 4\left[\frac{a}{a+e_s}\right]\left[\frac{b_1a_{22}-b_2a_{12}}{a_{11}a_{22}-a_{21}a_{12}}\right] \tag{C.18a}$$

$$\frac{u_{y2}}{u_y} = 4\left[\frac{a}{a+e_s}\right]\left[\left[\frac{a/2-e_s}{3a/2-e_s}\right]\left[\frac{b_1a_{22}-b_2a_{12}}{a_{11}a_{22}-a_{21}a_{12}}\right]+\frac{1}{4}\left[\frac{a+e_s}{3a/2-e_s}\right]\right] \tag{C.18b}$$

$$\frac{u_{y3}}{u_y} = 4\left[\frac{a}{a-e_s}\right]\left[\left[\frac{a/2+e_s}{3a/2+e_s}\right]\left[\frac{b_2a_{11}-b_1a_{21}}{a_{11}a_{22}-a_{21}a_{12}}\right]+\frac{1}{4}\left[\frac{a-e_s}{3a/2+e_s}\right]\right] \tag{C.18c}$$

$$\frac{u_{y4}}{u_y} = 4\left[\frac{a}{a-e_s}\right]\left[\frac{b_2a_{11}-b_1a_{21}}{a_{11}a_{22}-a_{21}a_{12}}\right] \tag{C.18d}$$

where $a_{11} = 2\left[\frac{a-e_s}{3a/2-e_s}\right]$, $a_{12} = 2\left[\frac{a+e_s}{3a/2+e_s}\right]$, $a_{21} = \left[\frac{7a-6e_s}{3a/2-e_s}\right]$, $a_{22} = -2$,

$b_1 = O_s - \frac{1}{4}\left[\frac{a+e_s}{3a/2-e_s}\right] + \frac{1}{4}\left[\frac{a-e_s}{3a/2+e_s}\right]$, and $b_2 = O_s\left[\frac{a+2e_p}{a}\right] - \frac{1}{2}\left[\frac{a+e_s}{3a/2-e_s}\right]$

APPENDIX D

LIMITING VALUES OF RESPONSE QUANTITIES FOR ELASTIC SYSTEMS

The frequencies and mode shapes of a one-story, linearly elastic system of Figure 5.1 are given as [11]:

$$\bar{\omega}_n = \frac{\omega_n}{\omega} = \left[\frac{1+(e_s/r)^2+\Omega_\theta^2}{2} \pm \sqrt{\left[\frac{1+(e_s/r)^2-\Omega_\theta^2}{2} \right]^2 + (e_s/r)^2\Omega_\theta^2} \right]^{1/2} \tag{D.1}$$

$$\boldsymbol{\alpha}_n = \begin{Bmatrix} \alpha_{yn} \\ \alpha_{\theta n} \end{Bmatrix} = \frac{1}{\sqrt{(e_s/r)^2+(1-\bar{\omega}_n^2)^2}} \begin{Bmatrix} -e_s/r \\ 1-\bar{\omega}_n^2 \end{Bmatrix} \tag{D.2}$$

where

$$\boldsymbol{\alpha}_n^T \boldsymbol{\alpha}_n = \alpha_{yn}^2+\alpha_{\theta n}^2 = 1 \tag{D.3}$$

Since the two modes are orthogonal to each other, it can be shown that $\alpha_{y1}=\alpha_{\theta 2}$ and $\alpha_{y2}=-\alpha_{\theta 1}$. The various symbols appearing in the above equations have been defined earlier.

In the n^{th} mode of vibration, the lateral and torsional deformations at the CM are then given by:

$$\mathbf{u}_n = \begin{Bmatrix} u_n \\ ru_{\theta n} \end{Bmatrix} = \frac{\alpha_{yn}}{\omega_n^2} \begin{Bmatrix} \alpha_{yn} \\ \alpha_{\theta n} \end{Bmatrix} S_{an} \tag{D.4}$$

the lateral deformation at the CS by:

$$u_{sn} = u_n+(e_s/r)(ru_{\theta n}) = \frac{\alpha_{yn}^2}{\omega^2} S_{an} \tag{D.5}$$

and the base torque at the CS by:

$$T_{sn} = rm\alpha_{yn}[\alpha_{\theta n}-(e_s/r)\alpha_{yn}]S_{an} \tag{D.6}$$

where S_{an} is the pseudo-acceleration ordinate associated with the vibration frequency ω_n.

Furthermore, the dynamic eccentricity in the n^{th} mode may be defined as:

$$e_{dn} = \frac{T_{sn}}{K_y u_o} = \frac{T_{sn}}{mS_a} \tag{D.7}$$

in which S_a is the pseudo-acceleration associated with the frequency ω of the corresponding uncoupled system. Note that for linearly elastic systems, dynamic eccentricity based on matching the torque becomes equal to that based on matching the deformation.

D.1 For Extreme Values of System Periods

When the vibration periods T_1 and T_2 become extremely short, the pseudo-acceleration spectrum ordinates for the two modes become identical and equal to the peak ground acceleration, i.e., $S_{a1}=S_{a2}=a_{go}$. Therefore, the lateral deformations at the CS in the two modes are given as:

$$u_{s1} = \frac{\alpha_{y1}^2}{\omega^2} a_{go} \quad \text{and} \quad u_{s2} = \frac{\alpha_{y2}^2}{\omega^2} a_{go} \tag{D.8}$$

Moreover, the peak values of the modal responses occur simultaneously at the same time as the peak value of the ground acceleration and the total deformation is given by the algebraic sum of the modal responses:

$$u_s = u_{s1}+u_{s2} = (\alpha_{y1}^2+\alpha_{y2}^2)\frac{a_{go}}{\omega^2} \tag{D.9}$$

Since $\alpha_{y2}=-\alpha_{\theta 1}$, equation (D.7) can be rewritten as:

$$u_s = (\alpha_{y1}^2+\alpha_{\theta 1}^2)\frac{a_{go}}{\omega^2} = \frac{a_{go}}{\omega^2} = u_o \tag{D.10}$$

in which equation (D.3) has been utilized.

Equation (D.10) indicates that the lateral deformation, u_s, at the CS of asymmetric-plan systems with very-short periods becomes independent of the parameters Ω_θ and e_s/r, approaches the lateral deformation u_o of the corresponding uncoupled system, and tends to zero in the limit as $T\rightarrow 0$ (or $\omega\rightarrow\infty$).

Furthermore, the base torque at the CS in the two modes are given as:

$$T_{s1} = rm[\alpha_{y1}\alpha_{\theta 1} - (e_s/r)\alpha_{y1}^2]a_{go} \quad \text{and} \quad T_{s2} = rm[\alpha_{y2}\alpha_{\theta 2} - (e_s/r)\alpha_{y2}^2]a_{go} \tag{D.11}$$

and the total torque as:

$$T_s = T_{s1} + T_{s2} = rm[\alpha_{y1}\alpha_{\theta 1} + \alpha_{y2}\alpha_{\theta 2} - (e_s/r)(\alpha_{y1}^2 + \alpha_{y2}^2)]a_{go} \tag{D.12}$$

Since $(\alpha_{y1}^2 + \alpha_{y2}^2) = 1$ and $\alpha_{y2}\alpha_{\theta 2} = -\alpha_{y1}\alpha_{\theta 1}$, equation (D.12) can be rewritten as

$$T_s = -ma_{go}e_s \tag{D.13}$$

Because $ma_{go} = V_o$ is the base shear of the corresponding uncoupled system, equation (D.13) implies that the dynamic torque in very-short period systems approaches static torque obtained by applying the base shear V_o at a distance e_s away from the CS.

Because the dynamic base torque is equal to the static torque, the total torsional deformation is obtained by

$$ru_\theta = \frac{rT_s}{K_{\theta s}} = \frac{-rma_{go}e_s}{r^2 m\omega_\theta^2} = -a_{go}\frac{e_s/r}{\omega_\theta^2} \tag{D.14}$$

Equation (D.14) indicates that the torsional deformation, which approaches the static value, in very-short period systems is proportional to $(e_s/r)/\omega_\theta^2$.

The dynamic eccentricity is given as:

$$e_d = e_{d1} + e_{d2} = \frac{(T_{s1} + T_{s1})}{ma_{go}} = \frac{T_s}{ma_{go}} = -e_s \tag{D.15}$$

Thus, absolute value of the dynamic eccentricity of very-short period systems approaches the static eccentricity.

When the vibration periods T_1 and T_2 of the system are very long, deformation spectrum ordinates for the two modes become equal to the peak ground displacement, i.e., $S_{d1} = S_{d2} = u_{go}$. Therefore, the peak modal displacements at the CM are given as:

$$u_1 = \frac{\alpha_{y1}^2}{\omega_1^2}\omega_1^2 u_{go} = \alpha_{y1}^2 u_{go} \quad \text{and} \quad u_2 = \frac{\alpha_{y2}^2}{\omega_2^2}\omega_2^2 u_{go} = \alpha_{y2}^2 u_{go} \tag{D.16}$$

Moreover, the peak values of the modal displacements occur simultaneously at the same time as the peak value of the ground displacement and the total deformation at the CM is given as the absolute sum of the modal responses:

$$u = u_1 + u_2 = (\alpha_{y1}^2 + \alpha_{y2}^2)u_{go} = u_{go} \tag{D.17}$$

Equation (D.17) implies that in the displacement-sensitive region, the lateral displacement, u, at the CM of asymmetric-plan systems is not affected by plan-asymmetry. Since the torsional component of the response becomes very small in the limit as T approaches infinity, as shown next, the lateral deformation at the CS becomes equal to that at the CM.

The peak torsional deformations in the two modes are given as:

$$ru_{\theta 1} = \alpha_{y1}\alpha_{\theta 1} u_{go} \quad \text{and} \quad ru_{\theta 2} = \alpha_{y2}\alpha_{\theta 2} u_{go} \tag{D.18}$$

and the total deformation as

$$ru_\theta = ru_{\theta 1} + ru_{\theta 2} = (\alpha_{y1}\alpha_{\theta 1} + \alpha_{y2}\alpha_{\theta 2})u_{go} = 0 \tag{D.19}$$

in which the relationship $\alpha_{y2}\alpha_{\theta 2} = -\alpha_{y1}\alpha_{\theta 1}$ has been utilized. Equation (D.19) implies that the torsional deformation approaches zero as system periods become very long. Thus, the dynamic eccentricity would also approach zero in the limit as $T \to \infty$.

D.2 For Extreme Values of Frequency Ratio

When the frequency ratio is very large, i.e., $\Omega_\theta \to \infty$, equations (D.1) and (D.2) lead to

$$\bar{\omega}_1 = 1 \quad \text{and} \quad \bar{\omega}_2 = \Omega_\theta \tag{D.20}$$

$$\boldsymbol{\alpha}_1 = \begin{Bmatrix} 1 \\ 0 \end{Bmatrix} \quad \text{and} \quad \boldsymbol{\alpha}_2 = \begin{Bmatrix} 0 \\ 1 \end{Bmatrix} \tag{D.21}$$

Equations (D.21) and (D.4) indicate that the second mode is not excited by the lateral

ground motion along the Y-direction. Furthermore, pseudo-acceleration ordinate corresponding to the vibration frequency ω_1 becomes equal to that for the corresponding uncoupled system, i.e, $S_{a1}=S_a$.

Thus the total response of the system is equal to the response in the first mode. The lateral deformation at the CS is then given as:

$$u_s = \frac{\alpha_{y1}^2}{\omega^2} S_{a1} = \frac{S_a}{\omega^2} = u_o \tag{D.22}$$

Equation (D.22) indicates that the lateral deformation of the asymmetric-plan system becomes equal to that of the corresponding uncoupled system, i.e., $u_s/u_o = 1$, as Ω_θ becomes very large.

The dynamic eccentricity for the system is also given as:

$$e_d = e_{d1} = \frac{rm\alpha_{y1}[\alpha_{\theta 1}-(e_s/r)\alpha_{y1}]S_a}{mS_a} \tag{D.23}$$

Substituting the values of α_{y1} and $\alpha_{\theta 1}$ from equation (D.21), equation (D.23) leads to

$$e_d = -e_s \tag{D.24}$$

Thus the absolute value of the dynamic eccentricity becomes equal to the absolute value of the static stiffness eccentricity as Ω_θ becomes very large.

When the frequency ratio Ω_θ becomes very small, i.e., $\Omega_\theta \rightarrow 0$, the mode shapes and frequencies of the system are given as:

$$\bar{\omega}_1 = 0 \quad \text{and} \quad \bar{\omega}_2 = \sqrt{1+(e_s/r)^2} \tag{D.25}$$

$$\boldsymbol{\alpha}_1 = \frac{1}{\sqrt{1+(e_s/r)^2}} \begin{Bmatrix} -e_s/r \\ 1 \end{Bmatrix} \quad \text{and} \quad \boldsymbol{\alpha}_2 = \frac{1}{\sqrt{1+(e_s/r)^2}} \begin{Bmatrix} -1 \\ -e_s/r \end{Bmatrix} \tag{D.26}$$

The lateral deformations at the CS due to the two vibration modes are given as:

$$u_{s1} = \frac{\alpha_{y1}^2}{\omega^2} S_{a1} = \frac{(e_s/r)^2}{1+(e_s/r)^2} \frac{S_{a1}}{\omega^2} \quad \text{and} \quad u_{s2} = \frac{1}{1+(e_s/r)^2} \frac{S_{a2}}{\omega^2} \tag{D.27}$$

Equation (D.27) suggests that the contribution, u_{s1}, of the first mode to the total response would be small for small values of the stiffness eccentricity. Thus, the total response, u_s, becomes approximately equal to the response in the second mode, i.e,

$$u_s \approx u_{s2} = \frac{1}{1+(e_s/r)^2} \frac{S_{a2}}{\omega^2} \tag{D.28}$$

Because ω_2 is not much different than ω (equation (D.25)), the pseudo-acceleration ordinate S_{a2} may be assumed to be approximately equal to S_a. Thus,

$$u_s \approx \frac{1}{1+(e_s/r)^2} \frac{S_a}{\omega^2} = \frac{1}{1+(e_s/r)^2} u_o \tag{D.29}$$

Equation (D.29) implies that the ratio u_s/u_o approaches $1/[1+(e_s/r)^2]$ as Ω_θ becomes very small. If the stiffness eccentricity of the system is also small, equation (D.29) indicates that u_s/u_o becomes one, i.e., u_s approaches u_o. Note that the approximation given by equation (D.29) deteriorates as the stiffness eccentricity increases.

The modal dynamic eccentricities for this case can be written as:

$$e_{d1} = -e_s \frac{S_{a1}}{S_a} \quad \text{and} \quad e_{d2} = 0 \tag{D.30}$$

in which values of α_1 and α_2 from equation (D.26) have been utilized. Equation (D.30) implies that the total dynamic eccentricity becomes equal to the dynamic eccentricity in the first mode. Since the pseudo-acceleration, S_{a1}, corresponding to the vibration frequency $\omega_1 \approx 0$ may be written as $\omega_1^2 u_{go} \approx 0$, the dynamic eccentricity approaches zero as Ω_θ becomes very small.

APPENDIX E

STRENGTH ECCENTRICITY OF CODE-DESIGNED SYMMETRIC-PLAN SYSTEM

The design force in the j^{th} resisting element of a code-designed symmetric-plan system, in which effects of accidental torsion are included, is given as:

$$V_{jo} = \frac{k_{jy}}{K_y} V + \frac{\beta b V}{K_{\theta s}} k_{jy} \mid x'_j \mid \tag{E.1}$$

in which the absolute value of x'_j has been used to emphasize that the accidental eccentricity always leads to an increased force in all resisting elements.

The strength eccentricity, e_p, defined earlier, for the symmetric-plan system is then given as:

$$e_p = \frac{\sum_j V_{jo} x'_j}{\sum_j V_{jo}} = \frac{1}{\sum_j V_{jo}} \left[V \sum_j \frac{k_{jy} x'_j}{K_y} + \frac{\beta b V}{K_{\theta s}} \sum_j k_{jy} x'_j \mid x'_j \mid \right] \tag{E.2}$$

Because stiffness eccentricity of the symmetric-plan system is zero, i.e.,

$$e_s = \frac{k_{jy} x'_j}{K_y} = 0 \tag{E.3}$$

and $x'_j = x_j$ when $e_s = 0$, equation (E.2) may be re-written as:

$$e_p = \frac{1}{\sum_j V_{jo}} \frac{\beta b V}{K_{\theta s}} \left[\sum_j k_{jy} x_j \mid x_j \mid \right] \tag{E.4}$$

in which equation (E.3) has been utilized.

It is apparent from equation (E.4) that the strength eccentricity of code-designed symmetric-plan system would be zero only when the term in square brackets of equation (E.4) vanishes. Such would be the case, for example, if the resisting elements in system plan appear in pairs, each pair having equal stiffness and located symmetrically about the CS. In general, the strength eccentricity $e_p \neq 0$ for a system designed to include the effects of accidental eccentricity although its stiffness eccentricity $e_s = 0$. In particular, $e_p \neq 0$ for the symmetric-

plan system corresponding to the asymmetric-plan ($e_s \neq 0$) system of Figure 5.1 because the element stiffnesses, which are the same in the two systems, would not be identical.

EARTHQUAKE ENGINEERING RESEARCH CENTER REPORT SERIES

EERC reports are available from the National Information Service for Earthquake Engineering(NISEE) and from the National Technical Information Service(NTIS). Numbers in parentheses are Accession Numbers assigned by the National Technical Information Service; these are followed by a price code. Contact NTIS, 5285 Port Royal Road, Springfield Virginia, 22161 for more information. Reports without Accession Numbers were not available from NTIS at the time of printing. For a current complete list of EERC reports (from EERC 67-1) and availablity information, please contact University of California, EERC, NISEE, 1301 South 46th Street, Richmond, California 94804.

UCB/EERC-81/01 "Control of Seismic Response of Piping Systems and Other Structures by Base Isolation," by Kelly, J.M., January 1981, (PB81 200 735)A05.

UCB/EERC-81/02 "OPTNSR- An Interactive Software System for Optimal Design of Statically and Dynamically Loaded Structures with Nonlinear Response," by Bhatti, M.A., Ciampi, V. and Pister, K.S., January 1981, (PB81 218 851)A09.

UCB/EERC-81/03 "Analysis of Local Variations in Free Field Seismic Ground Motions," by Chen, J.-C., Lysmer, J. and Seed, H.B., January 1981, (AD-A099508)A13.

UCB/EERC-81/04 "Inelastic Structural Modeling of Braced Offshore Platforms for Seismic Loading," by Zayas, V.A., Shing, P.-S.B., Mahin, S.A. and Popov, E.P., January 1981, INEL4, (PB82 138 777)A07.

UCB/EERC-81/05 "Dynamic Response of Light Equipment in Structures," by Der Kiureghian, A., Sackman, J.L. and Nour-Omid, B., April 1981, (PB81 218 497)A04.

UCB/EERC-81/06 "Preliminary Experimental Investigation of a Broad Base Liquid Storage Tank," by Bouwkamp, J.G., Kollegger, J.P. and Stephen, R.M., May 1981, (PB82 140 385)A03.

UCB/EERC-81/07 "The Seismic Resistant Design of Reinforced Concrete Coupled Structural Walls," by Aktan, A.E. and Bertero, V.V., June 1981, (PB82 113 358)A11.

UCB/EERC-81/08 "Unassigned," by Unassigned, 1981.

UCB/EERC-81/09 "Experimental Behavior of a Spatial Piping System with Steel Energy Absorbers Subjected to a Simulated Differential Seismic Input," by Stiemer, S.F., Godden, W.G. and Kelly, J.M., July 1981, (PB82 201 898)A04.

UCB/EERC-81/10 "Evaluation of Seismic Design Provisions for Masonry in the United States," by Sveinsson, B.I., Mayes, R.L. and McNiven, H.D., August 1981, (PB82 166 075)A08.

UCB/EERC-81/11 "Two-Dimensional Hybrid Modelling of Soil-Structure Interaction," by Tzong, T.-J., Gupta, S. and Penzien, J., August 1981, (PB82 142 118)A04.

UCB/EERC-81/12 "Studies on Effects of Infills in Seismic Resistant R/C Construction," by Brokken, S. and Bertero, V.V., October 1981, (PB82 166 190)A09.

UCB/EERC-81/13 "Linear Models to Predict the Nonlinear Seismic Behavior of a One-Story Steel Frame," by Valdimarsson, H., Shah, A.H. and McNiven, H.D., September 1981, (PB82 138 793)A07.

UCB/EERC-81/14 "TLUSH: A Computer Program for the Three-Dimensional Dynamic Analysis of Earth Dams," by Kagawa, T., Mejia, L.H., Seed, H.B. and Lysmer, J., September 1981, (PB82 139 940)A06.

UCB/EERC-81/15 "Three Dimensional Dynamic Response Analysis of Earth Dams," by Mejia, L.H. and Seed, H.B., September 1981, (PB82 137 274)A12.

UCB/EERC-81/16 "Experimental Study of Lead and Elastomeric Dampers for Base Isolation Systems," by Kelly, J.M. and Hodder, S.B., October 1981, (PB82 166 182)A05.

UCB/EERC-81/17 "The Influence of Base Isolation on the Seismic Response of Light Secondary Equipment," by Kelly, J.M., April 1981, (PB82 255 266)A04.

UCB/EERC-81/18 "Studies on Evaluation of Shaking Table Response Analysis Procedures," by Blondet, J. M., November 1981, (PB82 197 278)A10.

UCB/EERC-81/19 "DELIGHT.STRUCT: A Computer-Aided Design Environment for Structural Engineering," by Balling, R.J., Pister, K.S. and Polak, E., December 1981, (PB82 218 496)A07.

UCB/EERC-81/20 "Optimal Design of Seismic-Resistant Planar Steel Frames," by Balling, R.J., Ciampi, V. and Pister, K.S., December 1981, (PB82 220 179)A07.

UCB/EERC-82/01 "Dynamic Behavior of Ground for Seismic Analysis of Lifeline Systems," by Sato, T. and Der Kiureghian, A., January 1982, (PB82 218 926)A05.

UCB/EERC-82/02 "Shaking Table Tests of a Tubular Steel Frame Model," by Ghanaat, Y. and Clough, R.W., January 1982, (PB82 220 161)A07.

UCB/EERC-82/03 "Behavior of a Piping System under Seismic Excitation: Experimental Investigations of a Spatial Piping System supported by Mechanical Shock Arrestors," by Schneider, S., Lee, H.-M. and Godden, W. G., May 1982, (PB83 172 544)A09.

UCB/EERC-82/04 "New Approaches for the Dynamic Analysis of Large Structural Systems," by Wilson, E.L., June 1982, (PB83 148 080)A05.

UCB/EERC-82/05 "Model Study of Effects of Damage on the Vibration Properties of Steel Offshore Platforms," by Shahrivar, F. and Bouwkamp, J.G., June 1982, (PB83 148 742)A10.

UCB/EERC-82/06 "States of the Art and Pratice in the Optimum Seismic Design and Analytical Response Prediction of R/C Frame Wall Structures," by Aktan, A.E. and Bertero, V.V., July 1982, (PB83 147 736)A05.

UCB/EERC-82/07 "Further Study of the Earthquake Response of a Broad Cylindrical Liquid-Storage Tank Model," by Manos, G.C. and Clough, R.W., July 1982, (PB83 147 744)A11.

UCB/EERC-82/08 "An Evaluation of the Design and Analytical Seismic Response of a Seven Story Reinforced Concrete Frame," by Charney, F.A. and Bertero, V.V., July 1982, (PB83 157 628)A09.

UCB/EERC-82/09 "Fluid-Structure Interactions: Added Mass Computations for Incompressible Fluid," by Kuo, J.S.-H., August 1982, (PB83 156 281)A07.

UCB/EERC-82/10 "Joint-Opening Nonlinear Mechanism: Interface Smeared Crack Model," by Kuo, J.S.-H., August 1982, (PB83 149 195)A05.

UCB/EERC-82/11 "Dynamic Response Analysis of Techi Dam," by Clough, R.W., Stephen, R.M. and Kuo, J.S.-H., August 1982, (PB83 147 496)A06.

UCB/EERC-82/12 "Prediction of the Seismic Response of R/C Frame-Coupled Wall Structures," by Aktan, A.E., Bertero, V.V. and Piazzo, M., August 1982, (PB83 149 203)A09.

UCB/EERC-82/13 "Preliminary Report on the Smart 1 Strong Motion Array in Taiwan," by Bolt, B.A., Loh, C.H., Penzien, J. and Tsai, Y.B., August 1982, (PB83 159 400)A10.

UCB/EERC-82/14 "Seismic Behavior of an Eccentrically X-Braced Steel Structure," by Yang, M.S., September 1982, (PB83 260 778)A12.

UCB/EERC-82/15 "The Performance of Stairways in Earthquakes," by Roha, C., Axley, J.W. and Bertero, V.V., September 1982, (PB83 157 693)A07.

UCB/EERC-82/16 "The Behavior of Submerged Multiple Bodies in Earthquakes," by Liao, W.-G., September 1982, (PB83 158 709)A07.

UCB/EERC-82/17 "Effects of Concrete Types and Loading Conditions on Local Bond-Slip Relationships," by Cowell, A.D., Popov, E.P. and Bertero, V.V., September 1982, (PB83 153 577)A04.

UCB/EERC-82/18 "Mechanical Behavior of Shear Wall Vertical Boundary Members: An Experimental Investigation," by Wagner, M.T. and Bertero, V.V., October 1982, (PB83 159 764)A05.

UCB/EERC-82/19 "Experimental Studies of Multi-support Seismic Loading on Piping Systems," by Kelly, J.M. and Cowell, A.D., November 1982, (PB90 262 684)A07.

UCB/EERC-82/20 "Generalized Plastic Hinge Concepts for 3D Beam-Column Elements," by Chen, P. F.-S. and Powell, G.H., November 1982, (PB83 247 981)A13.

UCB/EERC-82/21 "ANSR-II: General Computer Program for Nonlinear Structural Analysis," by Oughourlian, C.V. and Powell, G.H., November 1982, (PB83 251 330)A12.

UCB/EERC-82/22 "Solution Strategies for Statically Loaded Nonlinear Structures," by Simons, J.W. and Powell, G.H., November 1982, (PB83 197 970)A06.

UCB/EERC-82/23 "Analytical Model of Deformed Bar Anchorages under Generalized Excitations," by Ciampi, V., Eligehausen, R., Bertero, V.V. and Popov, E.P., November 1982, (PB83 169 532)A06.

UCB/EERC-82/24 "A Mathematical Model for the Response of Masonry Walls to Dynamic Excitations," by Sucuoglu, H., Mengi, Y. and McNiven, H.D., November 1982, (PB83 169 011)A07.

UCB/EERC-82/25 "Earthquake Response Considerations of Broad Liquid Storage Tanks," by Cambra, F.J., November 1982, (PB83 251 215)A09.

UCB/EERC-82/26 "Computational Models for Cyclic Plasticity, Rate Dependence and Creep," by Mosaddad, B. and Powell, G.H., November 1982, (PB83 245 829)A08.

UCB/EERC-82/27 "Inelastic Analysis of Piping and Tubular Structures," by Mahasuverachai, M. and Powell, G.H., November 1982, (PB83 249 987)A07.

UCB/EERC-83/01 "The Economic Feasibility of Seismic Rehabilitation of Buildings by Base Isolation," by Kelly, J.M., January 1983, (PB83 197 988)A05.

UCB/EERC-83/02 "Seismic Moment Connections for Moment-Resisting Steel Frames.," by Popov, E.P., January 1983, (PB83 195 412)A04.

UCB/EERC-83/03 "Design of Links and Beam-to-Column Connections for Eccentrically Braced Steel Frames," by Popov, E.P. and Malley, J.O., January 1983, (PB83 194 811)A04.

UCB/EERC-83/04 "Numerical Techniques for the Evaluation of Soil-Structure Interaction Effects in the Time Domain," by Bayo, E. and Wilson, E.L., February 1983, (PB83 245 605)A09.

UCB/EERC-83/05 "A Transducer for Measuring the Internal Forces in the Columns of a Frame-Wall Reinforced Concrete Structure," by Sause, R. and Bertero, V.V., May 1983, (PB84 119 494)A06.

UCB/EERC-83/06 "Dynamic Interactions Between Floating Ice and Offshore Structures," by Croteau, P., May 1983, (PB84 119 486)A16.

UCB/EERC-83/07 "Dynamic Analysis of Multiply Tuned and Arbitrarily Supported Secondary Systems," by Igusa, T. and Der Kiureghian, A., July 1983, (PB84 118 272)A11.

UCB/EERC-83/08 "A Laboratory Study of Submerged Multi-body Systems in Earthquakes," by Ansari, G.R., June 1983, (PB83 261 842)A17.

UCB/EERC-83/09 "Effects of Transient Foundation Uplift on Earthquake Response of Structures," by Yim, C.-S. and Chopra, A.K., June 1983, (PB83 261 396)A07.

UCB/EERC-83/10 "Optimal Design of Friction-Braced Frames under Seismic Loading," by Austin, M.A. and Pister, K.S., June 1983, (PB84 119 288)A06.

UCB/EERC-83/11 "Shaking Table Study of Single-Story Masonry Houses: Dynamic Performance under Three Component Seismic Input and Recommendations," by Manos, G.C., Clough, R.W. and Mayes, R.L., July 1983, (UCB/EERC-83/11)A08.

UCB/EERC-83/12 "Experimental Error Propagation in Pseudodynamic Testing," by Shiing, P.B. and Mahin, S.A., June 1983, (PB84 119 270)A09.

UCB/EERC-83/13 "Experimental and Analytical Predictions of the Mechanical Characteristics of a 1/5-scale Model of a 7-story R/C Frame-Wall Building Structure," by Aktan, A.E., Bertero, V.V., Chowdhury, A.A. and Nagashima, T., June 1983, (PB84 119 213)A07.

UCB/EERC-83/14 "Shaking Table Tests of Large-Panel Precast Concrete Building System Assemblages," by Oliva, M.G. and Clough, R.W., June 1983, (PB86 110 210/AS)A11.

UCB/EERC-83/15 "Seismic Behavior of Active Beam Links in Eccentrically Braced Frames," by Hjelmstad, K.D. and Popov, E.P., July 1983, (PB84 119 676)A09.

UCB/EERC-83/16 "System Identification of Structures with Joint Rotation," by Dimsdale, J.S., July 1983, (PB84 192 210)A06.

UCB/EERC-83/17 "Construction of Inelastic Response Spectra for Single-Degree-of-Freedom Systems," by Mahin, S. and Lin, J., June 1983, (PB84 208 834)A05.

UCB/EERC-83/18 "Interactive Computer Analysis Methods for Predicting the Inelastic Cyclic Behaviour of Structural Sections," by Kaba, S. and Mahin, S., July 1983, (PB84 192 012)A06.

UCB/EERC-83/19 "Effects of Bond Deterioration on Hysteretic Behavior of Reinforced Concrete Joints," by Filippou, F.C., Popov, E.P. and Bertero, V.V., August 1983, (PB84 192 020)A10.

UCB/EERC-83/20 "Correlation of Analytical and Experimental Responses of Large-Panel Precast Building Systems," by Oliva, M.G., Clough, R.W., Velkov, M. and Gavrilovic, P., May 1988, (PB90 262 692)A06.

UCB/EERC-83/21 "Mechanical Characteristics of Materials Used in a 1/5 Scale Model of a 7-Story Reinforced Concrete Test Structure," by Bertero, V.V., Aktan, A.E., Harris, H.G. and Chowdhury, A.A., October 1983, (PB84 193 697)A05.

UCB/EERC-83/22 "Hybrid Modelling of Soil-Structure Interaction in Layered Media," by Tzong, T.-J. and Penzien, J., October 1983, (PB84 192 178)A08.

UCB/EERC-83/23 "Local Bond Stress-Slip Relationships of Deformed Bars under Generalized Excitations," by Eligehausen, R., Popov, E.P. and Bertero, V.V., October 1983, (PB84 192 848)A09.

UCB/EERC-83/24 "Design Considerations for Shear Links in Eccentrically Braced Frames," by Malley, J.O. and Popov, E.P., November 1983, (PB84 192 186)A07.

UCB/EERC-84/01 "Pseudodynamic Test Method for Seismic Performance Evaluation: Theory and Implementation," by Shing, P.-S.B. and Mahin, S.A., January 1984, (PB84 190 644)A08.

UCB/EERC-84/02 "Dynamic Response Behavior of Kiang Hong Dian Dam," by Clough, R.W., Chang, K.-T., Chen, H.-Q. and Stephen, R.M., April 1984, (PB84 209 402)A08.

UCB/EERC-84/03 "Refined Modelling of Reinforced Concrete Columns for Seismic Analysis," by Kaba, S.A. and Mahin, S.A., April 1984, (PB84 234 384)A06.

UCB/EERC-84/04 "A New Floor Response Spectrum Method for Seismic Analysis of Multiply Supported Secondary Systems," by Asfura, A. and Der Kiureghian, A., June 1984, (PB84 239 417)A06.

UCB/EERC-84/05 "Earthquake Simulation Tests and Associated Studies of a 1/5th-scale Model of a 7-Story R/C Frame-Wall Test Structure," by Bertero, V.V., Aktan, A.E., Charney, F.A. and Sause, R., June 1984, (PB84 239 409)A09.

UCB/EERC-84/06 "R/C Structural Walls: Seismic Design for Shear," by Aktan, A.E. and Bertero, V.V., 1984.

UCB/EERC-84/07 "Behavior of Interior and Exterior Flat-Plate Connections subjected to Inelastic Load Reversals," by Zee, H.L. and Moehle, J.P., August 1984, (PB86 117 629/AS)A07.

UCB/EERC-84/08 "Experimental Study of the Seismic Behavior of a Two-Story Flat-Plate Structure," by Moehle, J.P. and Diebold, J.W., August 1984, (PB86 122 553/AS)A12.

UCB/EERC-84/09 "Phenomenological Modeling of Steel Braces under Cyclic Loading," by Ikeda, K., Mahin, S.A. and Dermitzakis, S.N., May 1984, (PB86 132 198/AS)A08.

UCB/EERC-84/10 "Earthquake Analysis and Response of Concrete Gravity Dams," by Fenves, G. and Chopra, A.K., August 1984, (PB85 193 902/AS)A11.

UCB/EERC-84/11 "EAGD-84: A Computer Program for Earthquake Analysis of Concrete Gravity Dams," by Fenves, G. and Chopra, A.K., August 1984, (PB85 193 613/AS)A05.

UCB/EERC-84/12 "A Refined Physical Theory Model for Predicting the Seismic Behavior of Braced Steel Frames," by Ikeda, K. and Mahin, S.A., July 1984, (PB85 191 450/AS)A09.

UCB/EERC-84/13 "Earthquake Engineering Research at Berkeley - 1984," by , August 1984, (PB85 197 341/AS)A10.

UCB/EERC-84/14 "Moduli and Damping Factors for Dynamic Analyses of Cohesionless Soils," by Seed, H.B., Wong, R.T., Idriss, I.M. and Tokimatsu, K., September 1984, (PB85 191 468/AS)A04.

UCB/EERC-84/15 "The Influence of SPT Procedures in Soil Liquefaction Resistance Evaluations," by Seed, H.B., Tokimatsu, K., Harder, L.F. and Chung, R.M., October 1984, (PB85 191 732/AS)A04.

UCB/EERC-84/16 "Simplified Procedures for the Evaluation of Settlements in Sands Due to Earthquake Shaking," by Tokimatsu, K. and Seed, H.B., October 1984, (PB85 197 887/AS)A03.

UCB/EERC-84/17 "Evaluation of Energy Absorption Characteristics of Highway Bridges Under Seismic Conditions - Volume I (PB90 262 627)A16 and Volume II (Appendices) (PB90 262 635)A13," by Imbsen, R.A. and Penzien, J., September 1986.

UCB/EERC-84/18 "Structure-Foundation Interactions under Dynamic Loads," by Liu, W.D. and Penzien, J., November 1984, (PB87 124 889/AS)A11.

UCB/EERC-84/19 "Seismic Modelling of Deep Foundations," by Chen, C.-H. and Penzien, J., November 1984, (PB87 124 798/AS)A07.

UCB/EERC-84/20 "Dynamic Response Behavior of Quan Shui Dam," by Clough, R.W., Chang, K.-T., Chen, H.-Q., Stephen, R.M., Ghanaat, Y. and Qi, J.-H., November 1984, (PB86 115177/AS)A07.

UCB/EERC-85/01 "Simplified Methods of Analysis for Earthquake Resistant Design of Buildings," by Cruz, E.F. and Chopra, A.K., February 1985, (PB86 112299/AS)A12.

UCB/EERC-85/02 "Estimation of Seismic Wave Coherency and Rupture Velocity using the SMART 1 Strong-Motion Array Recordings," by Abrahamson, N.A., March 1985, (PB86 214 343)A07.

UCB/EERC-85/03 "Dynamic Properties of a Thirty Story Condominium Tower Building," by Stephen, R.M., Wilson, E.L. and Stander, N., April 1985, (PB86 118965/AS)A06.

UCB/EERC-85/04 "Development of Substructuring Techniques for On-Line Computer Controlled Seismic Performance Testing," by Dermitzakis, S. and Mahin, S., February 1985, (PB86 132941/AS)A08.

UCB/EERC-85/05 "A Simple Model for Reinforcing Bar Anchorages under Cyclic Excitations," by Filippou, F.C., March 1985, (PB86 112 919/AS)A05.

UCB/EERC-85/06 "Racking Behavior of Wood-framed Gypsum Panels under Dynamic Load," by Oliva, M.G., June 1985, (PB90 262 643)A04.

UCB/EERC-85/07 "Earthquake Analysis and Response of Concrete Arch Dams," by Fok, K.-L. and Chopra, A.K., June 1985, (PB86 139672/AS)A10.

UCB/EERC-85/08 "Effect of Inelastic Behavior on the Analysis and Design of Earthquake Resistant Structures," by Lin, J.P. and Mahin, S.A., June 1985, (PB86 135340/AS)A08.

UCB/EERC-85/09 "Earthquake Simulator Testing of a Base-Isolated Bridge Deck," by Kelly, J.M., Buckle, I.G. and Tsai, H.-C., January 1986, (PB87 124 152/AS)A06.

UCB/EERC-85/10 "Simplified Analysis for Earthquake Resistant Design of Concrete Gravity Dams," by Fenves, G. and Chopra, A.K., June 1986, (PB87 124 160/AS)A08.

UCB/EERC-85/11 "Dynamic Interaction Effects in Arch Dams," by Clough, R.W., Chang, K.-T., Chen, H.-Q. and Ghanaat, Y., October 1985, (PB86 135027/AS)A05.

UCB/EERC-85/12 "Dynamic Response of Long Valley Dam in the Mammoth Lake Earthquake Series of May 25-27, 1980," by Lai, S. and Seed, H.B., November 1985, (PB86 142304/AS)A05.

UCB/EERC-85/13 "A Methodology for Computer-Aided Design of Earthquake-Resistant Steel Structures," by Austin, M.A., Pister, K.S. and Mahin, S.A., December 1985, (PB86 159480/AS)A10 .

UCB/EERC-85/14 "Response of Tension-Leg Platforms to Vertical Seismic Excitations," by Liou, G.-S., Penzien, J. and Yeung, R.W., December 1985, (PB87 124 871/AS)A08.

UCB/EERC-85/15 "Cyclic Loading Tests of Masonry Single Piers: Volume 4 - Additional Tests with Height to Width Ratio of 1," by Sveinsson, B., McNiven, H.D. and Sucuoglu, H., December 1985.

UCB/EERC-85/16 "An Experimental Program for Studying the Dynamic Response of a Steel Frame with a Variety of Infill Partitions," by Yanev, B. and McNiven, H.D., December 1985, (PB90 262 676)A05.

UCB/EERC-86/01 "A Study of Seismically Resistant Eccentrically Braced Steel Frame Systems," by Kasai, K. and Popov, E.P., January 1986, (PB87 124 178/AS)A14.

UCB/EERC-86/02 "Design Problems in Soil Liquefaction," by Seed, H.B., February 1986, (PB87 124 186/AS)A03.

UCB/EERC-86/03 "Implications of Recent Earthquakes and Research on Earthquake-Resistant Design and Construction of Buildings," by Bertero, V.V., March 1986, (PB87 124 194/AS)A05.

UCB/EERC-86/04 "The Use of Load Dependent Vectors for Dynamic and Earthquake Analyses," by Leger, P., Wilson, E.L. and Clough, R.W., March 1986, (PB87 124 202/AS)A12.

UCB/EERC-86/05 "Two Beam-To-Column Web Connections," by Tsai, K.-C. and Popov, E.P., April 1986, (PB87 124 301/AS)A04.

UCB/EERC-86/06 "Determination of Penetration Resistance for Coarse-Grained Soils using the Becker Hammer Drill," by Harder, L.F. and Seed, H.B., May 1986, (PB87 124 210/AS)A07.

UCB/EERC-86/07 "A Mathematical Model for Predicting the Nonlinear Response of Unreinforced Masonry Walls to In-Plane Earthquake Excitations," by Mengi, Y. and McNiven, H.D., May 1986, (PB87 124 780/AS)A06.

UCB/EERC-86/08 "The 19 September 1985 Mexico Earthquake: Building Behavior," by Bertero, V.V., July 1986.

UCB/EERC-86/09 "EACD-3D: A Computer Program for Three-Dimensional Earthquake Analysis of Concrete Dams," by Fok, K.-L., Hall, J.F. and Chopra, A.K., July 1986, (PB87 124 228/AS)A08.

UCB/EERC-86/10 "Earthquake Simulation Tests and Associated Studies of a 0.3-Scale Model of a Six-Story Concentrically Braced Steel Structure," by Uang, C.-M. and Bertero, V.V., December 1986, (PB87 163 564/AS)A17.

UCB/EERC-86/11 "Mechanical Characteristics of Base Isolation Bearings for a Bridge Deck Model Test," by Kelly, J.M., Buckle, I.G. and Koh, C.-G., November 1987, (PB90 262 668)A04.

UCB/EERC-86/12 "Effects of Axial Load on Elastomeric Isolation Bearings," by Koh, C.-G. and Kelly, J.M., November 1987.

UCB/EERC-87/01 "The FPS Earthquake Resisting System: Experimental Report," by Zayas, V.A., Low, S.S. and Mahin, S.A., June 1987.

UCB/EERC-87/02 "Earthquake Simulator Tests and Associated Studies of a 0.3-Scale Model of a Six-Story Eccentrically Braced Steel Structure," by Whittaker, A., Uang, C.-M. and Bertero, V.V., July 1987.

UCB/EERC-87/03 "A Displacement Control and Uplift Restraint Device for Base-Isolated Structures," by Kelly, J.M., Griffith, M.C. and Aiken, I.D., April 1987.

UCB/EERC-87/04 "Earthquake Simulator Testing of a Combined Sliding Bearing and Rubber Bearing Isolation System," by Kelly, J.M. and Chalhoub, M.S., 1987.

UCB/EERC-87/05 "Three-Dimensional Inelastic Analysis of Reinforced Concrete Frame-Wall Structures," by Moazzami, S. and Bertero, V.V., May 1987.

UCB/EERC-87/06 "Experiments on Eccentrically Braced Frames with Composite Floors," by Ricles, J. and Popov, E., June 1987.

UCB/EERC-87/07 "Dynamic Analysis of Seismically Resistant Eccentrically Braced Frames," by Ricles, J. and Popov, E., June 1987.

UCB/EERC-87/08 "Undrained Cyclic Triaxial Testing of Gravels-The Effect of Membrane Compliance," by Evans, M.D. and Seed, H.B., July 1987.

UCB/EERC-87/09 "Hybrid Solution Techniques for Generalized Pseudo-Dynamic Testing," by Thewalt, C. and Mahin, S.A., July 1987.

UCB/EERC-87/10 "Ultimate Behavior of Butt Welded Splices in Heavy Rolled Steel Sections," by Bruneau, M., Mahin, S.A. and Popov, E.P., September 1987.

UCB/EERC-87/11 "Residual Strength of Sand from Dam Failures in the Chilean Earthquake of March 3, 1985," by De Alba, P., Seed, H.B., Retamal, E. and Seed, R.B., September 1987.

UCB/EERC-87/12 "Inelastic Seismic Response of Structures with Mass or Stiffness Eccentricities in Plan," by Bruneau, M. and Mahin, S.A., September 1987, (PB90 262 650)A14.

UCB/EERC-87/13 "CSTRUCT: An Interactive Computer Environment for the Design and Analysis of Earthquake Resistant Steel Structures," by Austin, M.A., Mahin, S.A. and Pister, K.S., September 1987.

UCB/EERC-87/14 "Experimental Study of Reinforced Concrete Columns Subjected to Multi-Axial Loading," by Low, S.S. and Moehle, J.P., September 1987.

UCB/EERC-87/15 "Relationships between Soil Conditions and Earthquake Ground Motions in Mexico City in the Earthquake of Sept. 19, 1985," by Seed, H.B., Romo, M.P., Sun, J., Jaime, A. and Lysmer, J., October 1987.

UCB/EERC-87/16 "Experimental Study of Seismic Response of R. C. Setback Buildings," by Shahrooz, B.M. and Moehle, J.P., October 1987.

UCB/EERC-87/17 "The Effect of Slabs on the Flexural Behavior of Beams," by Pantazopoulou, S.J. and Moehle, J.P., October 1987, (PB90 262 700)A07.

UCB/EERC-87/18 "Design Procedure for R-FBI Bearings," by Mostaghel, N. and Kelly, J.M., November 1987, (PB90 262 718)A04.

UCB/EERC-87/19 "Analytical Models for Predicting the Lateral Response of R C Shear Walls: Evaluation of their Reliability," by Vulcano, A. and Bertero, V.V., November 1987.

UCB/EERC-87/20 "Earthquake Response of Torsionally-Coupled Buildings," by Hejal, R. and Chopra, A.K., December 1987.

UCB/EERC-87/21 "Dynamic Reservoir Interaction with Monticello Dam," by Clough, R.W., Ghanaat, Y. and Qiu, X-F., December 1987.

UCB/EERC-87/22 "Strength Evaluation of Coarse-Grained Soils," by Siddiqi, F.H., Seed, R.B., Chan, C.K., Seed, H.B. and Pyke, R.M., December 1987.

UCB/EERC-88/01 "Seismic Behavior of Concentrically Braced Steel Frames," by Khatib, I., Mahin, S.A. and Pister, K.S., January 1988.

UCB/EERC-88/02 "Experimental Evaluation of Seismic Isolation of Medium-Rise Structures Subject to Uplift," by Griffith, M.C., Kelly, J.M., Coveney, V.A. and Koh, C.G., January 1988.

UCB/EERC-88/03 "Cyclic Behavior of Steel Double Angle Connections," by Astaneh-Asl, A. and Nader, M.N., January 1988.

UCB/EERC-88/04 "Re-evaluation of the Slide in the Lower San Fernando Dam in the Earthquake of Feb. 9, 1971," by Seed, H.B., Seed, R.B., Harder, L.F. and Jong, H.-L., April 1988.

UCB/EERC-88/05 "Experimental Evaluation of Seismic Isolation of a Nine-Story Braced Steel Frame Subject to Uplift," by Griffith, M.C., Kelly, J.M. and Aiken, I.D., May 1988.

UCB/EERC-88/06 "DRAIN-2DX User Guide.," by Allahabadi, R. and Powell, G.H., March 1988.

UCB/EERC-88/07 "Cylindrical Fluid Containers in Base-Isolated Structures," by Chalhoub, M.S. and Kelly, J.M. , April 1988.

UCB/EERC-88/08 "Analysis of Near-Source Waves: Separation of Wave Types using Strong Motion Array Recordings," by Darragh, R.B., June 1988.

UCB/EERC-88/09 "Alternatives to Standard Mode Superposition for Analysis of Non-Classically Damped Systems," by Kusainov, A.A. and Clough, R.W., June 1988.

UCB/EERC-88/10 "The Landslide at the Port of Nice on October 16, 1979," by Seed, H.B., Seed, R.B., Schlosser, F., Blondeau, F. and Juran, I., June 1988.

UCB/EERC-88/11 "Liquefaction Potential of Sand Deposits Under Low Levels of Excitation," by Carter, D.P. and Seed, H.B., August 1988.

UCB/EERC-88/12 "Nonlinear Analysis of Reinforced Concrete Frames Under Cyclic Load Reversals," by Filippou, F.C. and Issa, A., September 1988.

UCB/EERC-88/13 "Implications of Recorded Earthquake Ground Motions on Seismic Design of Building Structures," by Uang, C.-M. and Bertero, V.V., November 1988.

UCB/EERC-88/14 "An Experimental Study of the Behavior of Dual Steel Systems," by Whittaker, A.S. , Uang, C.-M. and Bertero, V.V., September 1988.

UCB/EERC-88/15 "Dynamic Moduli and Damping Ratios for Cohesive Soils," by Sun, J.I., Golesorkhi, R. and Seed, H.B., August 1988.

UCB/EERC-88/16 "Reinforced Concrete Flat Plates Under Lateral Load: An Experimental Study Including Biaxial Effects," by Pan, A. and Moehle, J., October 1988.

UCB/EERC-88/17 "Earthquake Engineering Research at Berkeley - 1988," by EERC, November 1988.

UCB/EERC-88/18 "Use of Energy as a Design Criterion in Earthquake-Resistant Design," by Uang, C.-M. and Bertero, V.V., November 1988.

UCB/EERC-88/19 "Steel Beam-Column Joints in Seismic Moment Resisting Frames," by Tsai, K.-C. and Popov, E.P., November 1988.

UCB/EERC-88/20 "Base Isolation in Japan, 1988," by Kelly, J.M., December 1988.

UCB/EERC-89/01 "Behavior of Long Links in Eccentrically Braced Frames," by Engelhardt, M.D. and Popov, E.P., January 1989.

UCB/EERC-89/02 "Earthquake Simulator Testing of Steel Plate Added Damping and Stiffness Elements," by Whittaker, A., Bertero, V.V., Alonso, J. and Thompson, C., January 1989.

UCB/EERC-89/03 "Implications of Site Effects in the Mexico City Earthquake of Sept. 19, 1985 for Earthquake-Resistant Design Criteria in the San Francisco Bay Area of California," by Seed, H.B. and Sun, J.I., March 1989.

UCB/EERC-89/04 "Earthquake Analysis and Response of Intake-Outlet Towers," by Goyal, A. and Chopra, A.K., July 1989.

UCB/EERC-89/05 "The 1985 Chile Earthquake: An Evaluation of Structural Requirements for Bearing Wall Buildings," by Wallace, J.W. and Moehle, J.P., July 1989.

UCB/EERC-89/06 "Effects of Spatial Variation of Ground Motions on Large Multiply-Supported Structures," by Hao, H., July 1989.

UCB/EERC-89/07 "EADAP - Enhanced Arch Dam Analysis Program: Users's Manual," by Ghanaat, Y. and Clough, R.W., August 1989.

UCB/EERC-89/08 "Seismic Performance of Steel Moment Frames Plastically Designed by Least Squares Stress Fields," by Ohi, K. and Mahin, S.A., August 1989.

UCB/EERC-89/09 "Feasibility and Performance Studies on Improving the Earthquake Resistance of New and Existing Buildings Using the Friction Pendulum System," by Zayas, V., Low, S., Mahin, S.A. and Bozzo, L., July 1989.

UCB/EERC-89/10 "Measurement and Elimination of Membrane Compliance Effects in Undrained Triaxial Testing," by Nicholson, P.G., Seed, R.B. and Anwar, H., September 1989.

UCB/EERC-89/11 "Static Tilt Behavior of Unanchored Cylindrical Tanks," by Lau, D.T. and Clough, R.W., September 1989.

UCB/EERC-89/12 "ADAP-88: A Computer Program for Nonlinear Earthquake Analysis of Concrete Arch Dams," by Fenves, G.L., Mojtahedi, S. and Reimer, R.B., September 1989.

UCB/EERC-89/13 "Mechanics of Low Shape Factor Elastomeric Seismic Isolation Bearings," by Aiken, I.D., Kelly, J.M. and Tajirian, F., December 1989.

UCB/EERC-89/14 "Preliminary Report on the Seismological and Engineering Aspects of the October 17, 1989 Santa Cruz (Loma Prieta) Earthquake," by EERC, October 1989.

UCB/EERC-89/15 "Experimental Studies of a Single Story Steel Structure Tested with Fixed, Semi-Rigid and Flexible Connections," by Nader, M.N. and Astaneh-Asl, A., August 1989.

UCB/EERC-89/16 "Collapse of the Cypress Street Viaduct as a Result of the Loma Prieta Earthquake," by Nims, D.K., Miranda, E., Aiken, I.D., Whittaker, A.S. and Bertero, V.V., November 1989.

UCB/EERC-90/01 "Mechanics of High-Shape Factor Elastomeric Seismic Isolation Bearings," by Kelly, J.M., Aiken, I.D. and Tajirian, F.F., March 1990.

UCB/EERC-90/02 "Javid's Paradox: The Influence of Preform on the Modes of Vibrating Beams," by Kelly, J.M., Sackman, J.L. and Javid, A., May 1990.

UCB/EERC-90/03 "Earthquake Simulator Tests of Viscoelastic Dampers for Medium Rise Structures," by Kelly, J.M. and Aiken, I.D., May 1990.

UCB/EERC-90/04 "Damage to the San Francisco-Oakland Bay Bridge During the October 17, 1989 Earthquake," by Astaneh, A., June 1990.

UCB/EERC-90/05 "Preliminary Report on the Principal Geotechnical Aspects of the October 17, 1989 Loma Prieta Earthquake," by Seed, R.B., Dickenson, S.E., Riemer, M.F., Bray, J.D., Sitar, N., Mitchell, J.K., Idriss, I.M., Kayen, R.E., Kropp, A., Harder, L.F., Jr. and Power, M.S., April 1990.

UCB/EERC-90/06 "Models of Critical Regions in Reinforced Concrete Frames Under Seismic Excitations." by Zulfiqar, N. and Filippou, F., May 1990.

UCB/EERC-90/07 "A Unified Earthquake-Resistant Design Method for Steel Frames Using ARMA Models," by Takewaki, I., Conte, J.P., Mahin, S.A. and Pister, K.S., June 1990.

UCB/EERC-90/08 "Soil Conditions and Earthquake Hazard Mitigation in the Marina District of San Francisco," by Mitchell, J.K., Masood, T., Kayen, R.E. and Seed, R.B., May 1990.

UCB/EERC-90/09 "Influence of the Earthquake Ground Motion Process and Structural Properties on Response Characteristics of Simple Structures," by Conte, J.P., Pister, K.S. and Mahin, S.A., July 1990.

UCB/EERC-90/10 "Experimental Testing of the Resilient-Friction Base Isolation Sytsem," by Clark, P.W. and Kelly, J.M., July 1990.

UCB/EERC-90/11 "Seismic Hazard Analysis: Improved Models, Uncertainties and Sensitivities," by Araya, R. and Der Kiureghian, A., March 1988.

UCB/EERC-90/12 "Effects of Torsion on the Linear and Nonlinear Seismic Response of Structures," by Sedarat, H. and Bertero, V.V., September 1989.

UCB/EERC-90/13 "The Effects of Tectonic Movements on Stresses and Deformations in Earth Embankments," by Bray, J. D., Seed, R. B. and Seed, H. B., September 1989.

UCB/EERC-90/14 "Inelastic Seismic Response of One-Story, Asymmetric-Plan Systems," by Goel, R. K. and Chopra, A. K., November 1990.